

# Annexes

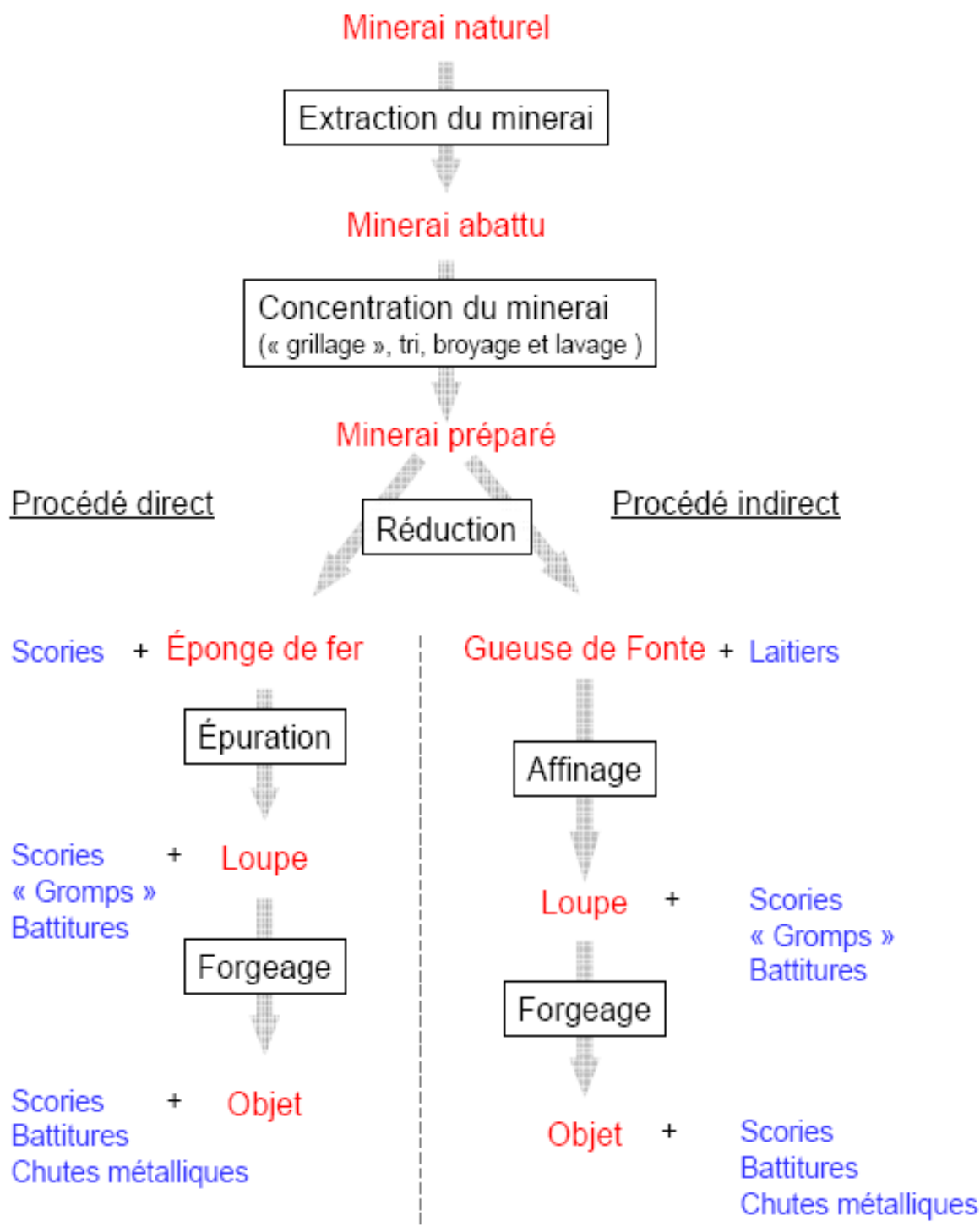
<b>Annexe A</b>	Schéma descriptif des chaînes opératoires directe et indirecte (tiré de Desaulty,2008)	3
<b>Annexe B</b>	Description de la production de la filière directe et notions de « qualité »	5
<b>Annexes C</b>	Plans de fouille et localisation des zones de prélèvements	9
<b>Annexe D</b>	Application de l'analyse discriminante aux données de l'Ariège et à celles d'échantillons d'origine ariégeoise et non ariégeoise ; comparaison des distances médiane et quartile sur l'axe discriminant LD1	19
<b>Annexe E</b>	Application de l'analyse discriminante aux données de l'Andorre ; compatibilité de la signature chimique avec l'espace sidérurgique andorran	23
<b>Annexes F</b>	Distribution sur l'axe discriminant LD1 des projections des observations associées aux objets d'origine inconnue et aux échantillons définissant l'Ariège ou la Lombardie	27
<b>Annexe G</b>	Résultats de l'analyse discriminante de deux classes de données. Coefficients de la fonction discriminante canonique associée à l'axe LD1	41
<b>Annexes H</b>	Analyse discriminante des $X_{ij}$ des objets MdS29421, MIR9 et MIR11 d'origine à identifier et des échantillons définissant l'Ariège, la Montagne Noire et l'Andorre. Projections sur les plans discriminants formés par les axes LD1, LD2, LD3	49
<b>Annexes I</b>	Analyse discriminante des $X_{ij}$ des fers du Palais des Papes d'Avignon d'origine à identifier et des échantillons définissant l'Ariège, la Montagne Noire, le Dauphiné et la Lombardie. Projections sur les plans discriminants formés par les axes LD1, LD2, LD3, LD4	53
<b>Annexe J</b>	Commerce du minerai et des produits sidérurgiques fin XIV <sup>e</sup> –milieu XV <sup>e</sup> siècle (Verna, 2001)	65
<b>Annexe K</b>	Analyses ICP-MS réalisées au Laboratoire des Mécanismes et Transferts en Géologie	67
<b>Annexe L</b>	Etude de la provenance d'objets retrouvés à Milan et en Piémont	69
<b>Annexe M</b>	Etude de la provenance de fers de construction de la cathédrale d'Amiens	75

<b>Annexes N</b>	Comparaisons des rapports d'éléments majeurs ( $\%_{\text{mass}}\text{Al}_2\text{O}_3/\%_{\text{mass}}\text{SiO}_2, \%_{\text{mass}}\text{K}_2\text{O}/\%_{\text{mass}}\text{CaO}, \%_{\text{mass}}\text{MgO}/\%_{\text{mass}}\text{Al}_2\text{O}_3$ ) dans les objets et les échantillons issus des espaces ariégeois et lombard	79
<b>Annexes O</b>	Observations macroscopiques et microscopiques sur des scories de réduction de Castel-Minier. Analyses des phases de composition	93
<b>Annexes P</b>	Observations métallographiques du corpus d'objets	105
<b>Annexe Q</b>	Corpus des objets du site de Montréal-de-Sos étudiés dans ce travail	147
<b>Annexe R</b>	Liste des échantillons d'origine connue collectés et étudiés dans ce travail (minerais, scories, objets)	153
<b>Annexe S</b>	Article : Protocole de minéralisation par attaque acide $\text{NH}_4\text{F}$ pour les analyses ICP-MS (Talanta (77) 445-450, 2008)	165
<b>Annexe T</b>	Short English version	181



## Annexe A

SCHÉMA DESCRIPTIF DES CHAÎNES OPÉRATOIRES DIRECTE ET INDIRECTE  
(TIRÉ DE DESAULTY, 2008)





## Annexe B

### DESCRIPTION DE LA PRODUCTION DE LA FILIÈRE DIRECTE ET NOTIONS DE « QUALITÉ »

La réduction directe ayant lieu à une température inférieure à celle de la fusion du fer, le produit de la réduction est une éponge plus ou moins carburée de structure très hétérogène. Différentes catégories d'alliage ferreux peuvent être mises en évidence en fonction de la teneur en carbone dans le métal. Le fer doux contient moins de 0,02% de carbone, l'acier contient jusqu'à 2% de carbone, la fonte contient de 2% à 7% de carbone (Fluzin *et al.*, 2000). Pour le procédé direct, les teneurs en carbone n'excèdent généralement pas 1,2 à 1,4%. Cependant, de la fonte pouvait également être produite sur les sites de bas fourneau. Des exemples archéologiques montrent ainsi l'obtention accidentelle de fonte pour la filière directe (Pelet, 1993 ; Yalcin & Hauptmann, 1995). Dans d'autres cas, il pourrait s'agir d'une action délibérée. Par exemple, en Italie, des blocs de fonte blanche qui ont été décarburés ont été mis au jour à Ponte di Val Gabbia aux V<sup>e</sup>-VI<sup>e</sup> siècles (Fluzin ; 1998).

Du fait de la spécificité de leur mode d'élaboration<sup>1</sup>, les matériaux ferreux archéologiques présentent un certain nombre d'hétérogénéités de composition et de structure, liées à la distribution de certains éléments et des inclusions dans le matériau. Par exemple, la taille des grains, les teneurs en carbone et les microstructures (structure de widmanstätten, perlite lamellaire...) peuvent être très variées (Figure B.1).

---

<sup>1</sup> Variabilité des conditions thermodynamiques locales dans les foyers anciens et des traitements de mise en forme à haute température.

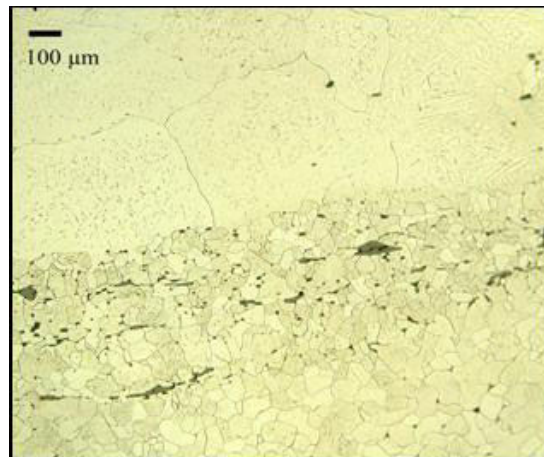


**Figure B.1 – Mise en évidence des hétérogénéités des matériaux ferreux anciens (attaque Nital). (Haut) taille des grains (Dillmann, 2006). (Bas) microteneur en carbone (L'Héritier, 2007)**

Ces hétérogénéités entraînent l'obtention de matériaux aux comportements mécaniques, à haute et température ambiante, qui diffèrent.

En fonction de la teneur variable de carbone dans le matériau, différents aciers sont mis en évidence. En ce sens, différentes qualités<sup>2</sup> de matériaux sont mentionnées dans les sources écrites dès le XIII<sup>e</sup> siècle et sont reconnues par les forgerons et les marchands sur les marchés. Certaines qualités seront recherchées pour une utilisation particulière, tandis que d'autres seront évitées par les acheteurs.

Verna (2000) fait référence à des sources qui donnent une idée de la diffusion et de l'emploi de matériaux dénommés de manière spécifique dans les Pyrénées. Par exemple, le fer du Minervois serait désigné comme « trop mou », tandis que celui du Comminges comme « trop dur ». En Ariège, la production des moulins était principalement du fer sous différentes formes : en barre ronde, des barres de fer plates, des tiges, des verges en fer, des morceaux, des ébauches, mais aussi du fer en plaque. Davantage que la forme, il existe surtout des qualités différentes de fers fabriquées dans les moulins. C. Verna rend compte de diverses appellations dans les sources: fer « fort », fer doux, fer *cédat*<sup>3</sup>. Le fer « fort » et le fer *cédat* sont davantage

<sup>2</sup> Il faut prendre ici cette notion de « qualité » au sens descriptif. Elle n'émet en aucun cas de jugement de valeur.

<sup>3</sup> Verna (2001), p.220.

carburés que le fer doux, le fer « fort » étant le plus carburé des trois. Les désignations de fer « fort » et fer *cédât* sont les plus fréquentes sur les marchés. Le fer « fort » y est vendu beaucoup plus cher que les autres fers.

L'une des caractéristiques du Vicdessos est de produire des barres de fer grossièrement martelées, les *merlaria*, qui ont pour caractéristique essentielle de rassembler différentes qualités de métal en fonction du degré de carburation. De ce produit hétérogène, de l'acier naturel pouvait être extrait. Verna (2001) décrit que les hommes, à cette époque, reconnaissaient dans les gisements de Vicdessos, un minerai qui donnait de l'acier naturel en réduction directe. Ils désignaient les mines de haute Ariège comme de « véritables montaignes » de fer et qualifiaient leur minerai de *mineriis de ferro calybe vel axero*<sup>4</sup>.

Au XIV<sup>e</sup> siècle, la compagnie Datini exportait de Brescia des aciers Lombards. Braunstein (2001) décrit, à partir de lettres de correspondants du marchand Datini, de nombreuses qualités d'acier désignées par des marques figurées. Une liste de dix sept variétés provenant du Valcamonica, quinze du Valtrompia et douze à travers les lettres de Brescia (« balestro », « campana », « gallo », etc.) peut être, à titre d'exemple, établie. Philippe Braunstein rapporte que le minerai d'origine, la qualité du charbon de bois, et le savoir-faire du maître, par son travail<sup>5</sup>, permettront d'obtenir un acier de plus ou moins bonne qualité.

---

<sup>4</sup> Cf. Verna (2001) p.65.

<sup>5</sup> Le choix des morceaux de la loupe, le martelage au feu, la trempe...



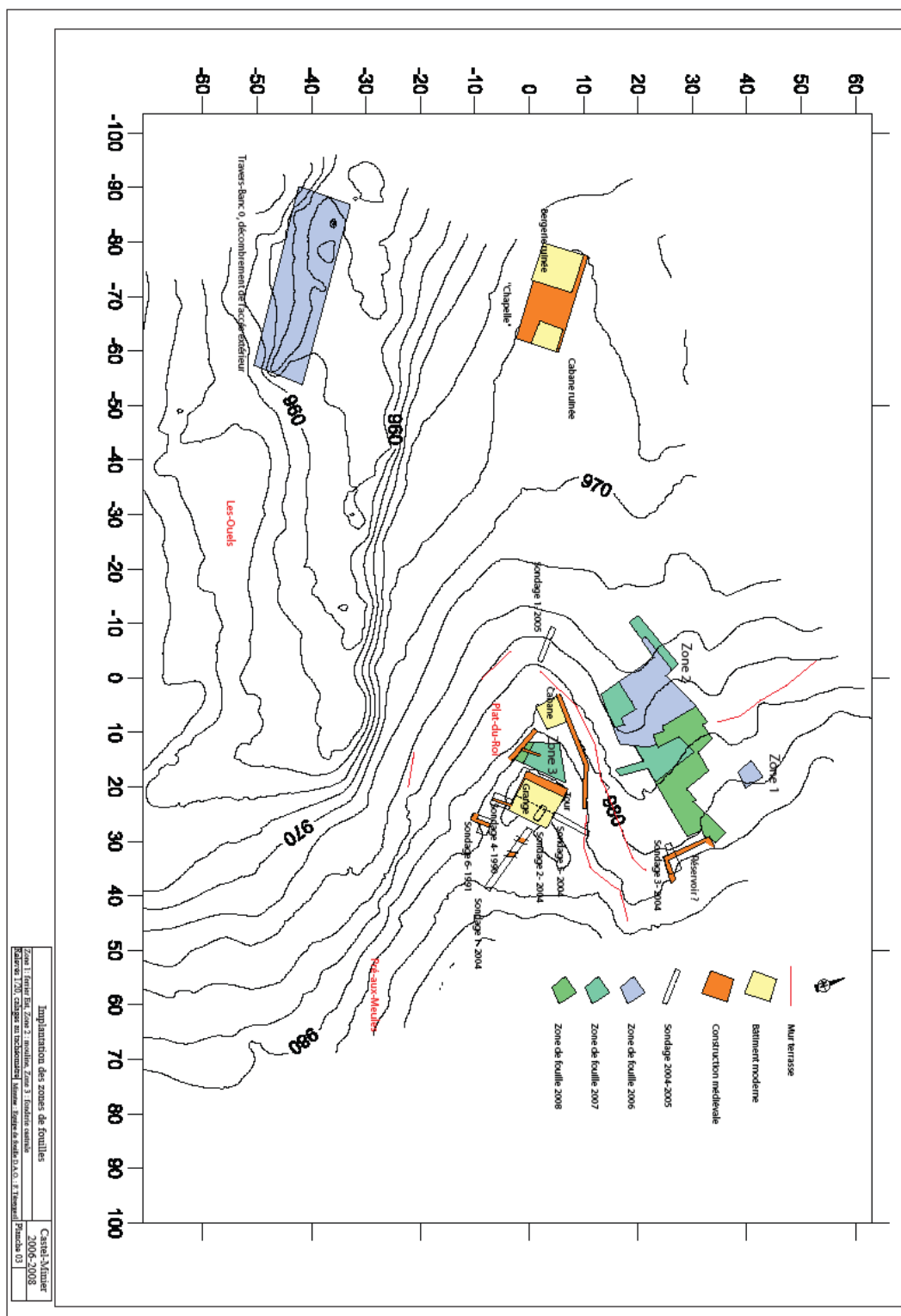
## **Annexes C**

### **PLANS DE FOUILLE ET LOCALISATION DES ZONES DE PRÉLÈVEMENTS**





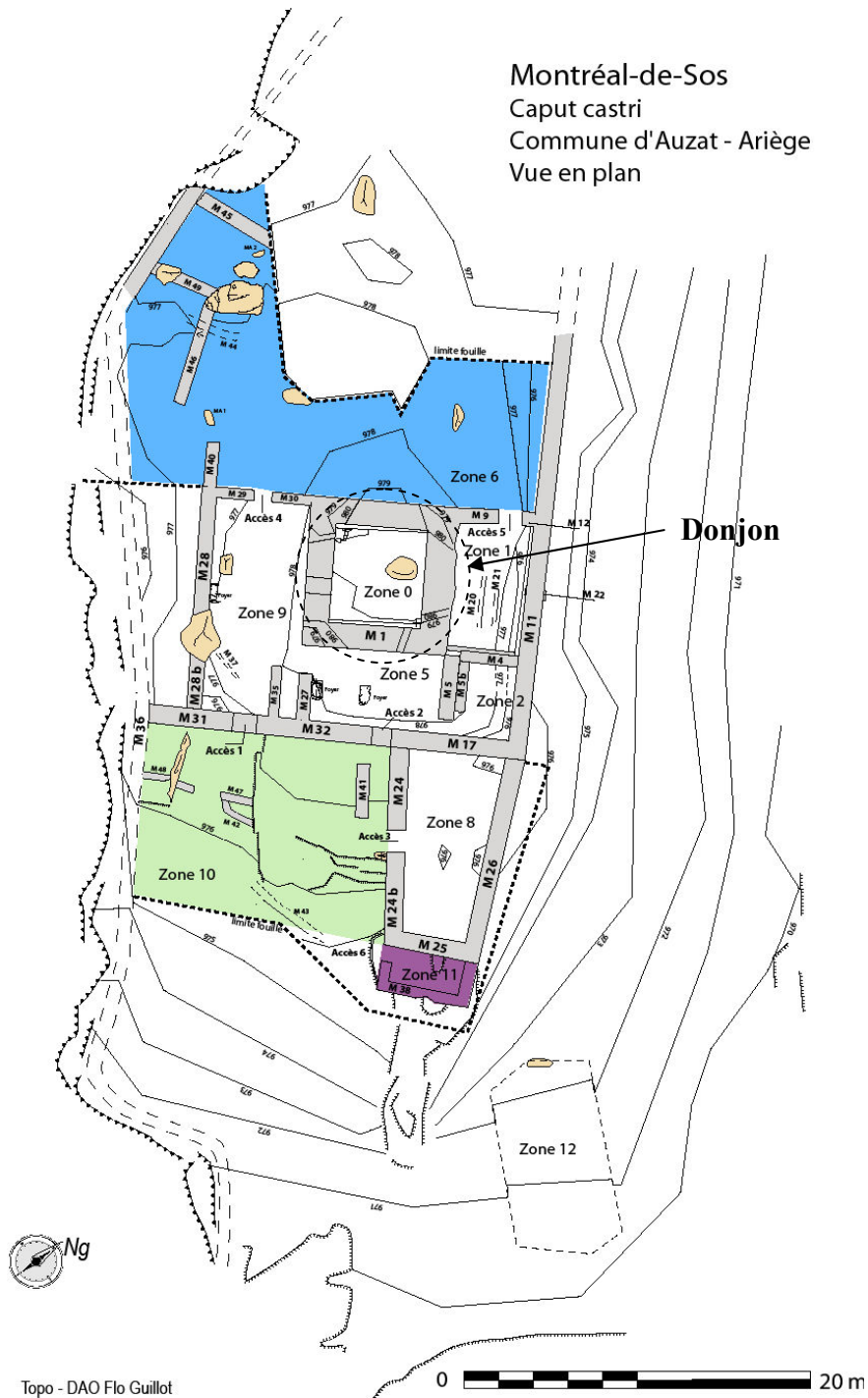
# Annexe C.1 - PLAN DE FOUILLE DU SITE DE CASTEL-MINIER. PRÉLÈVEMENT DES OBJETS FERREUX

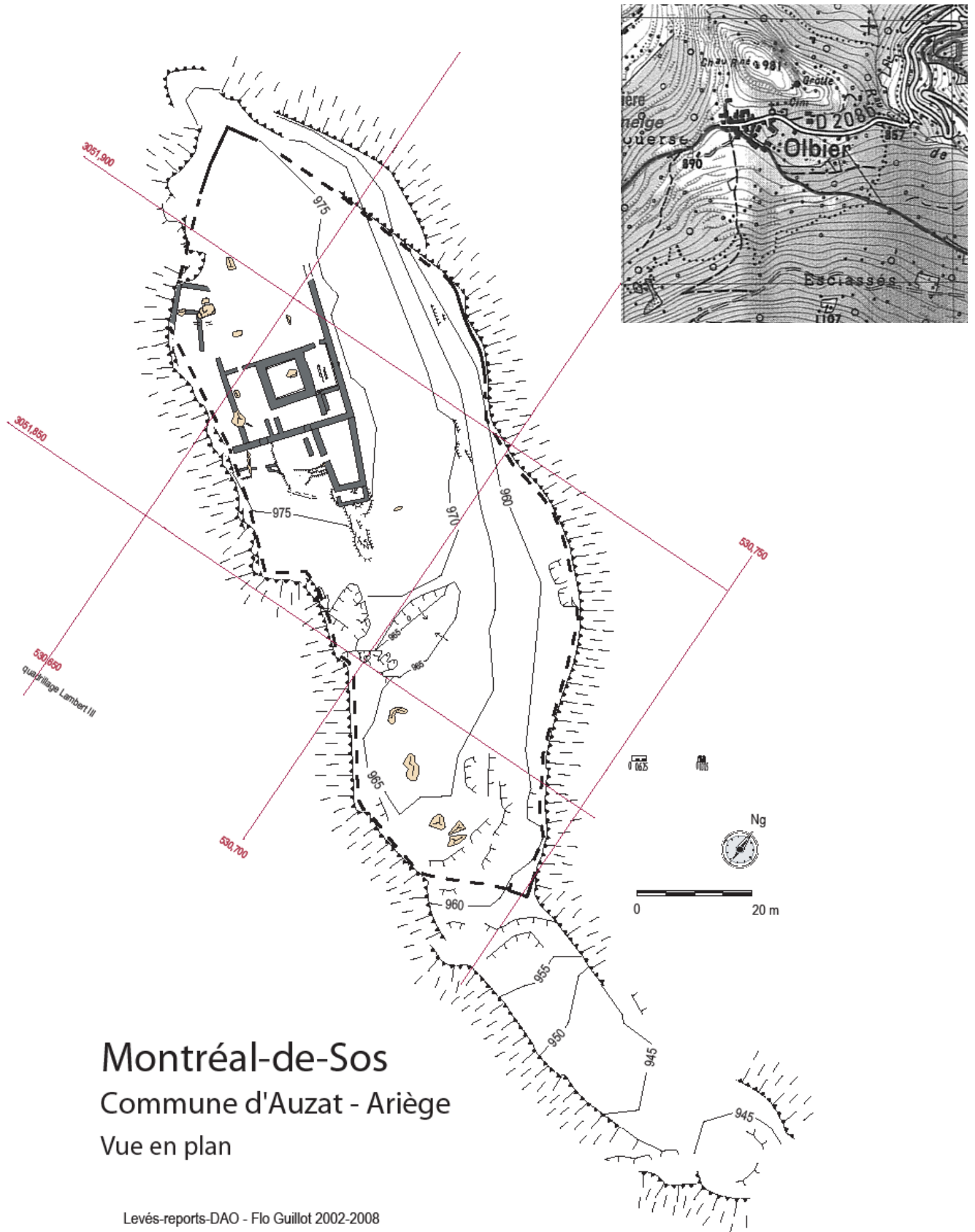




### Annexe C.3 - PLAN DE FOUILLE DU SITE DE MONTRÉAL-DE-SOS. PRÉLÈVEMENTS DES OBJETS FERREUX ET DESCRIPTION DES ZONES DE PRÉLÈVEMENTS (D'APRÈS GUILLOT, 2008)

Le mobilier ferreux étudié a été mis au jour à différents endroits du site : en zone 6 (face nord-ouest du donjon), en zone 10-11 pour le fer d'équidé (face sud-ouest du donjon) et au niveau du donjon (nord-est et coin-est) pour les couteaux (figure ci-dessous).





# Montréal-de-Sos

## Commune d'Auzat - Ariège

### Vue en plan

Levés-reports-DAO - Flo Guillot 2002-2008

DESCRIPTION DES ZONES DU DONJON DU SITE DE MONTRÉAL-DE-SOS**◆ Zones du donjon :**

**Zone 0** : centre du donjon, non fouillé en 2006 ; sondage en 2001.

**Zone 1** : face nord-est externe du donjon. Fouillée en 2005 + opérations 2003 et 2004. Cet espace est limité entre plusieurs murs (du donjon M1, de l'enceinte interne M11bis doublant M11, de l'accès à la plate-forme nord-est (=zone 1), M9 et M12, le mur 4)

**Zone 2** : coin est externe du donjon, fouillé en 2005 et en 2004/2003.

**Zone 5** : face sud-est externe du donjon. Fouillée en 2005 et en 2006.

**Zone 6** : face nord-ouest et coin ouest externes du donjon. Fouillée en partie en 2005. En 2006, seule l'U.S. de destruction a été fouillée sur cette face qui a fait l'objet de recherches en 2007. Cet espace est limité par les murs 9 et 12 qui limitent la zone 6 de la zone 1, le mur 11 (enceinte interne), le mur 1 du donjon -son coin ouest et sa face nord-ouest- (zone 6 à l'extérieur du donjon), une berme artificielle talutée et servant de limite à la fouille actuellement. La zone 6 devra donc être élargie et une limite artificielle avec les fouilles des sondages le long du mur d'enceinte qui ont eu lieu en 2002 et 2004.

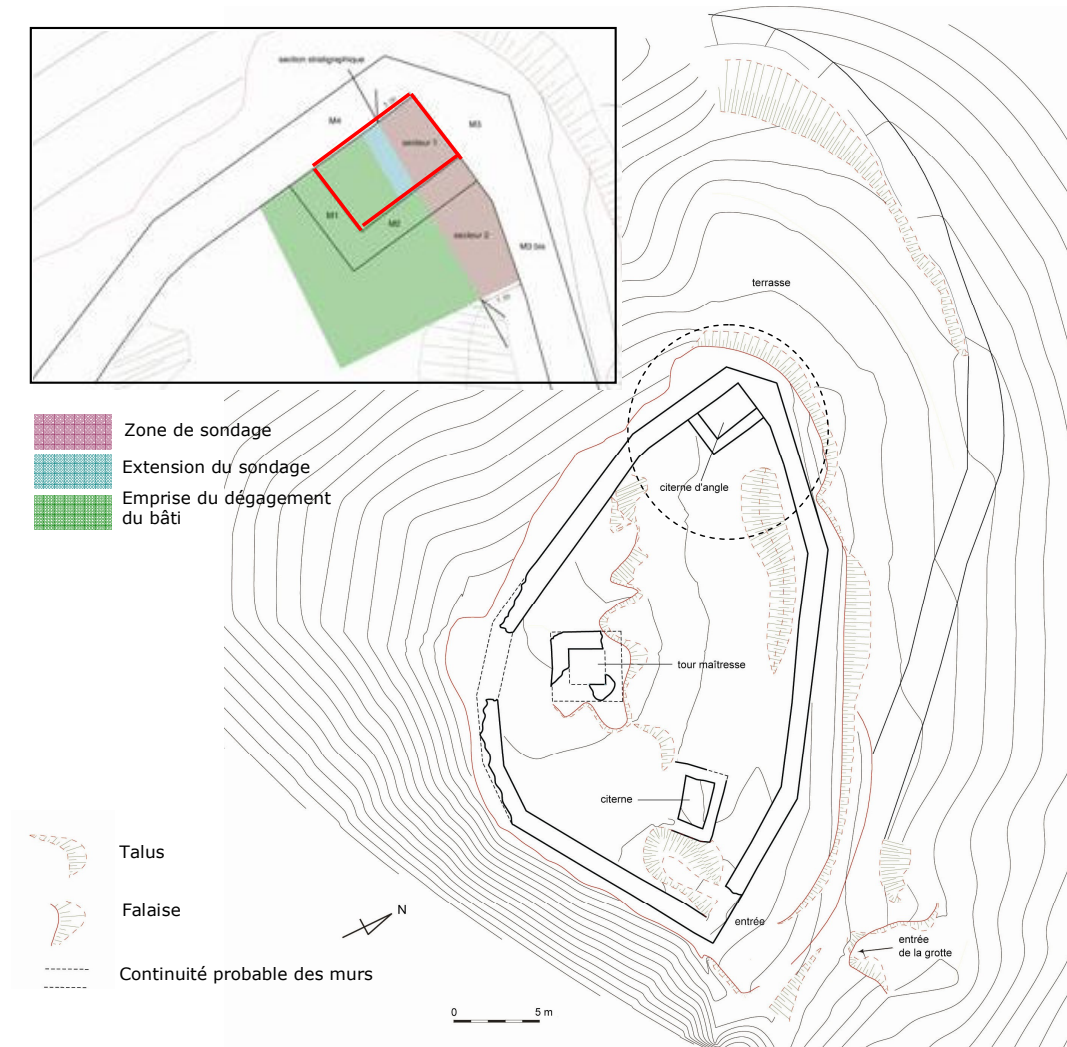
**Zone 3** : sondages le long du mur d'enceinte interne (M 11). Sondages réalisés en 2002 et 2004, regroupés car coalescents. Ils jonctionnent sur leur face sud-est avec la zone 6, qui forme donc le même groupe.

**Zone 8** : bâtiment sous-jacent au donjon, face sud-est. Cette zone est limitrophe des zones 5 et 2, donc limitée par les murs 17, 17 bis, puis 24, 25 et 26. Cet espace a été entièrement fouillé en 2006.

**Zone 9** : face sud-ouest du donjon.

**Zone 10** : secteur lié à l'accès des zones 8, 5 et 9. Non fouillé en 2006.

## Annexe C.4 - PLAN DE FOUILLE DU SITE DE MIRABAT. PRÉLÈVEMENTS DES OBJETS FERREUX ÉTUDIÉS DANS CE TRAVAIL



*Plan du site du château de Mirabat. Localisation des prélèvements des clous étudiés (citerne d'angle) (dessin T.Lasnier)*









## Annexe D

APPLICATION DE L'ANALYSE DISCRIMINANTE AUX DONNÉES DE L'ARIÈGE ET À CELLES D'ÉCHANTILLONS D'ORIGINE ARIÉGEOISE ET NON ARIÉGEOISE ; COMPARAISON DES DISTANCES MÉDIANE ET QUARTILE SUR L'AXE DISCRIMINANT LD1

Afin de mettre en évidence le fait que des échantillons d'origine ariégeoise ne se séparent pas aussi distinctement du corpus ariégeois que les échantillons d'une origine non ariégeoise, nous avons comparé en suivant la même approche que celle développée dans le Chapitre IV, le corpus ariégeois à des groupes de scories extraites de ce corpus mais aussi à des scories et des minerais non originaires de l'Ariège (lombards et dauphinois) (Tableau D.1). Ces groupes ont été formés de manière aléatoire. Les résultats des projections de l'analyse discriminante sont présentés dans la Figure D.2 pour les groupes de scories ariégeoises (Groupe n°1, 2, 3 -scories ariégeoises-) et la Figure D.3 pour les groupes d'échantillons non ariégeois (Groupe n°1, 2, 3 -scories et minerais lombards- ; et Groupe n°1-scories et minerais dauphinois-). Les valeurs des distances médiane et quartile sont consignées dans le Tableau D.2.

**Tableau D.1 – Composition des groupes de scories et minerais issus de l'Ariège, la Lombardie et le Dauphiné**

Scories ariégeoises			Scories et minerais lombards			Scories et minerais dauphinois
Groupe n°1	Groupe n°2	Groupe n°3	Groupe n°1	Groupe n°2	Groupe n°3	Groupe n°1
CM06-2002/1	CM06-2014/1	CM06-2018/1	SCH08/1	SCH07/1	SCH min Hab/M1	PEL 87 006
CM06-1004/1	CM06-2002/2	CM07-2099/1	SCH08/2	SCH03/1	SCH MINES /M2	PEL 87 007
SCCM2	CM06-2018/2	CM07-2088/1	SCH04/1	SCH02/1		PEL 87 008
CM06-1004/2	CM06-2020/2	CM07-2026/1	SCH01/1	SCH02/2	GAF1/1	PEL 87 001
CM06-2020/1	CM06-1004/3	CM06-2004/1	SCH06/1	SCH03/2	GAF1	PEL 87 002
			SCH06/2	SCH05/1	GAF1	PEL 87 003
				TIZ 002	ST1/M1	PEL 87 006
				TIZ 003	ST1/M1	PEL 87 007
				TIZ 004	ST4/M1	PEL 87 008
				TIZ 005	ST4/M1	PEL 87 001
				TIZ 006		
				TIZ 007		

La lecture des résultats confirme que les distances (médiane et quartile) obtenues pour les scories de l'espace ariégeois sont, systématiquement, significativement plus faibles que pour des minerais et scories d'autre provenance.

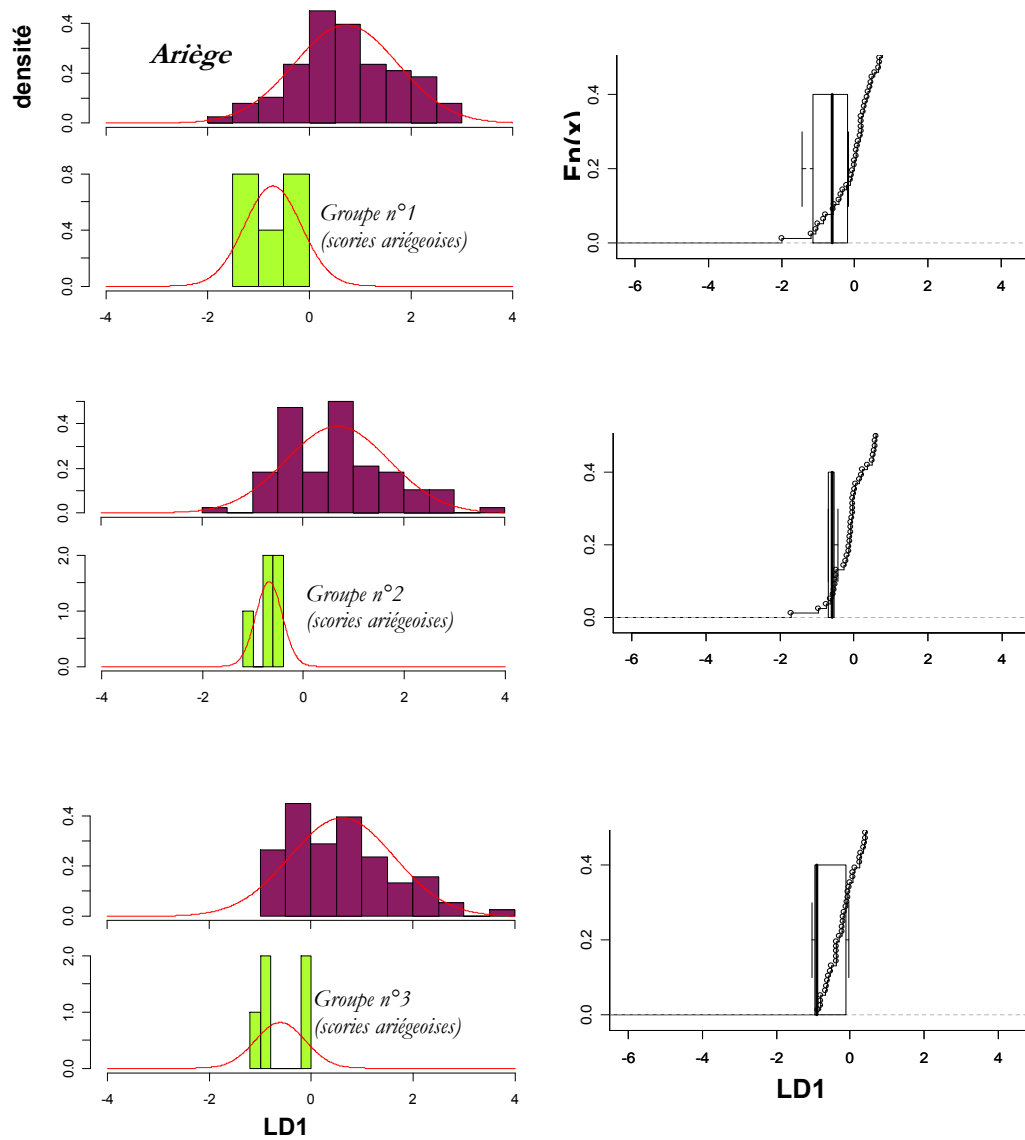


**Figure D.2 – Analyse discriminante linéaire appliquée aux données des groupes de scories ariégeoises et à celles du corpus définissant l'Ariège. Projections du premier axe discriminant  $LD_1$**

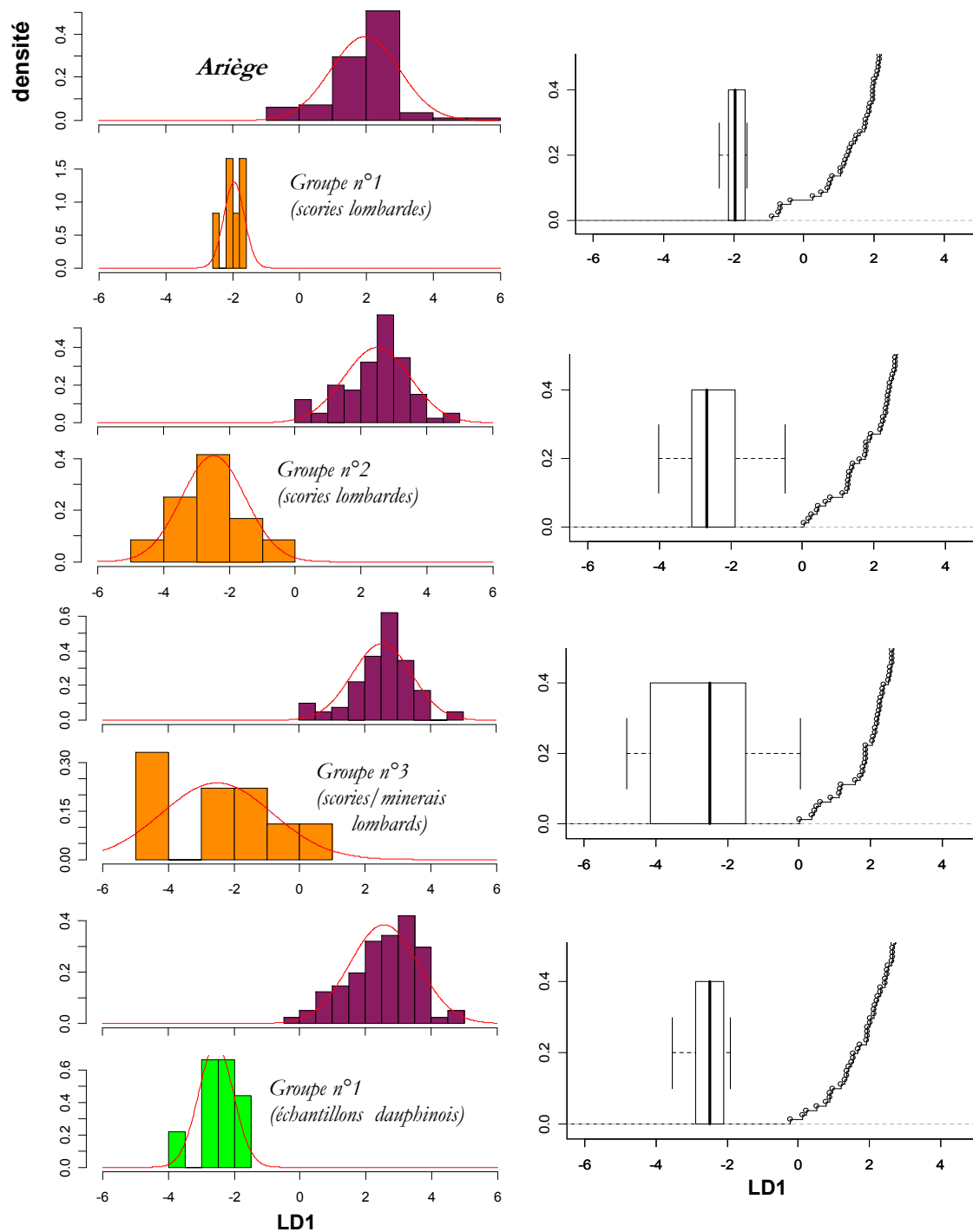


**Figure D.3** – Analyse discriminante linéaire appliquée aux données des groupes de minerais et scories non ariégeois (lombards et dauphinois) et à celles du corpus définissant l'Ariège. Projections du premier axe discriminant LD<sub>1</sub>

**Tableau D.2 – Distance de la médiane et du 3<sup>ème</sup> quartile des projections des différents groupes de scories et minerais au domaine des Proj. $X_{ES,Ariège}$  (sur l'axe le plus discriminant)**

<b>Groupes de scories extraites du corpus ariégeois</b>	<b>Groupe n°1</b>	<b>Groupe n°2</b>	<b>Groupe n°3</b>	
<b><math>D_{méd.}</math></b>	<b>-1,36</b>	<b>-1,08</b>	<b>0,03</b>	
<b><math>D_{quart.}</math></b>	<b>-1,79</b>	<b>-1,14</b>	<b>-0,76</b>	

<b>Groupes de minerais et scories extraits des corpus lombard et dauphinois</b>	<b>Groupe n°1 (Lombardie)</b>	<b>Groupe n°2 (Lombardie)</b>	<b>Groupe n°3 (Lombardie)</b>	<b>Groupe n°1 (Dauphiné)</b>
<b><math>D_{méd.}</math></b>	<b>1,03</b>	<b>2,70</b>	<b>2,49</b>	<b>2,26</b>
<b><math>D_{quart.}</math></b>	<b>0,79</b>	<b>1,97</b>	<b>1,48</b>	<b>1,87</b>

$D_{méd.}$ : distance de la médiane des projections du groupe de scories et minerais au domaine des Proj. $X_{ES,Ariège}$ .

$D_{quart.}$ : distance du troisième quartile des projections du groupe de scories et minerais au domaine des Proj. $X_{ES,Ariège}$ .

## Annexe E

APPLICATION DE L'ANALYSE DISCRIMINANTE AUX DONNÉES DE L'ANDORRE ;  
COMPATIBILITÉ DE LA SIGNATURE CHIMIQUE AVEC L'ESPACE SIDÉRURGIQUE ANDORRAN

L'analyse discriminante a été appliquée sur une classe sidérurgique définie par un nombre d'échantillons nettement moins élevé que ceux définissant l'Ariège et la Lombardie : la classe associée aux données de l'Andorre. Cet espace sidérurgique est caractérisé par vingt et un échantillons, soit quatre minerais, douze scories et cinq produits des forges Farga Areny et Farga Rossell. Les résultats de l'analyse sont présentés dans la figure suivante.

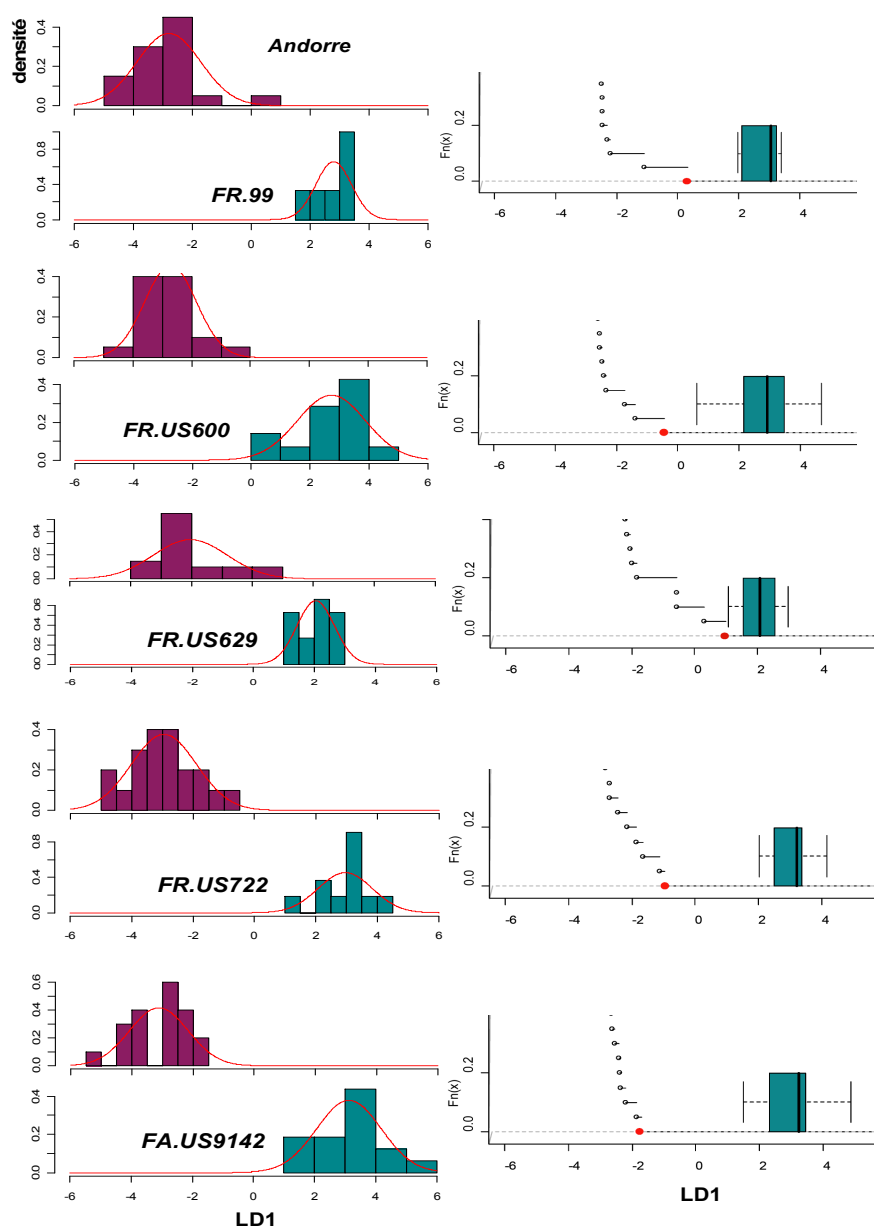


Figure E.4 – Analyse discriminante linéaire appliquée aux  $X_{ij}$  de l'Andorre et aux cinq produits d'origine andorrane. Projections du premier axe discriminant  $LD_1$

Dans une première approche, les projections sur l'axe LD1 montrent que toutes les valeurs des Proj. $X_{OI}$  sont exclues du domaine des Proj. $X_{ES.Andorre}$ . Aucune de ces valeurs ne se situent à proximité du domaine de l'espace sidérurgique, excepté pour l'échantillon FR.US629. Les valeurs des distances du premier quartile et de la médiane obtenues sont décrites dans le Tableau E.3. La distance quartile maximale est de 3,18 et la valeur maximale de la médiane est de 4,12.

**Tableau E.3 – Distance de la médiane et du 3<sup>ème</sup> quartile des Proj. $X_{OI}$  au domaine des Proj. $X_{ES.Andorre}$  sur l'axe le plus discriminant pour des objets d'origine andorrane**

échantillons	FR.99	FR.US600	FR.US629	FR.US722	FA.US9142
$\mathcal{D}_{méd.}$	1,99	2,66	0,55	3,45	4,12
$\mathcal{D}_{quart.}$	1,62	1,05	0,08	2,07	3,18

$\mathcal{D}_{méd.}$  : distance de la médiane des Proj. $X_{OI}$  au domaine des Proj. $X_{ES.Andorre}$ .

$\mathcal{D}_{quart.}$  : distance du troisième quartile des Proj. $X_{OI}$  au domaine des Proj. $X_{ES.Andorre}$ .

Si l'on compare ces valeurs à celles obtenues pour des objets qui ne sont pas d'origine andorrane, on constate une nette différence. Les objets considérés sont deux objets provenant d'Ariège (i10013 et 2008-1), l'objet de Mimet et la loupe lorraine. Les projections de l'axe LD1 des  $X_{ij}$  associés à cette analyse et les valeurs des distances sont présentées *infra* :

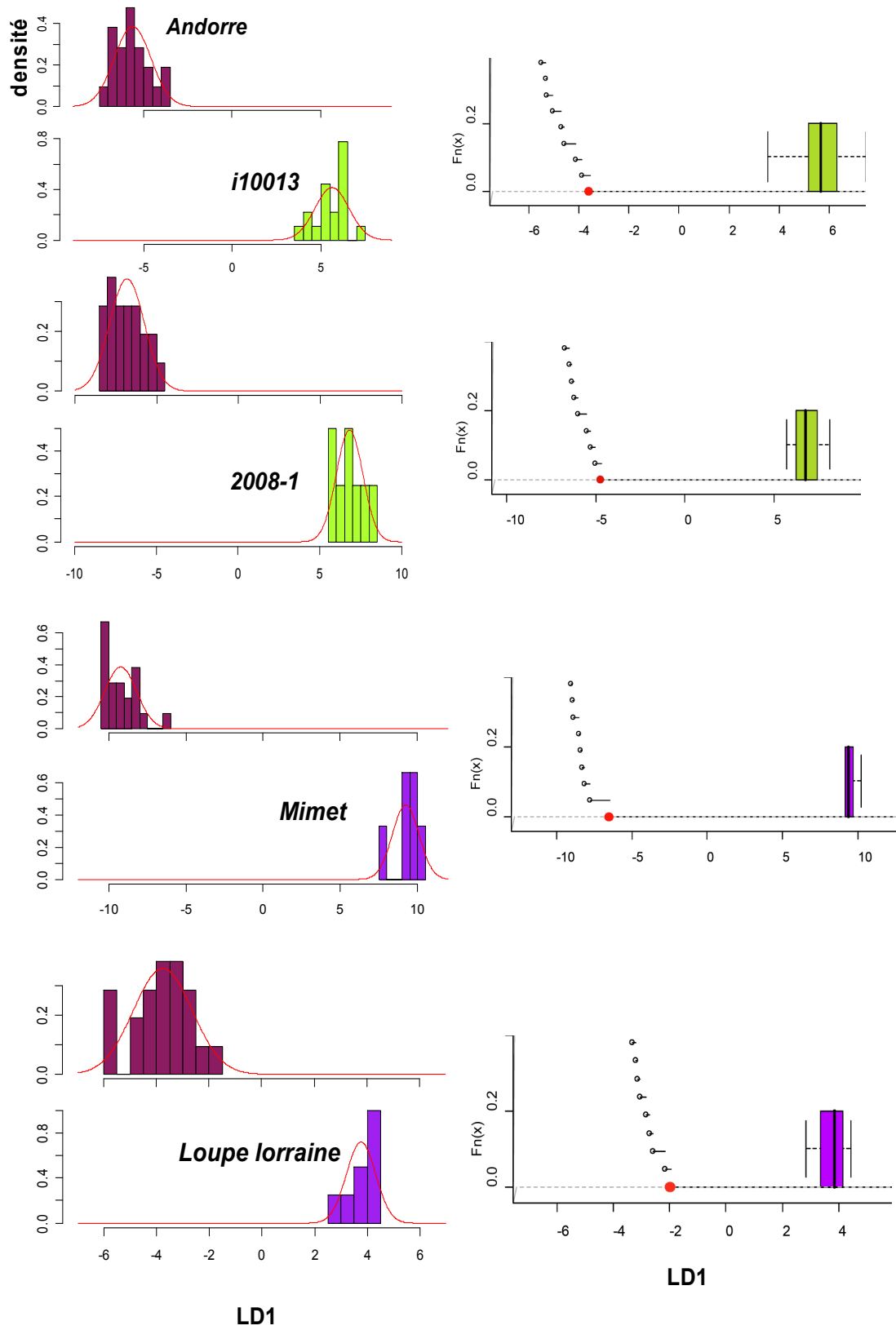


Figure E.5 – Analyse discriminante linéaire appliquée aux  $X_{ij}$  de l'Andorre et aux produits d'origine non andorrane. Projections du premier axe discriminant  $LD_1$

**Tableau E.4 – Distance de la médiane et du 1<sup>er</sup> quartile des Proj.X<sub>OI</sub> au domaine des Proj.X<sub>ES.Andorre</sub> sur l'axe le plus discriminant pour des objets d'origine non andorrane**

échantillons	i10013	2008-1	Mimet	Loupelorraine
$\mathcal{D}_{méd.}$	9,22	11,40	15,81	5,80
$\mathcal{D}_{quart.}$	8,76	10,96	15,60	5,43

$\mathcal{D}_{méd.}$  : distance de la médiane des Proj.X<sub>OI</sub> au domaine des Proj.X<sub>ES.Andorre</sub>.

$\mathcal{D}_{quart.}$  : distance du premier quartile des Proj.X<sub>OI</sub> au domaine des Proj.X<sub>ES.Andorre</sub>.

Ces valeurs sont très élevées en comparaison de celles calculées jusqu'à présent pour les espaces sidérurgiques ariégeois et lombard. Ainsi, les distances minimales sont ici de 5,43 et 5,80 pour la distance médiane et quartile respectivement.

Lorsque celles-ci sont confrontées aux valeurs trouvées pour les objets d'origine andorrane, il est donc possible de séparer les deux domaines de compatibilité. Il en résulte que pour des valeurs inférieures à 3,18 et 4,12 pour  $\mathcal{D}_{quart.}$  et  $\mathcal{D}_{méd.}$ , l'objet d'origine inconnue peut provenir de la région. En revanche, si ces valeurs sont supérieures à 5,43 et 5,80, il est possible d'exclure une origine andorrane.



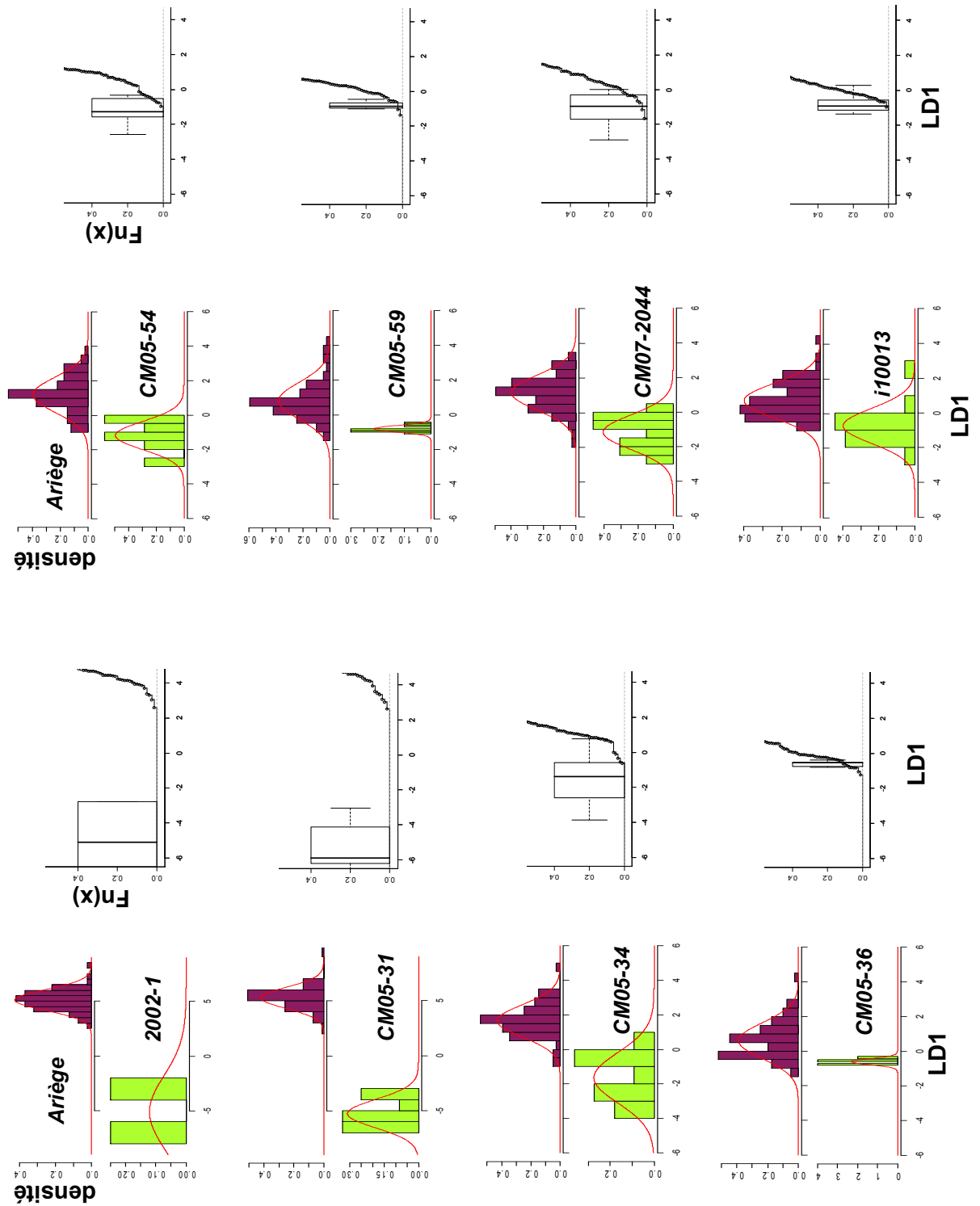
## **Annexes F**

DISTRIBUTION SUR L'AXE DISCRIMINANT LD1  
DES PROJECTIONS DES OBSERVATIONS ASSOCIEES AUX  
OBJETS D'ORIGINE INCONNUE ET AUX ECHANTILLONS  
DEFINISSANT L'ARIEGE OU LA LOMBARDIE

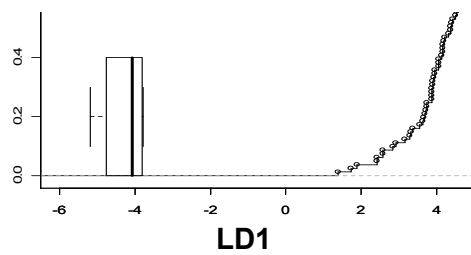
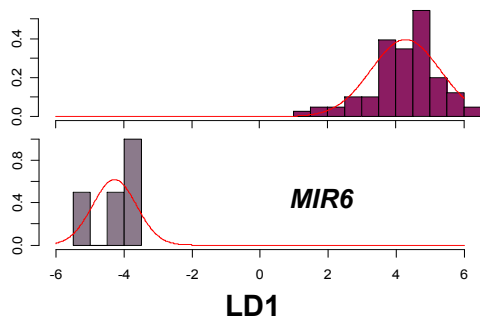
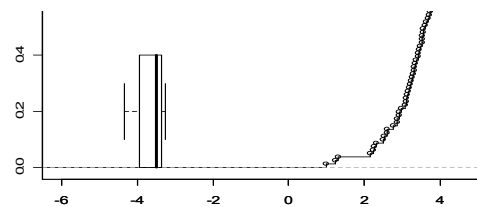
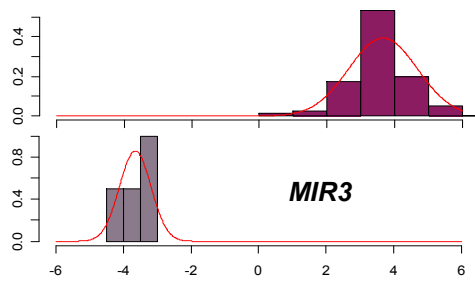
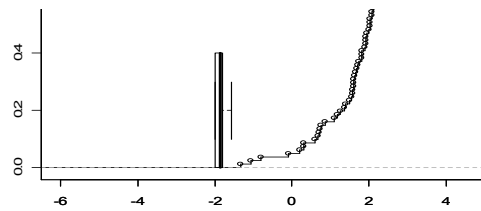
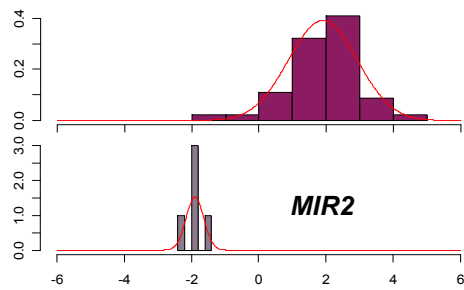
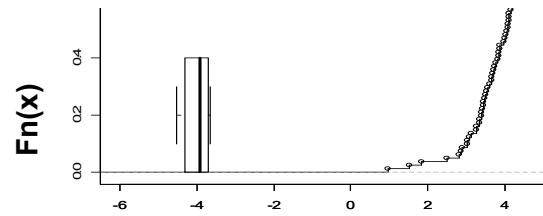
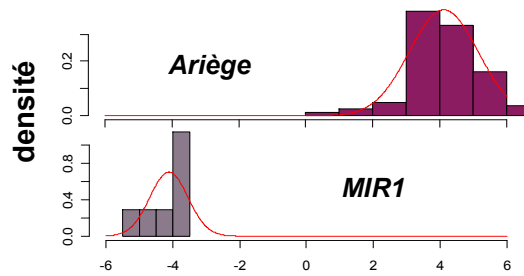


## Annexe F.1 -

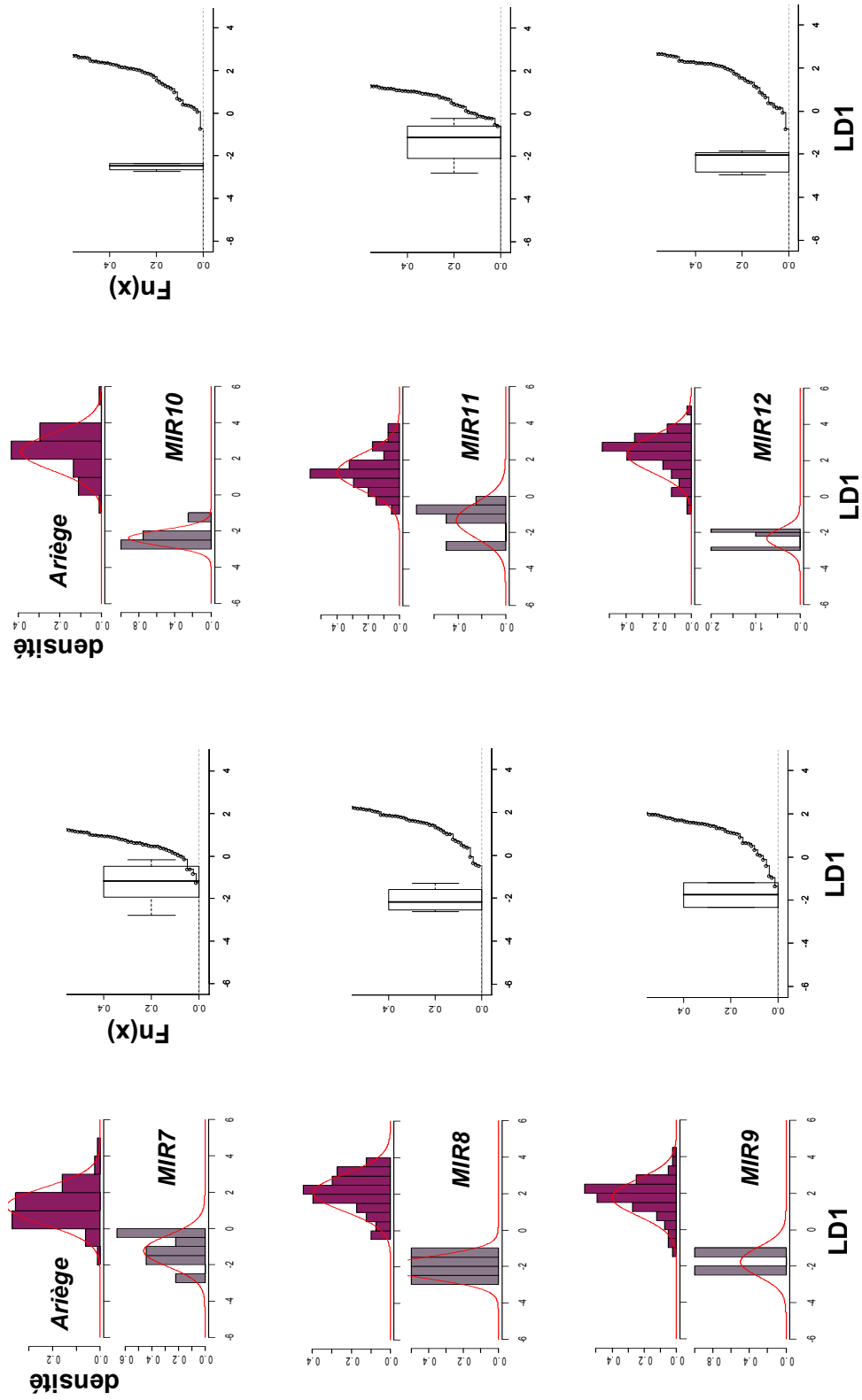
ANALYSE DISCRIMINANTE DES  $X_{ij}$  DES INCLUSIONS DES OBJETS D'ORIGINE INCONNUE MIS AU JOUR SUR LE SITE DE CASTELMINIER, ET DES ECHANTILLONS DEFINISSANT L'ARIEGE. PROJECTIONS SUR L'AXE DISCRIMINANT LD1



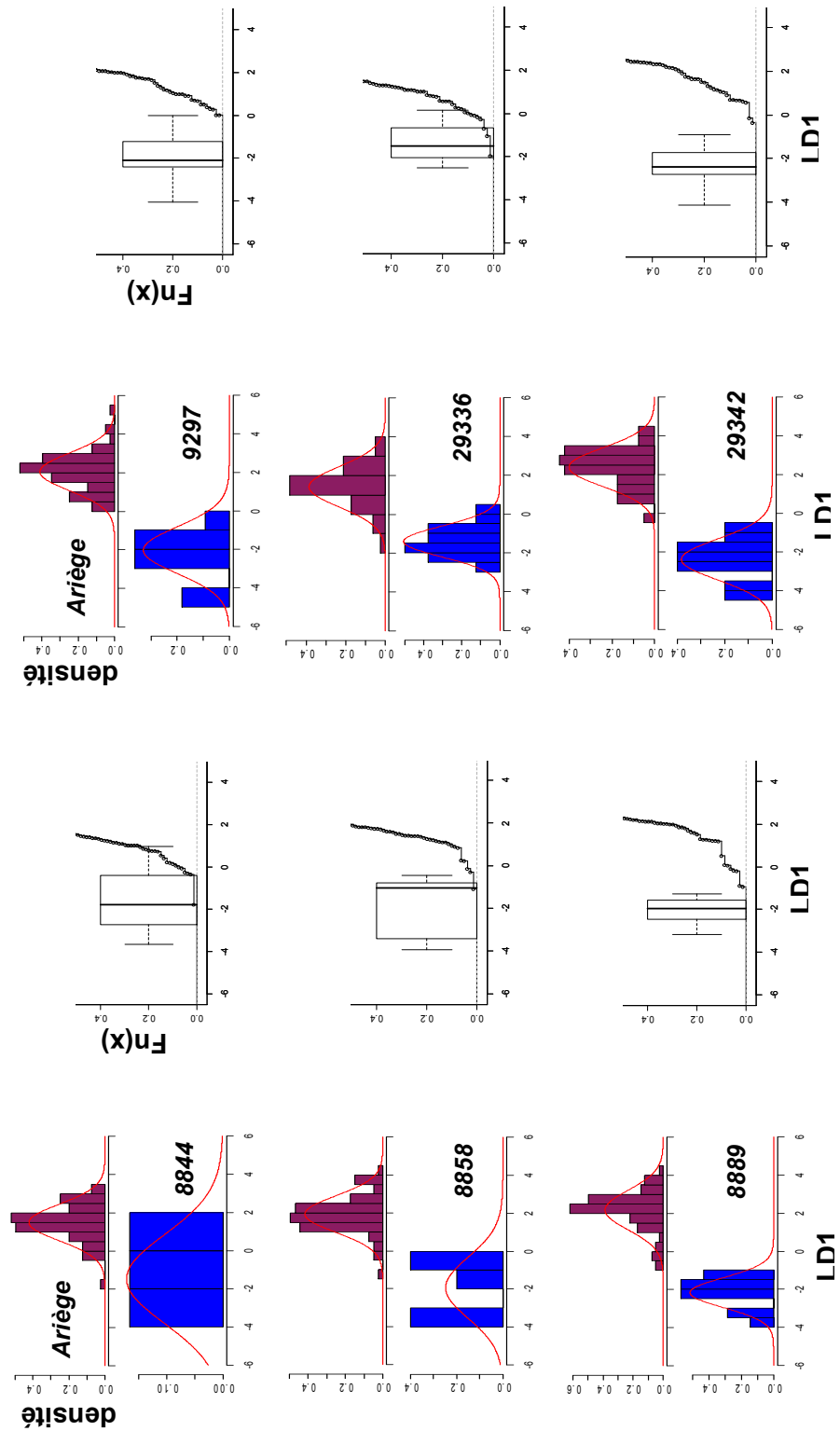
## Annexe F.2 - ANALYSE DISCRIMINANTE DES $X_{ij}$ DES INCLUSIONS DES CLOUS MIS AU JOUR SUR LE SITE DE MIRABAT ET DES ECHANTILLONS DEFINISSANT L'ARIEGE. PROJECTIONS SUR L'AXE DISCRIMINANT LD1



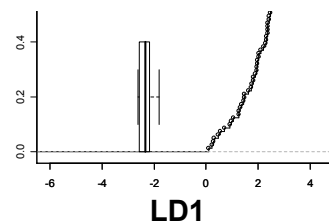
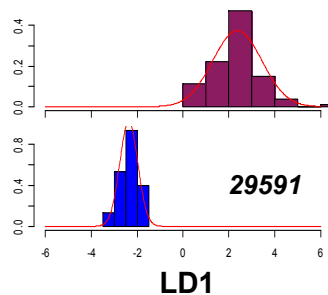
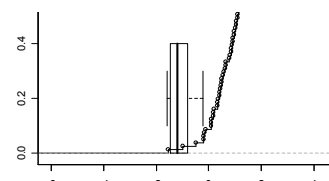
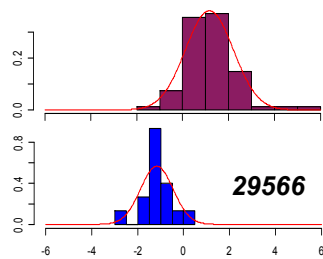
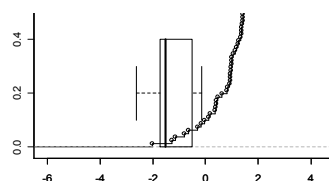
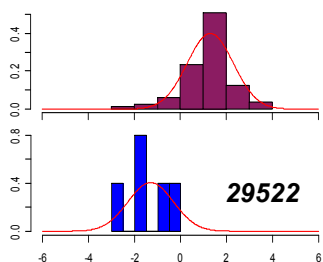
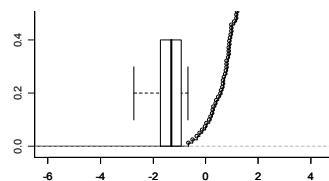
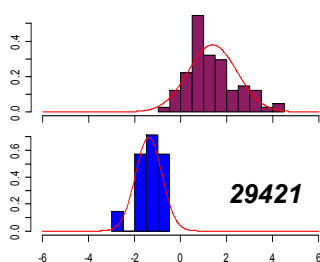
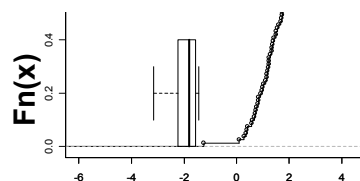
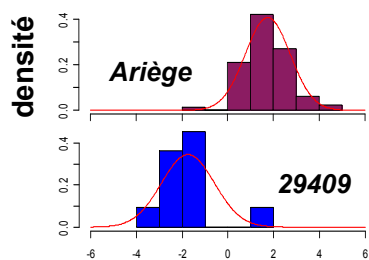
## Annexe F.2 - (suite)



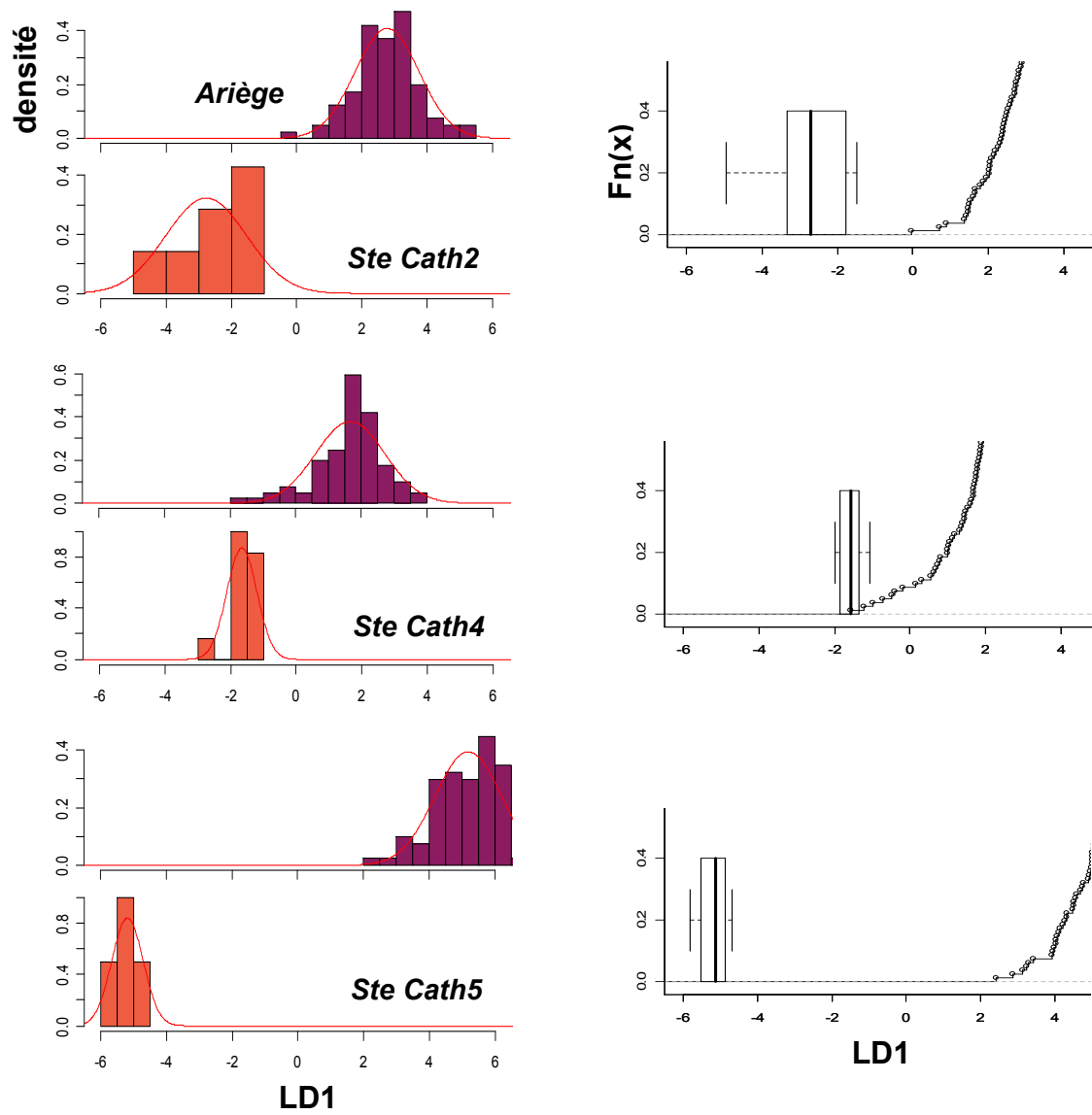
### Annexe F.3 - ANALYSE DISCRIMINANTE DES $X_{ij}$ DES INCLUSIONS DES OBJETS MIS AU JOUR SUR LE SITE DE MONTRÉAL-DE-SOS ET DES ÉCHANTILLONS DEFINISSANT L'ARIÈGE. PROJECTIONS SUR L'AXE DISCRIMINANT LD1



## Annexe F.3 - (suite)

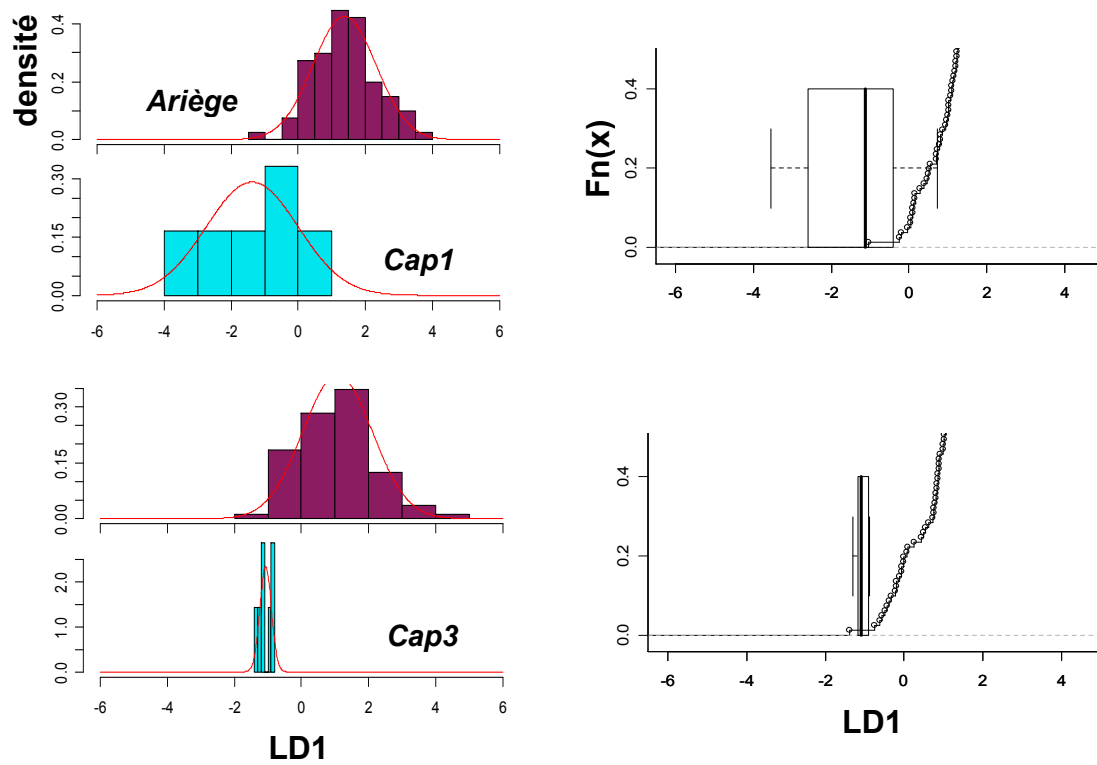


## Annexe F.4 -ANALYSE DISCRIMINANTE DES $X_j$ DES INCLUSIONS DES CLOUS MIS AU JOUR SUR LE SITE DE SAINTE-CATHERINE ET DES ECHANTILLONS DEFINISSANT L'ARIEGE. PROJECTIONS SUR L'AXE DISCRIMINANT LD1

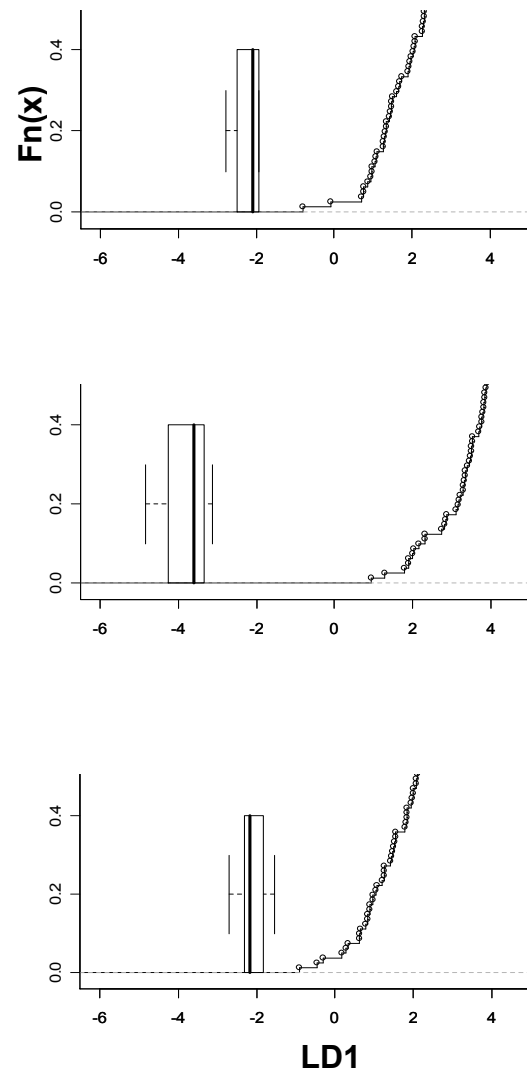
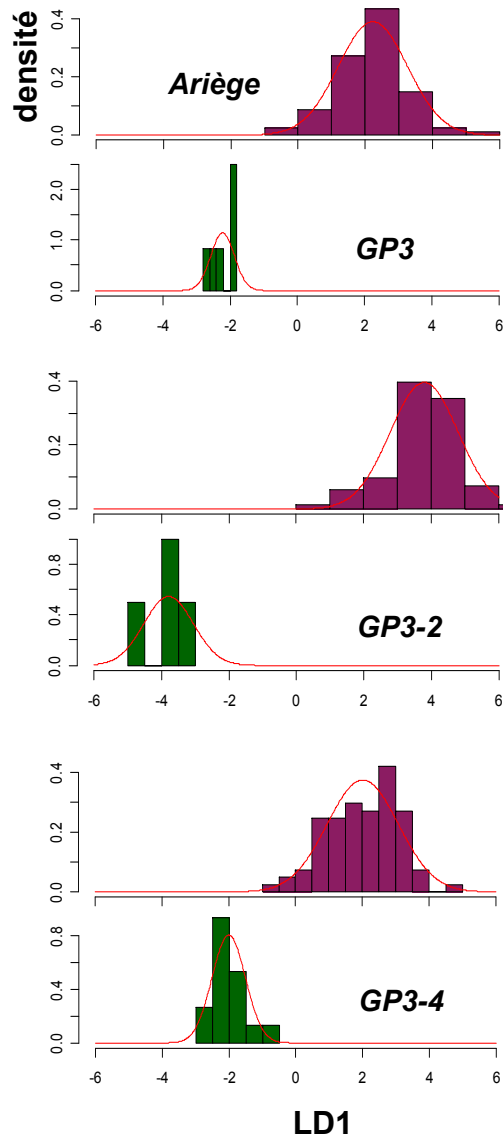




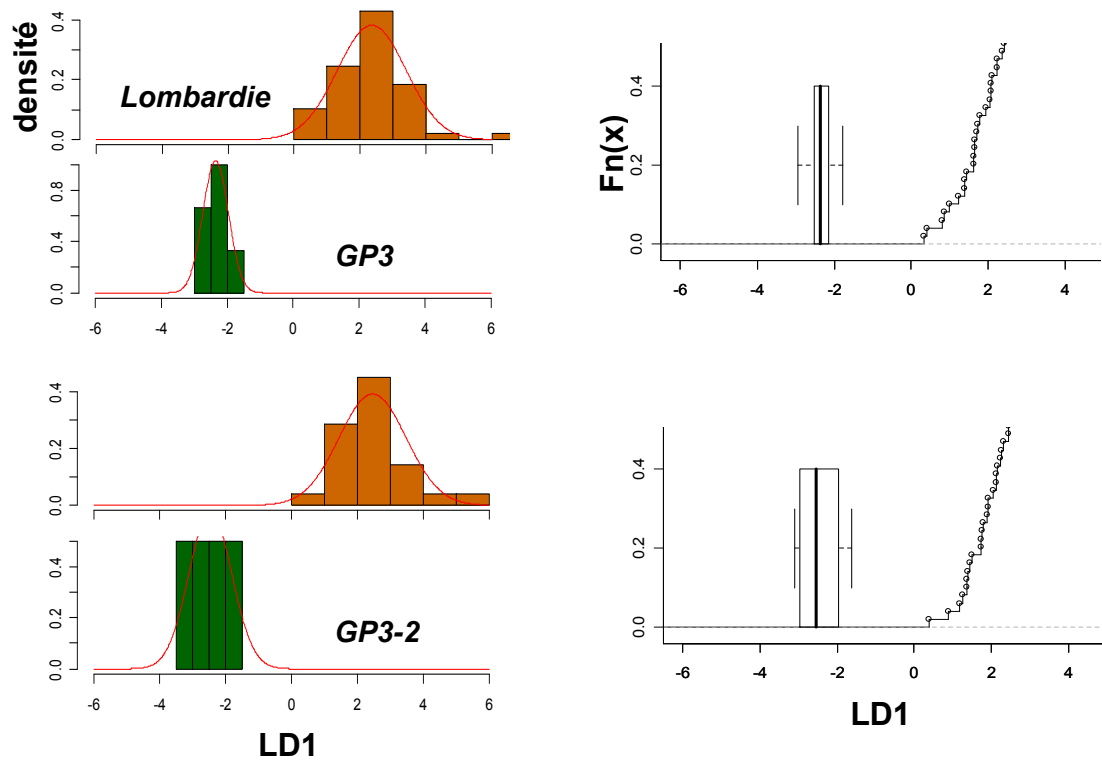
## Annexe F.5 - ANALYSE DISCRIMINANTE DES $X_{ij}$ DES INCLUSIONS DE CAP<sub>1</sub> ET CAP<sub>3</sub> ET DES ÉCHANTILLONS DEFINISSANT L'ARIÈGE. PROJECTIONS SUR L'AXE DISCRIMINANT LD1



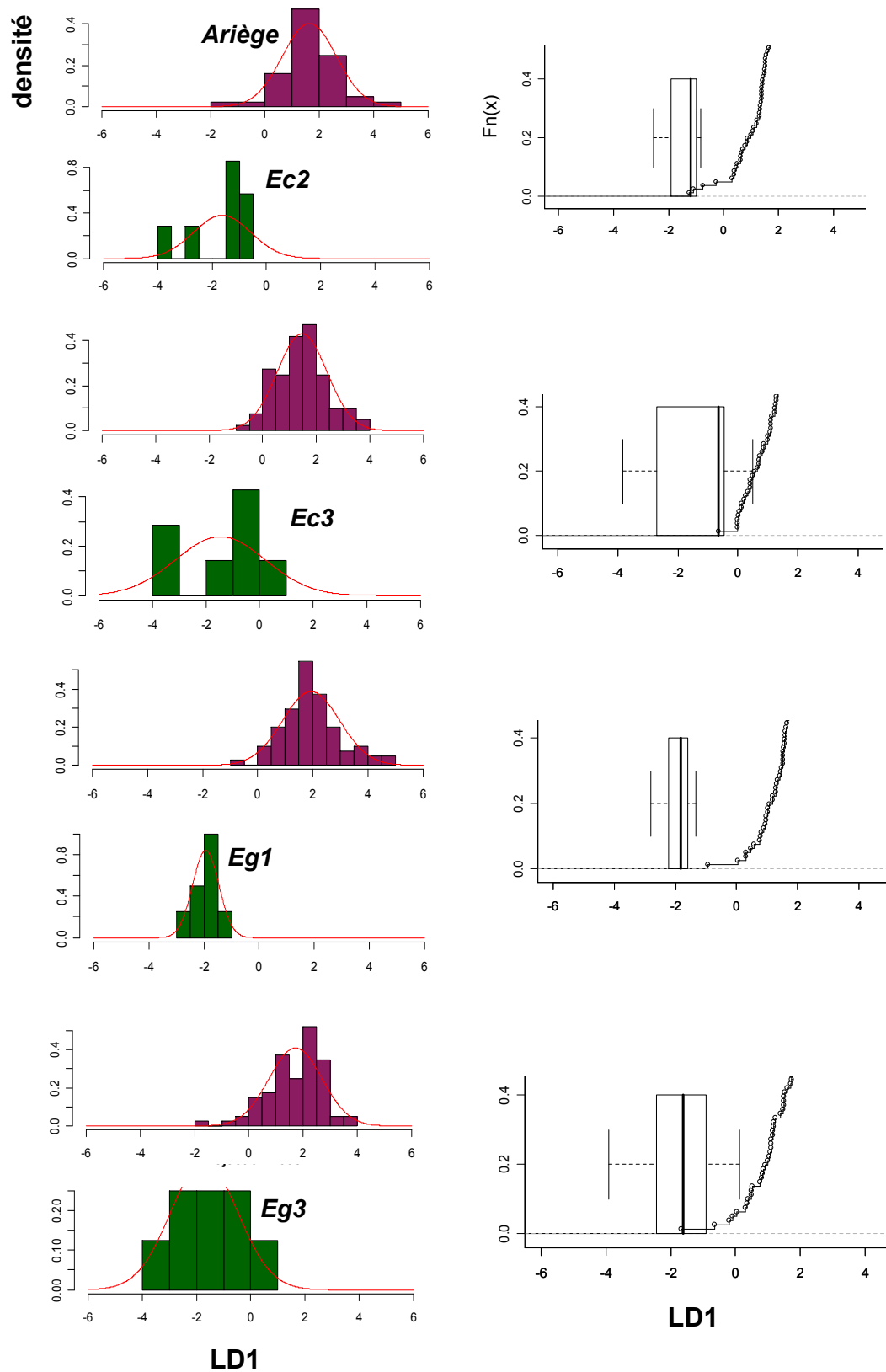
## Annexe F.6 - ANALYSE DISCRIMINANTE DES $X_{ij}$ DES INCLUSIONS DES TIRANTS DU GRAND PROMENOIR ET DES ÉCHANTILLONS DÉFINISSANT L'ARIÈGE. PROJECTIONS SUR L'AXE DISCRIMINANT LD1



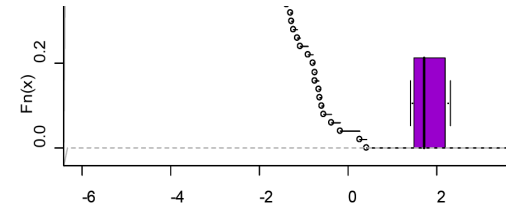
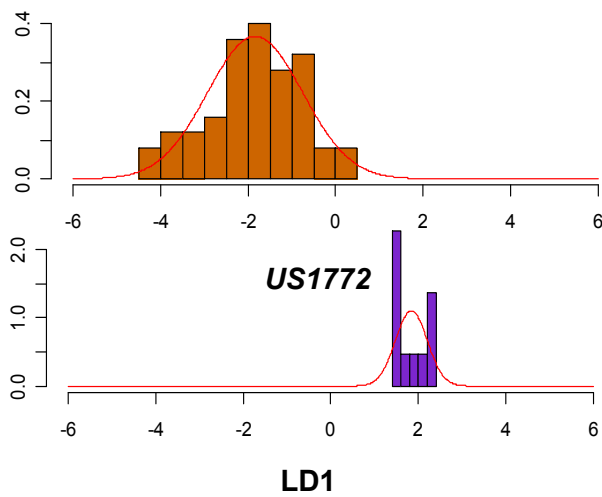
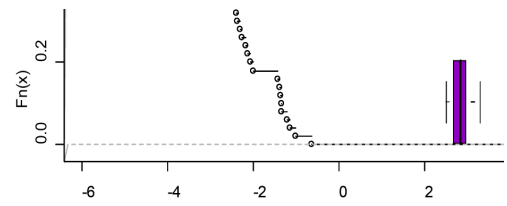
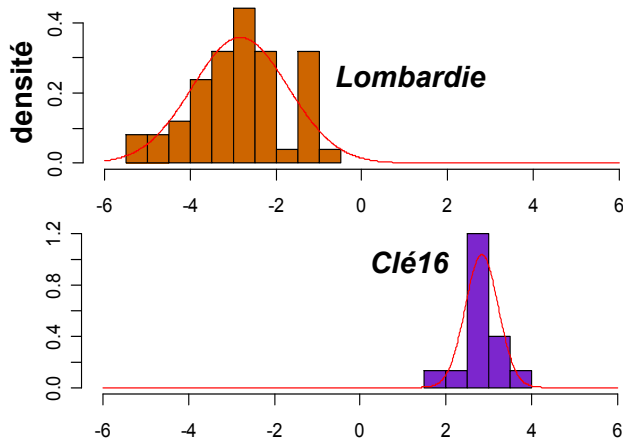
**Annexe F.7** - ANALYSE DISCRIMINANTE DES  $X_{ij}$  DES INCLUSIONS DES TIRANTS DU GRAND PROMENOIR (GP3 ET GP3.2) ET DES ÉCHANTILLONS DEFINISSANT LA LOMBARDIE. PROJECTIONS SUR L'AXE DISCRIMINANT LD1



## Annexe F.8 - ANALYSE DISCRIMINANTE DES $X_{ij}$ DES INCLUSIONS DES AGRAFES DE LA TOUR DES LATRINES (EC2, EC3, EG1, EG3) ET DES ÉCHANTILLONS DEFINISSANT L'ARIÈGE. PROJECTIONS SUR L'AXE DISCRIMINANT LD1

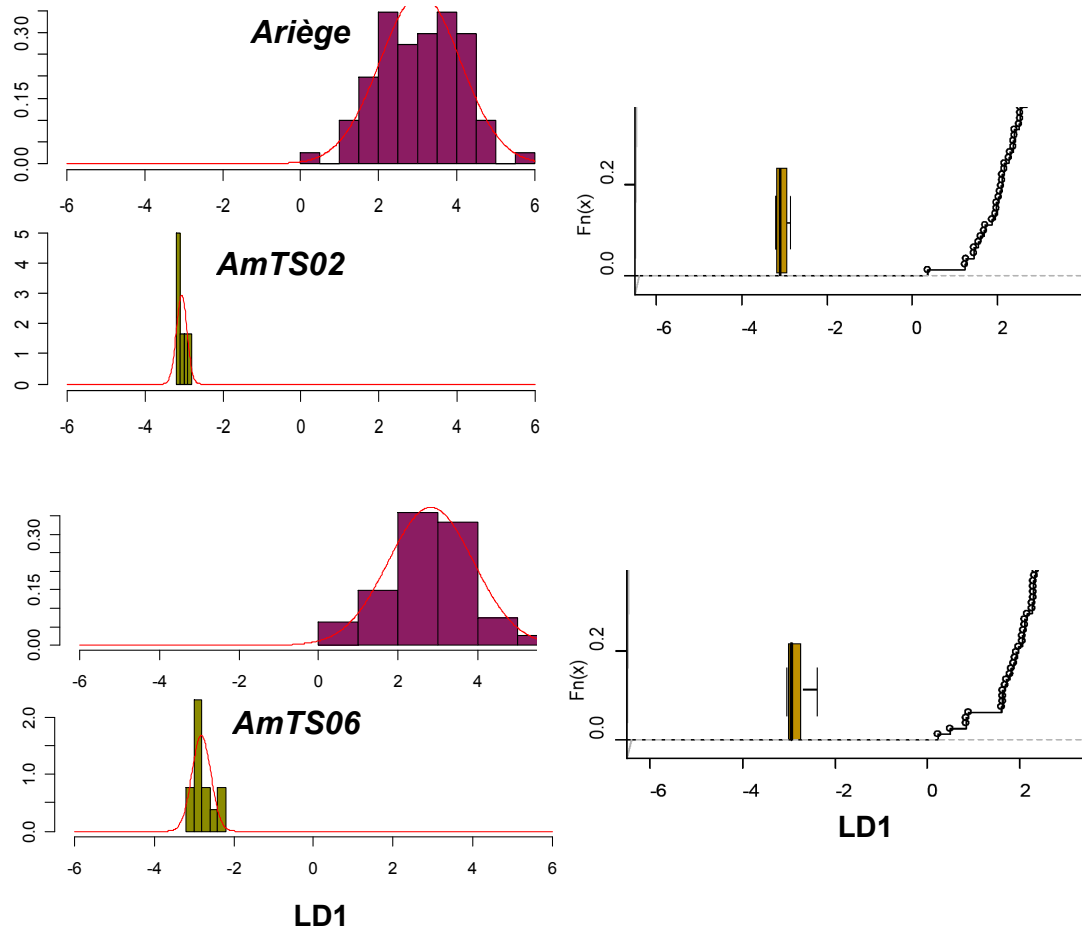


## Annexe F.9 - ANALYSE DISCRIMINANTE DES $X_{ij}$ DES INCLUSIONS DE CLÉ16 ET US1772, ET DES ÉCHANTILLONS DÉFINISSANT LA LOMBARDIE. PROJECTIONS SUR L'AXE DISCRIMINANT LD1



LD1

## Annexe F.10 - ANALYSE DISCRIMINANTE DES $X_{ij}$ DES INCLUSIONS DES FERS DE CONSTRUCTION DE LA CATHEDRALE D'AMIENS ET DES ÉCHANTILLONS DEFINISSANT L'ARIEGE. PROJECTIONS SUR L'AXE DISCRIMINANT LD1



## **Annexe G**

RESULTATS DE L'ANALYSE DISCRIMINANTE DE DEUX  
CLASSES DE DONNEES. COEFFICIENTS DE LA FONCTION  
DISCRIMINANTE CANONIQUE ASSOCIEE A L'AXE LD1





Comparaison sur l'axe LD1 avec la signature définissant l'espace ariégeois

But de l'analyse	Nom échantillons	Localisation	Y	Nb	Cs	La	Ce	Nd	Sm	Yb	Hf	Th	U
<u>Caractérisation des valeurs seuils de <math>D_{méd}</math> et <math>D_{quart}</math> échantillons d'origine ariégeoise</u>	CM06-2002-2	Castel-Minier	1,54	0,13	-0,39	-2,38	-0,21	0,02	-0,88	-2,81	0,88	-0,28	-0,84
	CM06-2003-2	Castel-Minier	-0,36	-0,13	-0,57	-2,78	-0,65	-0,01	-4,01	-1,21	0,76	-0,01	-0,75
	CM06-2004-3	Castel-Minier	-1,99	0,22	-0,87	-1,20	-3,13	0,15	-0,32	-0,91	-0,34	1,05	-0,43
	CM06-2004-1	Castel-Minier	0,11	0,67	0,29	2,77	-0,43	-0,02	4,31	0,68	0,09	-1,13	0,14
	CM06-2008-1	Castel-Minier	-1,87	0,16	0,38	-1,55	-1,06	-0,35	4,05	-0,40	0,33	-0,80	-0,04
	CM05-02-4	Castel-Minier	-0,89	-0,06	0,44	-2,98	-0,55	-0,45	0,95	-0,60	0,34	-0,44	-0,53
<u>Caractérisation des valeurs seuils de <math>D_{méd}</math> et <math>D_{quart}</math> échantillons d'origine non ariégeoise</u>	ling	Castel-Minier	-1,52	0,13	-0,31	-2,41	-1,35	-0,18	2,03	-1,32	-0,11	0,44	-0,36
	CM05-02-27	Castel-Minier	-1,90	0,04	-0,43	-2,87	-2,09	-0,18	0,15	-1,03	0,57	-0,31	-0,43
	Loupelorraine	Loupe expérimentale	-4,31	0,10	-0,04	-0,24	-4,08	0,17	0,43	-0,06	0,05	-0,34	0,84
	Clé16	Piémont	-4,09	-0,26	-0,22	-0,69	-2,61	0,07	-1,11	0,64	-0,29	0,20	0,88
<u>échantillons d'origine non ariégeoise</u>	SCHmet1	Schilpario	-0,66	0,10	-0,28	0,68	1,34	0,15	-3,68	1,14	-0,47	-0,31	0,52
	MIMET	Mimet	-4,47	0,02	-0,13	-1,23	-4,60	0,13	-0,96	-0,32	-0,07	0,17	0,53

But de l'analyse	Nom échantillons	Localisation	Y	Nb	Cs	La	Ce	Nd	Sm	Yb	Hf	Th	U
Test de l'hypothèse d'une provenance arégeoise	GP3.4	Palais des Papes	-4,07	0,10	-0,45	-0,21	-3,61	0,12	3,68	-0,82	0,15	0,42	0,68
	GP3.2	Palais des Papes	-5,45	0,17	-0,15	-0,85	-3,45	0,06	-0,96	1,02	-0,42	0,25	0,64
	GP3	Palais des Papes	-2,13	0,05	-0,44	-1,03	-3,26	0,33	-3,04	-1,33	0,13	0,13	0,07
	Ec2	Palais des Papes	-3,76	0,26	0,22	-1,06	0,55	-0,34	-0,14	1,85	-0,63	-0,12	0,17
	Ec3	Palais des Papes	-1,06	0,15	-0,06	-0,49	0,01	-0,21	4,77	-0,94	0,14	0,00	0,01
	Eg1	Palais des Papes	-0,32	0,13	1,22	-0,05	1,68	-0,40	1,51	0,59	0,14	-1,15	-0,10
	Eg3	Palais des Papes	-1,82	0,13	-0,97	-1,48	-1,05	0,01	0,98	-1,22	0,29	0,53	-0,05
Test de l'hypothèse d'une provenance arégeoise	CAP3	Collégiale St-Etienne de Caspeatang	-2,20	0,16	-0,02	-3,06	-0,56	-0,29	0,40	-0,35	-0,04	-0,38	-0,12
	CAP1	Collégiale St-Etienne de Caspeatang	-0,40	0,43	-0,06	-0,06	0,23	-0,13	4,18	-0,67	-0,40	0,12	-0,25
Test de l'hypothèse d'une provenance arégeoise	8844	Montréal-de-Sos	0,95	0,36	-0,19	0,89	1,40	0,17	-4,45	0,92	-0,94	0,29	0,07
	8858	Montréal-de-Sos	-1,69	0,32	0,19	-1,61	1,88	-0,40	-2,64	2,87	-1,10	0,26	-0,12
	8889	Montréal-de-Sos	-1,21	0,37	-0,80	-0,46	-0,70	0,34	-1,04	-0,65	-1,01	1,19	0,37
	9297	Montréal-de-Sos	2,28	0,06	-0,37	0,18	2,33	0,20	-3,27	-0,84	0,39	-0,40	0,27
	29336	Montréal-de-Sos	0,05	0,08	-1,17	-2,42	0,23	-0,03	0,16	-1,46	0,17	0,71	-0,25
	29342	Montréal-de-Sos	-2,66	0,17	-0,83	-1,00	-0,69	0,01	2,71	-0,03	-0,30	0,67	0,60

But de l'analyse	Nom échantillons	Localisation	Y	Nb	Cs	La	Ce	Nd	Sm	Yb	Hf	Th	U
Test de l'hypothèse d'une provenance arégoise	29409	Montréal-de-Sos	-3,32	0,16	-0,06	-1,01	-2,98	0,13	-0,66	0,13	-0,32	-0,29	0,58
	29421	Montréal-de-Sos	-2,62	-0,05	0,52	-2,66	0,27	-0,43	-0,52	1,35	-0,50	-0,45	0,46
	29522	Montréal-de-Sos	-0,79	0,37	-0,91	-1,76	-0,17	0,17	-2,69	-0,62	-0,56	0,70	-0,07
	29566	Montréal-de-Sos	2,15	0,09	0,61	-2,54	1,94	-0,36	-0,53	-1,05	0,01	-0,26	-0,60
	29591	Montréal-de-Sos	-2,13	-0,06	0,72	0,32	0,59	-0,05	-3,00	1,21	-1,19	0,64	0,15
Test de l'hypothèse d'une provenance arégoise	MIR1	Mirabat	4,58	-0,03	0,39	0,23	3,63	0,06	-3,74	-1,04	0,31	-0,51	-0,40
	MIR2	Mirabat	-1,58	0,04	0,29	0,19	1,89	-0,13	-0,01	0,67	0,09	-0,75	0,54
	MIR3	Mirabat	-5,36	0,22	-0,08	-0,83	-2,09	-0,24	0,69	2,56	-0,64	0,12	0,63
	MIR5	Mirabat	-3,26	0,31	-0,07	0,47	-1,71	0,12	1,59	-0,27	-0,32	0,38	0,44
	MIR6	Mirabat	-3,66	0,17	0,76	0,65	-1,21	-0,15	-0,23	2,10	-0,19	-0,64	0,82
	MIR7	Mirabat	-4,63	0,35	0,34	-1,23	-1,05	-0,43	0,19	2,85	-0,69	-0,28	0,29
	MIR8	Mirabat	2,15	-0,10	0,46	0,86	2,43	0,10	-3,57	-0,09	-0,18	-0,06	0,40
	MIR9	Mirabat	-0,46	0,35	-1,08	-1,58	-0,15	0,17	-0,41	-1,09	-0,43	0,97	-0,10
	MIR10	Mirabat	-0,43	0,13	0,89	0,88	0,84	-0,06	-2,12	1,14	-0,03	-0,76	0,67
	MIR11	Mirabat	-1,67	0,06	-0,01	-1,25	-0,91	-0,40	5,29	-0,05	-0,18	0,02	0,14
	MIR12	Mirabat	-0,64	0,13	0,81	0,49	1,22	-0,11	-3,40	1,49	-0,17	-0,50	0,52

But de l'analyse	Nom échantillons	Localisation	Y	Nb	Cs	La	Ce	Nd	Sm	Yb	Hf	Th	U
Test de l'hypothèse d'une provenance arigeoise	Ste Cath n2	Sainte-Catherine	-2,87	0,00	-0,26	0,17	-4,54	0,21	4,02	-1,22	0,16	0,06	0,58
	Ste Cath n4	Sainte-Catherine	0,10	0,10	-0,34	1,32	1,48	0,15	1,47	-0,20	-0,20	-0,37	0,79
	Ste Cath n5	Sainte-Catherine	-3,26	0,08	-0,55	0,82	-5,86	0,35	3,72	-0,96	-0,06	0,61	0,47
Test de l'hypothèse d'une provenance arigeoise	CM05-31	Castel-Minier	-2,62	0,14	-0,27	1,71	-5,65	0,49	0,18	-0,85	0,10	0,25	0,33
	2002-1	Castel-Minier	0,10	0,19	0,23	-1,11	2,34	-0,02	-6,54	1,40	-0,59	-0,09	-0,31
	CM05-02-34	Castel-Minier	-4,76	0,03	0,13	-1,00	-2,66	-0,28	1,10	2,07	-0,42	-0,04	0,64
	CM05-02-36	Castel-Minier	-0,38	-0,10	0,55	-1,97	2,15	-0,58	-1,48	1,95	-0,35	-0,68	0,28
	CM05-02-54	Castel-Minier	-2,75	0,08	0,36	-3,09	-0,34	-0,46	1,47	0,36	-0,27	-0,03	-0,10
	CM07-2044	Castel-Minier	-3,85	0,28	-0,57	-1,85	-2,32	-0,03	0,17	0,19	-0,84	1,04	0,01
Test de l'hypothèse d'une provenance arigeoise	CM05-02-59	Castel-Minier	-1,02	-0,05	-0,08	-3,09	0,39	-0,42	-3,10	1,22	-0,20	-0,10	0,13
	i10013	Castel-Minier	-1,74	-0,26	0,51	-1,79	0,88	-0,59	0,13	1,87	-0,26	-0,51	0,59
	TS02	Cathédrale d'Amiens	-2,45	0,06	-0,41	-0,69	-3,90	0,34	0,36	-2,23	0,32	0,78	0,28
	TS06	Cathédrale d'Amiens	-1,87	-0,02	0,09	-1,19	-2,80	0,14	1,40	-2,30	0,38	0,52	0,41

Comparaison sur l'axe LD1 avec la signature définissant l'espace lombard

But de l'analyse	Nom échantillons	Localisation	Y	Nb	Cs	La	Ce	Nd	Sm	Yb	Hf	Th	U
<b>Caractérisation des valeurs seuils de <math>D_{m\&amp;eacute;l}</math> et <math>D_{quartz}</math></b>	Louelloiraine	Loupe	1,63	0,31	-0,94	2,66	2,88	0,13	1,43	1,52	-0,14	-0,08	-0,37
	MIMET	Mimet	1,60	0,45	-1,00	2,99	2,92	0,09	1,95	1,15	-0,11	-0,49	-0,23
	i10013	Castel-Mimier	0,82	0,58	-0,85	2,81	1,75	0,05	1,81	-0,13	-0,09	-1,14	-0,05
	CM06-2008-1	Castel-Mimier	0,97	0,46	-0,96	2,62	1,95	0,07	1,37	0,29	-0,17	-0,80	0,12
<b>Test de l'hypothèse d'une provenance lombarde</b>	GP3.2	Palais des Papes	-2,23	-0,23	0,57	-3,55	-0,93	-0,06	-1,76	-1,02	0,07	0,06	0,18
	GP3	Palais des Papes	-1,75	-0,39	0,87	-2,97	-2,75	-0,10	-1,78	-1,46	0,14	0,14	0,22
	EG3	Palais des Papes	-1,04	-0,23	-0,11	-3,40	0,76	-0,07	0,14	-0,52	0,24	0,97	-0,07
	EG1	Palais des Papes	-1,01	-0,38	1,31	-2,04	-2,09	-0,09	-1,95	-0,18	0,29	0,38	-0,27
	EC2	Palais des Papes	-1,43	-0,41	0,66	-3,35	0,66	-0,01	-1,95	0,63	0,09	0,55	-0,37
	EC3	Palais des Papes	-0,83	-0,33	0,58	-2,57	-0,90	-0,08	-0,04	-0,58	0,21	0,96	-0,16
<b>Test de l'hypothèse d'une provenance lombarde</b>	GP3.4	Palais des Papes	-1,36	-0,33	0,59	-3,33	-1,59	-0,10	-0,25	-1,27	0,25	1,07	0,12
	US1772	Via Moneta (Milan)	1,58	0,53	-0,11	4,14	0,15	0,03	1,06	0,56	0,03	-0,77	-0,34
	Clé16	Piémont	1,62	0,76	-0,82	3,66	1,76	-0,01	2,08	0,55	0,08	-0,72	-0,29
	US1660	Via Moneta (Milan)	1,29	0,44	-0,22	3,24	1,89	0,09	1,07	1,04	-0,06	-1,23	-0,44

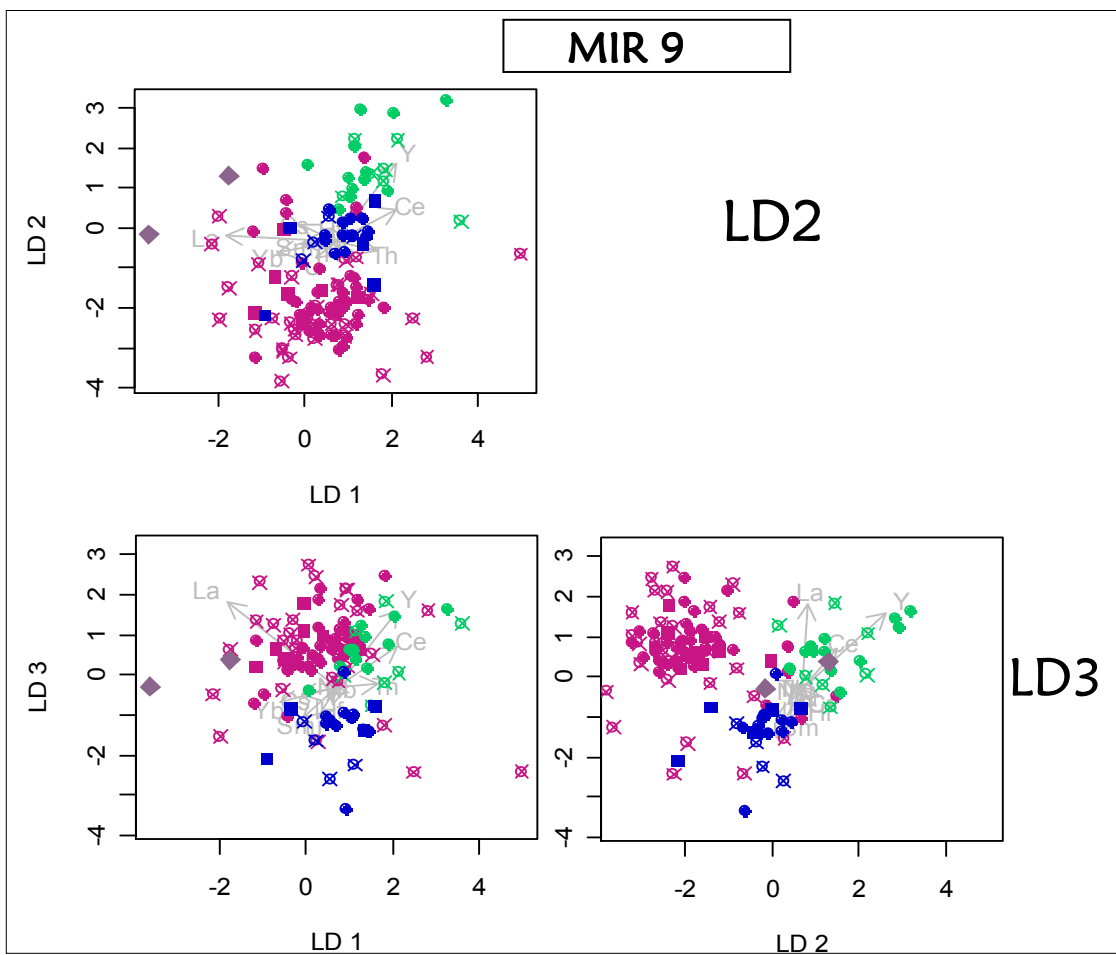
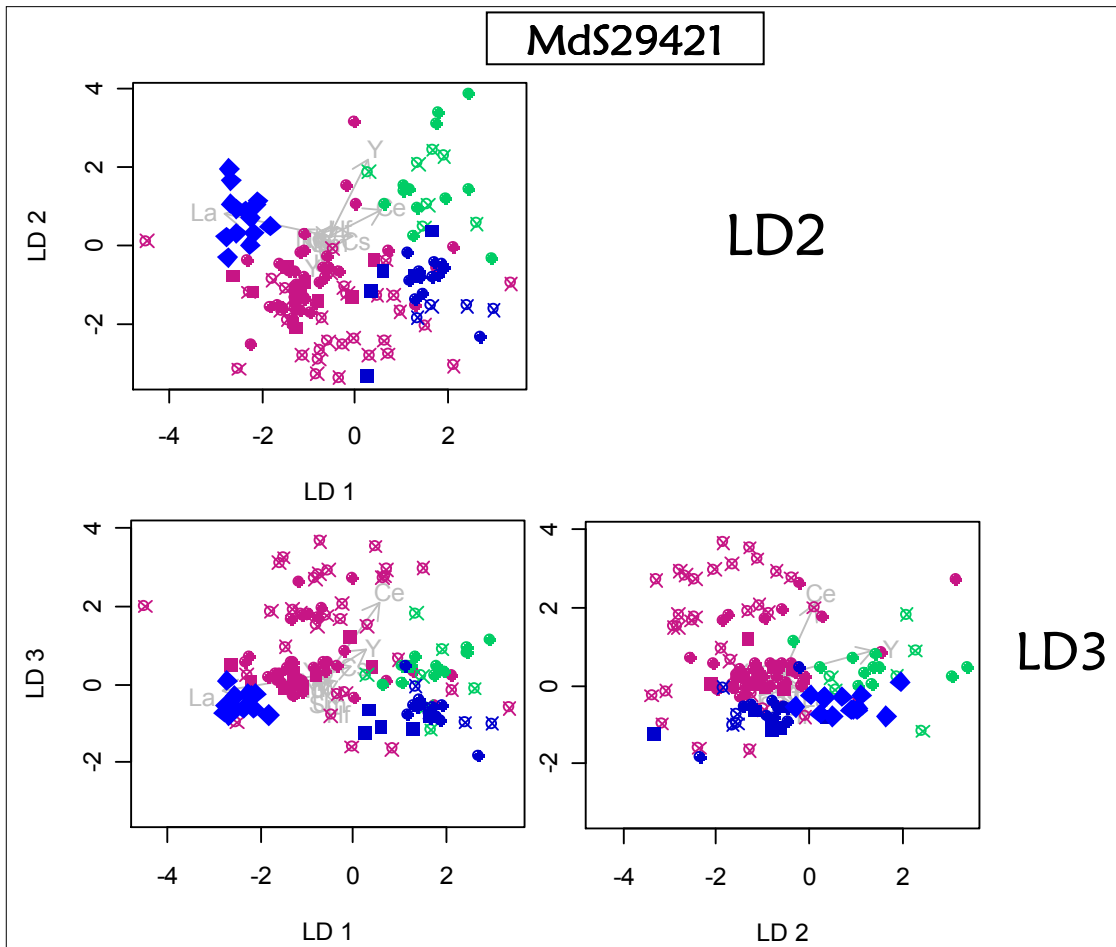


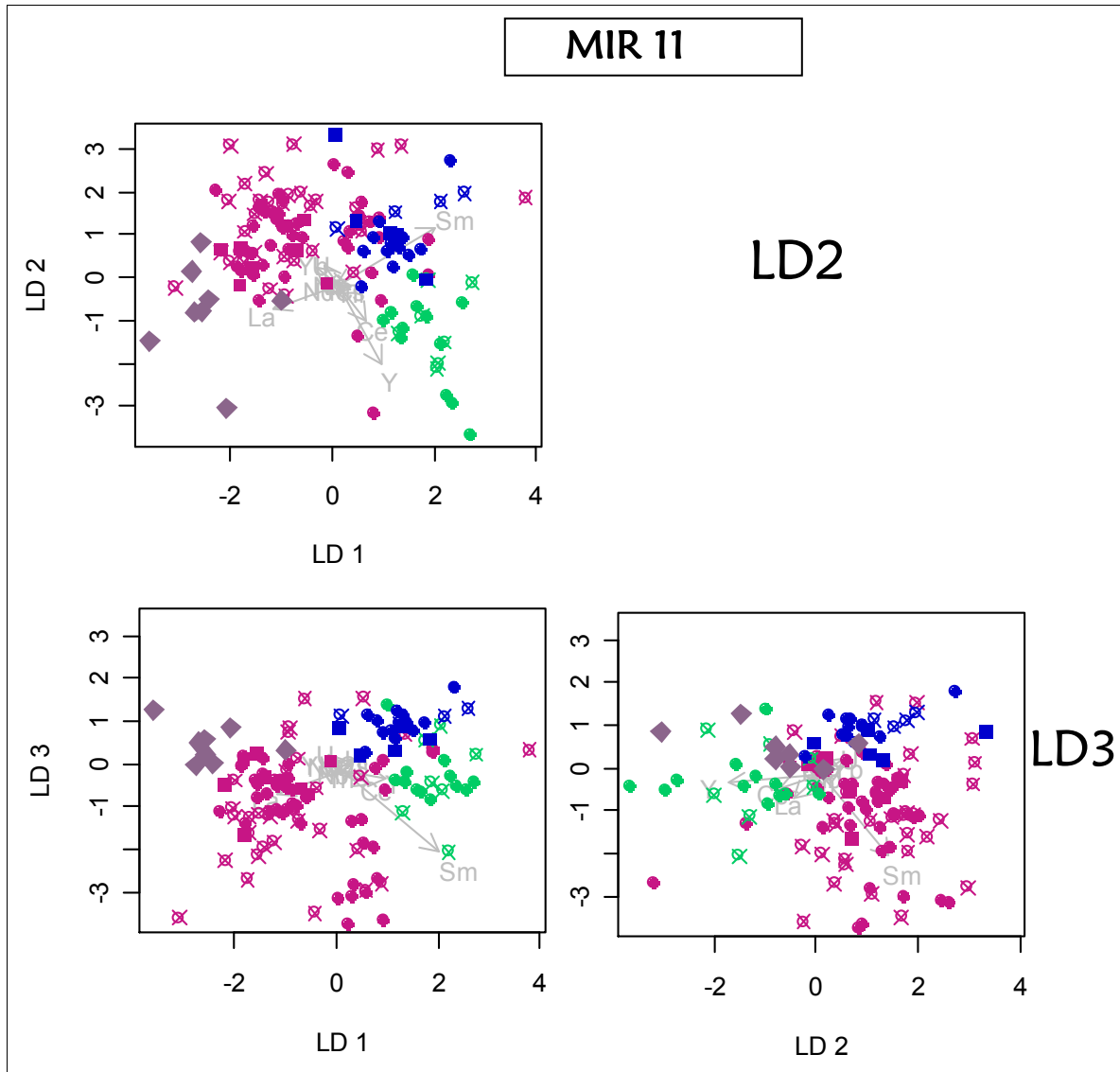
## Annexes H

ANALYSE DISCRIMINANTE DES  $X_{ij}$  DES OBJETS MdS29421, MIR9 ET MIR11 D'ORIGINE A IDENTIFIER ET DES ECHANTILLONS DEFINISSANT L'ARIEGE, LA MONTAGNE NOIRE ET L'ANDORRE. PROJECTIONS SUR LES PLANS DISCRIMINANTS FORMES PAR LES AXES LD1, LD2, LD3







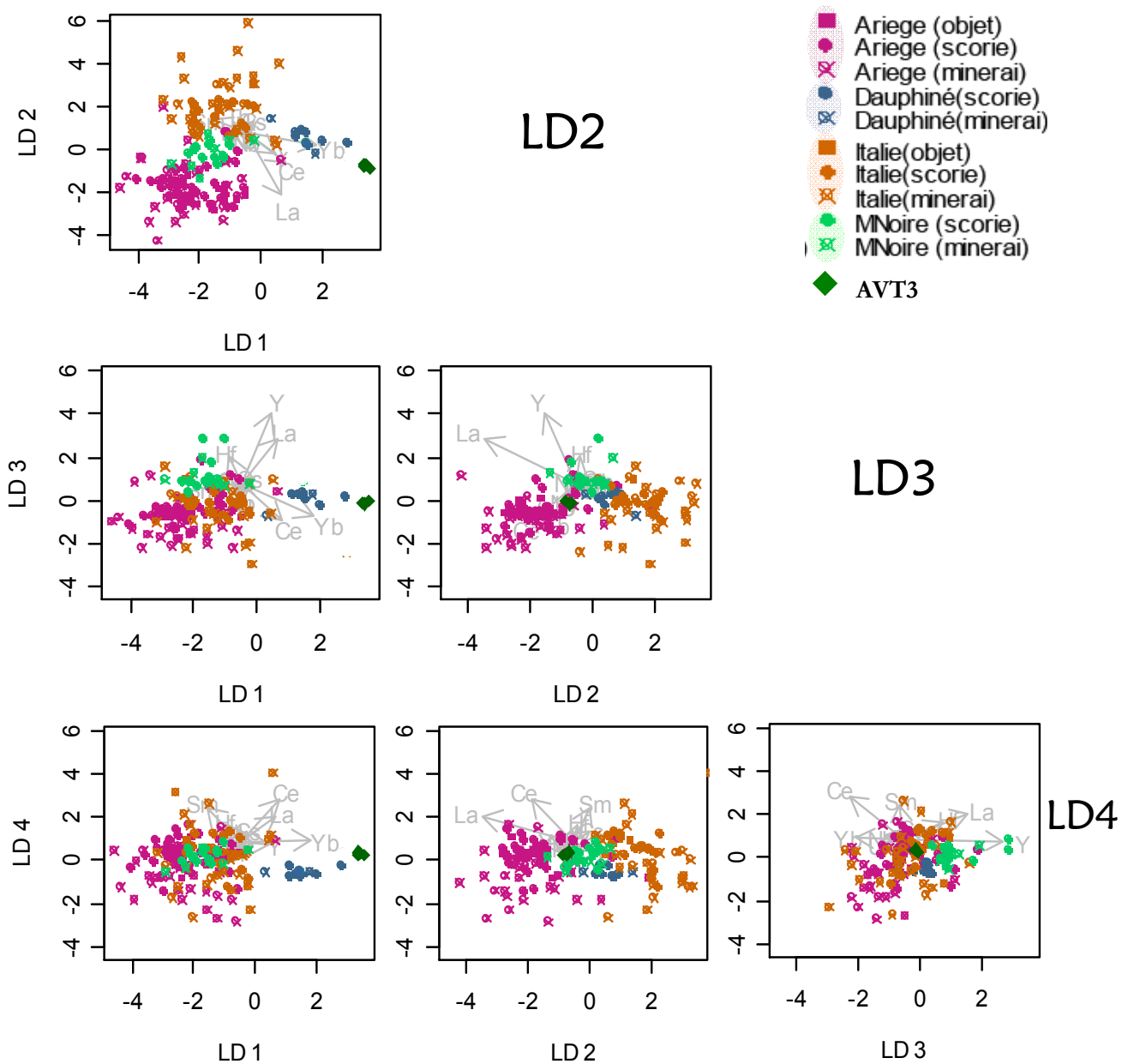


## **Annexes I**

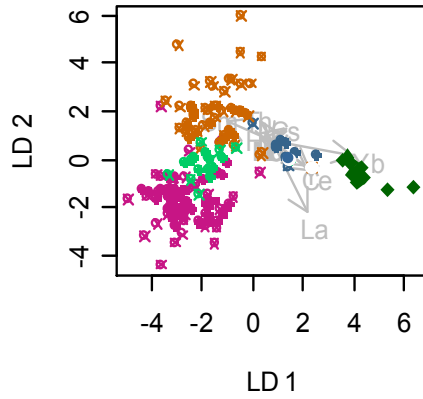
ANALYSE DISCRIMINANTE DES  $X_{ij}$  DES FERS DU PALAIS  
DES PAPES D'AVIGNON D'ORIGINE A IDENTIFIER ET  
DES ECHANTILLONS DEFINISSANT L'ARIEGE, LA  
MONTAGNE NOIRE, LE DAUPHINE ET LA LOMBARDIE.  
PROJECTIONS SUR LES PLANS DISCRIMINANTS FORMES  
PAR LES AXES LD1, LD2, LD3, LD4



## AVT3

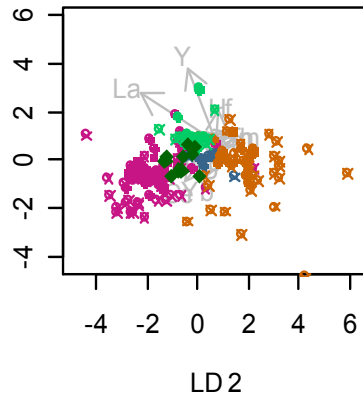
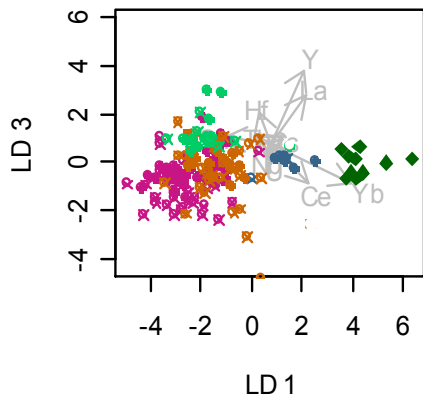


AVT4

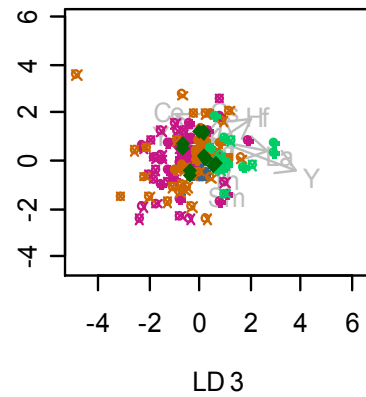
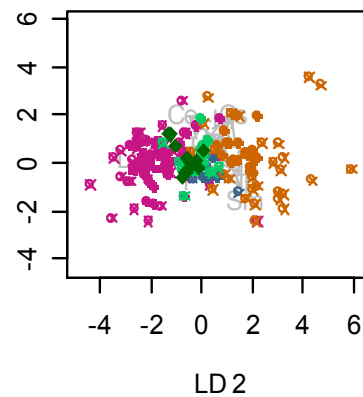
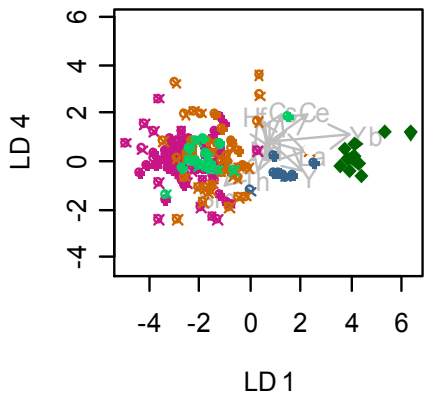


LD2

- Ariège (objet)
- Ariège (scorie)
- ✕ Ariège (minerai)
- Dauphiné (scorie)
- ✕ Dauphiné (minerai)
- Italie (objet)
- Italie (scorie)
- ✕ Italie (minerai)
- MNoire (scorie)
- ✕ MNoire (minerai)
- ◆ AVT4

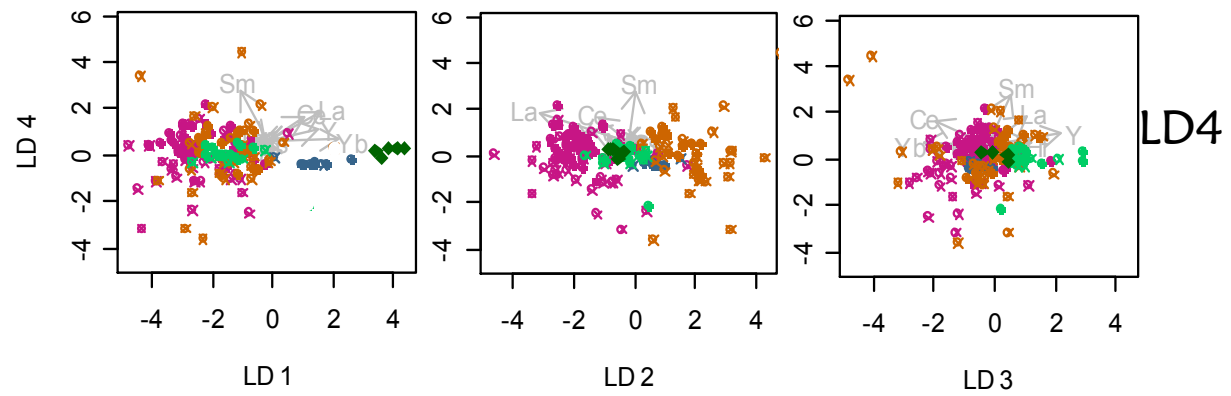
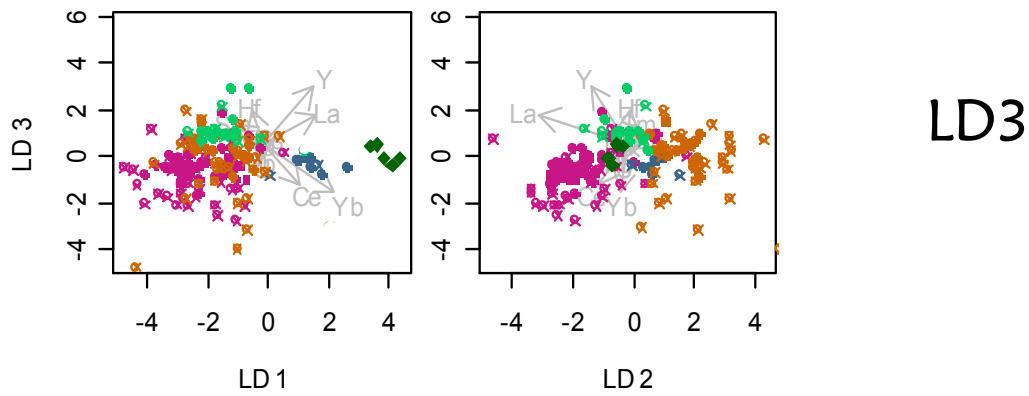


LD3

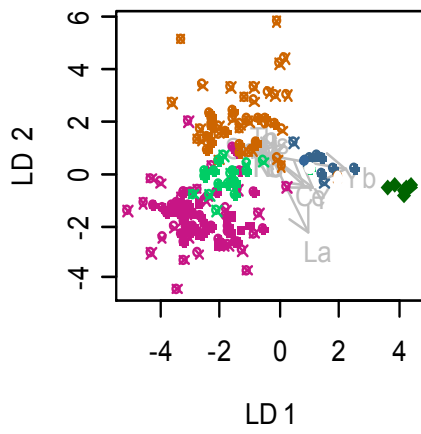


LD4

## AVT5

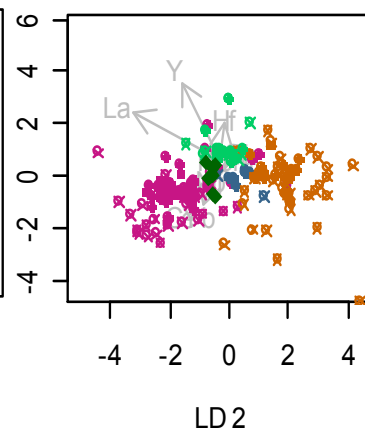
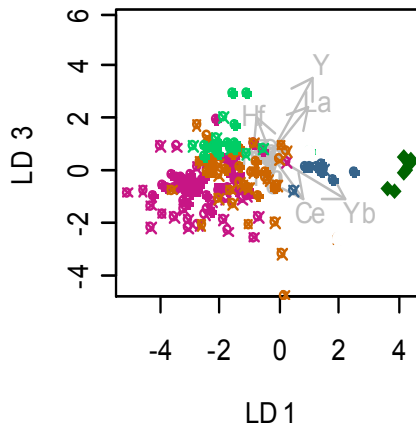


TRsud

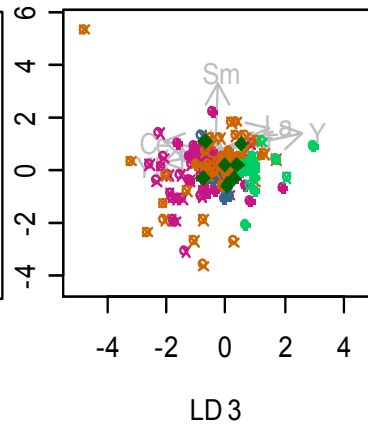
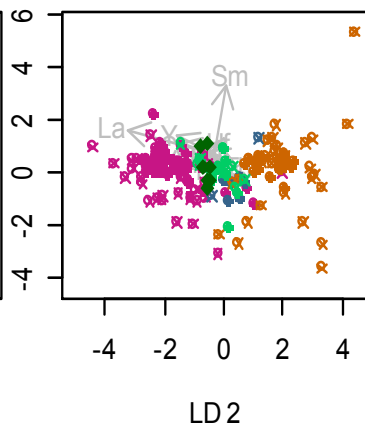
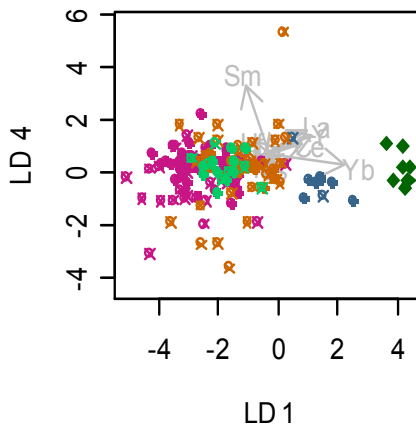


LD2

- Ariège (objet)
- Ariège (scorie)
- ✕ Ariège (minerai)
- Dauphiné(scorie)
- ✕ Dauphiné(minerai)
- Italie(objet)
- Italie(scorie)
- ✕ Italie(minerai)
- MNoire (scorie)
- ✕ MNoire (minerai)
- ◆ TRsud



LD3



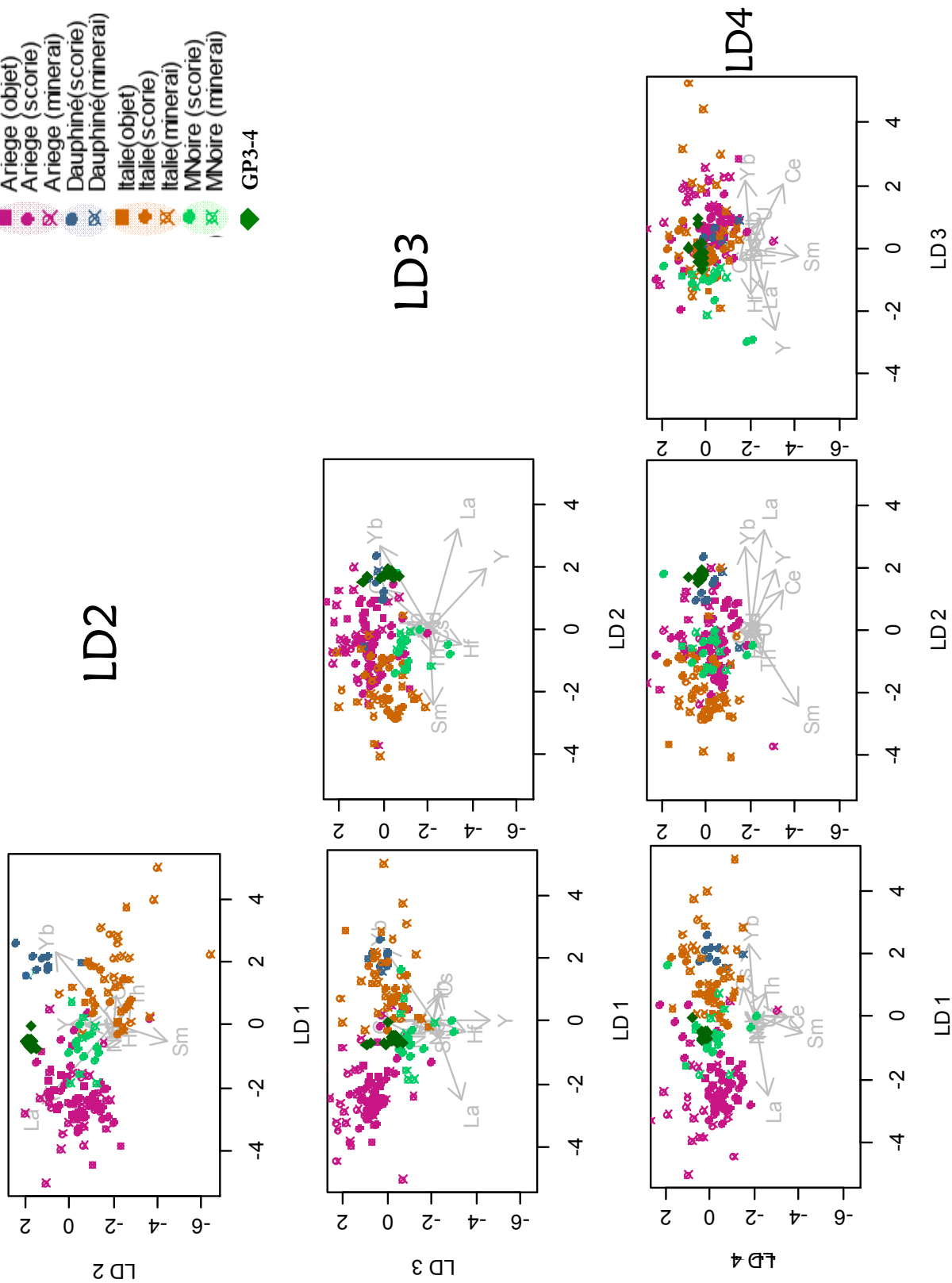
LD4

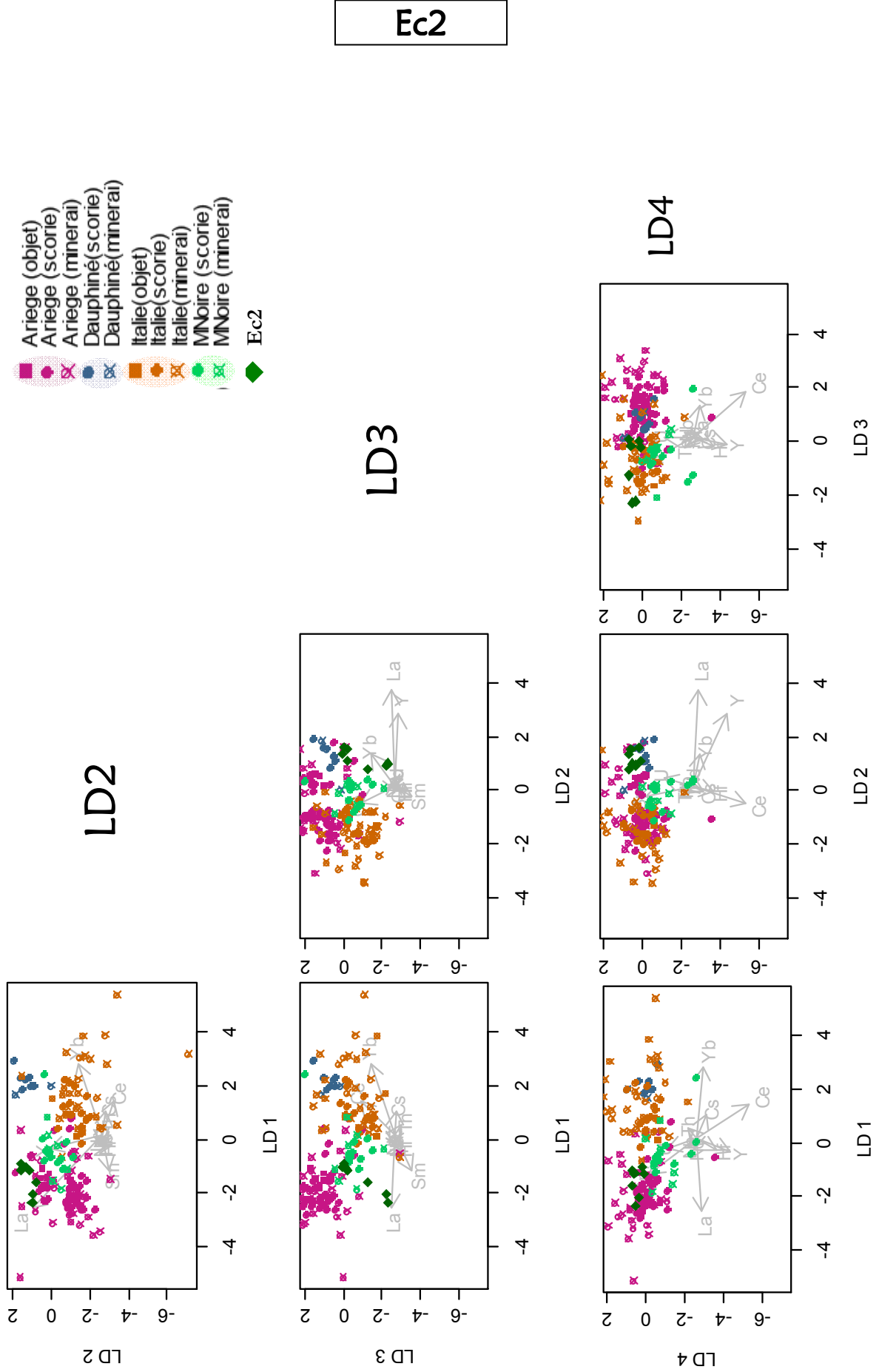
tel-00598796, version 1 - 7 Jun 2011

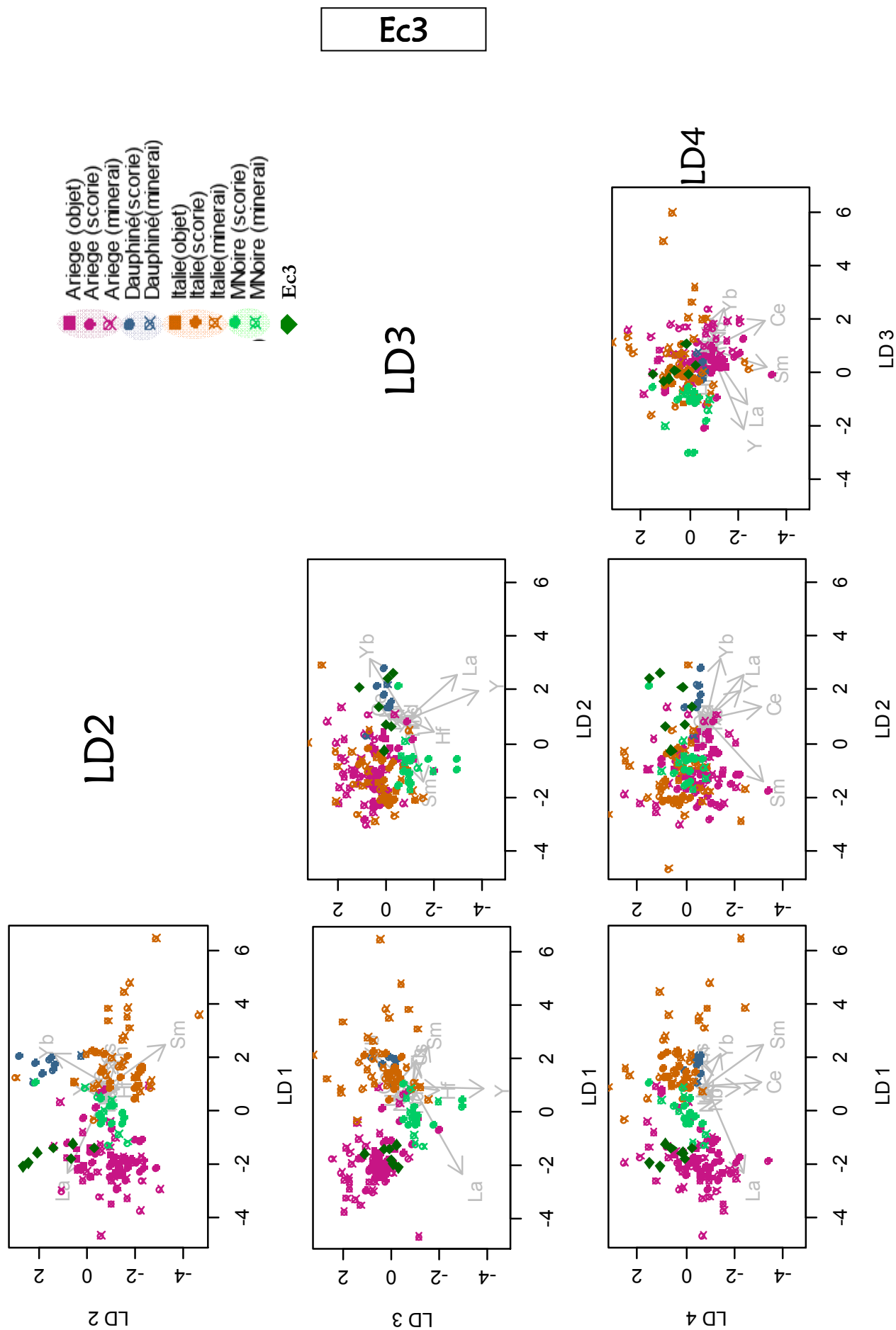


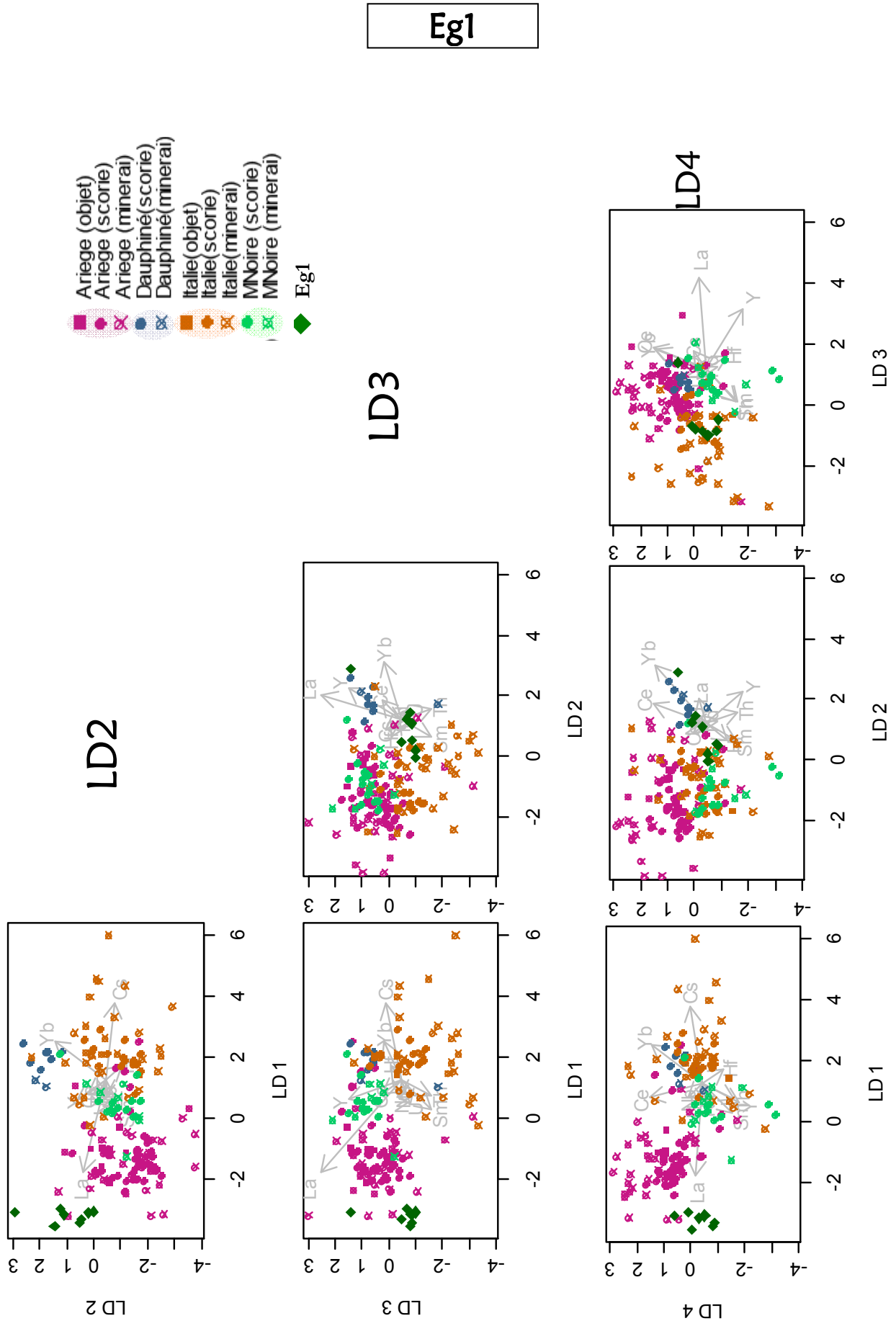
- Ariege (objet)
- Ariege (scorie)
- Ariege (mineral)
- Dauphiné(scorie)
- Dauphiné(mineral)
- Italie(objet)
- Italie(scorie)
- Italie(mineral)
- MNoire (scorie)
- MNoire (mineral)
- GP3-4

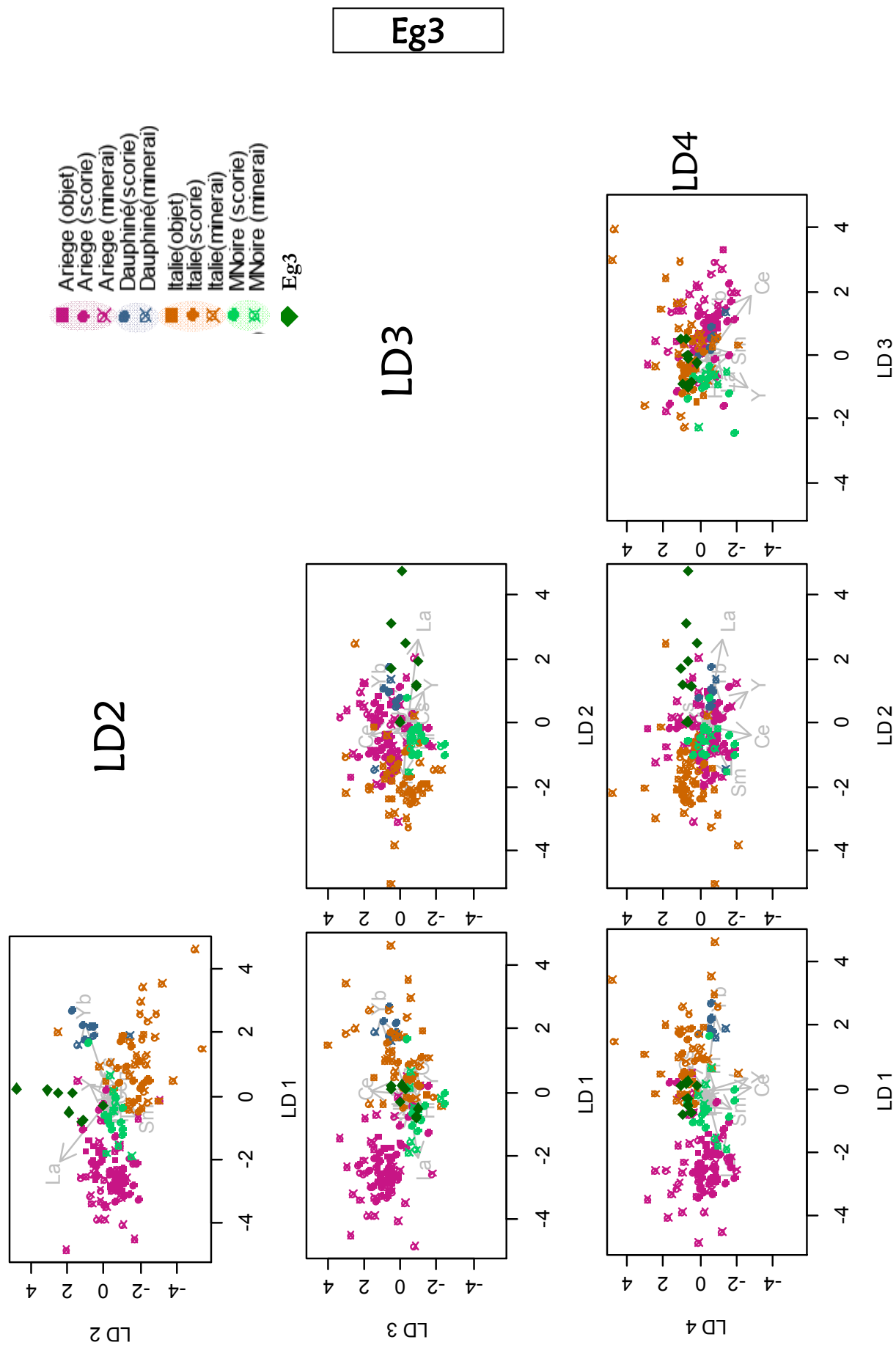
GP3-4









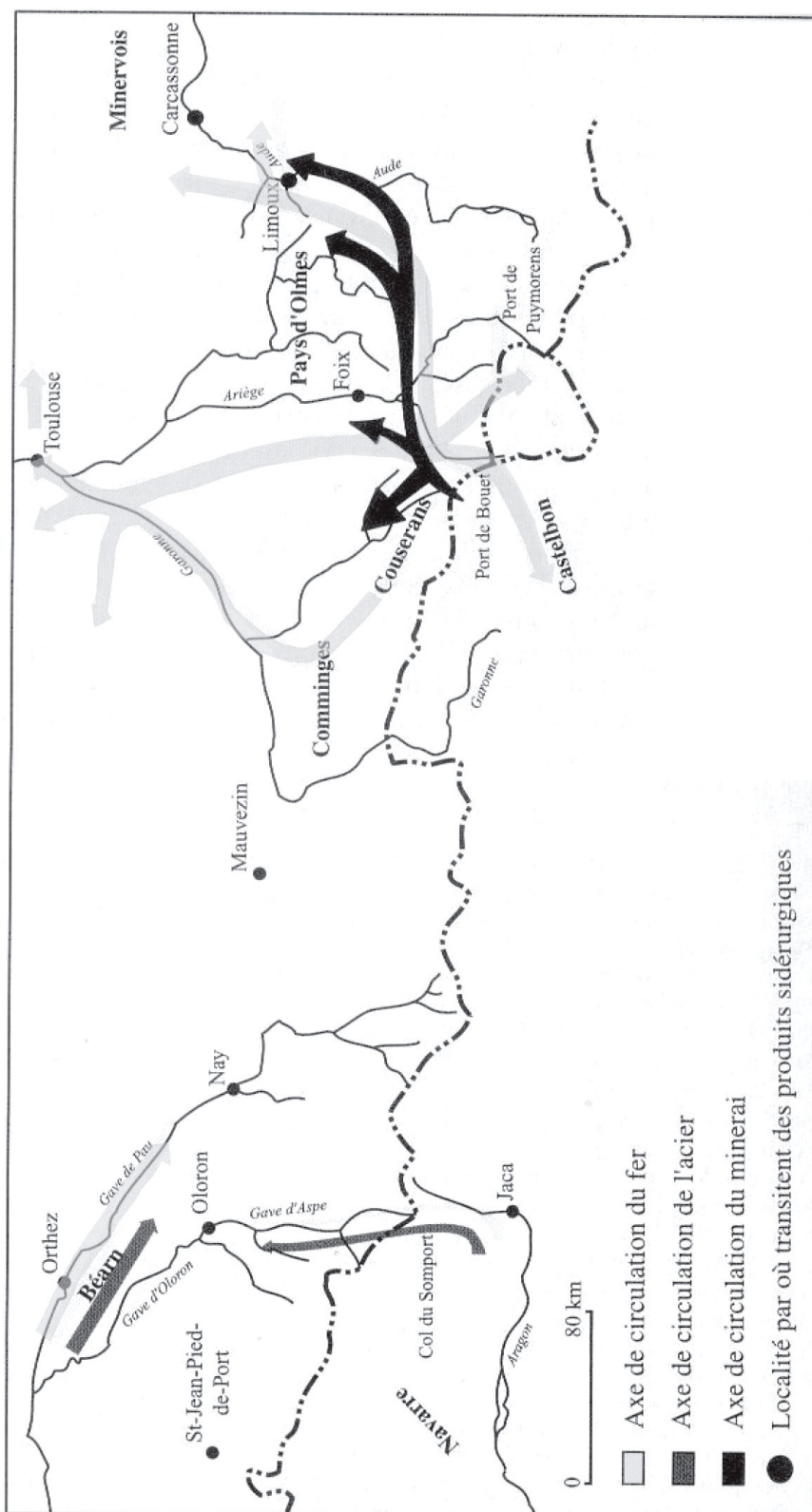


Eg3



## Annexe J

COMMERCE DU MINÉRAI ET DES PRODUITS SIDÉRURGIQUES  
FIN XIV<sup>e</sup> – MILIEU XV<sup>e</sup> SIÈCLE (Verna, 2001)







## Annexe K

### ANALYSES ICP-MS REALISÉES AU LABORATOIRE DES MÉCANISMES ET TRANSFERTS EN GÉOLOGIE

L'appareillage du L.M.T.G. est un ICP-MS quadripolaire, Perkin-Elmer Elan 6000, couplé à un laser du type Nd :YAG de longueur d'onde de 266 nm (Coustures *et al.*, 2003). Dans le cadre de nos analyses, le diamètre du cratère dû à l'ablation est de 20µm au point focal, tandis que le temps d'acquisition est de 80 secondes. Le standard interne considéré pour ces analyses est l'élément majeur aluminium. Une seule ablation est réalisée sur les inclusions. Comme pour les analyses menées à Orléans, la calibration a été réalisée à l'aide d'un standard NIST 612.

Pour traiter les résultats, nous avons travaillé directement sur les profils de concentrations obtenus en temps réel. Le signal brut a été intégré uniquement sur la durée de prélèvement de l'inclusion. Les signaux obtenus sont apparus courts et faibles, en raison de la petite taille des inclusions, ce qui limite la possibilité de quantifier un nombre important d'éléments traces. Seuls les plus concentrés ont pu être ainsi dosés. Le tableau ci-dessous résume les éléments qui ont pu être quantifiés pour les trois échantillons d'armures.

**Tableau K.5 – Bilan des éléments traces quantifiés par LA-ICP-MS sur les échantillons d'armures W.C A.143, W.C A.144 et W.C A.235. Le chiffre entre parenthèses indique le nombre d'inclusions pour lesquelles la teneur élémentaire a pu être quantifiée**

Echantillons	Eléments quantifiés	
	pour les 3 échantillons	Eléments parfois quantifiés
W.C A.143	Y. Nb. Ba. La.	Sc(1). Cs(4). Nd(8). Sm(1). Eu(1). Yb(2). Th(7). Hf(1)
W.C A.144	Ce. Ti. V. Cr. As. Rb. Sr. Zr	Cs(1). Nd(2). Tb(1). Yb(3). Hf(3). U(1)
W.C A.235		Be(2). Cs(1). Ta(1). U(2)



## Annexe L

### ÉTUDE DE LA PROVENANCE D'OBJETS RETROUVÉS À MILAN ET EN PIÉMONT

Trois pièces métalliques d'origine inconnue ont été retrouvées à Milan et en Piémont, à proximité de l'espace lombard étudié. Nous avons trouvé, par là même, l'occasion d'appliquer et tester l'approche multivariée mise en place dans ce travail de thèse à l'espace de production lombard.

Ces trois objets sont datés de l'Antiquité tardive et du XVI<sup>e</sup> siècle<sup>6</sup>. Ils correspondent à l'ancre d'une maison du XVI<sup>e</sup> siècle du village de Bugnate en Piémont, près du Lac d'Orta, et deux lingots collectés près de Milan (Figure L.6 et Tableau L.6). Ces derniers ont été mis au jour lors de la fouille Via Moneta.



Figure L.6 – Objets d'origine à identifier retrouvés à Milan et en Piémont

Tableau L.6 – Corpus des objets retrouvés en Lombardie et étudiés dans ce travail

Echantillons	Provenance	Description	Métallographie	Datation
Clé16	Village de Bugnate	Clé	Hétérogène : ferritique à 0,8% de C	XVI <sup>e</sup> s.
US1660	Milan- Via Moneta US1660	Lingot	Hétérogène : ferritique à 0,8% de C	500-600 A.D*

<sup>6</sup> Objets collectés par M. Tizzoni et confiés pour analyse.

US1772	Milan- Via Moneta US1772	Lingot	Hétérogène : ferritique à 0,8% de C	0-100 A.D*
--------	-----------------------------	--------	--	------------

\* Datations actuellement en cours de révision

Ces objets pourraient avoir été produits en Lombardie, zone proche d'une centaine de kilomètres. Dans une première approche, la comparaison de leurs signatures avec celle de cet espace sidérurgique permettra de tester cette hypothèse.

Rappelons que seuls les objets issus de la filière directe contiennent des inclusions susceptibles de porter les traces de la signature chimique du minerai d'origine. Pour l'échantillon datant du XVI<sup>e</sup> siècle, la question du procédé d'élaboration peut se poser<sup>7</sup>. Ainsi, comme évoqué dans la partie méthodologique du Chapitre IV § V.1, nous utilisons l'abaque proposé par Dillmann & L'Héritier (2007) permettant de distinguer les objets issus de la filière directe et indirecte. Celui-ci révèle que l'objet se place dans le domaine du procédé direct (Figure L.7; Gauche). L'étude de la signature chimique de cet échantillon peut donc être envisagée. Les analyses en éléments majeurs sont reportées dans l'Annexe N.9<sup>8</sup>. La comparaison des compositions en oxydes de manganèse et de phosphore des inclusions des objets avec celles des échantillons définissant la Lombardie montre qu'un des objets, US1660, ne peut provenir de l'espace sidérurgique lombard, en raison de la faible teneur en manganèse détectée (<0,5 %<sub>mass</sub> MnO\*) (Figure L.7 ; Droite). Dans ce qui suit, nous ne considérerons donc pas la signature en éléments traces de cet objet dans l'analyse multivariée.

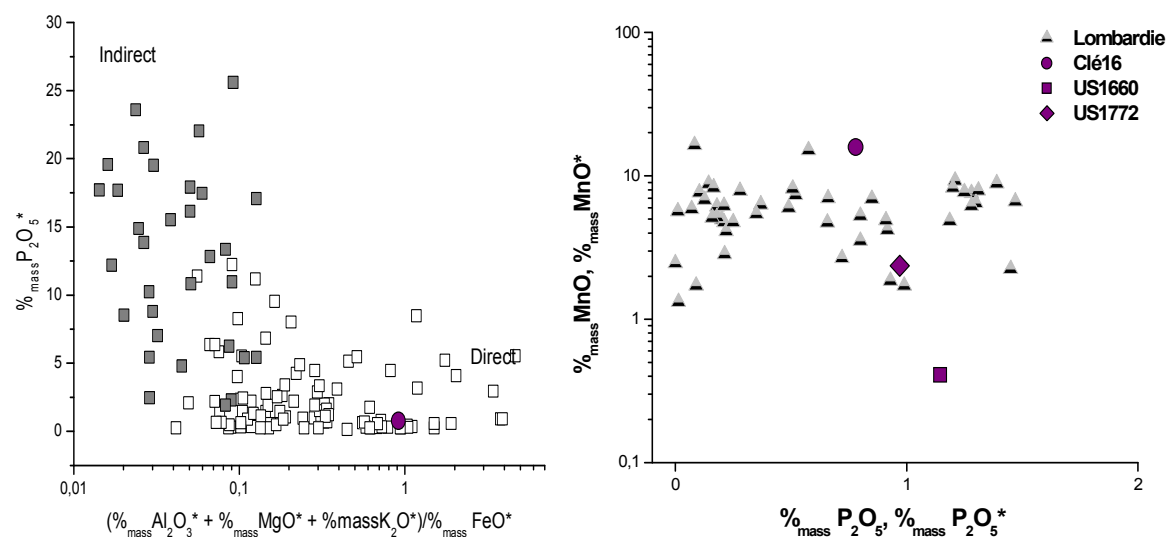


**Figure L.7 – (Gauche): Discrimination des procédés pour les inclusions de l'objet Clé16<sup>9</sup>. (Droite): Comparaison des teneurs absolues en oxydes de manganèse et phosphore dans les inclusions des objets et les échantillons définissant la signature lombarde (EDS)**

<sup>7</sup> En effet, même si des traces de martelage sont visibles sur la clé, l'aspect régulier de la clavette pose plus de questions.

<sup>8</sup> A titre indicatif, notons que les inclusions de l'échantillon Clé16 contiennent des quantités notables en titane (~0,7%<sub>mass</sub>) et en soufre (~0,6%<sub>mass</sub>).

<sup>9</sup> Pour l'échantillon Clé16 uniquement, le point représente une composition moyenne pondérée.

Le tableau ci-dessous réunit les résultats de l'analyse par approche multivariée réalisée selon la démarche n°1 de notre méthodologie (voir Chapitre IV § V.2) pour les deux échantillons Clé16 et US1772. Les observations tirées des comparaisons des distances médiane et quartile avec celles des domaines de compatibilité avec une origine lombarde dans l'abaque (voir la Figure L.8) mettent en évidence deux résultats différents. Le lingot US1772 présente des distances appartenant au domaine « indéterminé » avec une origine lombarde. Une provenance de cet espace ne peut donc être exclue. En revanche, l'objet Clé16 n'est pas originaire de cette zone sidérurgique.

**Tableau L.7 – Distances de la médiane et du premier quartile des Proj.X<sub>OI</sub> au domaine des Proj.X<sub>ES.Lombardie</sub> sur l'axe LD1 pour Clé16 et US1772**

Echantillons		Clé16	US1772
$D_{méd.}$		2,90	1,15
$D_{quart.}$		2,80	0,80

$D_{méd.}$  : distance de la médiane des Proj.X<sub>OI</sub> au domaine des Proj.X<sub>ES.Lombardie</sub>  
 $D_{quart.}$  : distance du troisième quartile des Proj.X<sub>OI</sub> au domaine des Proj.X<sub>ES.Lombardie</sub>

$D_{méd.} \leq 0,37$	$0,37 < D_{méd.}$	$0,37 < D_{méd.} < 2,75$	$D_{méd.} \geq 2,75$
$D_{quart.} \leq 0,19$	$D_{quart.} < 0,19$	$0,19 < D_{quart.} < 2,60$	$D_{quart.} \geq 2,60$
Compatible	Probable	Indéterminé	Non compatible

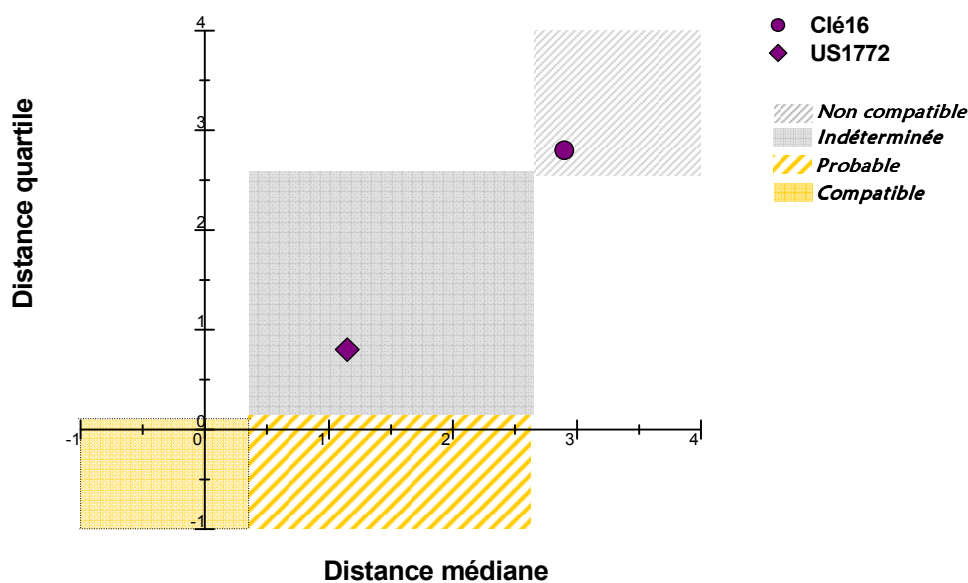


**Figure L.8 – Compatibilité avec une origine lombarde pour les objets Clé16 et US1772 en fonction des distances médiane et quartile**

► Nous avons montré en début de cette annexe, que l'échantillon nommé US1660 ne provenait pas de l'espace lombard étudié car ces inclusions contenaient trop peu de manganèse ( $\sim 0,41\%_{\text{mass}}$  de MnO) en comparaison des échantillons lombards. A ce titre, il faut souligner qu'à l'ouest de la Lombardie existe une zone de minéralisation particulière que nous n'avons pas incluse dans l'espace lombard étudié ici: les gisements du Piani d'Erna. Ces derniers, situés près de Lecco, ne possèdent pas les mêmes caractéristiques que ceux couramment rencontrés dans la zone bergamasque, à savoir des gisements de minerais carbonatés riches en oxydes de manganèse. Les minéralisations de cette région sont atypiques et les minerais de fer ne contiennent pas de manganèse. C'est pourquoi, d'après la démarche n°1 de la méthodologie mise en place, nous avons souhaité confronter les données inclusionnaires du lingot US1660 à celles des minerais et scories du Piani d'Erna<sup>10</sup>. Les projections obtenues à partir de l'analyse multivariée appliquée aux variables des échantillons définissant la Lombardie dans ce travail, le Piani d'Erna et le lingot US1660 sont présentées dans le plan discriminant (LD1, LD2) (Figure L.9). Les domaines de projection des observations des différentes classes sont clairement isolés. Ainsi, les minerais du Piani d'Erna n'ont pu, non plus, être à l'origine du lingot.

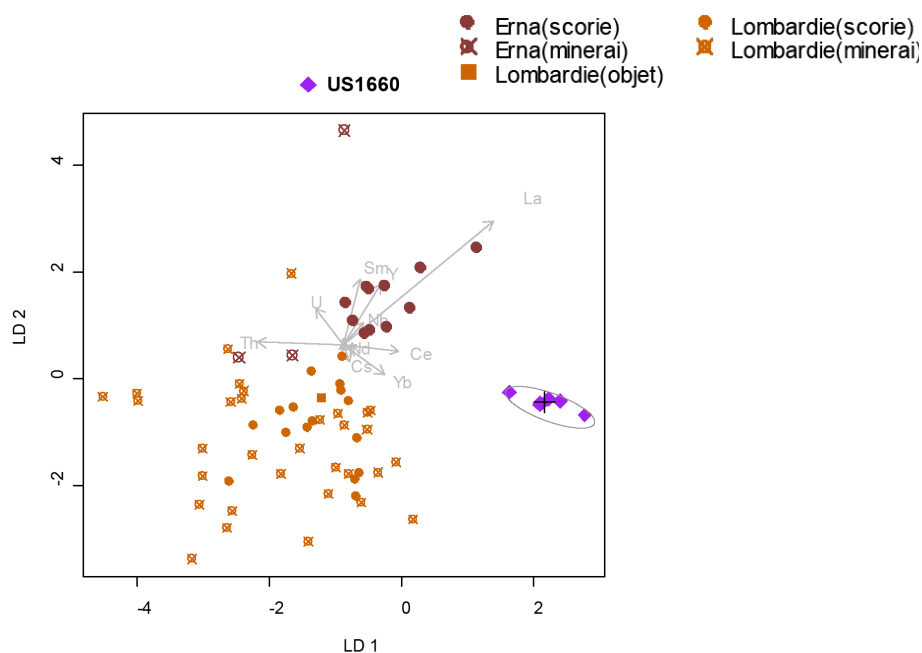


**Figure L.9 – Analyse discriminante des  $X_{ij}$  des échantillons définissant la Lombardie, le Piani d'Erna, et du lingot US1660 sur le plan discriminant (LD1,LD2)**

<sup>10</sup> Les données élémentaires utilisées ici, sont tirées de la publication Cucini & Tizzoni (2006). *Gli scarti della produzione siderurgica*. p.109-110. Pour plus de renseignements sur les recherches archéométallurgiques menées dans cette région, se reporter aux travaux de M. Tizzoni et C. Cucini (2006).

► Enfin, la région du Piémont avoisine celle du Dauphiné. Au XVI<sup>e</sup> siècle, dans cette zone, transitaient des fers provenant des Alpes italiennes mais certainement également du bassin dauphinois. Aussi, il ne nous a pas semblé inutile de comparer, toujours selon la démarche n°1, les signatures chimiques de ces deux zones sidérurgiques avec celle de la Clé retrouvée en Piémont et pour laquelle une origine lombarde a pu être préalablement écartée. Les résultats de l'analyse multivariée sont illustrés dans la Figure L.10. Les projections associées à chacune des classes sont suffisamment distinctes pour mettre en lumière une provenance autre que celles proposées pour l'objet Clé16.

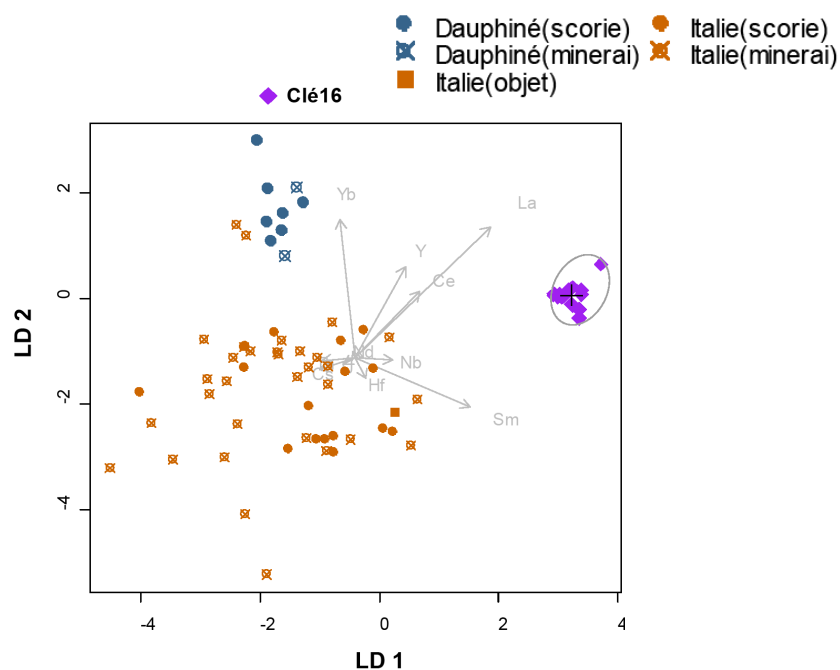


Figure L.10 – Analyse discriminante des  $X_{ij}$  des échantillons définissant la Lombardie, le Dauphiné, et du lingot US1772 sur le plan discriminant (LD1, LD2)





## Annexe M

### ÉTUDE DE LA PROVENANCE DE FERS DE CONSTRUCTION DE LA CATHÉDRALE D'AMIENS

Les comptes de la fabrique de la cathédrale d'Amiens, construite au XIII<sup>e</sup> siècle, font mention de commandes de fer d'Espagne, pour le chaînage du *triforium* de la cathédrale (L'Héritier, 2007). Par conséquent, il semblerait que les fabriques de la cathédrale aient cherché à se procurer ce matériau. Cependant, comme l'affirment certains auteurs, il est « difficile de définir exactement ce qui était vendu sous le nom de fer d'Espagne ». Au-delà d'une simple provenance de la péninsule ibérique, cette appellation peut faire référence à des matériaux de qualité supérieure. D'après L'Héritier (2007), plusieurs types de fer pouvaient être vendus sous cette appellation.

A la fin de la période médiévale, le fer espagnol est vraisemblablement un fer du procédé de réduction directe, provenant des Pyrénées, région qui utilise un minerai manganésifère. Les études effectuées sur les fers d'œuvre de la cathédrale ont montré que, pour certains d'entre eux, les inclusions contenaient une teneur élevée en manganèse. Une provenance ariégeoise n'est donc pas à exclure pour ces chantiers. Il est légitime, sans chercher à se questionner sur l'origine véritable du fer d'Espagne, de comparer les signatures de l'Ariège à celles des fers de construction de la cathédrale d'Amiens.

La plupart des échantillons prélevés sur le chaînage d'Amiens ne sont pas issus du procédé direct<sup>11</sup>. Jusqu'à présent, seuls les prélèvements effectués sur le chaînage situé à l'extrémité du transept sud pourraient correspondre au fer d'Espagne. Ils montrent en effet l'utilisation de fer de réduction directe (Figure M.11 ; Gauche) et leurs inclusions contiennent des teneurs très élevées en manganèse (~10% de MnO), caractéristique de la région pyrénéenne. La Figure M.11 (Droite) montre que les teneurs en cet élément et en phosphore sont en effet comparables à celles présentes dans les échantillons ariégeois.

---

<sup>11</sup> Une soixantaine de prélèvements avait été effectuée par P.Dillmann sur les chaînages du *triforium*. Les analyses métallographiques ont montré que ces fers étaient essentiellement constitués de fer phosphoreux issu de l'affinage de la fonte. Dillmann (2006), *De Soissons à Beauvais : le fer des cathédrales de Picardie, une approche archéométrique*. Dans L'Homme et la Matière. L'emploi du plomb et du fer dans l'architecture gothique. Actes du colloque 2006.

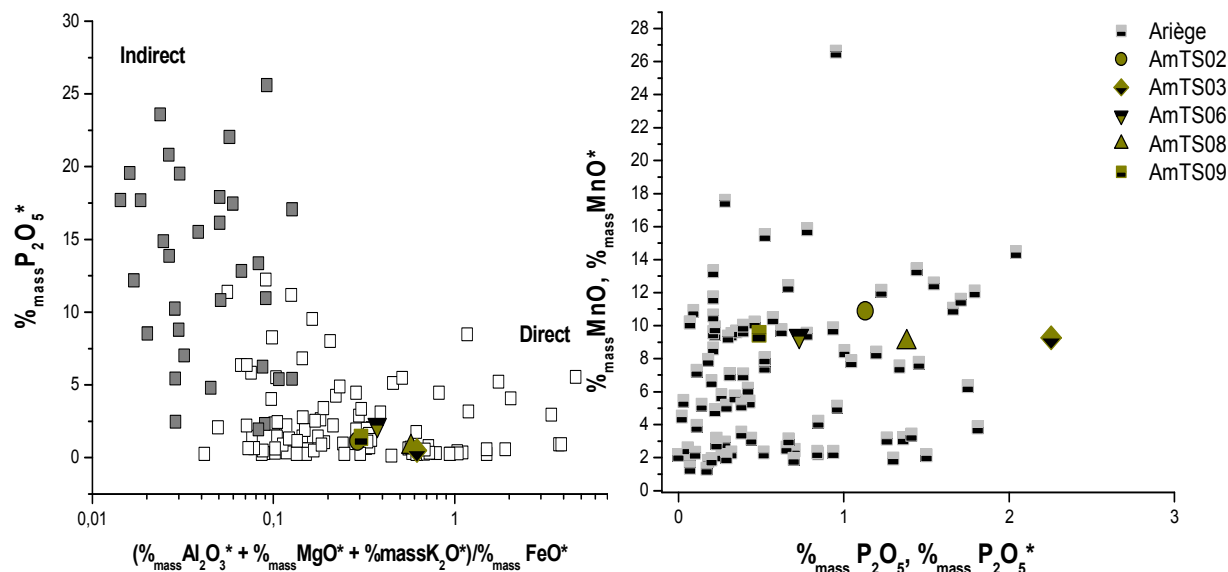


**Figure M.11 – (Gauche) : Discrimination des procédés pour les inclusions des échantillons de la cathédrale d'Amiens (EDS). (Droite) : Comparaison des teneurs absolues (moyennes pondérées) en MnO (MnO\*) et P<sub>2</sub>O<sub>5</sub> (P<sub>2</sub>O<sub>5</sub>\*) dans les échantillons ariégeois et les inclusions des échantillons d'Amiens (EDS)**

Pour vérifier la compatibilité de ces fers de construction avec une provenance du bassin sidérurgique ariégeois, nous avons utilisé la démarche n°1 de la méthodologie développée pour l'approche multivariée. Etant donné la petite taille des inclusions observées dans le métal des échantillons, seuls deux prélèvements, AmTS02 et AmTS06, ont pu faire l'objet de cette analyse<sup>12</sup>. Ci-dessous, sont présentés les résultats des projections de l'analyse discriminante (Tableau M.8 et Figure M.12). Les valeurs des distances médiane et quartile obtenues sont élevées, nettement supérieures aux valeurs seuils de non compatibilité. Celles-ci nous permettent d'écarter, avec certitude, l'Ariège comme zone de production pour ces fers.

<sup>12</sup> Rappelons que pour les analyses LA-ICP-MS, la taille d'ablation laser utilisée au Centre Ernest Babelon (Orléans) dans une matrice scoritique est d'environ 80 µm. Dans ce cas, les inclusions de taille trop petite (<80 µm) ne peuvent être analysées. À propos de la méthodologie de travail pour les analyses ICP-MS par ablation laser, se référer au Chapitre II § III.3.3.

**Tableau M.8 – Distances de la médiane et du troisième quartile des Proj. $X_{O1}$  au domaine des Proj. $X_{ES,Ariège}$  sur l'axe LD1 pour AmTS02 et AmTS06**

Echantillons	AmTS02	AmTS06
$D_{méd.}$	<b>3,45</b>	<b>3,15</b>
$D_{quart.}$	<b>3,31</b>	<b>2,94</b>

$D_{méd.}$  : distance de la médiane des Proj. $X_{O1}$  au domaine des Proj. $X_{ES,Ariège}$ .

$D_{quart.}$  : distance du troisième quartile des Proj. $X_{O1}$  au domaine des Proj. $X_{ES,Ariège}$ .

$D_{méd.} \leq 0,27$	$0,27 < D_{méd.}$	$0,27 < D_{méd.} < 1,16$	$D_{méd.} \geq 1,16$
$D_{quart.} \leq 0,01$	$D_{quart.} < 0,01$	$0,01 < D_{quart.} < 0,92$	$D_{quart.} \geq 0,92$
Compatible	Probable	Indéterminé	Non compatible

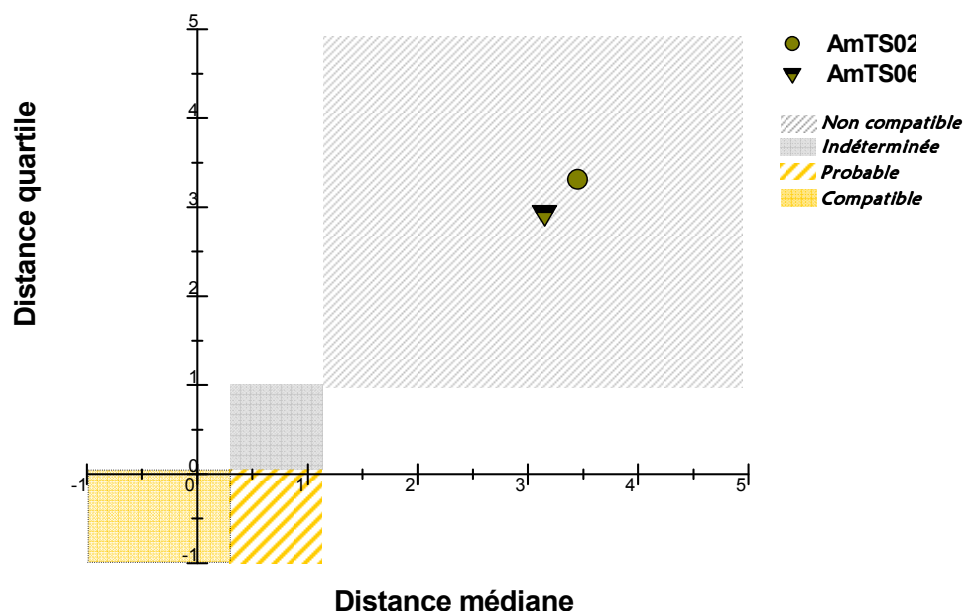


**Figure M.12 – Compatibilité avec une origine ariégeoise pour les fers de construction AmTS02 et AmTS06 en fonction des distances médiane et quartile**

Dans la mesure où nous ne disposons que de la signature de la zone ariégeoise, seules des comparaisons avec ce bassin ont pu être réalisées dans ce travail. Il est évident que les signatures chimiques de ces prélèvements devront, par la suite, être confrontées à celle du Pays Basque. Les minerais de cet autre espace pyrénéen sont également caractérisés par de fortes teneurs en manganèse (Serneels, 2002) et les forges basques ont exporté leur fer dans une partie de l'Europe médiévale (Verna, 2001). Si le « fer d'Espagne » a effectivement été utilisé, en faibles quantités néanmoins, sur le chaînage de la cathédrale d'Amiens et si, pour ce cas précis, il désigne réellement une provenance de la péninsule ibérique, c'est donc avant tout

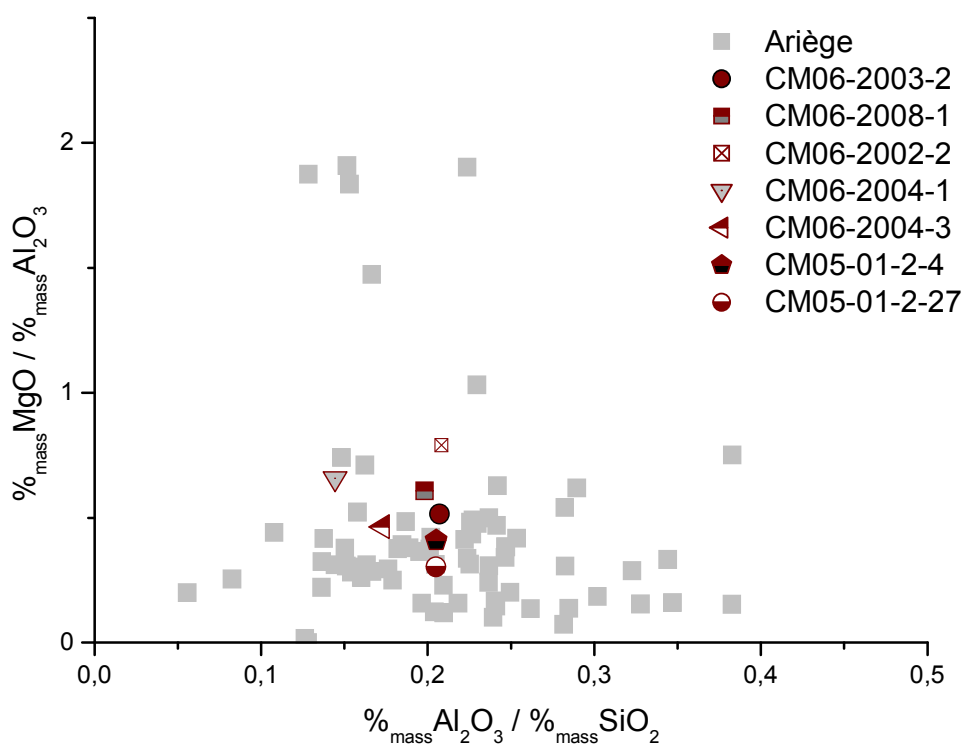
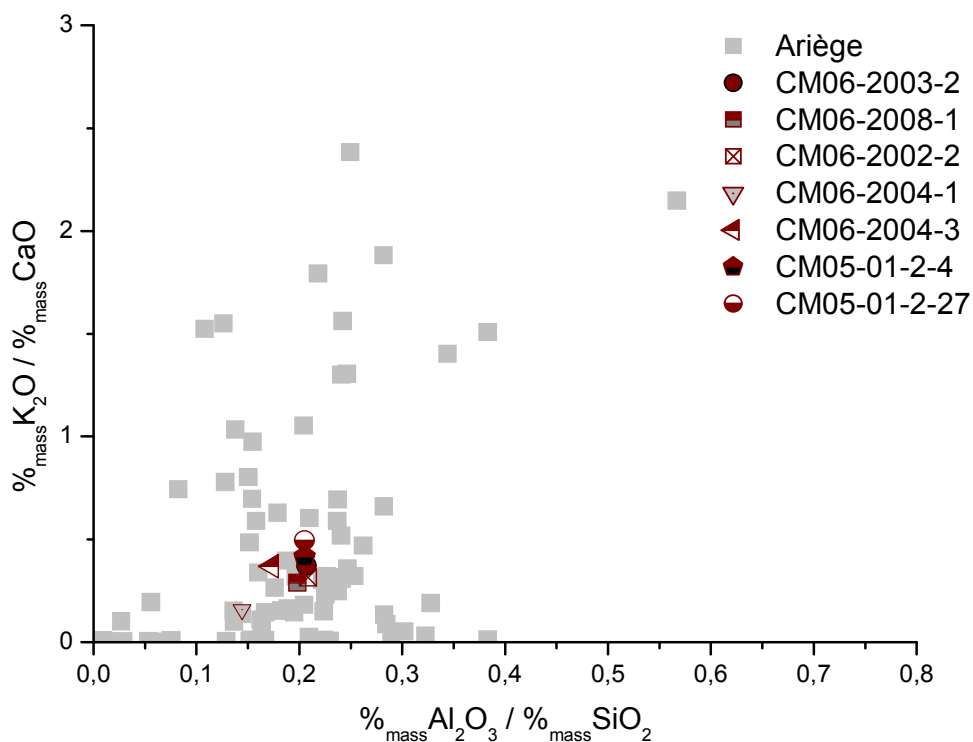
vers cet espace qu'il faudra se tourner. Une étude de plus grande envergure devra donc être menée sur cette partie occidentale des Pyrénées.

## Annexes N

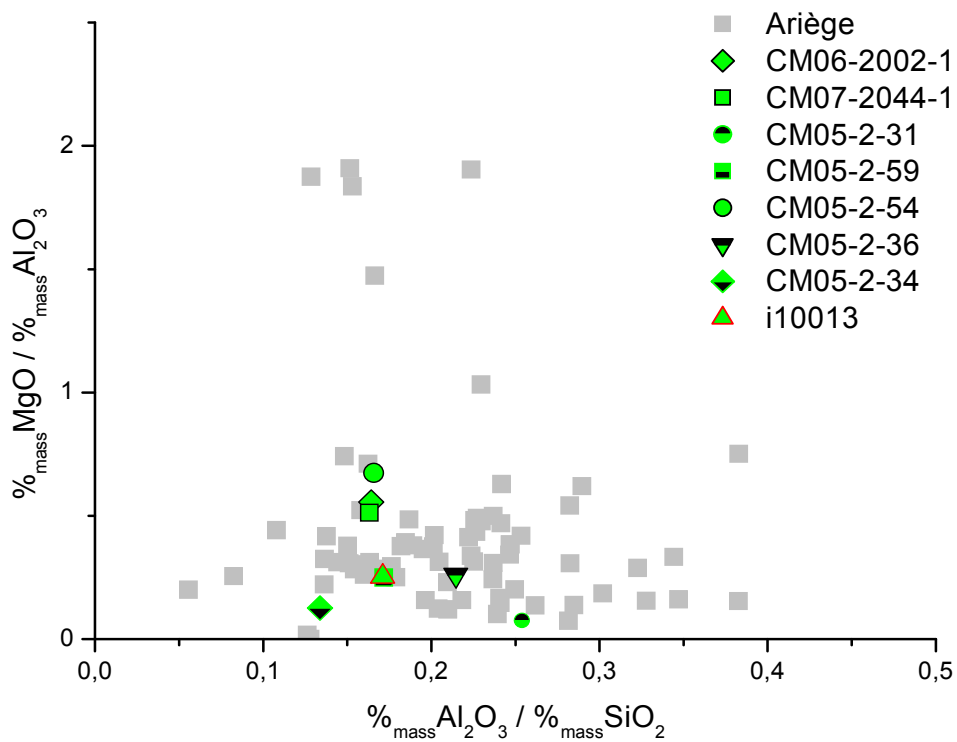
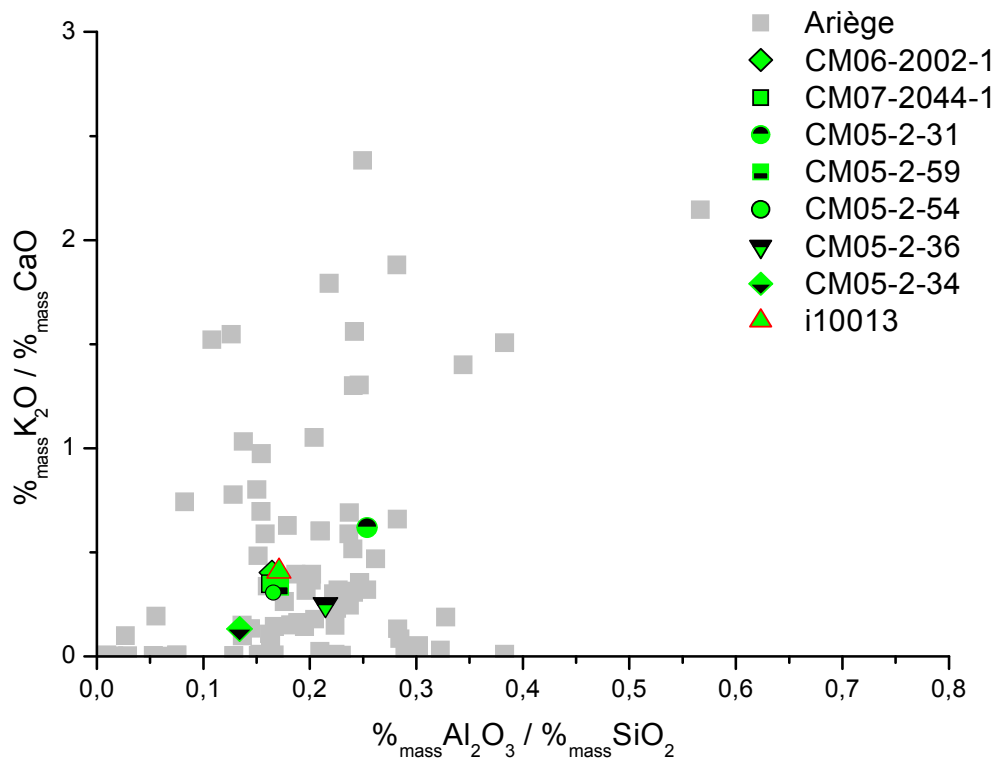
COMPARAISONS DES RAPPORTS D'ÉLÉMENTS MAJEURS  
( $\%_{\text{mass}}\text{Al}_2\text{O}_3/\%_{\text{mass}}\text{SiO}_2$ ,  $\%_{\text{mass}}\text{K}_2\text{O}/\%_{\text{mass}}\text{CaO}$ ,  $\%_{\text{mass}}\text{MgO}/\%_{\text{mass}}\text{Al}_2\text{O}_3$ )  
DANS LES OBJETS ET LES ÉCHANTILLONS ISSUS DES  
ESPACES ARIÉGEOIS ET LOMBARD



## Annexe N.1 - COMPARAISON DES RAPPORTS DES COMPOSÉS NON RÉDUITS DANS LES OBJETS PRODUITS SUR LE SITE DE CASTEL-MINIER ET LES ÉCHANTILLONS DÉFINISSANT L'ESPACE ARIÉGEOIS

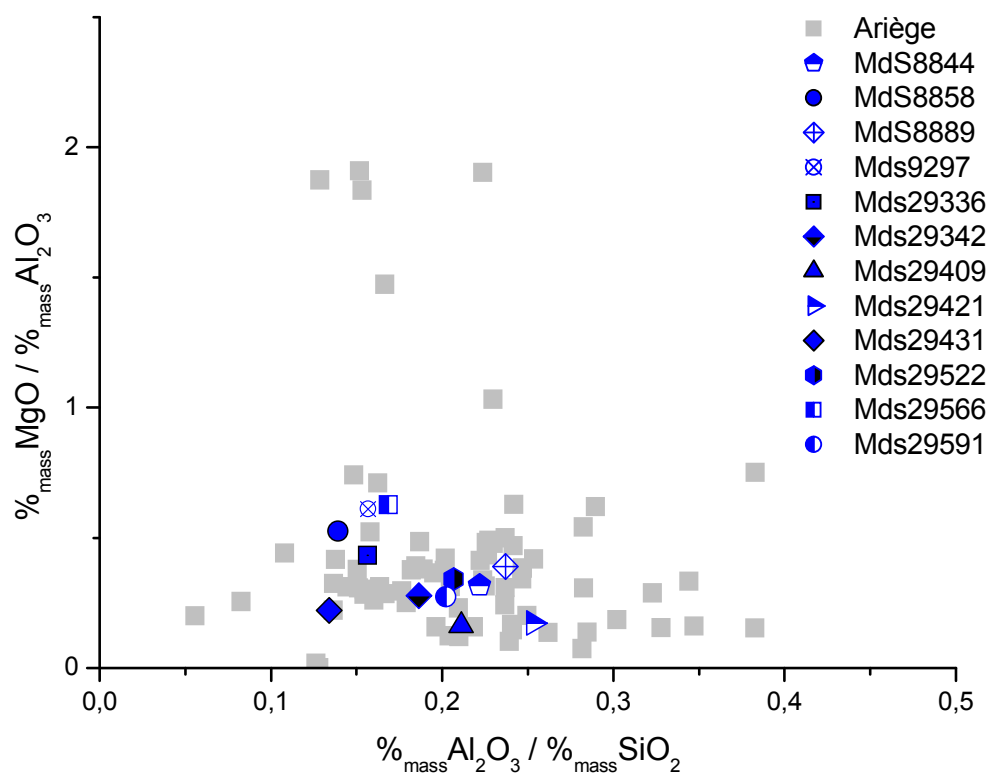
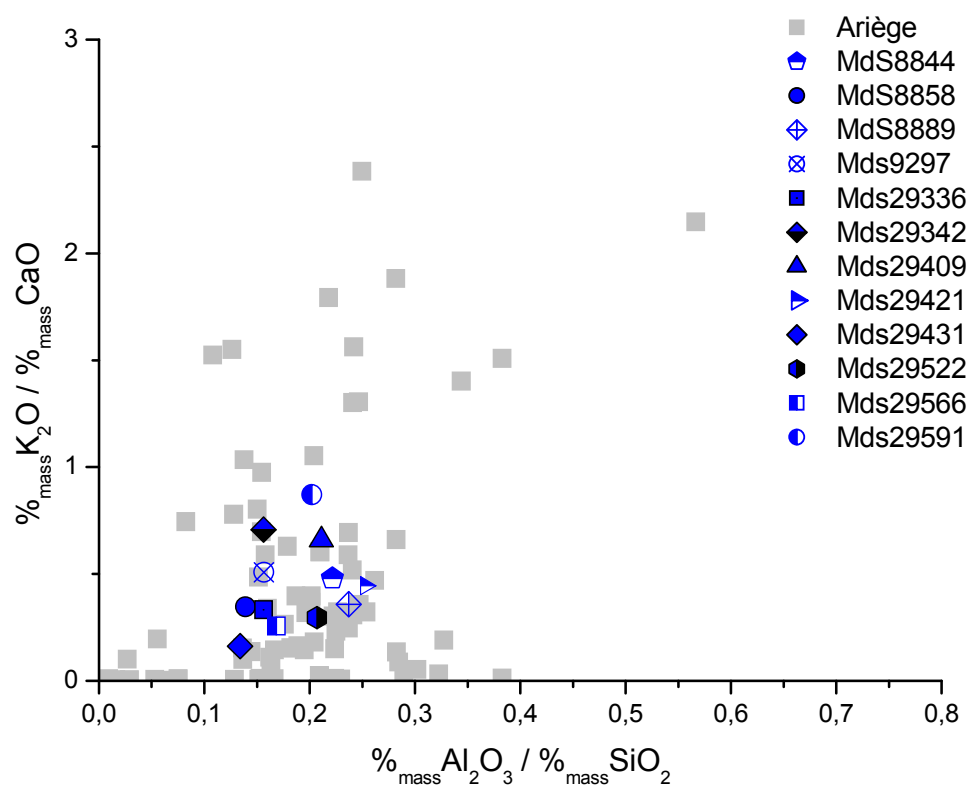


## Annexe N.2 - COMPARAISON DES RAPPORTS DES COMPOSÉS NON RÉDUITS DANS LES OBJETS, D'ORIGINE À IDENTIFIER, MIS AU JOUR À CASTELMINIER ET LES ÉCHANTILLONS DÉFINISSANT L'ESPACE ARIÉGEAIS

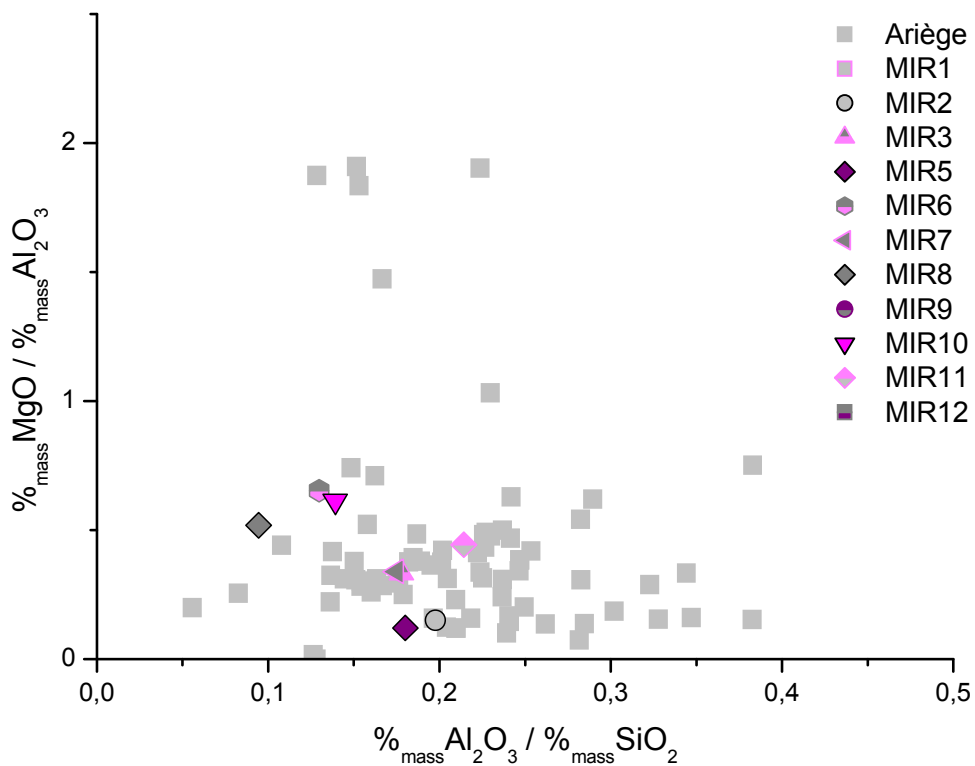
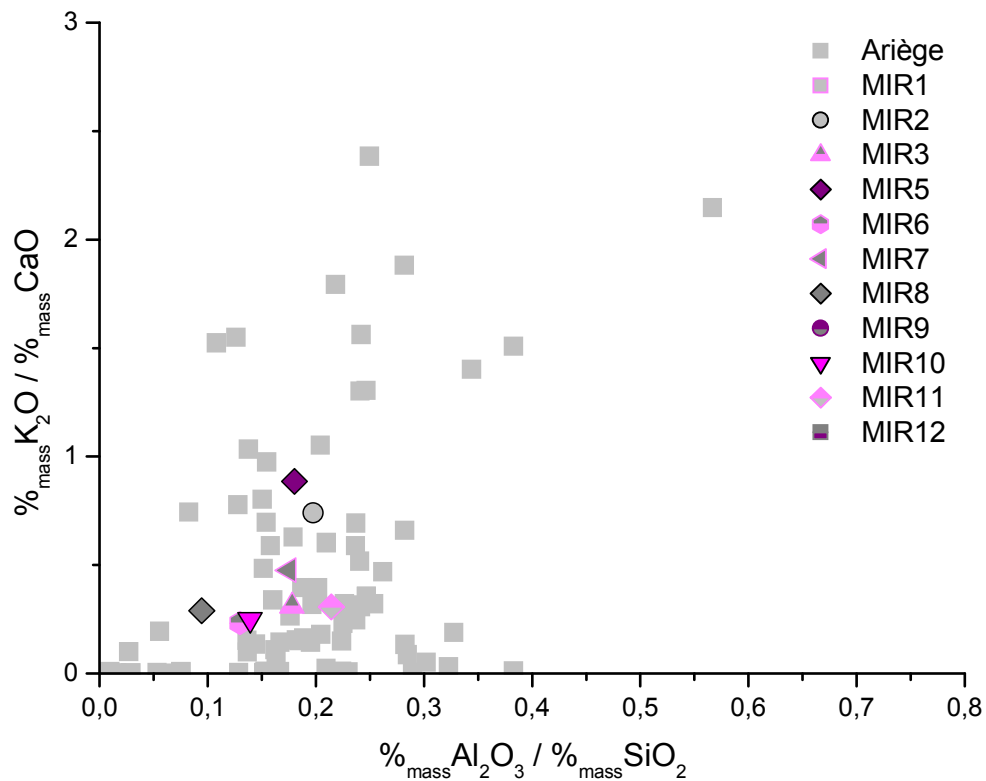




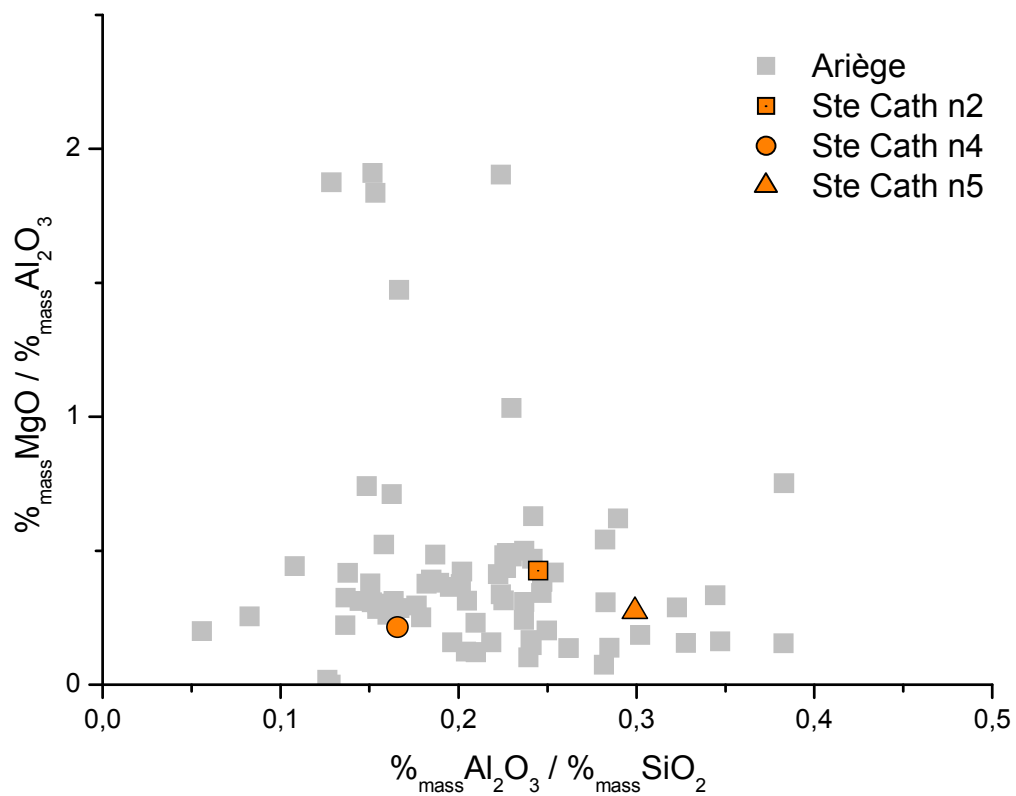
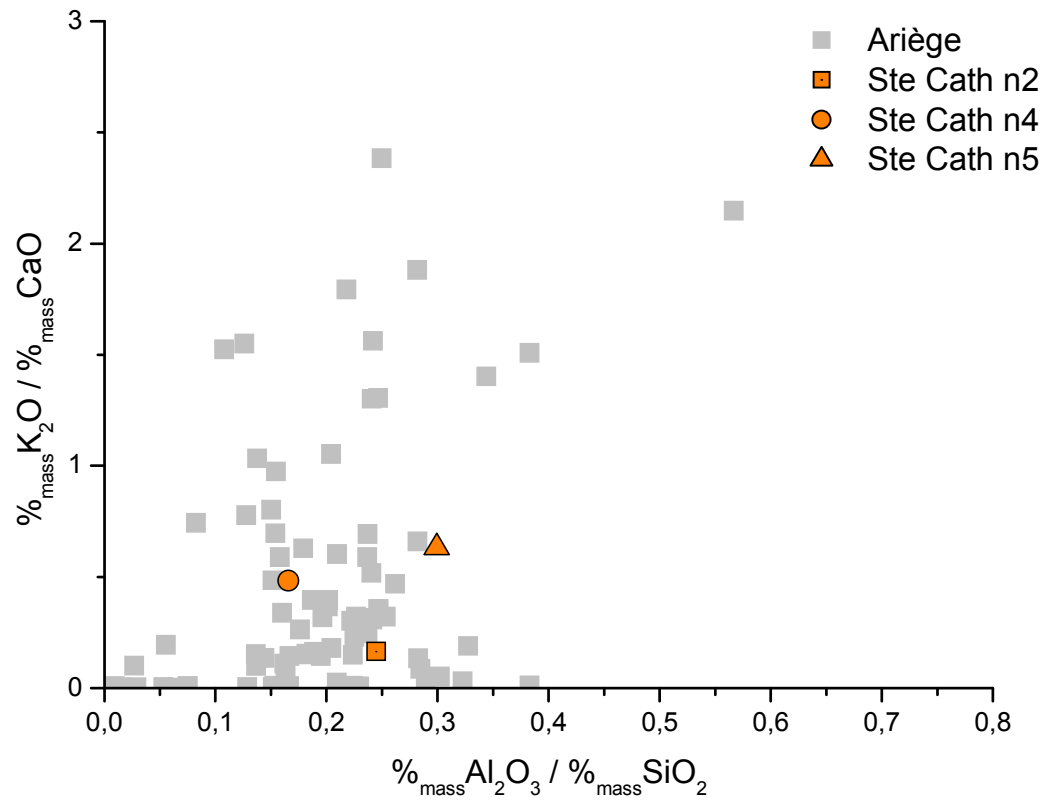
### Annexe N.3 - COMPARAISON DES RAPPORTS DES COMPOSÉS NON RÉDUITS DANS LES OBJETS, D'ORIGINE À IDENTIFIER, MIS AU JOUR À MONTRÉAL-DE-SOS ET LES ÉCHANTILLONS DÉFINISSANT L'ESPACE ARIÉGOIS



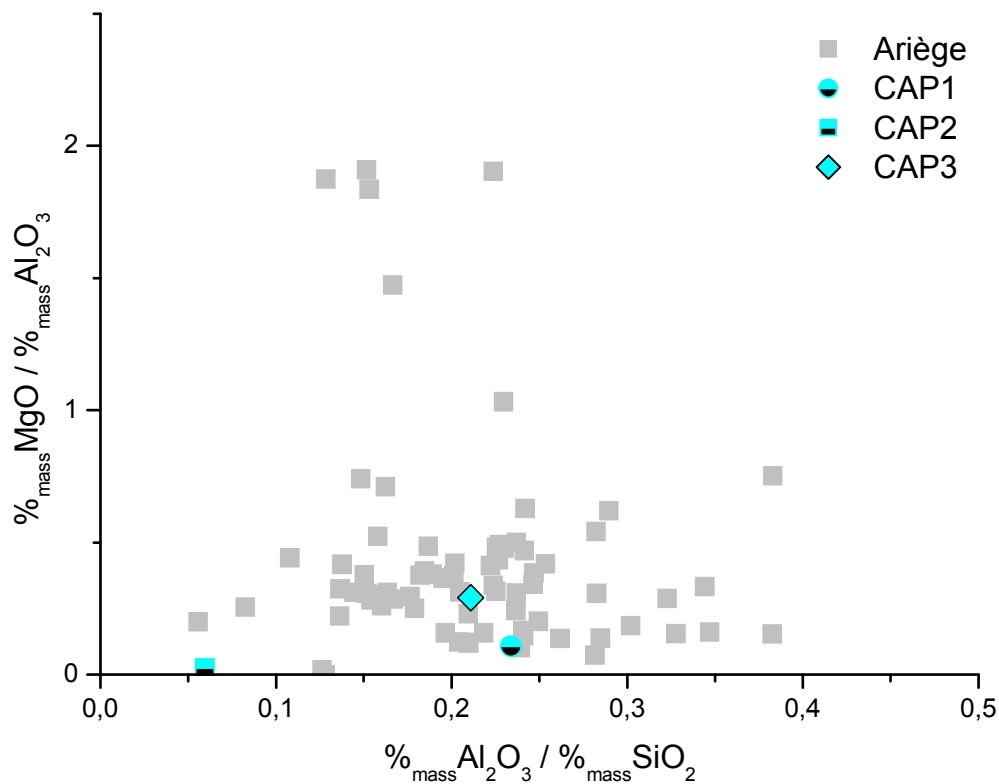
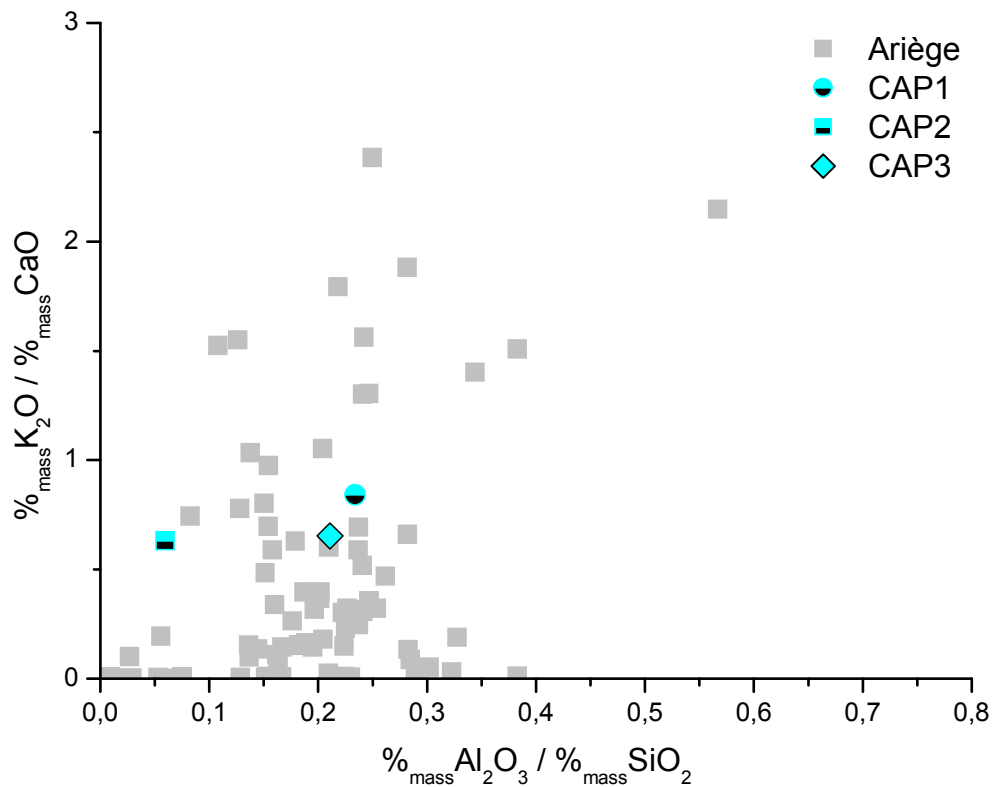
## Annexe N.4 - COMPARAISON DES RAPPORTS DES COMPOSÉS NON RÉDUITS DANS LES CLOUS, D'ORIGINE À IDENTIFIER, MIS AU JOUR À MIRABAT ET LES ÉCHANTILLONS DÉFINISSANT L'ESPACE ARIÉGEAIS



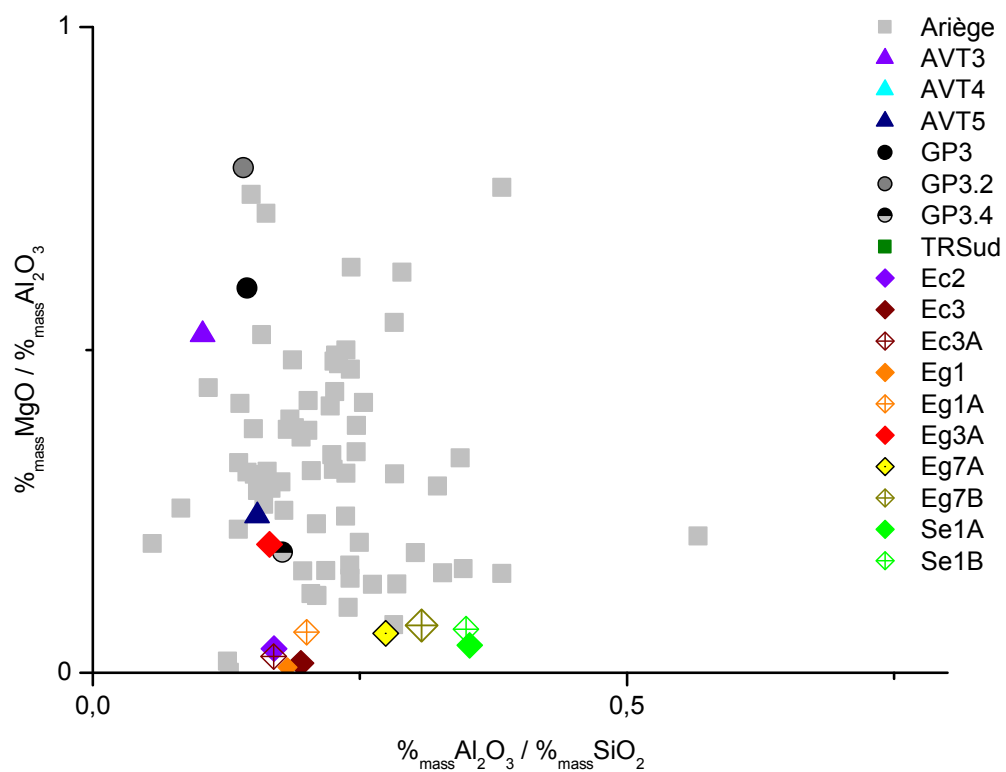
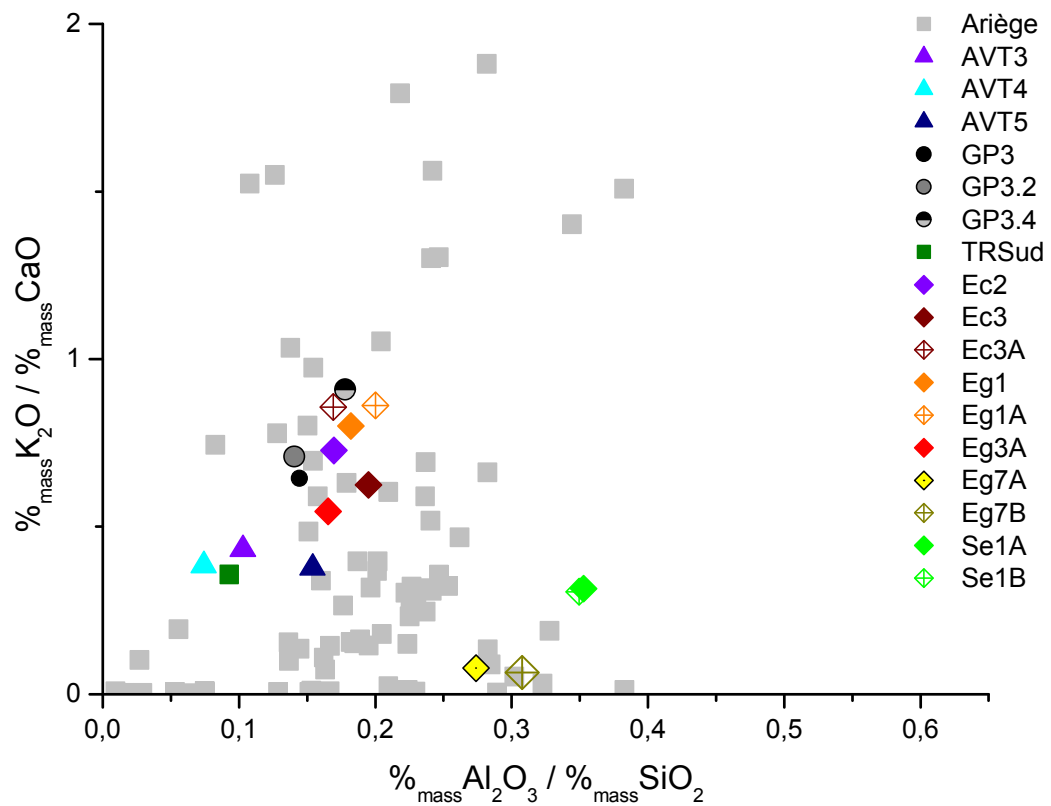
## Annexe N.5 - COMPARAISON DES RAPPORTS DES COMPOSÉS NON RÉDUITS DANS LES CLOUS, D'ORIGINE À IDENTIFIER, MIS AU JOUR À STE-CATHERINE ET LES ÉCHANTILLONS DÉFINISSANT L'ESPACE ARIÉGEOIS



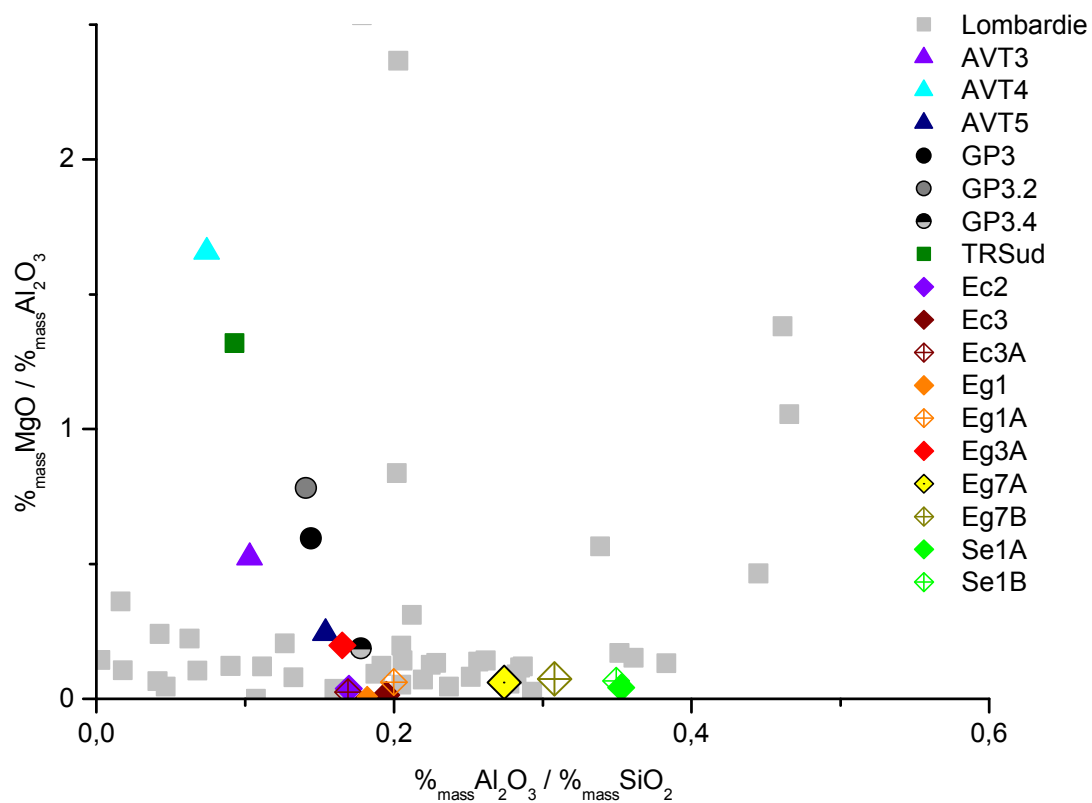
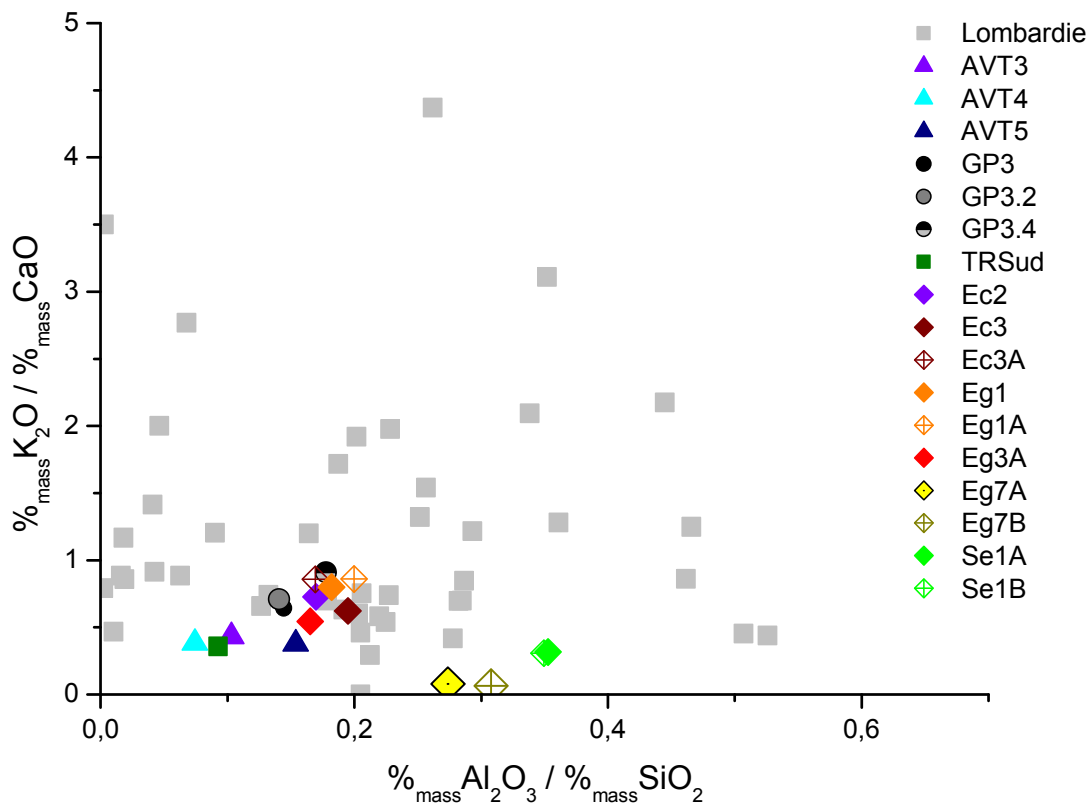
## Annexe N.6 - COMPARAISON DES RAPPORTS DES COMPOSÉS NON RÉDUITS DANS LES TIRANTS DE LA COLLÉGIALE DE CAPESTANG ET LES ÉCHANTILLONS DÉFINISSANT L'ESPACE ARIÉGIOIS



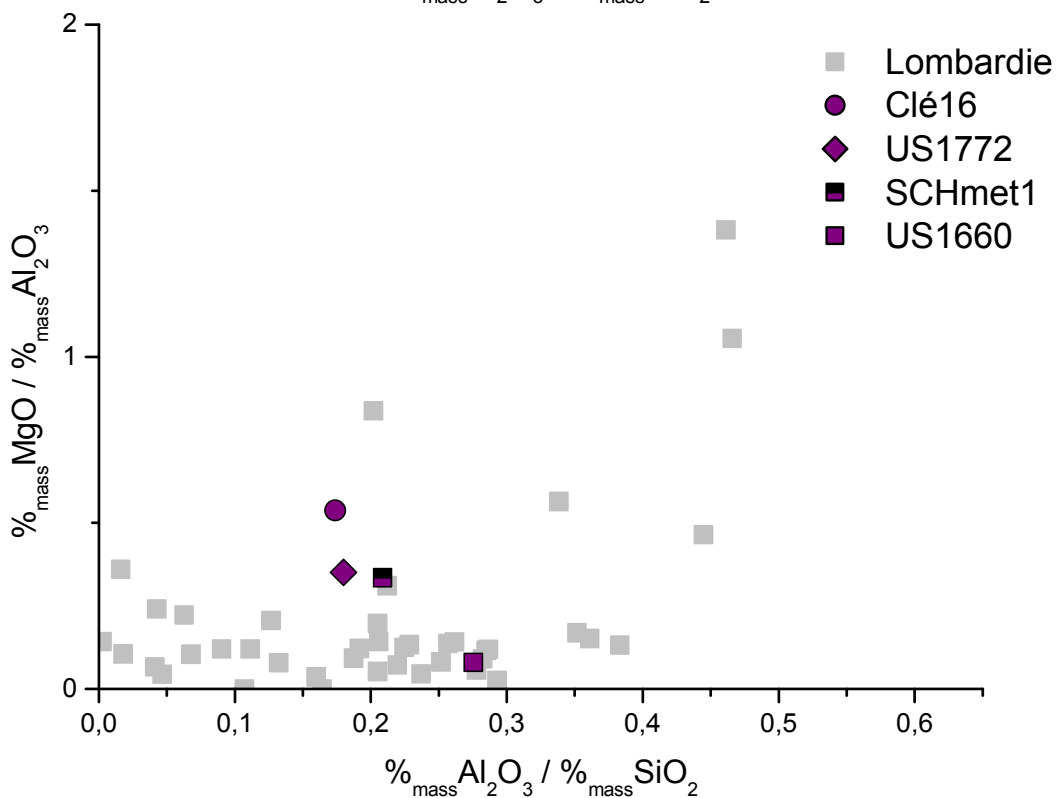
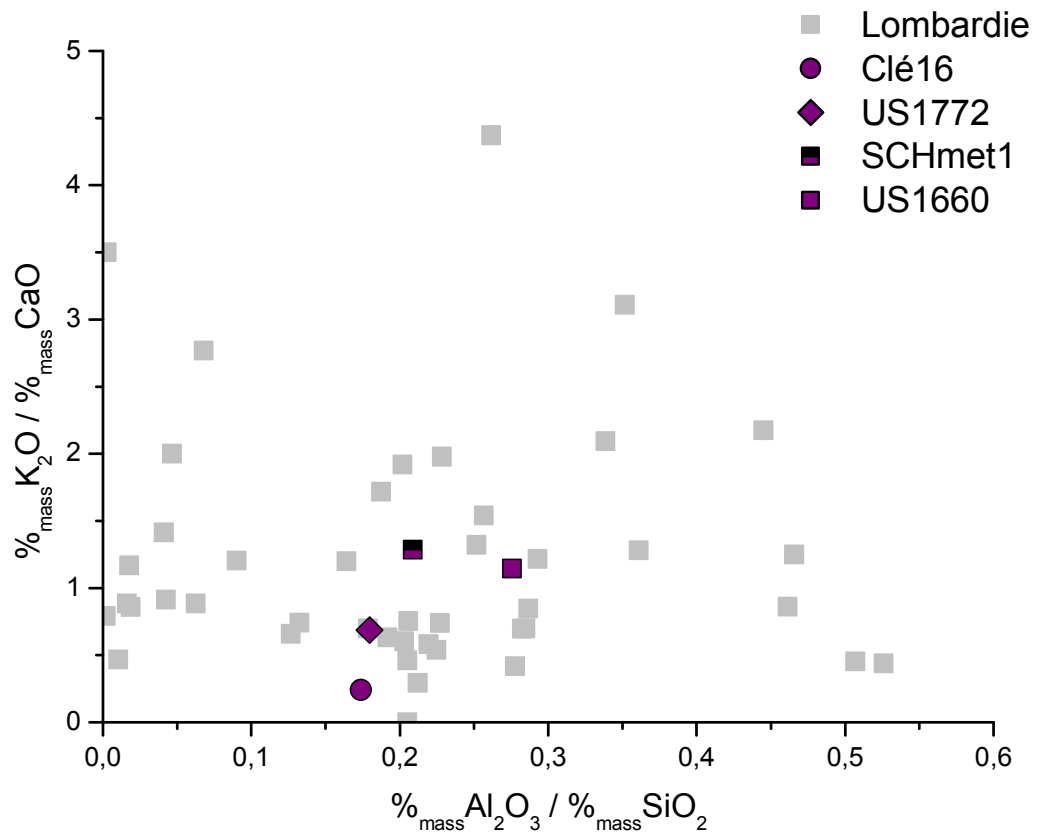
## Annexe N.7 - COMPARAISON DES RAPPORTS DES COMPOSÉS NON RÉDUITS DANS LES FERS DE CONSTRUCTION DU PALAIS DES PAPES D'AVIGNON ET LES ÉCHANTILLONS DÉFINISSANT L'ESPACE ARIÉGEAIS



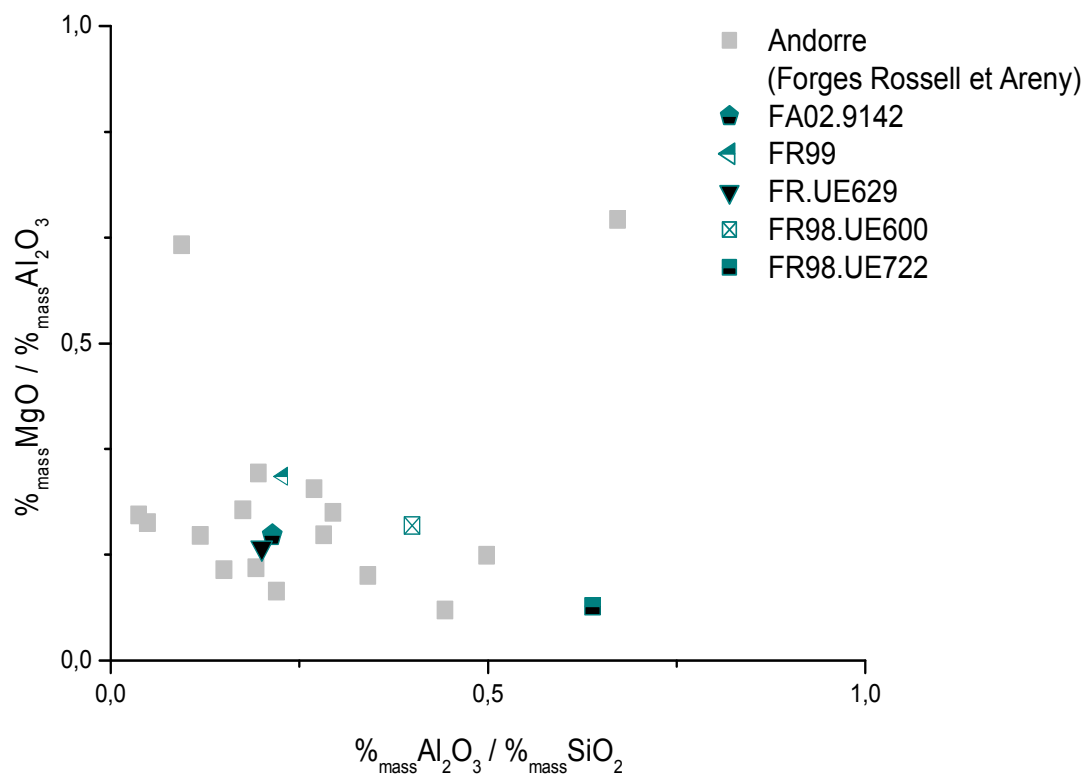
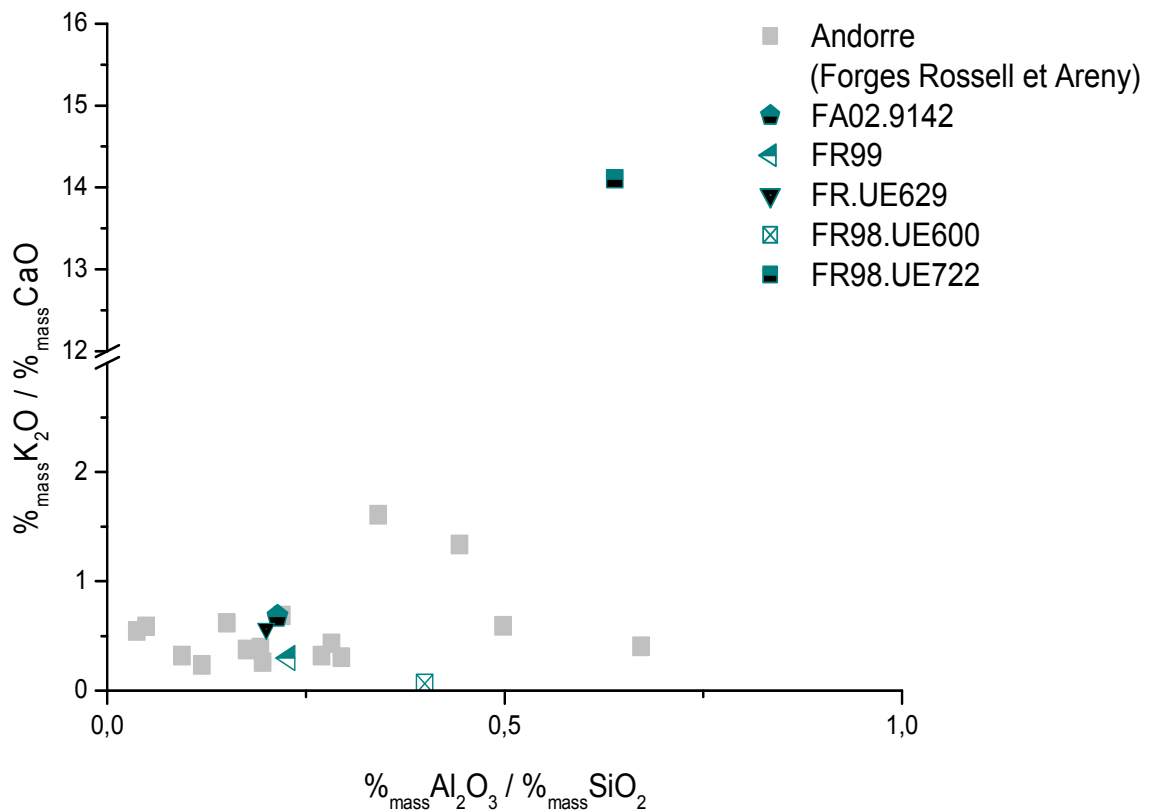
## Annexe N.8 - COMPARAISON DES RAPPORTS DES COMPOSÉS NON RÉDUITS DANS LES FERS DE CONSTRUCTION DU PALAIS DES PAPES D'AVIGNON ET LES ÉCHANTILLONS DÉFINISSANT L'ESPACE LOMBARDE



## Annexe N.9 - COMPARAISON DES RAPPORTS DES COMPOSÉS NON RÉDUITS DANS LES OBJETS DE MILAN ET DU PIÉMONT, ET LES ÉCHANTILLONS DÉFINISSANT L'ESPACE LOMBARDE

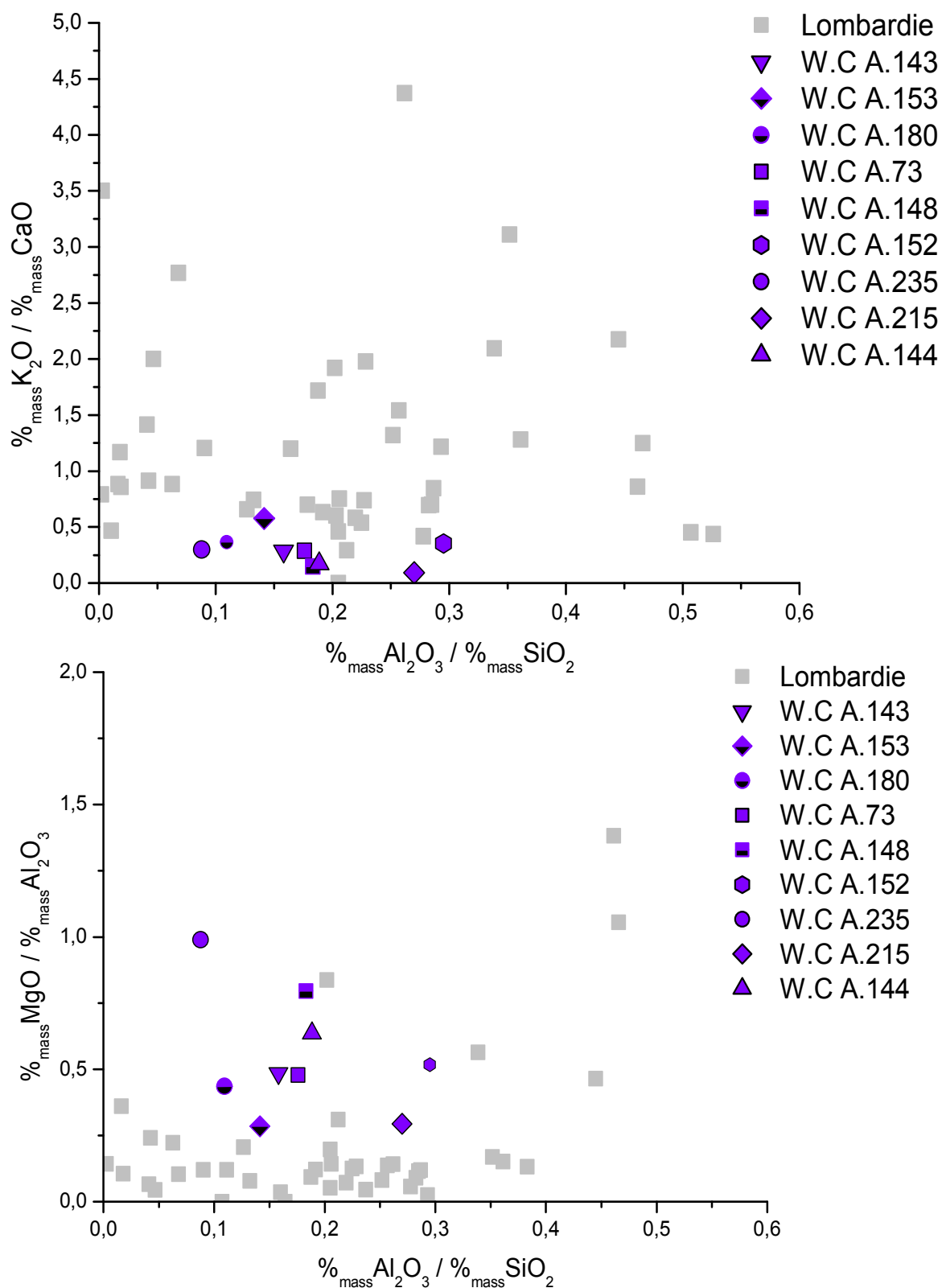


## Annexe N.10 - COMPARAISON DES RAPPORTS DES COMPOSÉS NON RÉDUITS DANS LES ÉCHANTILLONS MIS AU JOUR SUR LES FORGES ROSSELL ET ARENY (MINÉRAIS, SCORIES, OBJETS)





## Annexe N.11 - COMPARAISON DES RAPPORTS DES COMPOSÉS NON RÉDUITS DANS LES PRÉLÈVEMENTS D'ARMURES DE LA WALLACE COLLECTION ET LES ÉCHANTILLONS DÉFINISSANT L'ESPACE LOMBARDE





## **Annexes O**

OBSERVATIONS MACROSCOPIQUES ET MICROSCOPIQUES  
SUR DES SCORIES DE RÉDUCTION DE CASTEL-MINIER.  
ANALYSES DES PHASES DE COMPOSITION



Nous allons présenter dans cette annexe, quelques observations résultantes de l'analyse de scories de réduction provenant des deux ferriers (ferrier 1 et 2) du site de Castel-Minier.

### **SCORIE DE FOND DE FOUR : CM05-01-4-2**

- *Morphologie et observations macroscopiques*

Le fond de four est de taille relativement importante. Il pèse 9.3 kg pour des dimensions de 33 cm x 23 cm et une épaisseur maximale de 8 cm (Figure O.13).

On peut observer une accumulation de coulures de scories superposées. Sur la partie supérieure, on note la présence de cordons très larges. La face inférieure moule la forme du sol et porte les empreintes des matériaux sur lesquelles le liquide s'est déversé.

La pièce a été tronçonnée dans la partie centrale sur son plus petit axe, de manière à obtenir trois coupes transversales. L'une d'entre elles (Figure O.13) laisse apparaître un fond de four majoritairement constitué de scorie, aucun fragment métallique n'est visible. La porosité est abondante (51%) et de taille variable (tailles centimétriques à millimétriques) avec une répartition aléatoire. Des stratifications de différentes coulées sont perceptibles et sont délimitées par un léger liseré dans la figure. Il a également été possible d'identifier des traces de charbon consumé sur d'autres coupes transversales mais jamais en grande quantité (une seule coupe transversale en possède une quantité < 10%).

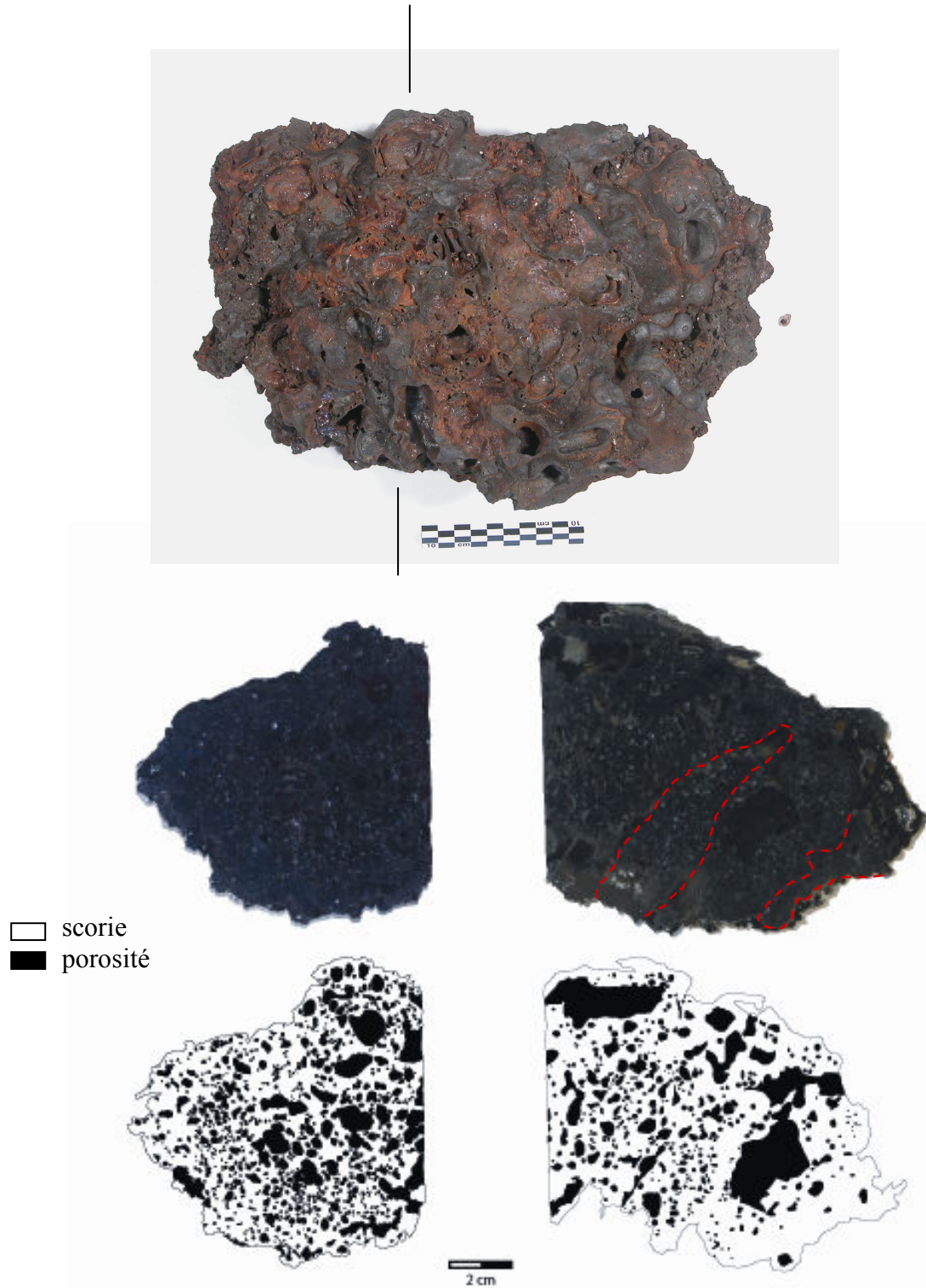
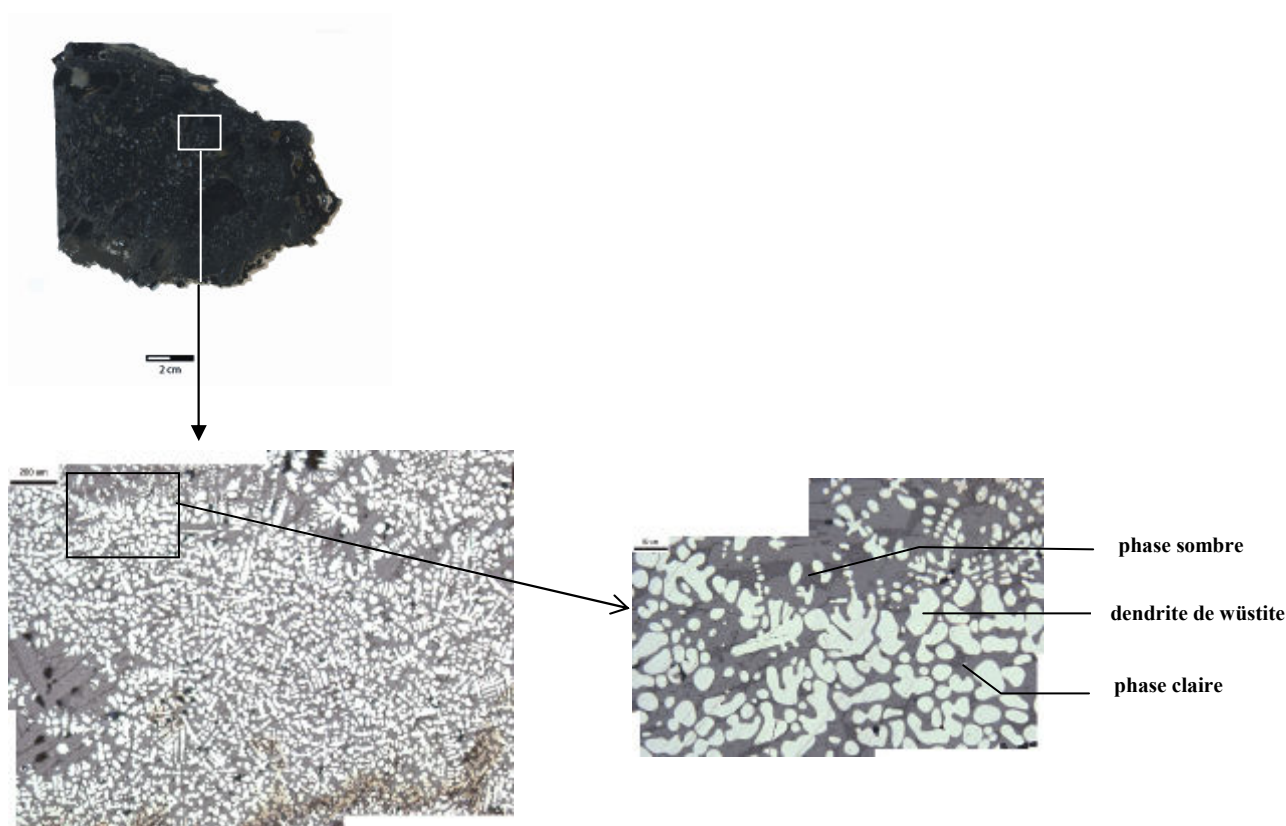


Figure O.13 – Macrographie du fond de four CM05-01-4-2

- *Observations microscopiques*

Un balayage complet de l'échantillon est effectué au microscope optique, pour appréhender la structure du matériau. Des fragments de métal (de tailles micrométriques) sont visibles sur certaines zones mais restent rares. Le plus souvent, on les retrouve à proximité des porosités. L'observation microscopique nous permet d'identifier trois phases différentes (Figure O.14). Par endroit, des dendrites sont présentes en forte proportion, ce qui indique que la scorie est passée à l'état liquide pendant la réduction. Une phase gris clair cristallisée (sous forme de lattes) qui constitue la majorité de la matrice scoritique semble correspondre à une phase siliceuse. Entre ces lattes, on trouve une phase plus particulière, beaucoup plus sombre.



**Figure O.14 – Microscopie optique de l'échantillon CM05-01-4-2**

- *Analyses élémentaires*

Nous allons procéder en deux temps. Dans une première étape, nous considérerons les phases particulières qui constituent la matrice du fond de four. Dans une deuxième étape, nous considérerons l'ensemble des analyses globales sur toute la surface de l'échantillon.

Des analyses ponctuelles ont été effectuées par spectrométrie EDS pour connaître la composition des différentes phases observées au microscope optique. Les résultats sont

exprimés en teneurs massiques pour chaque élément puis, à partir de ces teneurs ils sont exprimés en oxydes (Tableau O.9 et Tableau O.10).

**Tableau O.9 – Composition (en %<sub>mass</sub>) des différentes phases qui composent la matrice scoritique**

Eléments % <sub>mass</sub>	O	Fe	Al	Si	Mn	Ca	K	Na	Mg	P
oxyde de fer	23,38	66,43	tr	tr	6,77	0,5	tr	n.d.	tr	tr
phase claire	35,78	23,96	1,37	16,45	10,96	6,68	0,7	tr	2,48	0,5
phase sombre	38,83	11,06	9,24	16,88	4,17	7,29	9,61	0,78	0,62	0,8

**Tableau O.10 – Composition (en %<sub>mass</sub> d'oxydes) des différentes phases qui composent la matrice scoritique**

Oxydes % <sub>mass</sub>	FeO	Al <sub>2</sub> O <sub>3</sub>	SiO <sub>2</sub>	MnO	CaO	K <sub>2</sub> O	NaO	MgO	P <sub>2</sub> O <sub>5</sub>
oxyde de fer	85,46	0,77	1	8,74	0,71	tr	n.d.	0,78	0,48
phase claire	30,82	2,58	35,2	14,15	9,34	0,84	tr	4,12	1,14
phase sombre	14,23	17,45	36,12	5,39	10,19	11,58	1,05	1,02	1,84

On retrouve dans la scorie une quantité importante de manganèse. Cet élément se partage entre les trois phases de la matrice. La stoechiométrie de la phase d'oxyde de fer est compatible avec une phase d'oxyde de fer de type wüstite. Ainsi, on vérifie en même temps que la valence du fer est +2. Cependant, une quantité élevée de MnO (8,74%) est détectable dans ces dendrites. Le manganèse viendrait donc se substituer dans cette phase sous forme : (Fe<sub>x</sub>,Mn<sub>y</sub>)O. La phase plus sombre semble, quant à elle, être constituée du groupement silicate. D'autres éléments sont également présents: Fe, Al, Ca, K et Mn (4-5%). Il n'est pas possible pour l'instant de déterminer cette phase. L'analyse élémentaire de la phase claire suggère qu'il s'agit d'olivine : (Fe, Mn, Mg, Ca)SiO<sub>4</sub>. Une forte proportion de MnO passe préférentiellement dans cette phase (14%).

Ainsi :

- l'élément Mn se partage entre les trois phases (mais une majorité passe dans l'olivine).
- les éléments K et Al se trouvent dans la même phase (phase sombre).
- l'élément Ca se partage entre les deux phases siliceuses.



### SCORIE DE FOND DE FOUR : CM05-01-4-4

- *Morphologie et observations macroscopiques*

Ce fond de four présente une morphologie assez identique au fond de four précédent mais la masse de scorie est moins importante. Son diamètre est de 15cm pour une longueur maximale de 29 cm (Figure O.15).

Tronçonné selon son petit axe dans sa partie centrale, le plan de coupe ne révèle à ce stade aucune présence de charbon de bois mais quelques fragments métalliques (de tailles millimétriques). Comme pour l'autre fond de four, la porosité est abondante (le cœur de la scorie est entièrement poreux, c'est pourquoi le pourcentage de porosité n'a pas été calculé) et de taille variable (tailles centimétriques à millimétriques). Les contours des porosités peuvent être très globuleux ou très déchiquetés.

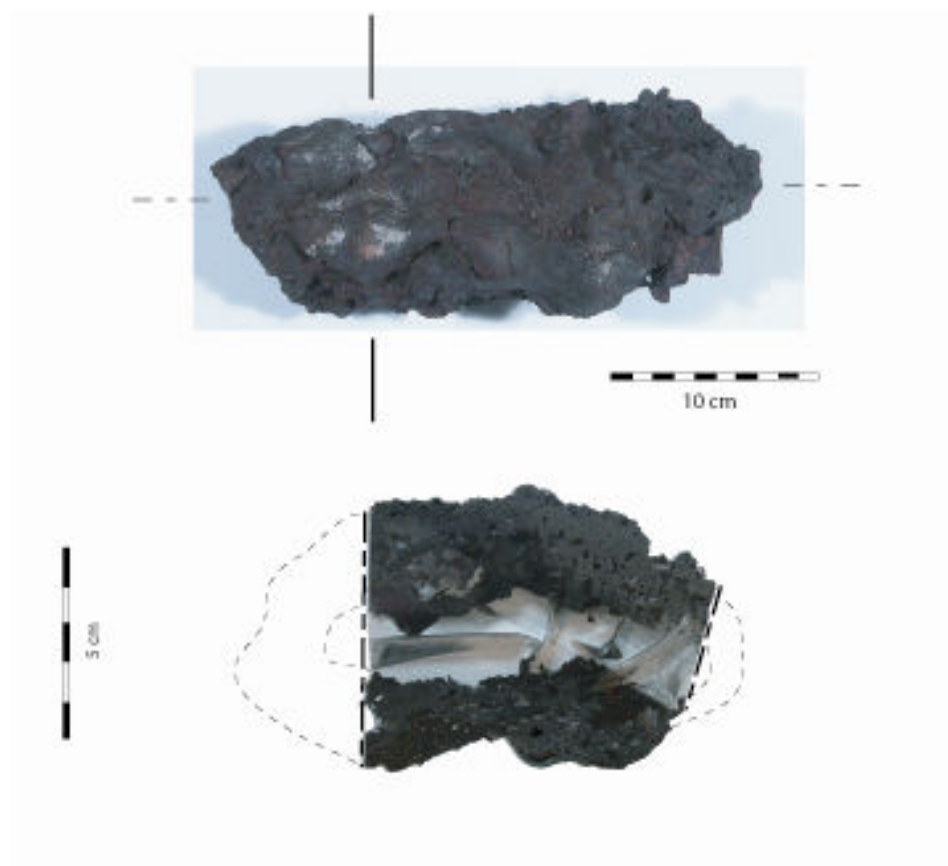


**Figure O.15 – Macrographie du fond de four CM05-01-4-4**

- *Observations microscopiques*

Il existe du métal par endroits (de tailles micrométriques à millimétriques), sans forme particulière, et quelques fois réoxydé (notamment à proximité des porosités). Notons que ces fragments de métal se situent le plus souvent entre les zones dendritiques. Des traces de charbon de bois sont également perceptibles. En outre, il semblerait que l'on retrouve les mêmes phases dans la matrice scoritique que pour l'autre fond de four, c'est-à-dire (Figure O.16) :

- une phase sous forme dendritique qui correspond probablement à un oxyde de fer
- une phase gris clair (sous forme cristallisée)
- une phase sombre

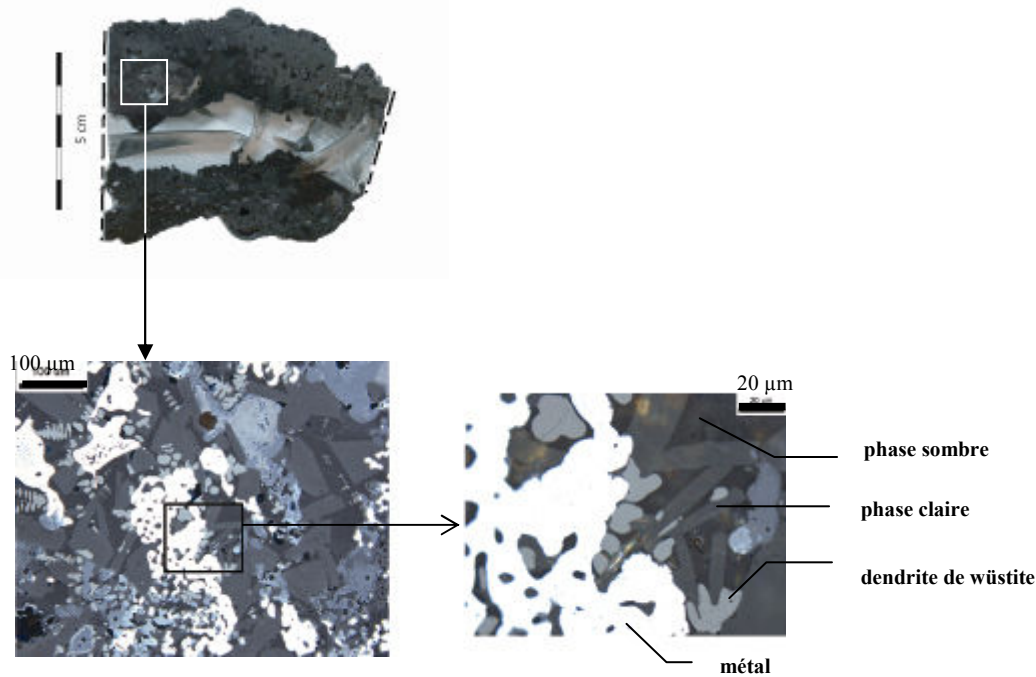


**Figure O.16 – Microscopie optique de la CM05-01-4-4**

Ces phases sont réparties de façon homogène dans la scorie.

- *Analyses élémentaires*

Dans un deuxième temps, des analyses ponctuelles ont été réalisées sur ces différentes phases. Les résultats sont présentés dans le Tableau O.11 et le Tableau O.12. De la même façon, ils sont exprimés en teneurs massiques puis convertis en %<sub>mass</sub> d'oxydes :

**Tableau O.11 – Composition moyenne (en %<sub>mass</sub>) des différentes phases qui composent la matrice scoritique**

Eléments % <sub>mass</sub>	O	Fe	Al	Si	Mn	Ca	K	Na	Mg	P	S
oxyde de fer	22,8	68,7	tr	tr	6,1	tr	tr	0,8	0,5	tr	tr
phase claire	34,4	28,7	tr	16,1	12,2	4,65	tr	0,5	2,3	tr	tr
phase sombre	40,3	12,5	10,87	17	3,8	9,74	2,7	1,1	0,5	0,6	tr

**Tableau O.12 – Composition moyenne (en %<sub>mass</sub> d'oxydes) des différentes phases qui composent la matrice scoritique**

Oxydes % <sub>mass</sub>	FeO	Al <sub>2</sub> O <sub>3</sub>	SiO <sub>2</sub>	MnO	CaO	K <sub>2</sub> O	NaO	MgO	P <sub>2</sub> O <sub>5</sub>	SO <sub>2</sub>
oxyde de fer	88,4	0,5	tr	7,8	tr	tr	1,1	0,9	tr	tr
phase claire	36,9	0,4	34,3	15,7	6,5	tr	0,7	3,8	0,4	tr
phase sombre	16,1	20,5	36,4	4,9	13,6	3,22	1,5	0,9	1,4	0,9

Comme pour l'autre fond de four, une quantité importante d'oxyde de manganèse est détectée et se partage entre les trois phases. Les résultats des analyses élémentaires obtenus sur la phase claire (tableau 10) montrent qu'il s'agirait d'une phase d'olivine. La plupart du manganèse (12%) se retrouve dans cette phase (en substitution). La composition élémentaire de la phase dendritique suggère qu'elle est constituée d'oxyde de fer de type wüstite. Une partie non négligeable du manganèse (6%) passe également dans cette phase. La phase sombre semble être une phase de type silicate, contenant la majorité de la quantité d'aluminium (4-5%), de calcium (10%) et de potassium (2-3%).

Il est ainsi intéressant d'effectuer une analyse structurale, par spectrométrie Raman, sur ces différentes phases pour les identifier et tenter de comprendre le comportement du manganèse.

- *Analyses structurales*

Une analyse de structure a été réalisée sur les trois phases qui composent la matrice. Les spectres Raman sont présentés dans la Figure O.17.

Grâce aux comparaisons avec les spectres de référence, on retrouve sur le spectre Raman de l'oxyde de fer, les pics principaux de la wüstite: 652 cm<sup>-1</sup>, 211 cm<sup>-1</sup> et une bande à 467cm<sup>-1</sup>, ce qui confirme l'identification faite avec les analyses élémentaires. Une bande à 587 cm<sup>-1</sup> serait liée à la présence de manganèse. Le profil de la phase claire (olivine ((Ca, Mn, Mg, Fe)<sub>2</sub>SiO<sub>4</sub>))

nous indique qu'il s'agit bien d'un silicate. En effet, d'après les références bibliographiques (Piriou *et al.*, 1983 ; Chopelas, 1991), on détecte la présence d'une double bande à  $811\text{ cm}^{-1}$  et  $841\text{ cm}^{-1}$  caractéristique d'un silicate. De part la complexité de la composition, il n'est pas possible d'associer ce spectre au spectre de référence de la fayalite. Cependant, certains groupements ( $167, 244, 517\text{ cm}^{-1}$ ) sont également présents sur le spectre de référence. Le profil de la phase sombre est assez semblable. Bien que les compositions soient différentes, on retrouve certains pics du profil de la phase précédente ( $384\text{ cm}^{-1}, 819\text{ cm}^{-1}$  et  $840\text{ cm}^{-1}$ ). On reconnaît ainsi toujours le double pic silicate ( $819\text{ cm}^{-1}$  et  $840\text{ cm}^{-1}$ ). Cependant, à ce stade de l'étude, il est difficile d'identifier avec exactitude les différentes phases présentes sous forme de mélanges dans le volume analysé.

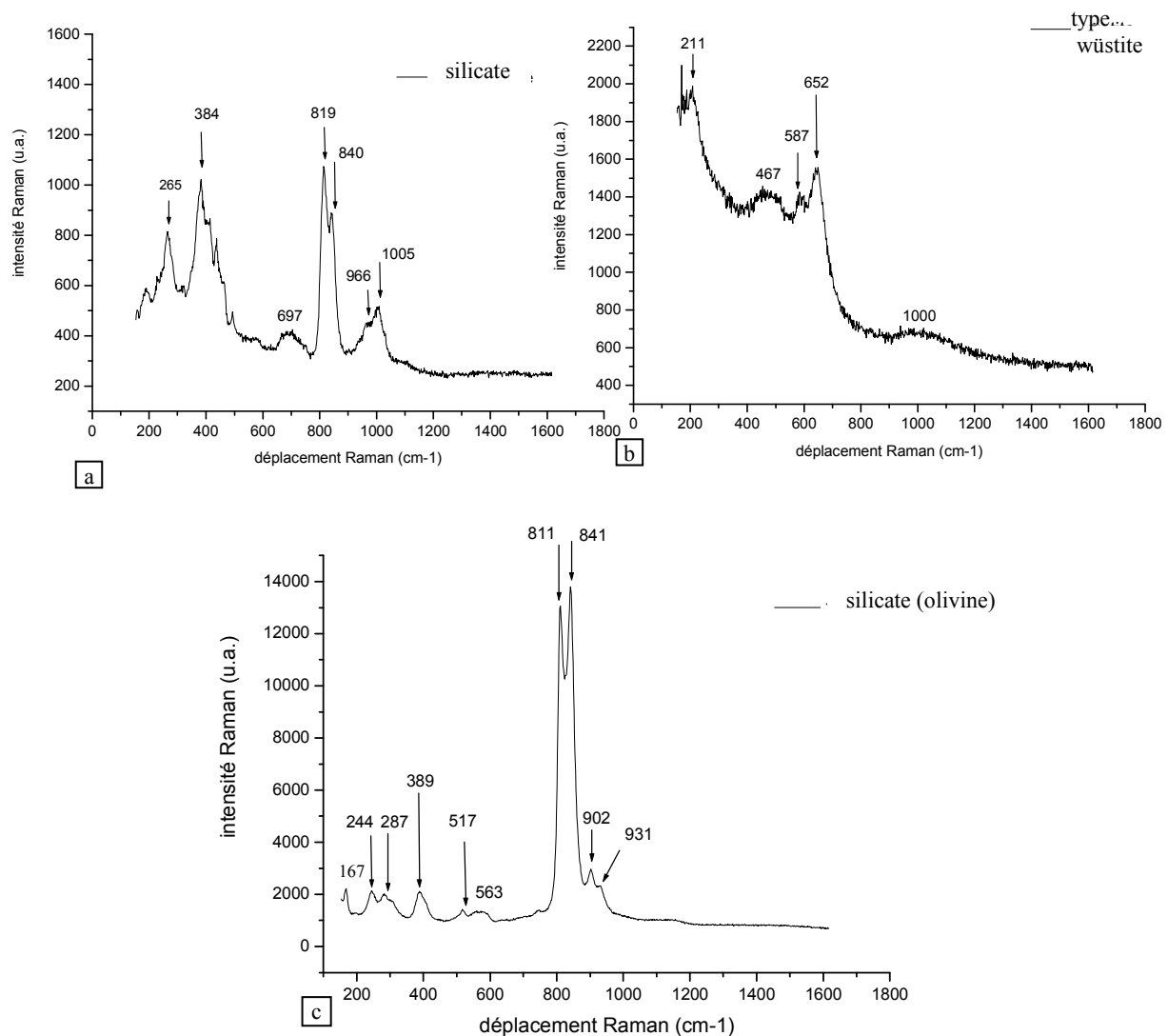
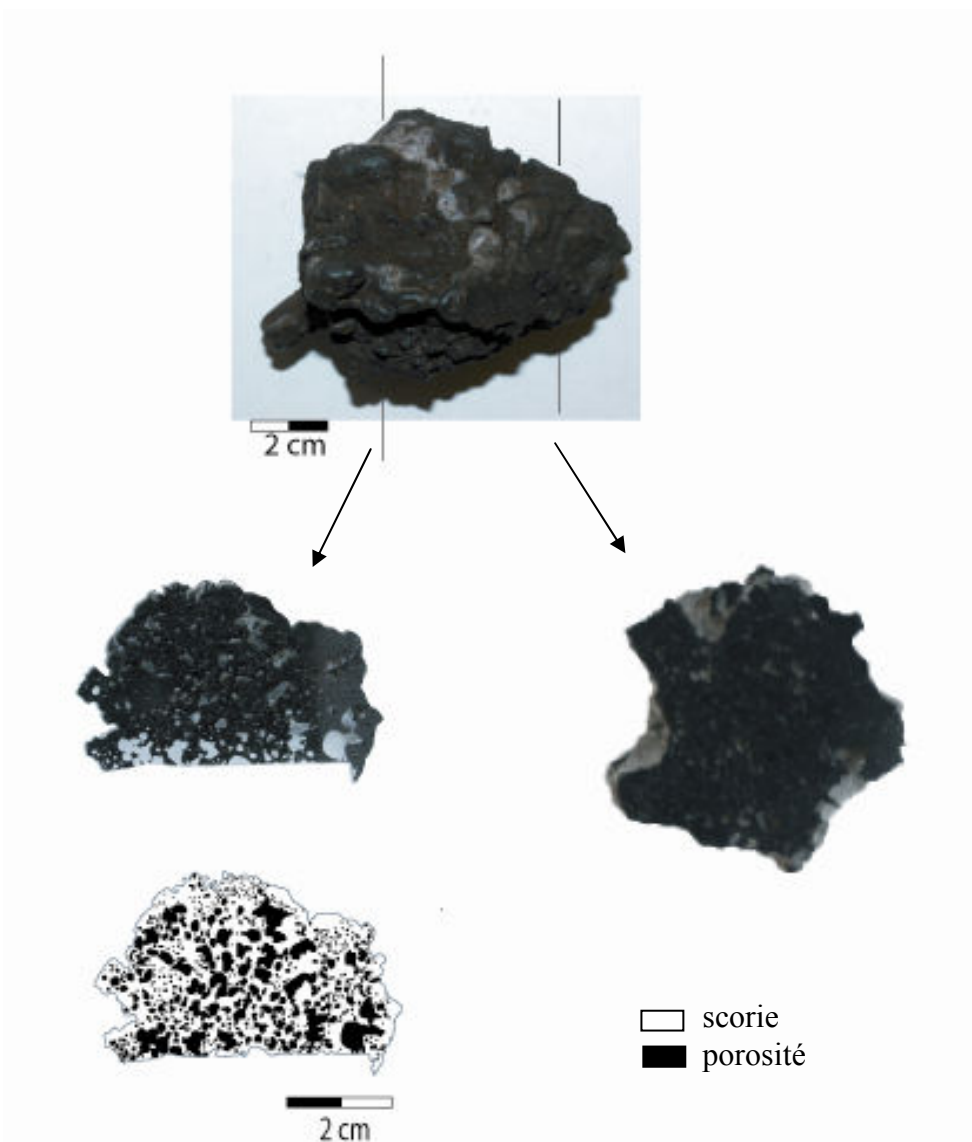


Figure O.17 – Spectres Raman ; [a- phase sombre ; b- type wüstite ; c- olivine]

### SCORIE DE FOND DE FOUR : CM04-04-4-5

- *Morphologie et observations macroscopiques*

Cette scorie a une masse de 500g (Figure O.18) pour des dimensions de 7x6 cm. On observe sur la partie supérieure différentes coulées qui se sont accumulées au fur et à mesure de l'étape de réduction. Plusieurs coupes ont été réalisées sur cet échantillon.



**Figure O.18 – Macrographie de la scorie coulée CM04-04-4-5**

Les différentes sections indiquent une porosité importante (51% pour une seule coupe), répartie de façon aléatoire au sein de la matrice. Aucune trace de charbon ou de métal n'est visible.

- *Observations microscopiques et composition élémentaire*

On observe au microscope optique le même type de matrice, aussi homogène que celle des fonds de four et composée des mêmes phases (Figure O.19). Des globules métalliques concentrés en périphérie des porosités sont également visibles. L'analyse EDS a permis d'identifier quatre phases :

- oxyde de fer de type wüstite ( $(\text{Fe}_x, \text{Mn}_y)\text{O}$ ) avec 9% de MnO.
- olivine  $((\text{Ca}, \text{Mn}, \text{Mg}, \text{Ca}, \text{Fe})\text{SiO}_4)$  avec 17% de MnO
- phase silicatée avec 3% de MnO.
- globules de métal

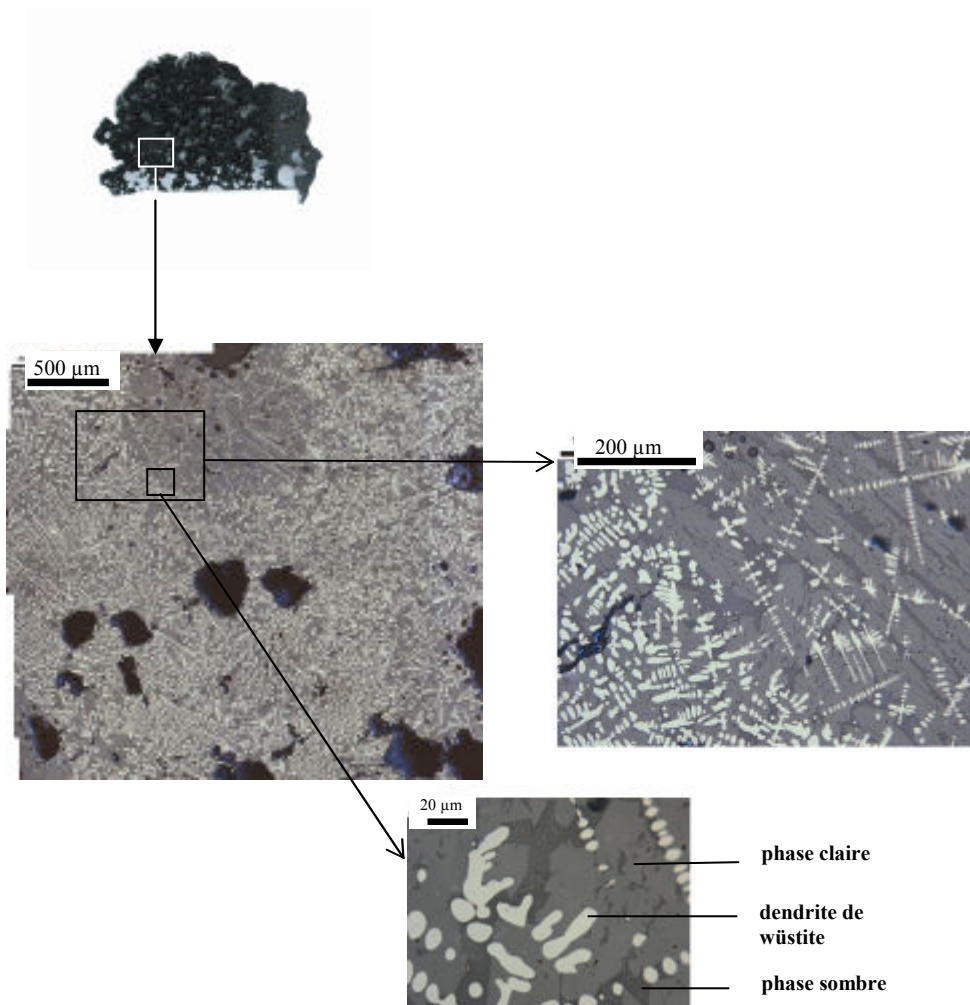


Figure O.19 – Microscopie de la scorie coulée CMo<sub>4</sub>-04-4-5

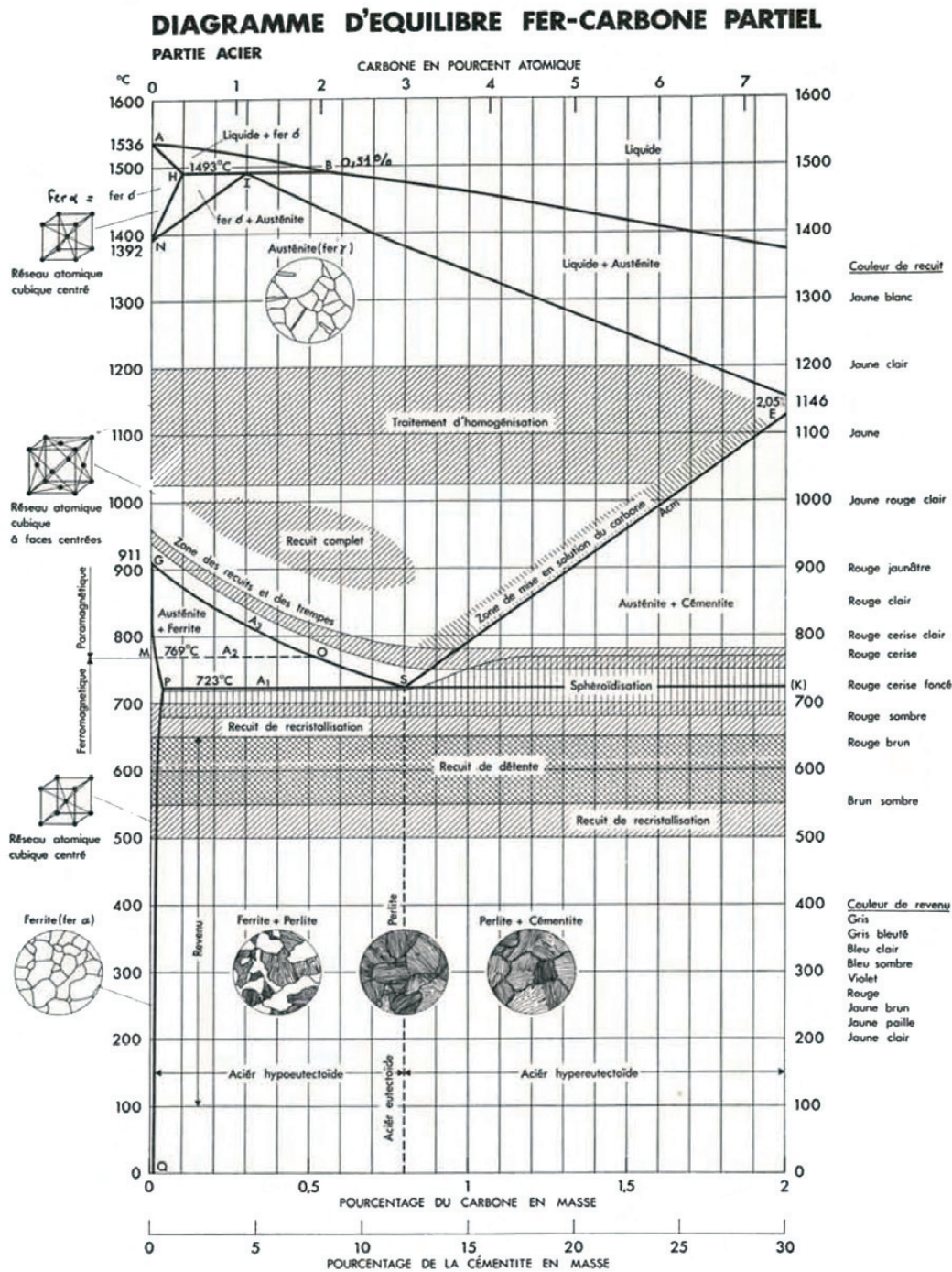
## **Annexes P**

### **OBSERVATIONS MÉTALLOGRAPHIQUES DU CORPUS D'OBJETS**





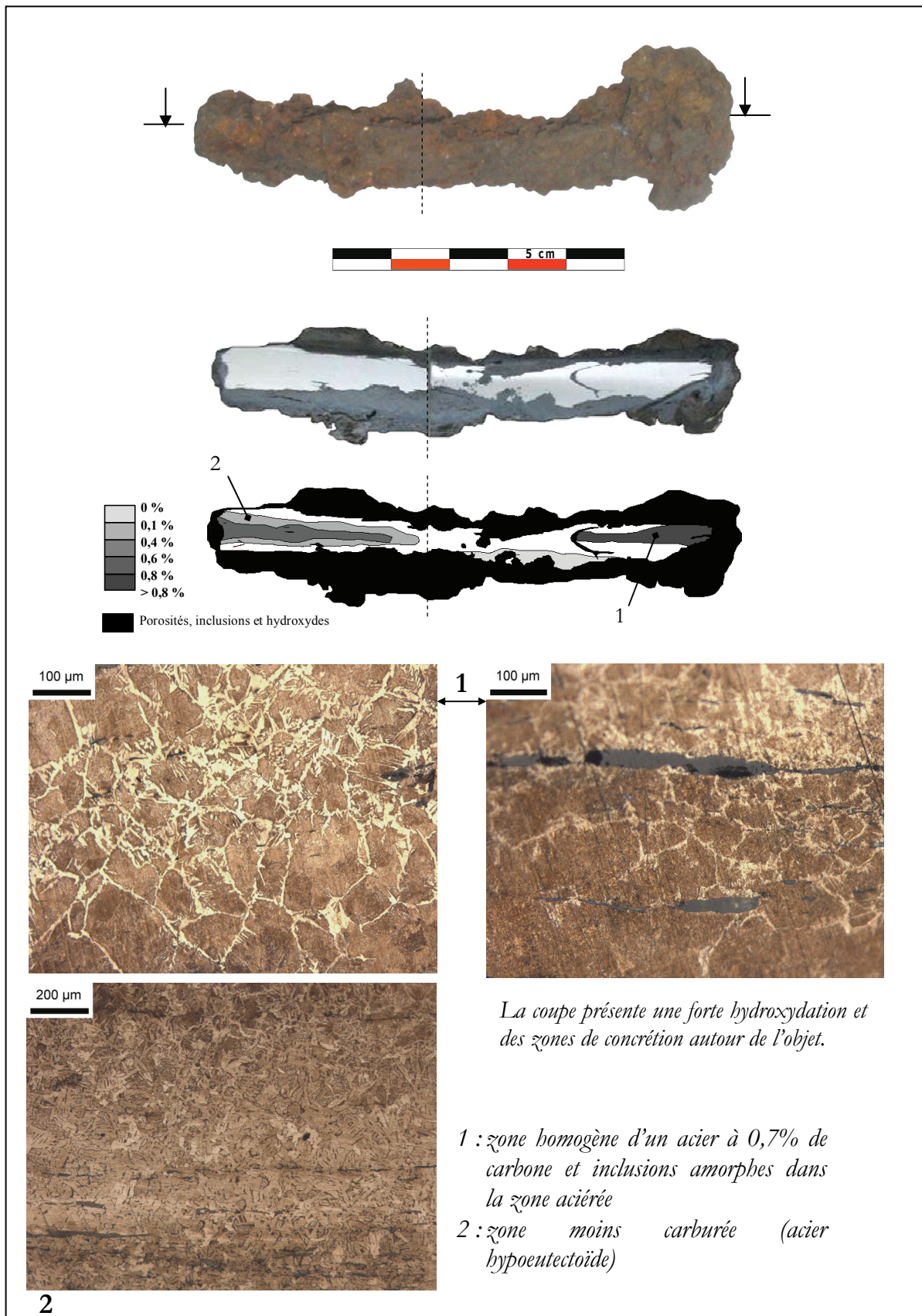
# Annexe P.1 - DIAGRAMME D'ÉQUILIBRE FER-CARBONE (D'APRÈS FLUZIN, 1983)



COMPILED BY S. ENGBEL-HILSEN  
Met. Eng. Technological Institute, Copenhagen

tel-00598796, version 1 - 7 Jun 2011

## Annexe P.2 - OBSERVATIONS METALLOGRAPHIQUES DE L'ECHANTILLON CM06-2002-1 (CASTEL-MINIER)

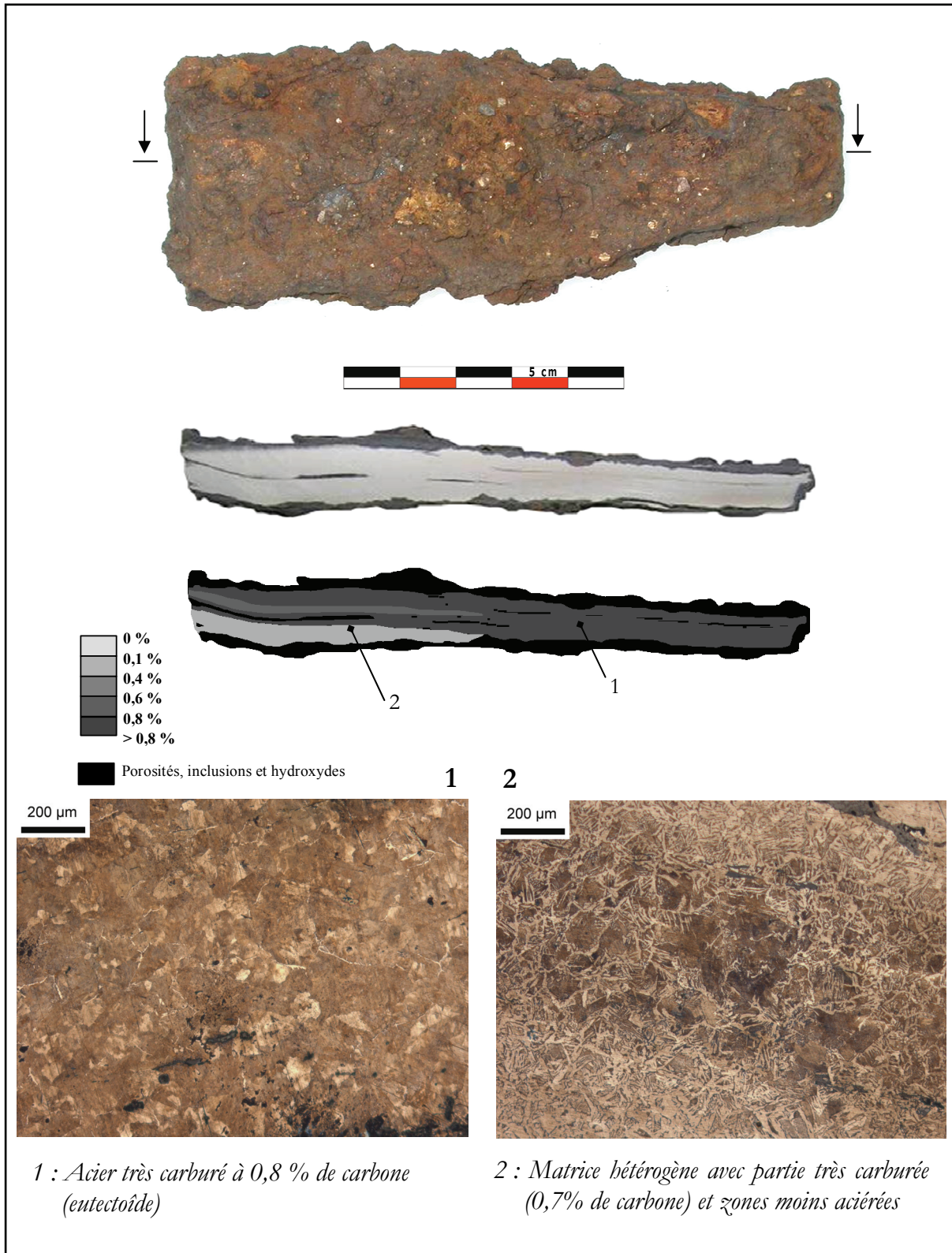


**MICROGRAPHIE :**

Le produit métallique est constitué en son centre d'un acier à 0,7% de carbone avec des zones de moins en moins aciérées vers la périphérie. Le reste est constitué de ferrite. Dans la partie la moins carburée et la partie ferritique, plusieurs inclusions polyphasées ont été observées. Il n'est pas étonnant d'observer ce type d'inclusions dans une matrice moins riche en carbone. Celles-ci sont souvent constituées de dendrites de wüstite (FeO) et d'une phase fayalitique.



### Annexe P.3 - OBSERVATIONS METALLOGRAPHIQUES DE L'ECHANTILLON CM06-2002-2 (CASTEL-MINIER)



**MACROGRAPHIE :**

Cet objet est un élément métallique plus manufacturé que les autres produits. On observe deux faces relativement planes qui témoignent d'un martelage. L'objet possède une forme régulière et un effilement à l'une de ses extrémités. La section longitudinale de l'objet révèle un métal relativement propre avec très peu d'inclusions

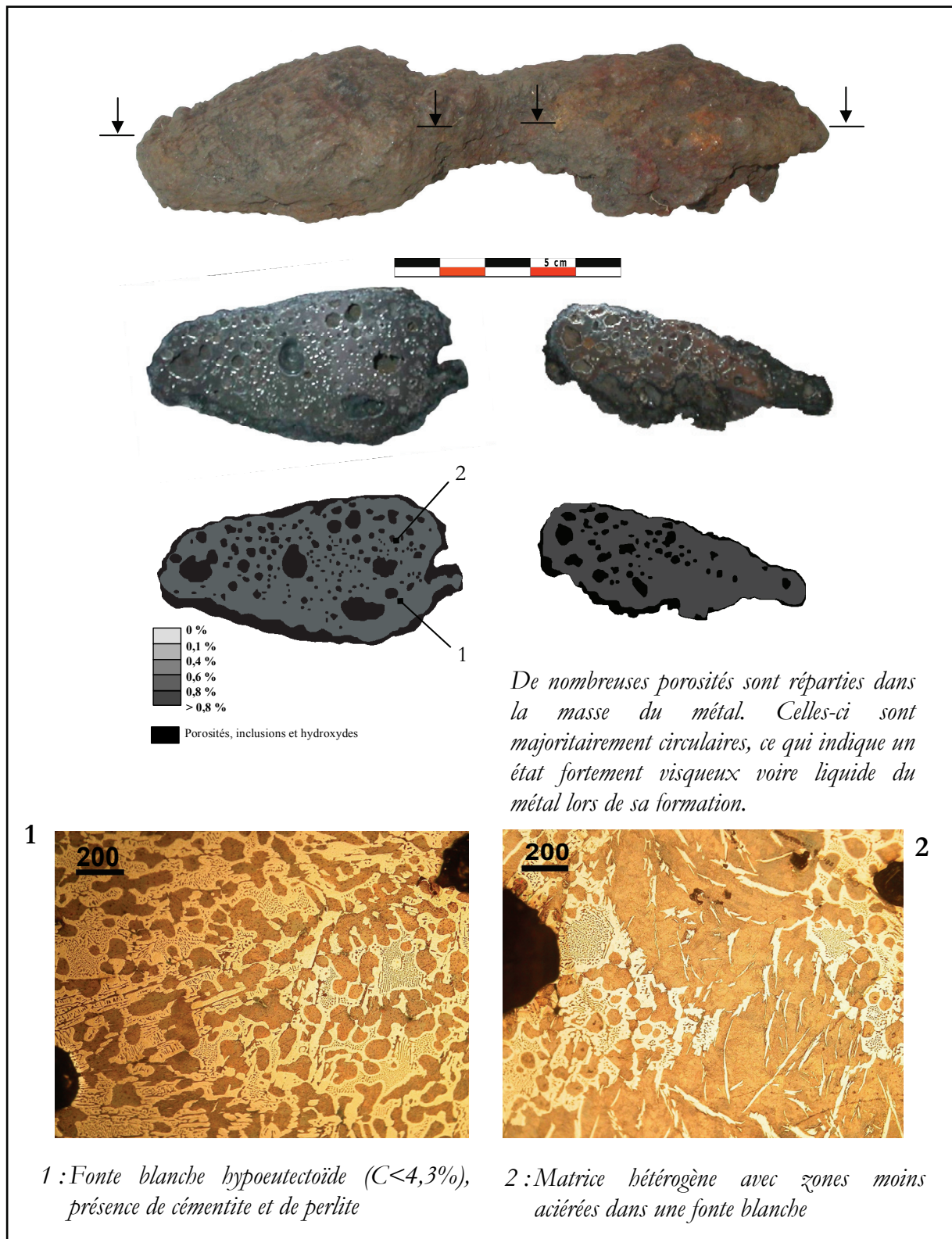
Les replis sont abondants et sont en majorité bien fermés ce qui confirme le travail de compactage. Tous les replis fermés indiquent un écrouissage important sur tout l'objet. Une ligne de soudure médiane peut être mise en évidence.

**MICROGRAPHIE :**

Après attaque chimique, on peut remarquer la faible hétérogénéité structurale du métal. Il s'agit d'un acier eutectoïde (à 0,8% de carbone). Seules quelques parties présentent une structure plus hétérogène : de 0,3 % à 0,7% de carbone.

Il y a relativement peu d'inclusions dans le métal. Lorsqu'elles existent, elles sont majoritairement amorphes. Très localement on observe quelques rares inclusions de type fayalitique avec de fréquentes dendrites de wüstite.

## Annexe P.4 - OBSERVATIONS METALLOGRAPHIQUES DE L'ÉCHANTILLON CM06-2002-3 (CASTEL-MINIER)



**MACROGRAPHIE :**

Cet échantillon correspond à deux masses métalliques importantes informes et compactes reliées entre elles par de la scorie. Il semble qu'elles correspondent à la perte de gros morceaux en début d'opération d'épuration. Ces deux masses correspondent donc à des déchets qui pourraient s'apparenter à ce que l'on appelle « *gromps* » et seraient caractéristiques de l'activité de compactage de la loupe. Le métal présente des porosités vides de scorie.

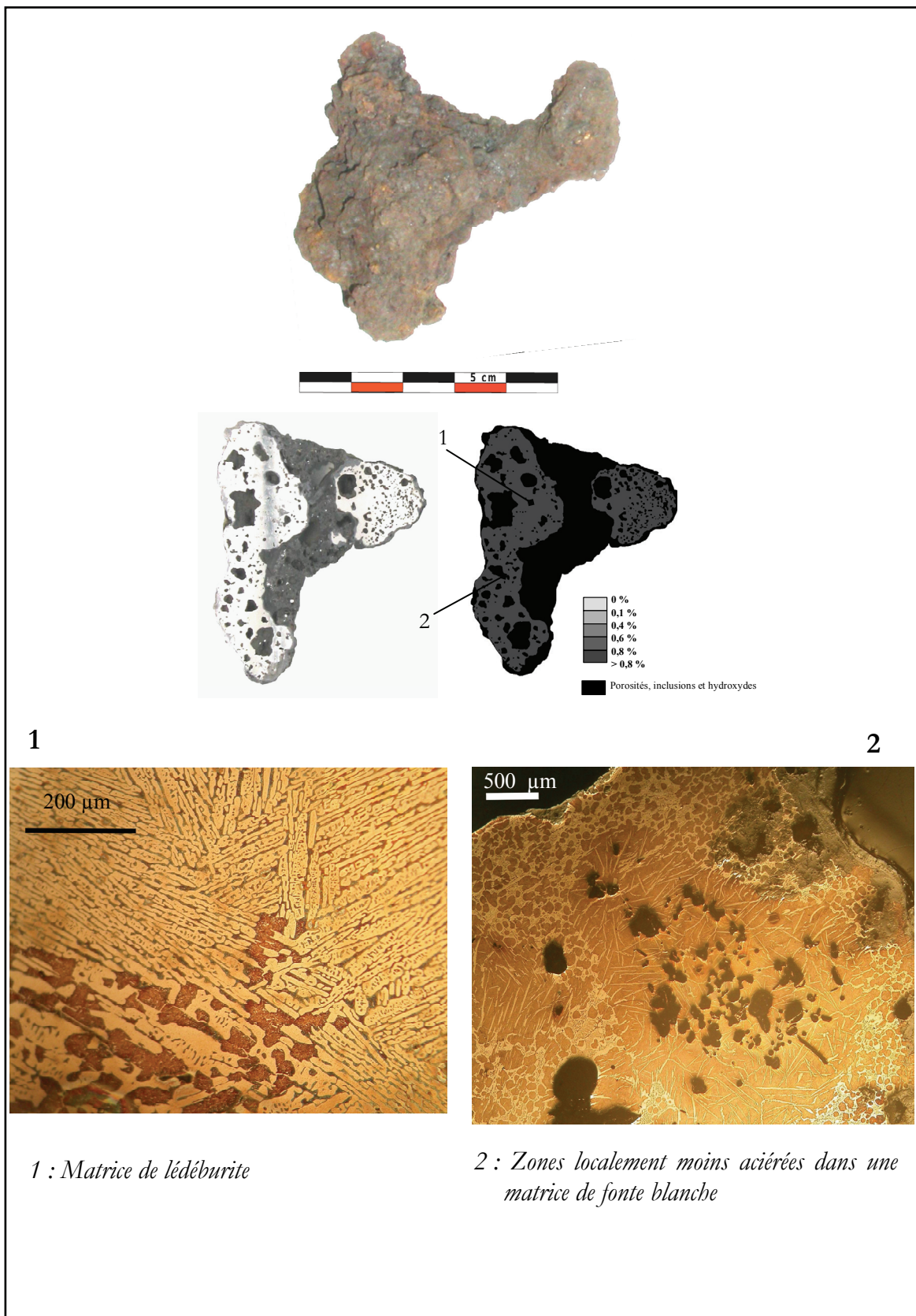
**MICROGRAPHIE :**

L'attaque chimique révèle que, pour les deux masses, nous sommes en présence d'une fonte blanche hypoeutectoïde (1) avec certaines zones moins carburées (2). La teneur en carbone pour ces échantillons varie donc de 1,7% à 4,3% de carbone. La fonte blanche est favorisée par des teneurs en carbone plus faibles que pour la fonte grise, un refroidissement rapide et par la présence d'éléments cémentisants comme le manganèse ou le chrome qui forment avec la cémentite ( $\text{Fe}_3\text{C}$ ) des carbures spécifiques.

Les deux fragments de loupe sont donc majoritairement constitués de fonte blanche eutectique. Quelques zones en acier hypereutectoïdes donc moins carburées peuvent être observées en certains endroits comme le montre le cliché 2.



## Annexe P.5 - OBSERVATIONS METALLOGRAPHIQUES DE L'ECHANTILLON CM06-2003-2 (CASTEL-MINIER)





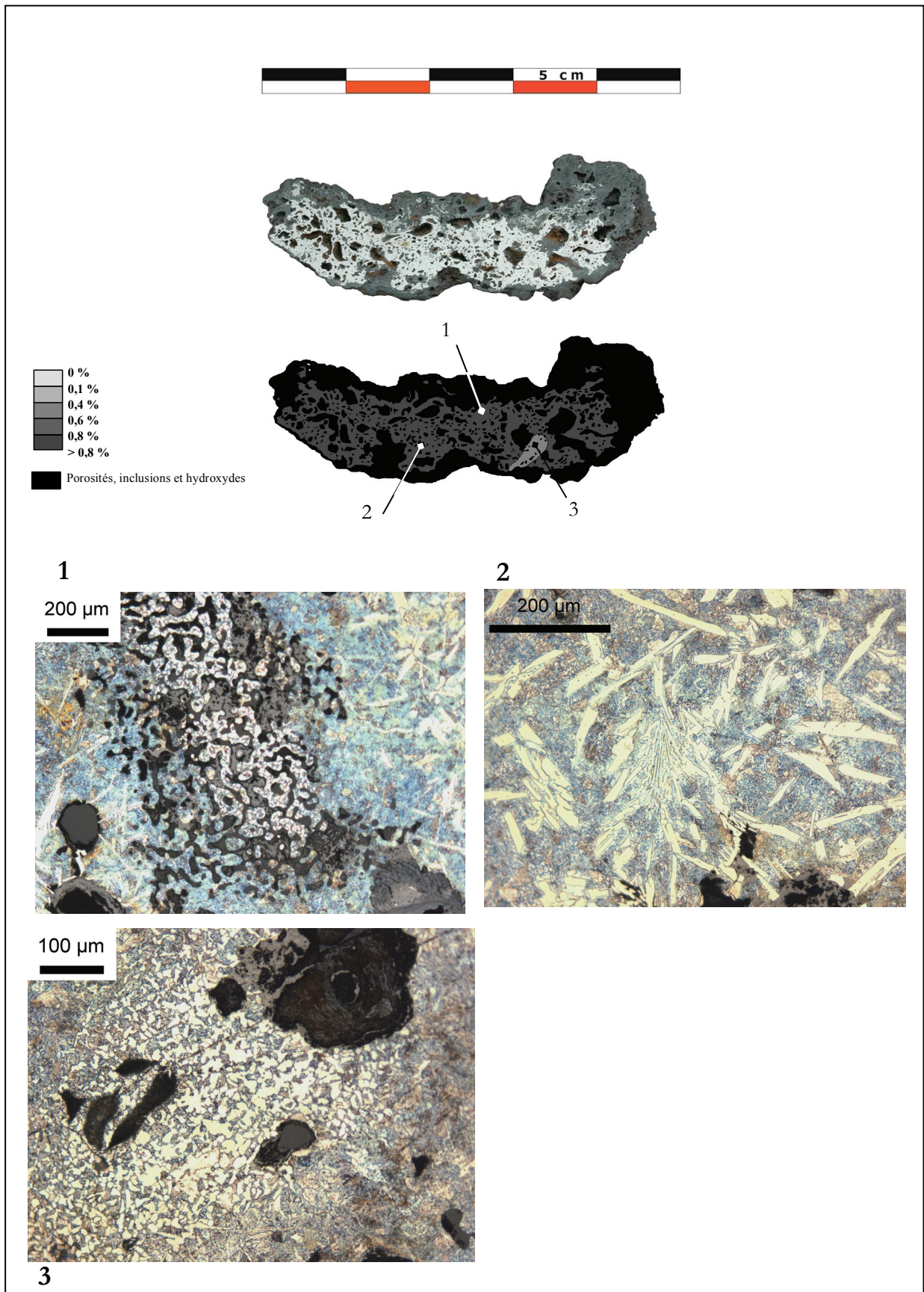
**MACROGRAPHIE :**

Il s'agit comme pour l'échantillon précédent d'un fragment métallique déchiqueté, également qualifié de *gromps*. Sa section dévoile une texture d'un fragment de loupe qui semble avoir été légèrement épuré. Le métal est hétérogène et contient de très nombreuses inclusions porosités. Ces porosités ont des contours relativement déchiquetés. En revanche, très peu d'inclusions scoritiques ont été observées.

**MICROGRAPHIE :**

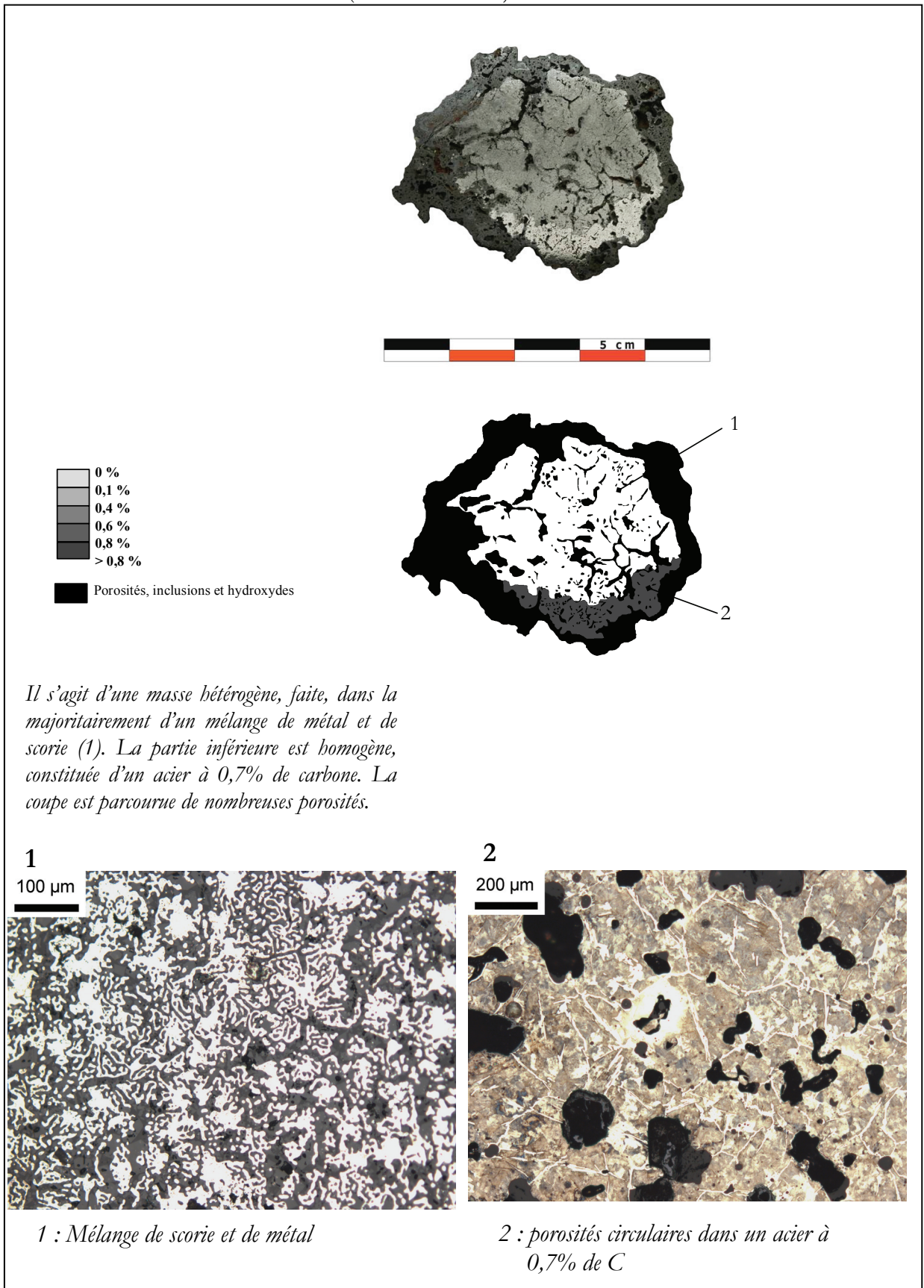
L'examen au microscope optique après attaque chimique permet d'identifier une structure de lédéburite qui correspond à un mélange hétérogène eutectique des deux phases : austénite à 1,7% de carbone et cémentite primaire. Il semble que le métal ait une composition proche de l'eutectique car la présence de lédéburite est pratiquement généralisée sur toute la surface. Seules quelques parties montrent une tendance à la décarburation notamment visible sur le cliché 2. Il s'agit donc également d'une fonte blanche à majorité eutectique.

# Annexe P.6 - OBSERVATIONS METALLOGRAPHIQUES DE L'ECHANTILLON CM05-01-2-4 (CASTEL-MINIER)



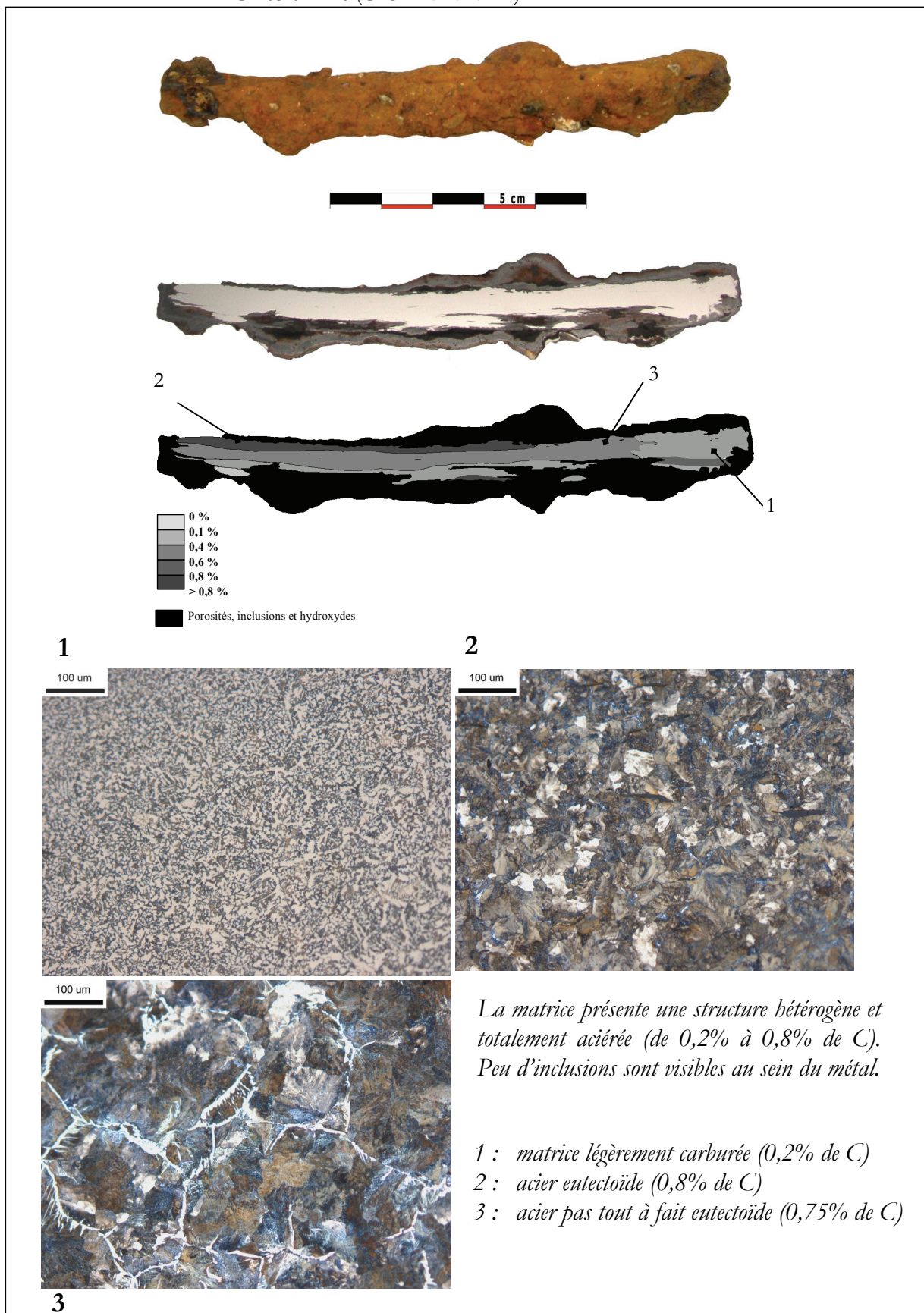
tel-00598796, version 1 - 7 Jun 2011

## Annexe P.7 - OBSERVATIONS METALLOGRAPHIQUES DE L'ÉCHANTILLON CM05-01-2-17 (CASTEL-MINIER)

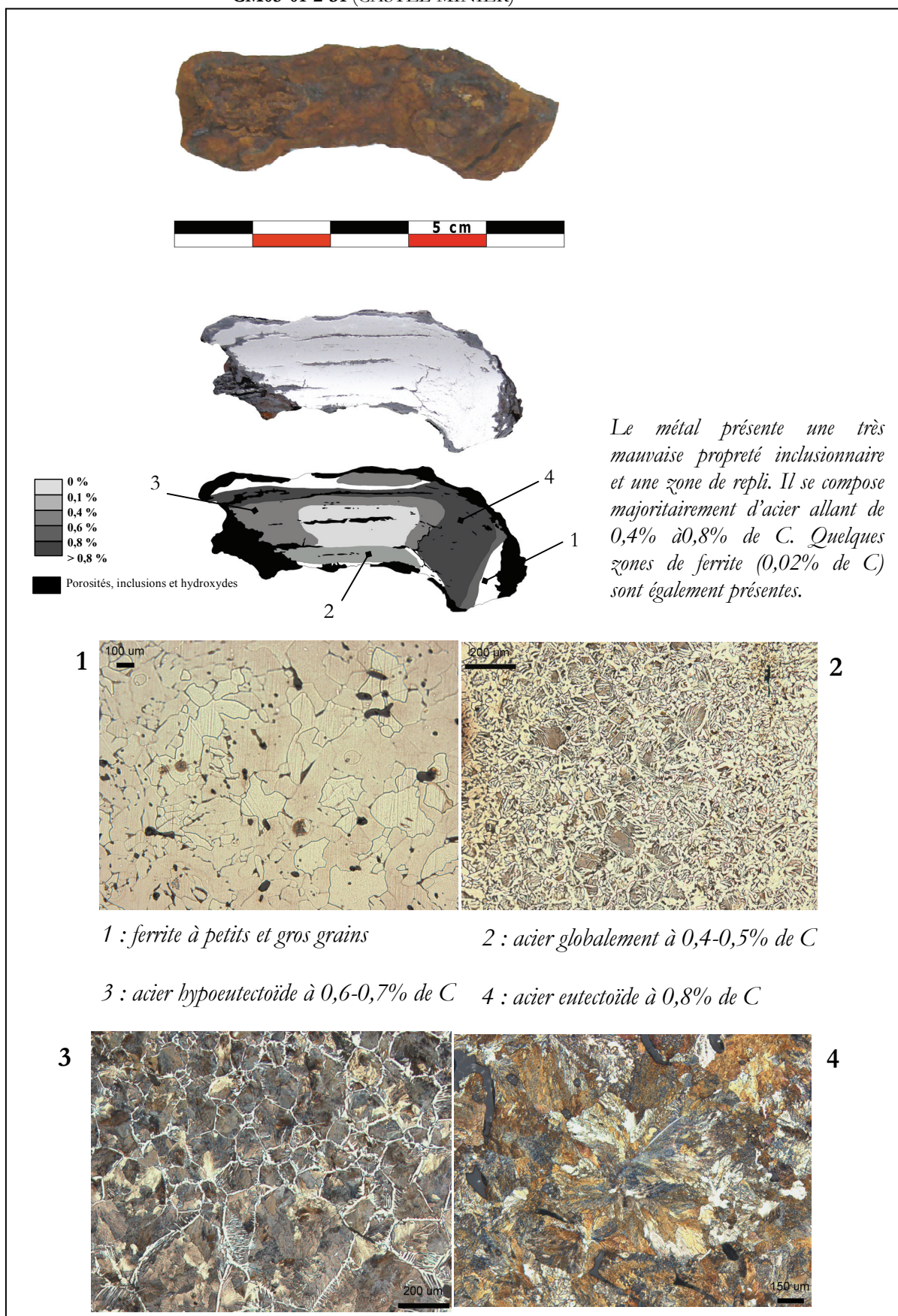




## Annexe P.8 - OBSERVATIONS METALLOGRAPHIQUES DE L'ECHANTILLON CM05-01-2-27 (CASTEL-MINIER)

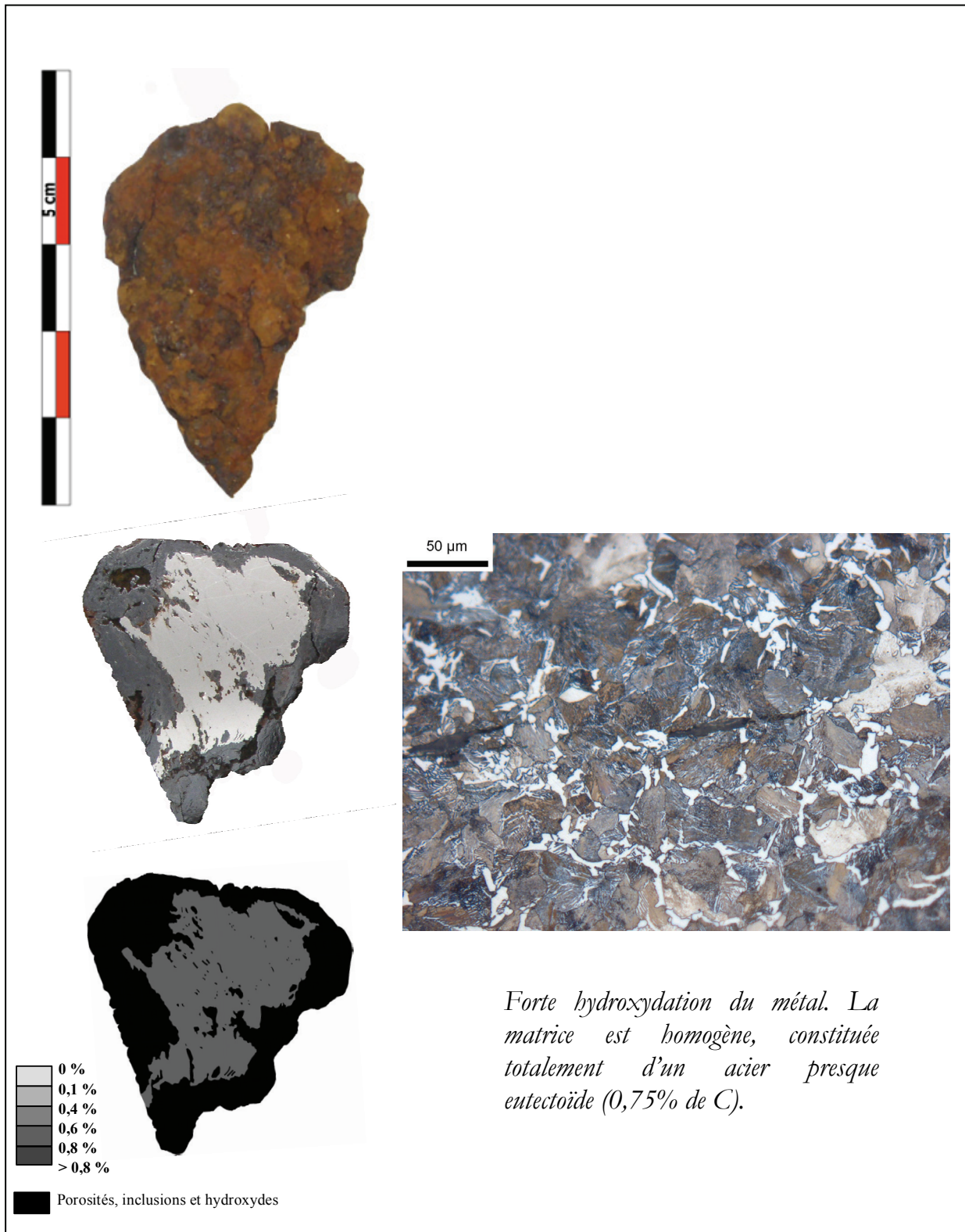


## Annexe P.9 - OBSERVATIONS METALLOGRAPHIQUES DE L'ÉCHANTILLON CM05-01-2-31 (CASTEL-MINIER)

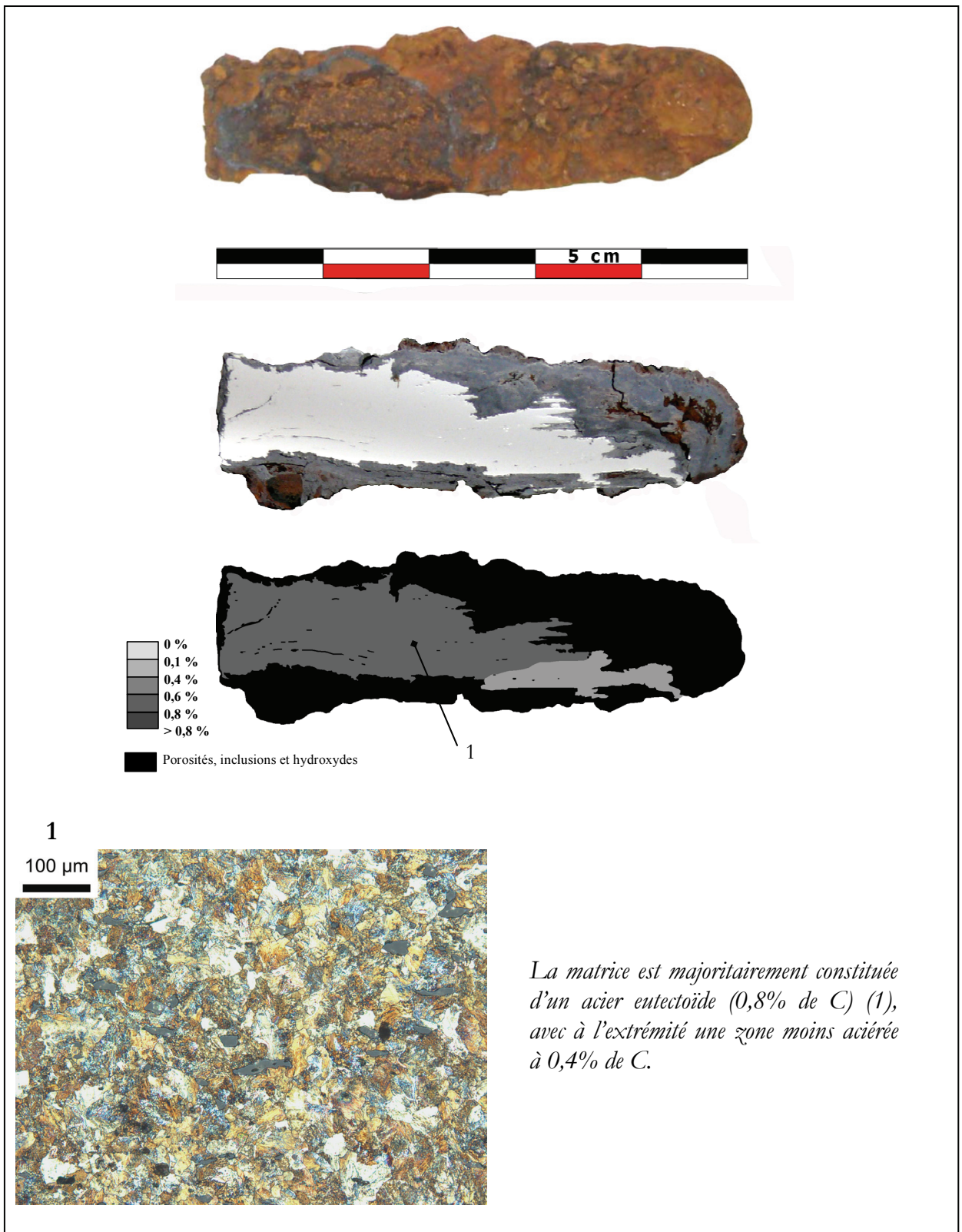




## Annexe P.10 - OBSERVATIONS METALLOGRAPHIQUES DE L'ECHANTILLON CM05-01-2-34 (CASTEL-MINIER)

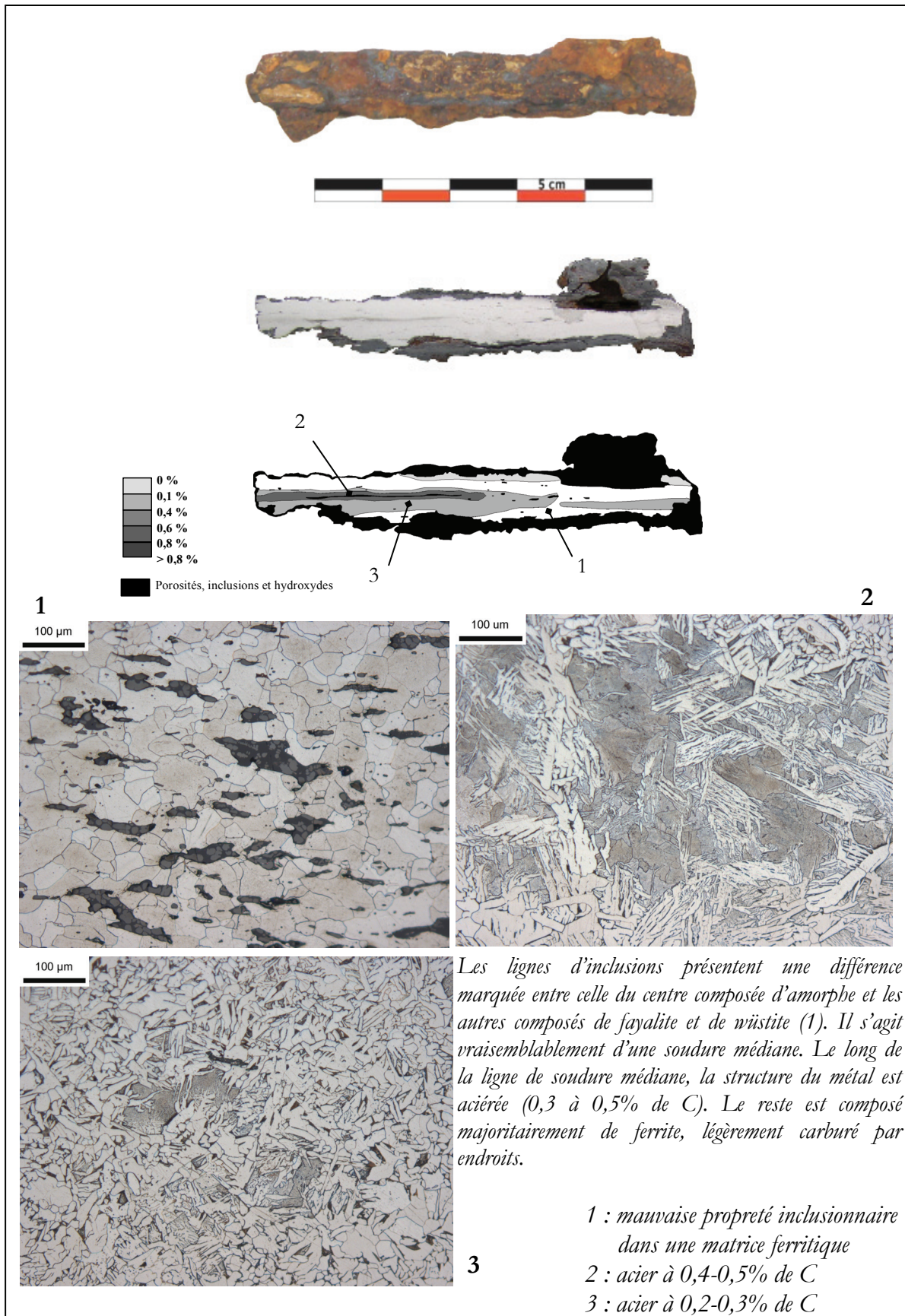


## Annexe P.11 - OBSERVATIONS METALLOGRAPHIQUES DE L'ÉCHANTILLON CM05-01-2-36 (CASTEL-MINIER)



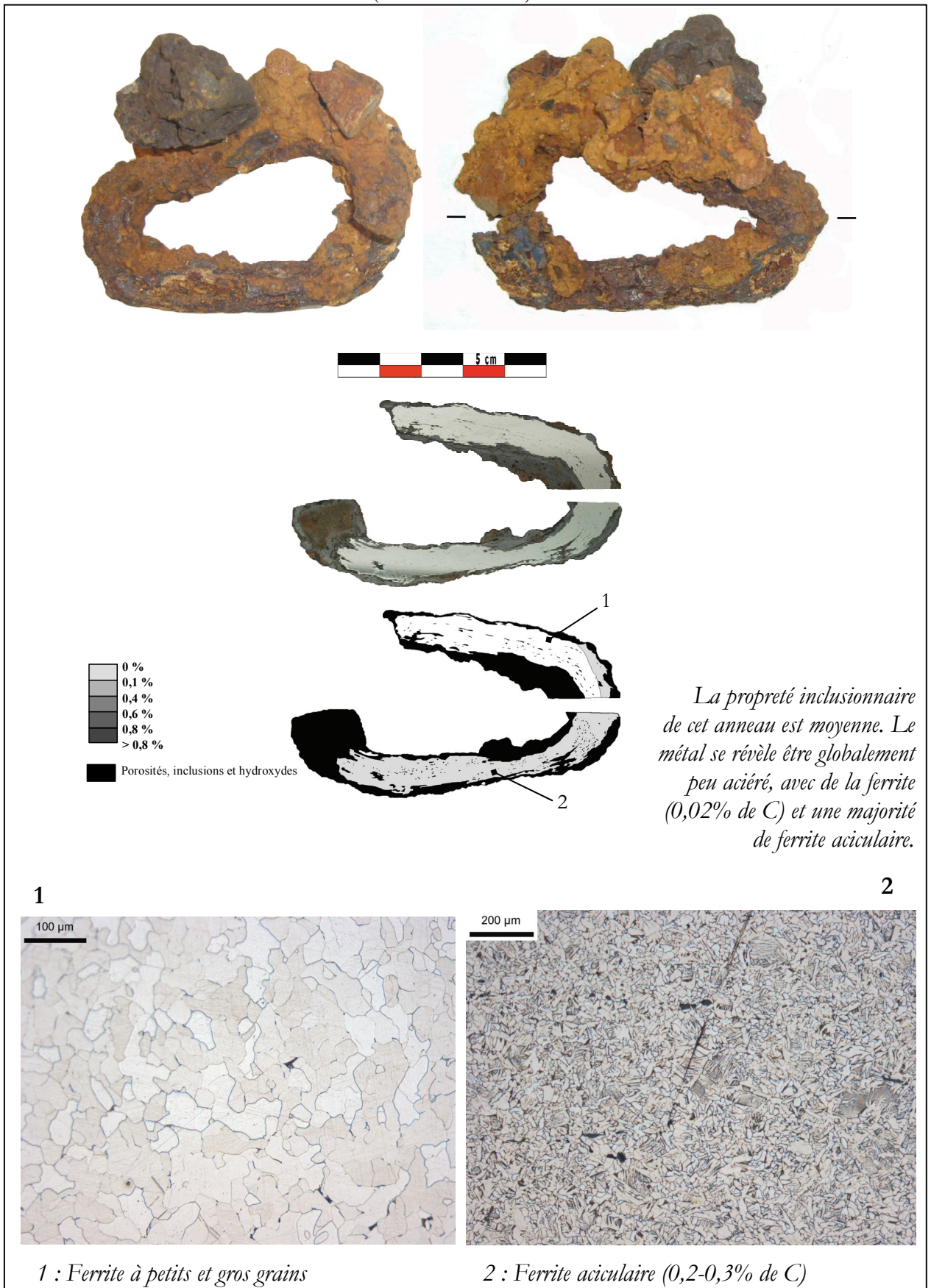


## Annexe P.12 - OBSERVATIONS METALLOGRAPHIQUES DE L'ECHANTILLON CM05-01-2-54 (CASTEL-MINIER)

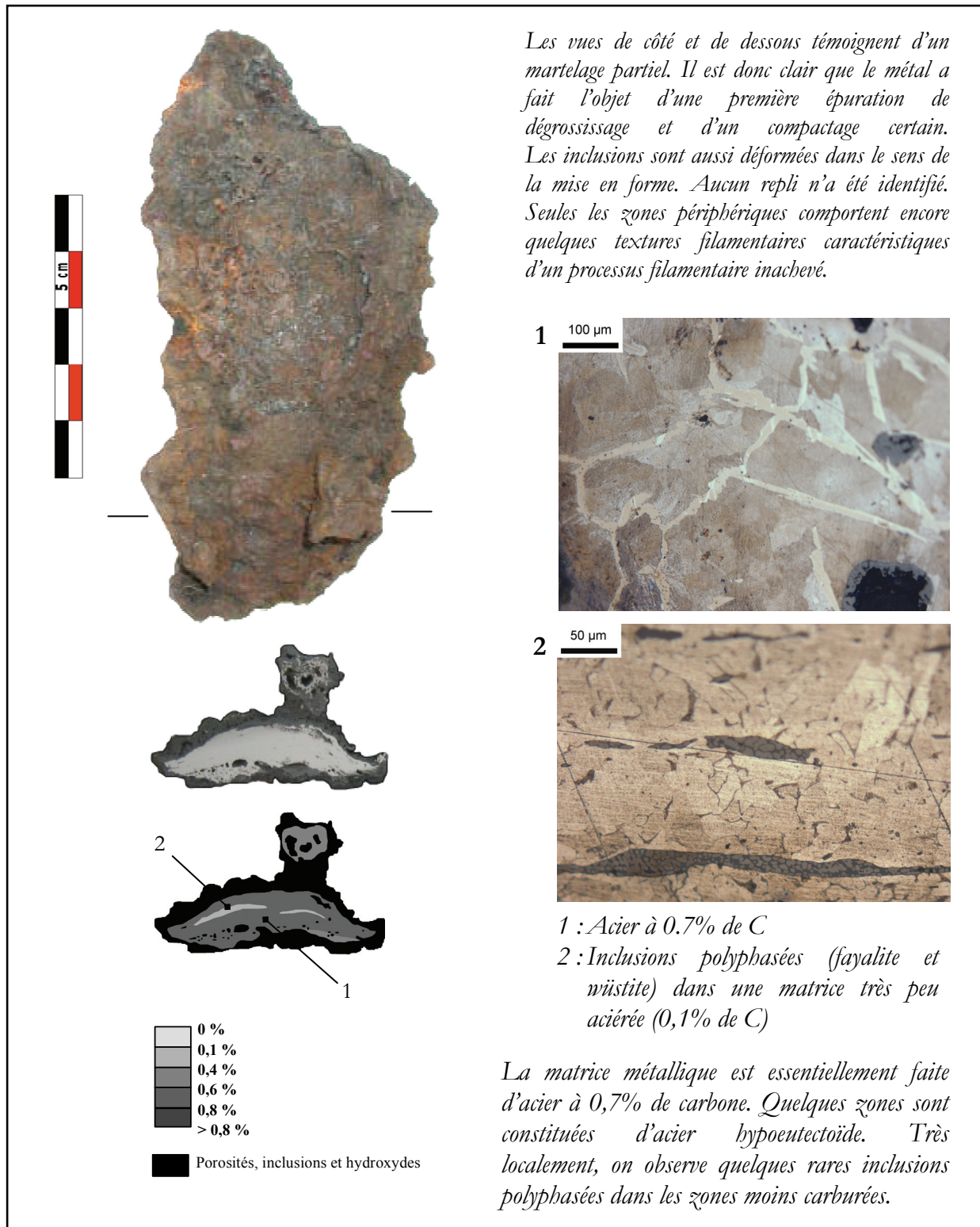




## Annexe P.13 - OBSERVATIONS METALLOGRAPHIQUES DE L'ÉCHANTILLON CM05-01-2-59 (CASTEL-MINIER)

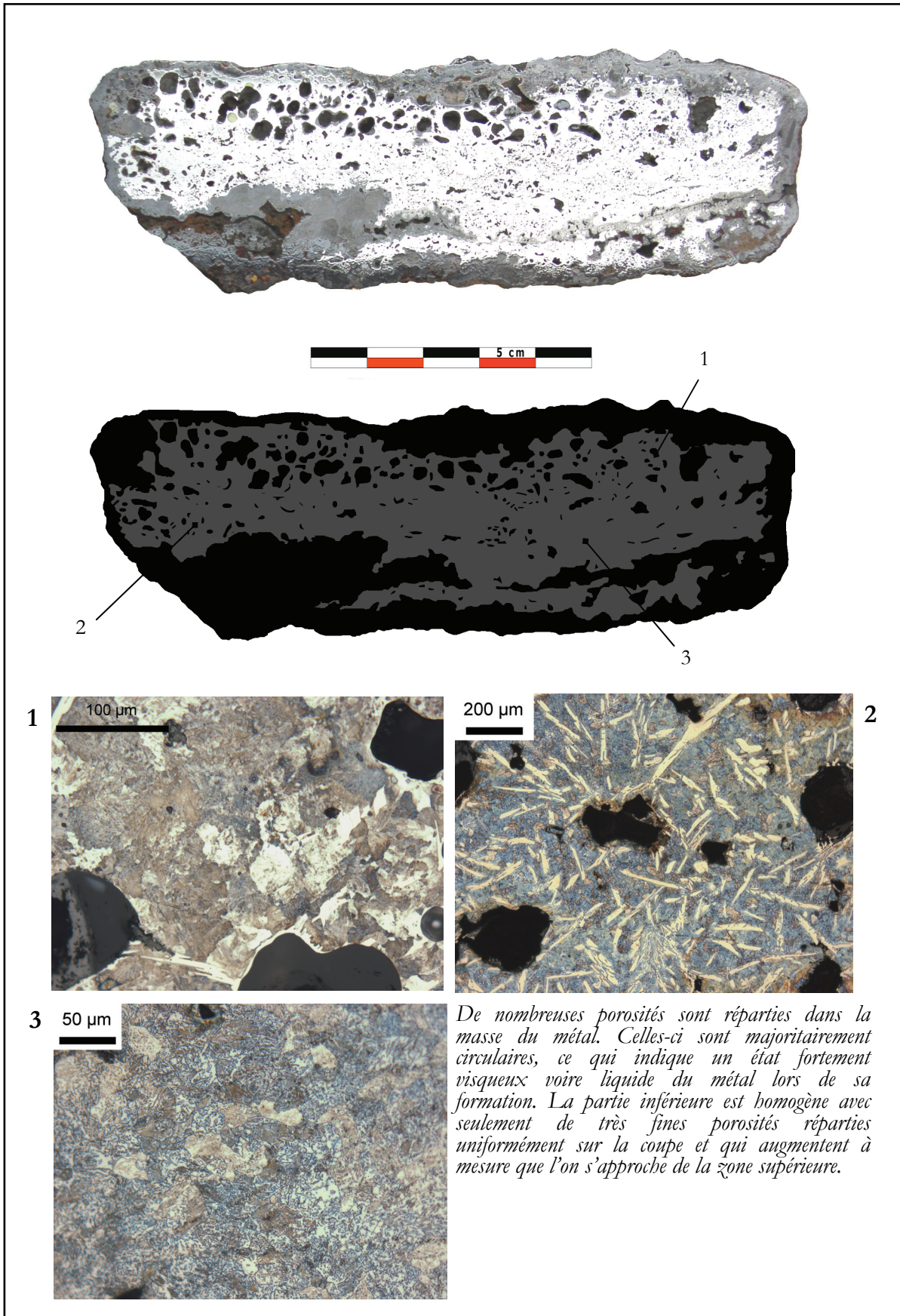


## Annexe P.14 - OBSERVATIONS METALLOGRAPHIQUES DE L'ECHANTILLON CM06-2004-1 (CASTEL-MINIER)

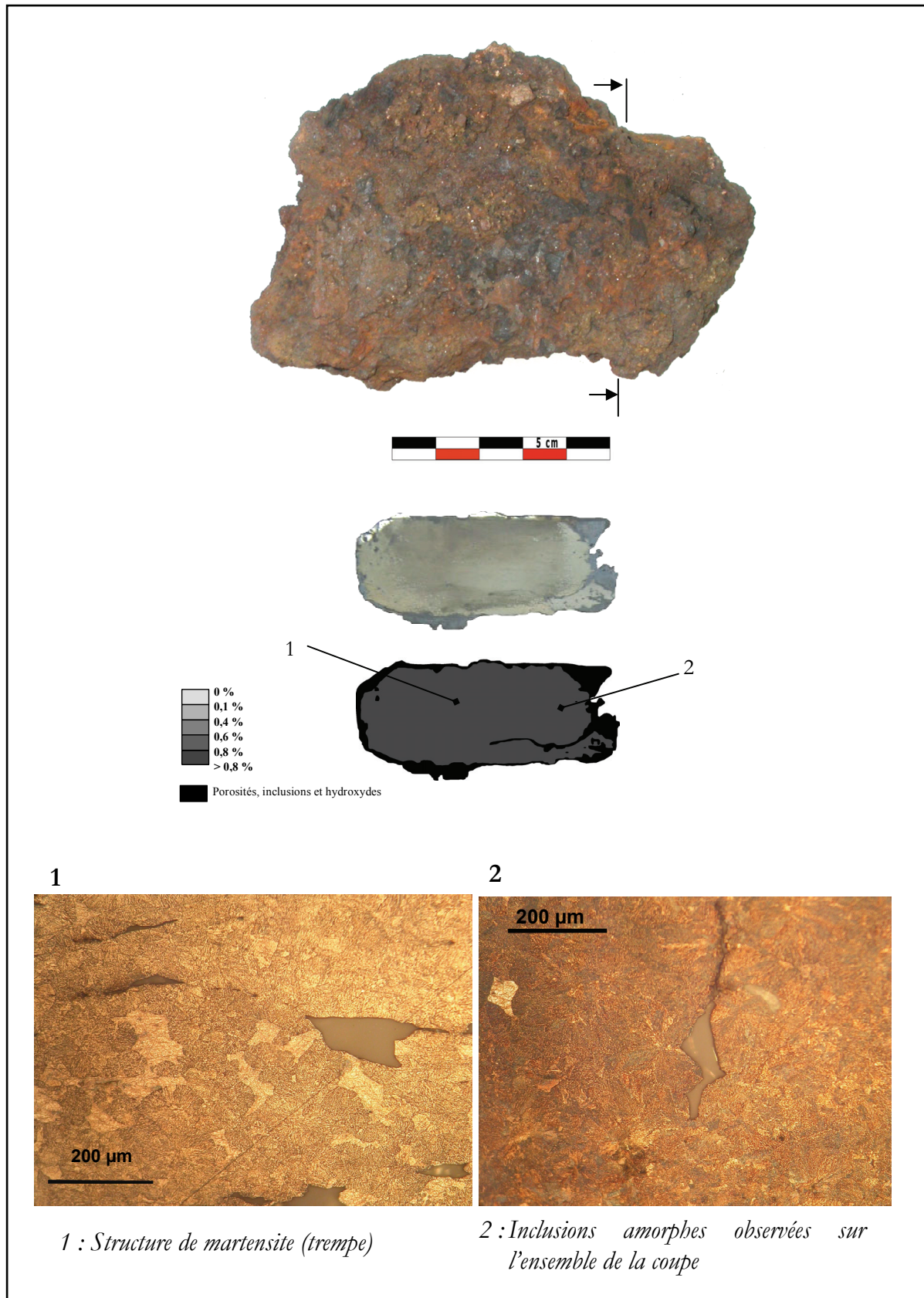




## Annexe P.15 - OBSERVATIONS METALLOGRAPHIQUES DE L'ÉCHANTILLON CM06-2004-2 (CASTEL-MINIER)



## Annexe P.16 - OBSERVATIONS METALLOGRAPHIQUES DE L'ECHANTILLON CM06-2008-1 (CASTEL-MINIER)



**MACROGRAPHIE :**

Il s'agit d'un demi-produit en forme de lingot provenant de la plus ancienne US fouillée sur le site. On décèle un écrasement dans le sens transversal. Les vues de dessus et de dessous témoignent ainsi d'un martelage partiel. Les autres faces ne semblent pas avoir été particulièrement travaillées. Le métal a donc fait l'objet d'une première épuration de dégrossissage et d'un compactage au moins sur deux faces.

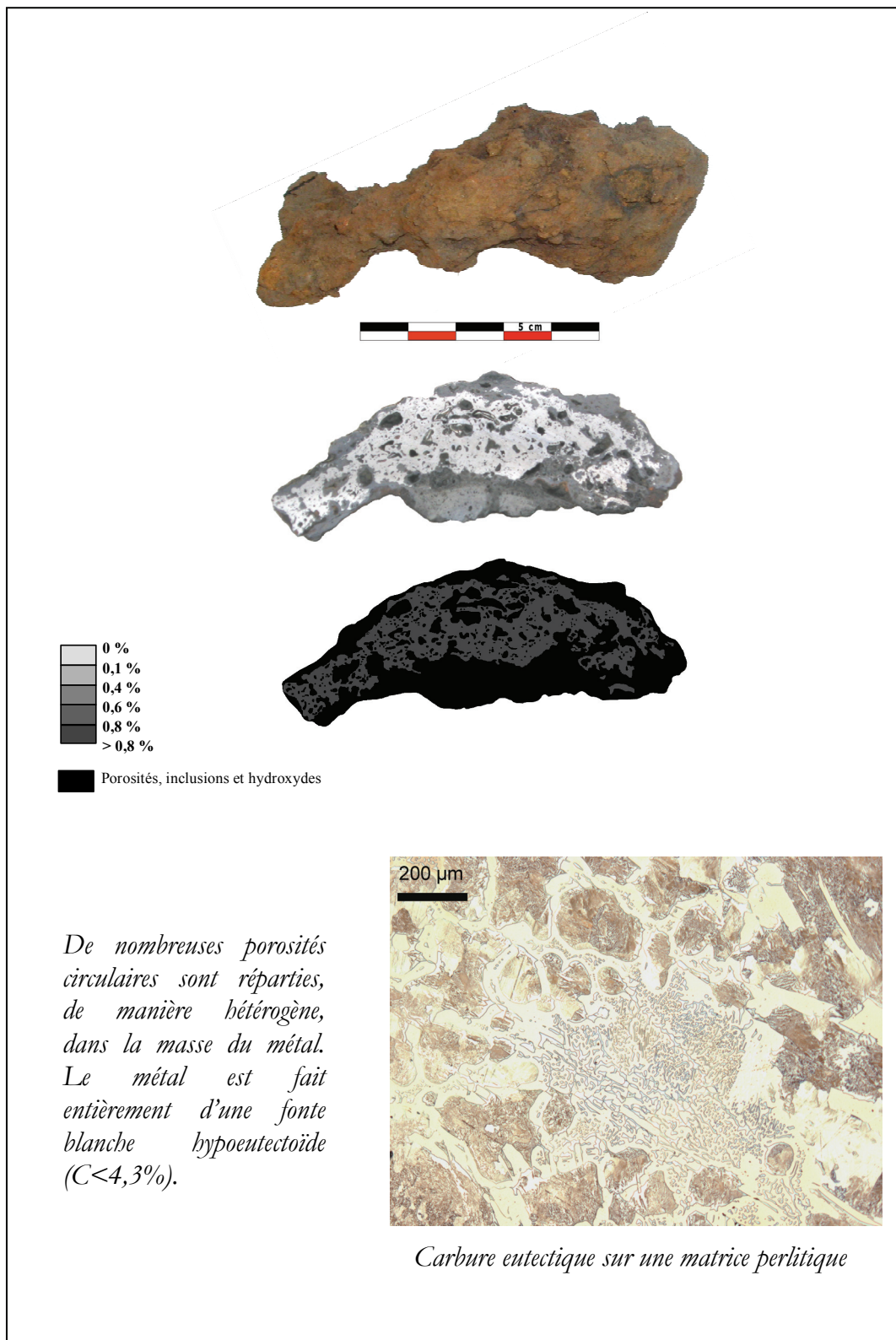
**MICROGRAPHIE :**

L'ensemble des inclusions observées sur toute la surface est amorphe. L'attaque au réactif Nital révèle qu'il s'agit d'une structure de trempe. En effet, sur toute la surface on observe des aiguilles qui caractérisent une structure de martensite, engendrée au cours de la décomposition de l'austénite. La matrice est parfaitement homogène sur le plan micrographique. La trempe homogène dans la masse lui confère une grande dureté. Le traitement thermique de la trempe qui lui donne cette dureté s'accompagne également d'une fragilité aux chocs mécaniques.

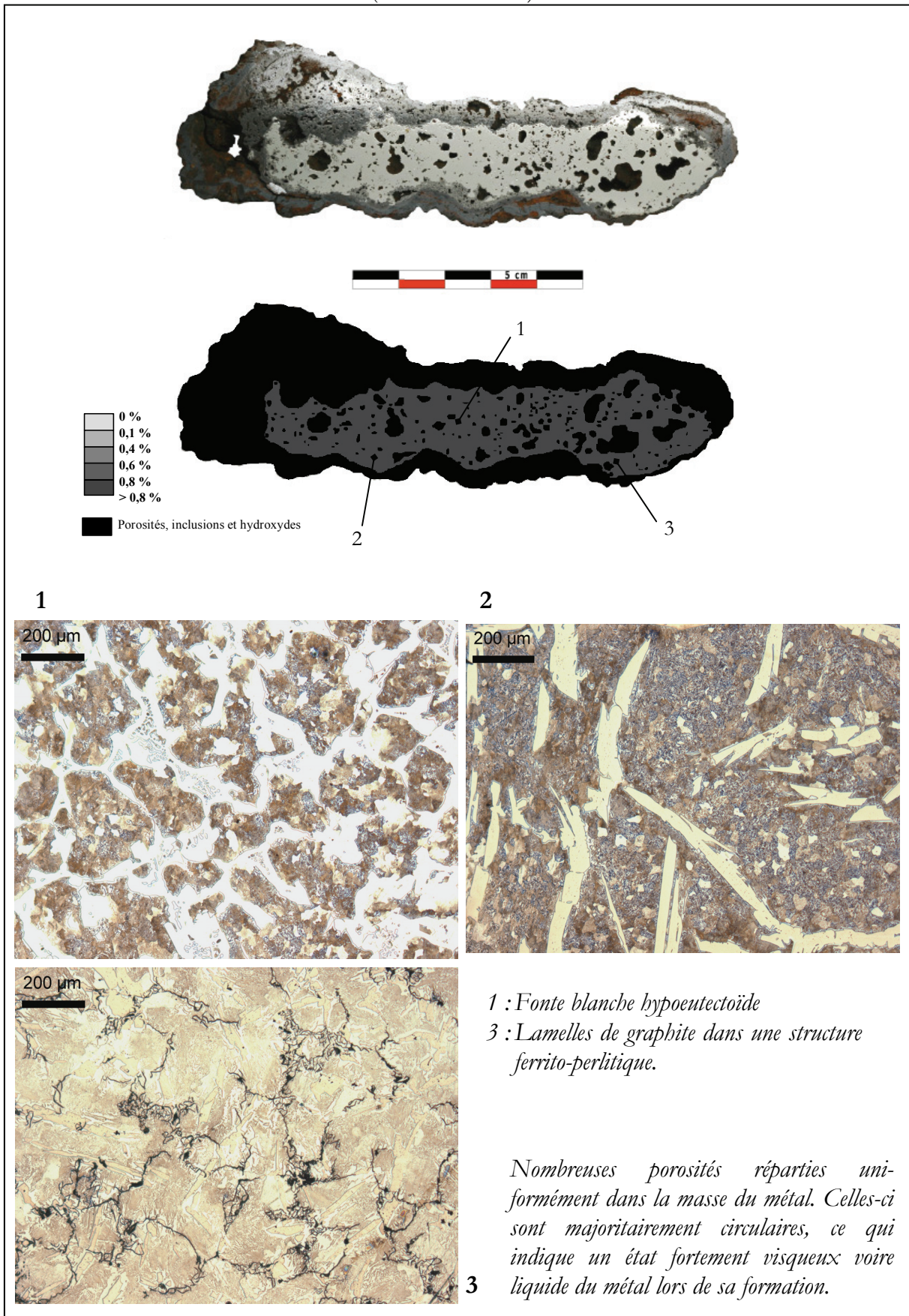
Il convient de noter qu'un objet qui a subi une trempe rend presque impossible le travail de forge du métal. L'observation d'une trempe sur du métal qui n'est pas manufacturé est étonnante. Cette structure de trempe résulte-t-elle d'actions délibérées de la part du forgeron de renforcer le matériau ?



## Annexe P.17 - OBSERVATIONS METALLOGRAPHIQUES DE L'ECHANTILLON CM06-F3 (CASTEL-MINIER)

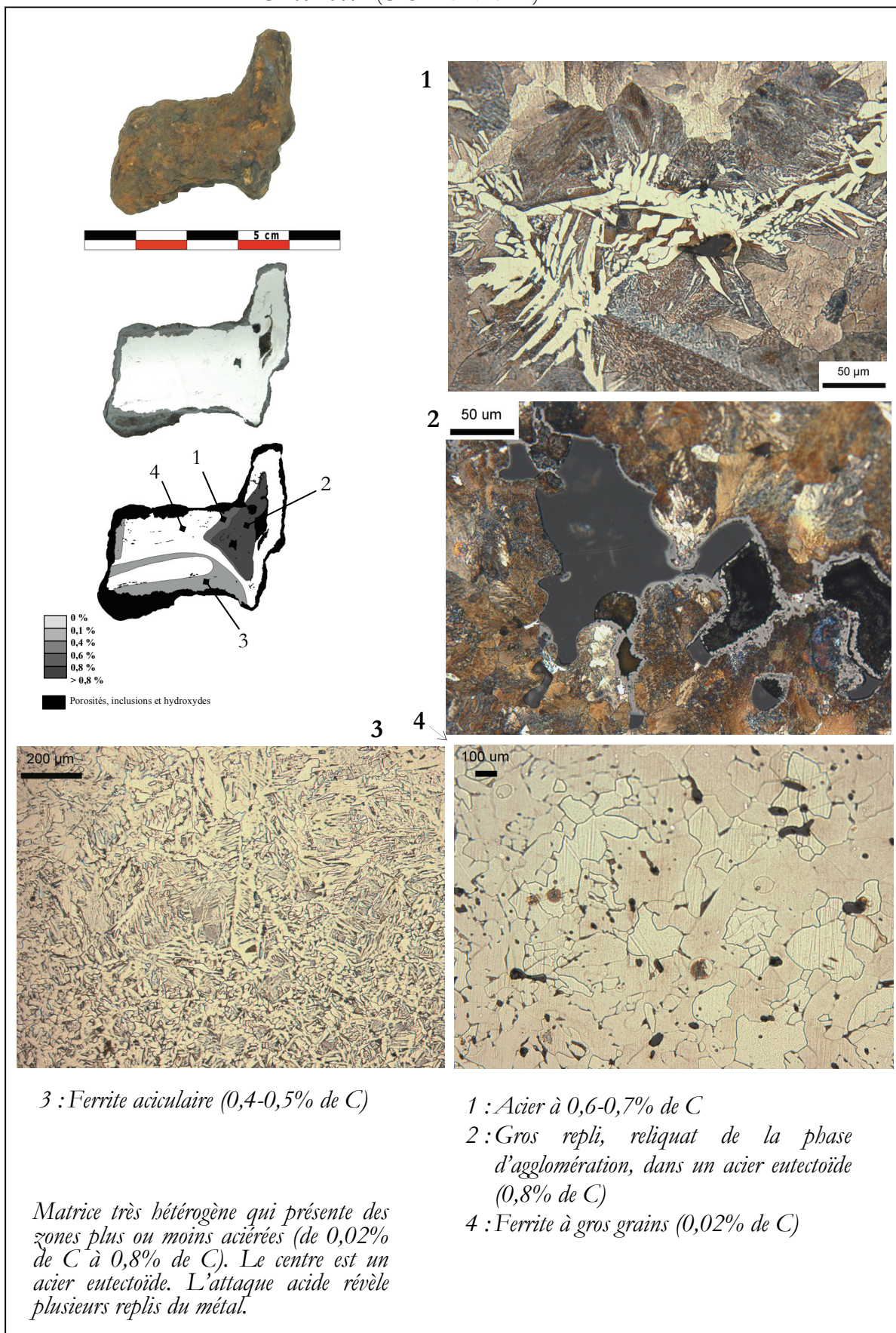


## Annexe P.18 - OBSERVATIONS METALLOGRAPHIQUES DE L'ÉCHANTILLON CM07-2010-1 (CASTEL-MINIER)



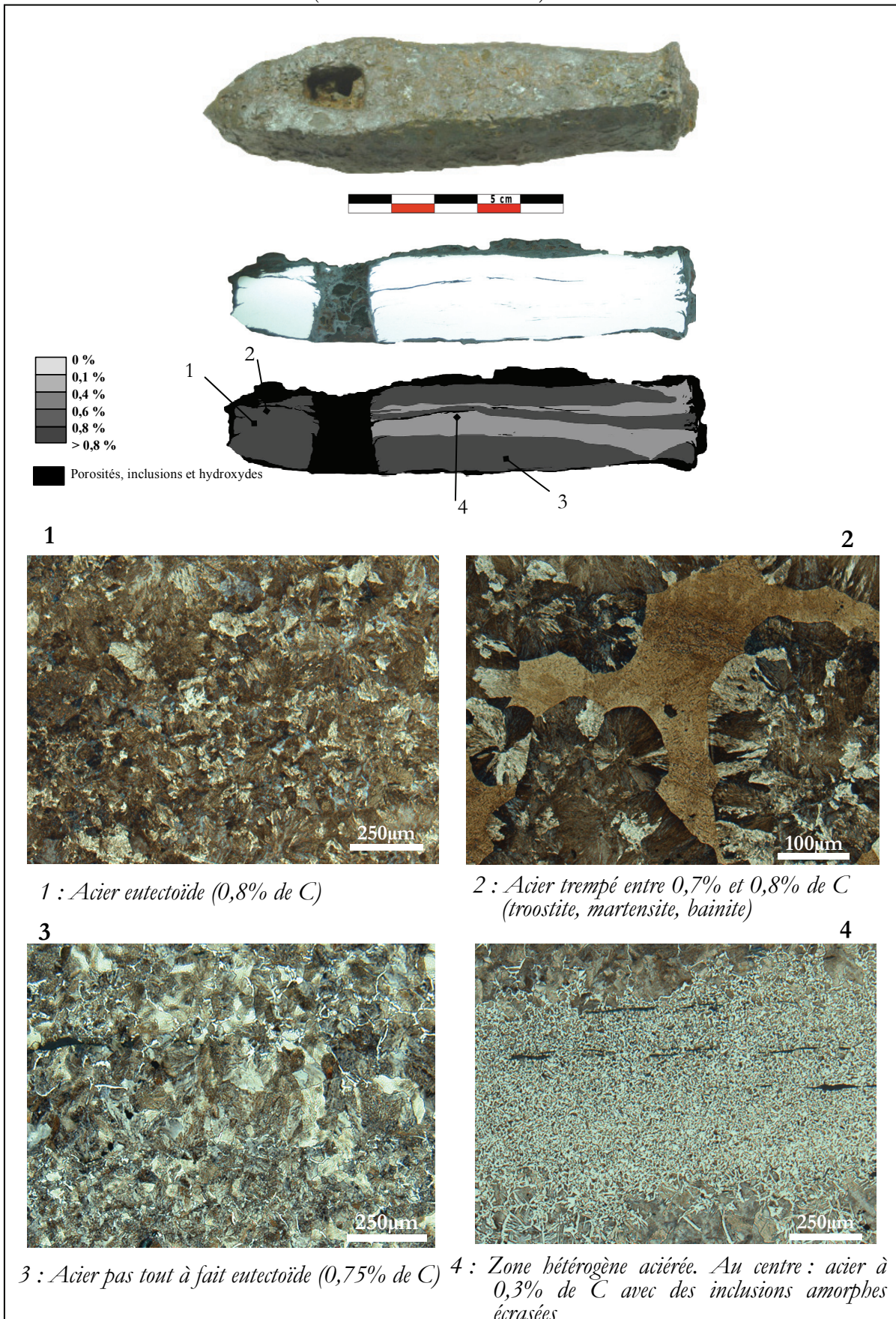


## Annexe P.19 - OBSERVATIONS METALLOGRAPHIQUES DE L'ECHANTILLON CM07-2044-1 (CASTEL-MINIER)

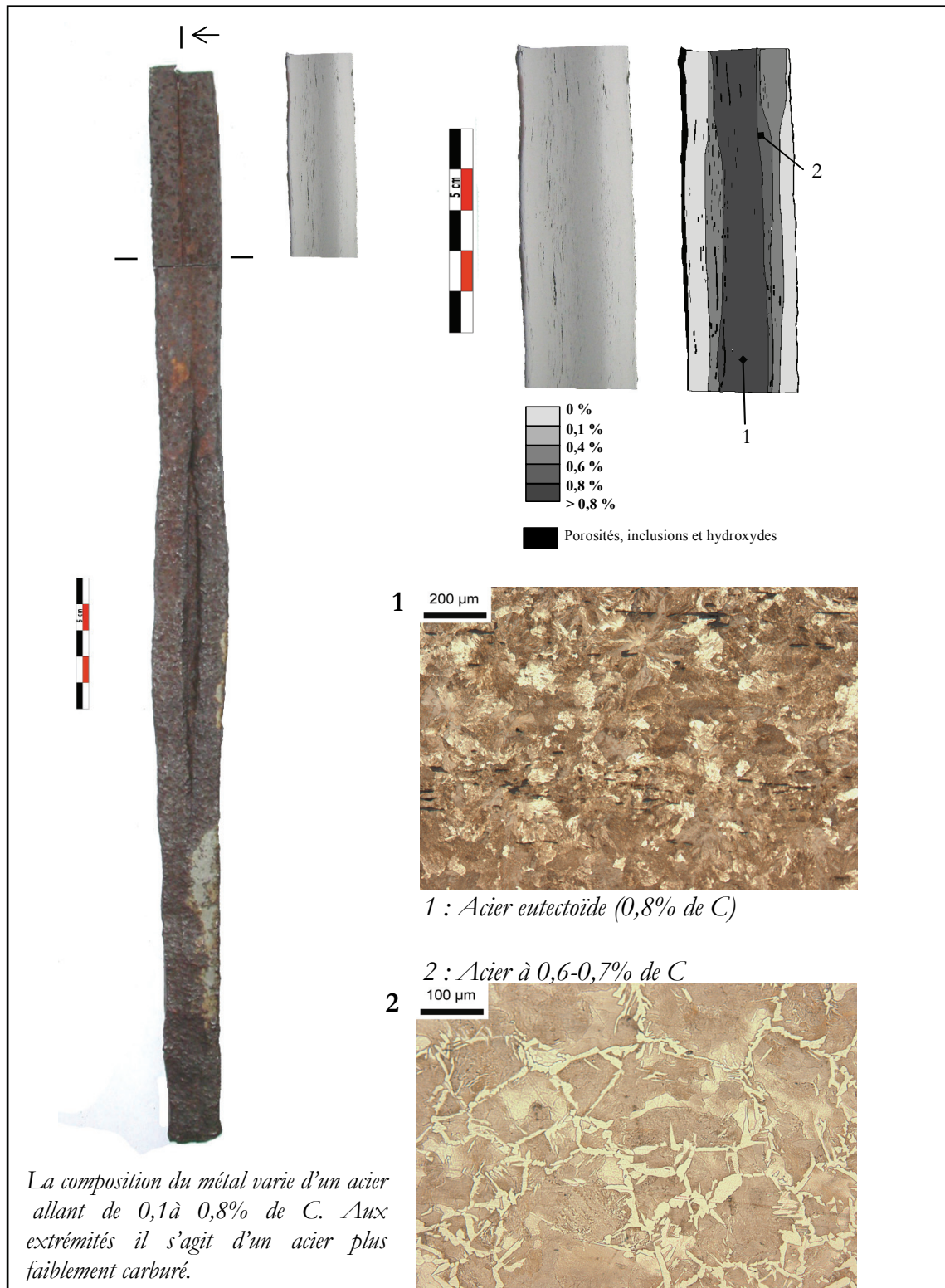




## Annexe P.20 - OBSERVATIONS METALLOGRAPHIQUES DE LA POINTEROLLE i10013 (GALERIE DES ANCIENS)

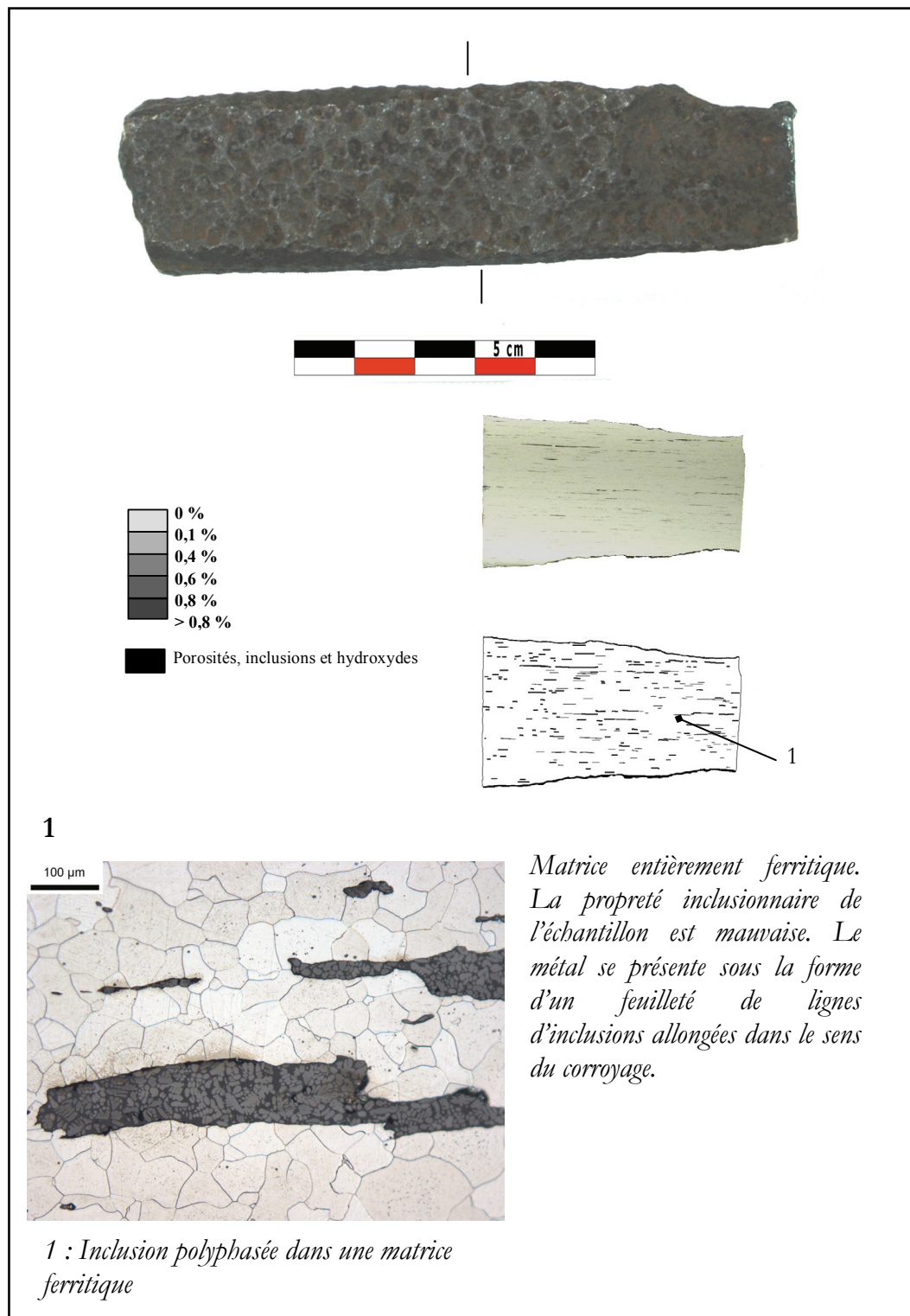


# Annexe P.21 - OBSERVATIONS METALLOGRAPHIQUES DU TIRANT CAP1 (CAPESTANG)

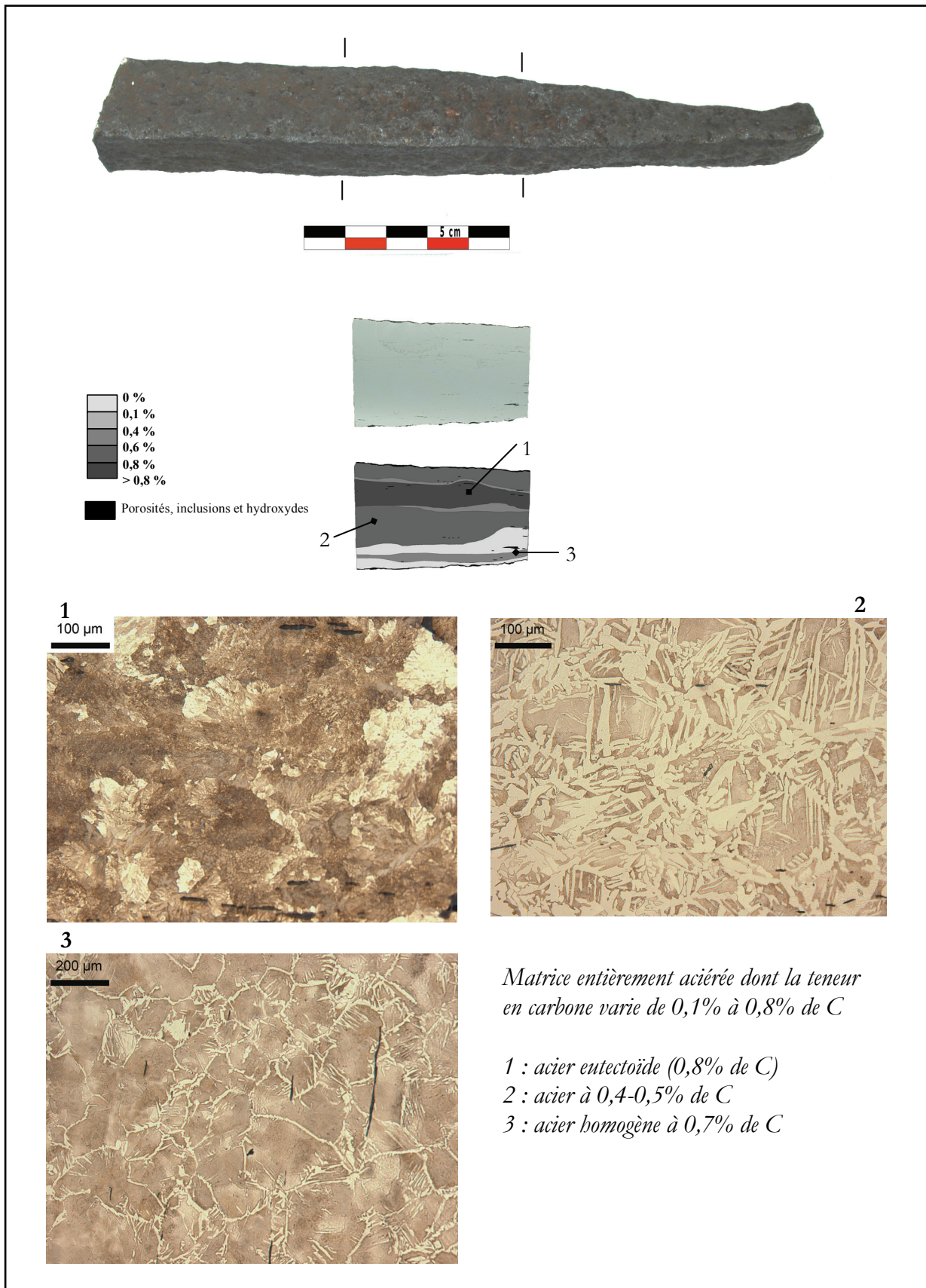




## Annexe P.22 - OBSERVATIONS METALLOGRAPHIQUES DU TIRANT CAP2 (CAPESTANG)

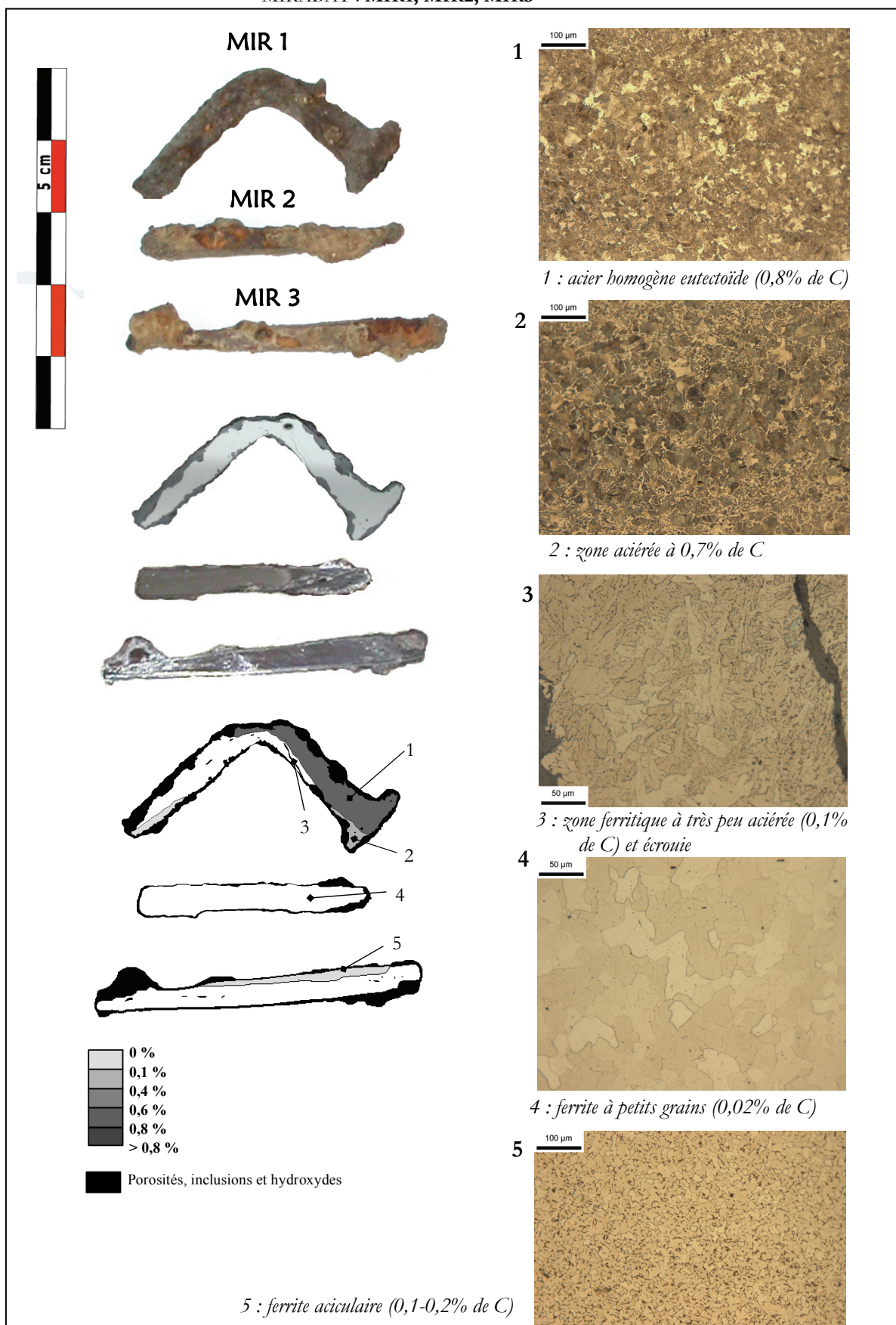


## Annexe P.23 - OBSERVATIONS METALLOGRAPHIQUES DU TIRANT CAP3 (CAPESTANG)

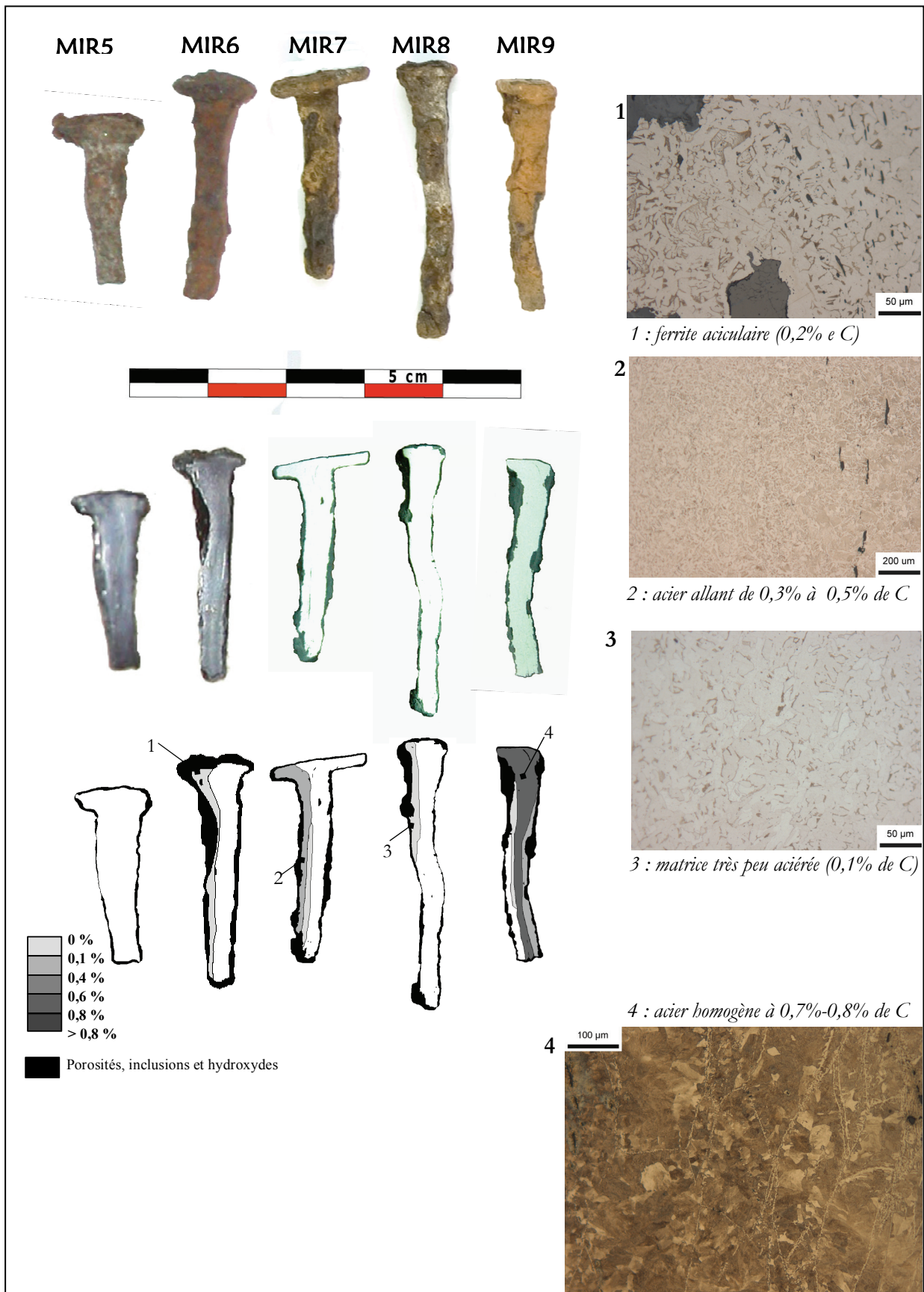




## Annexe P.24 - OBSERVATIONS METALLOGRAPHIQUES DES CLOUS DE MIRABAT : MIR1, MIR2, MIR3



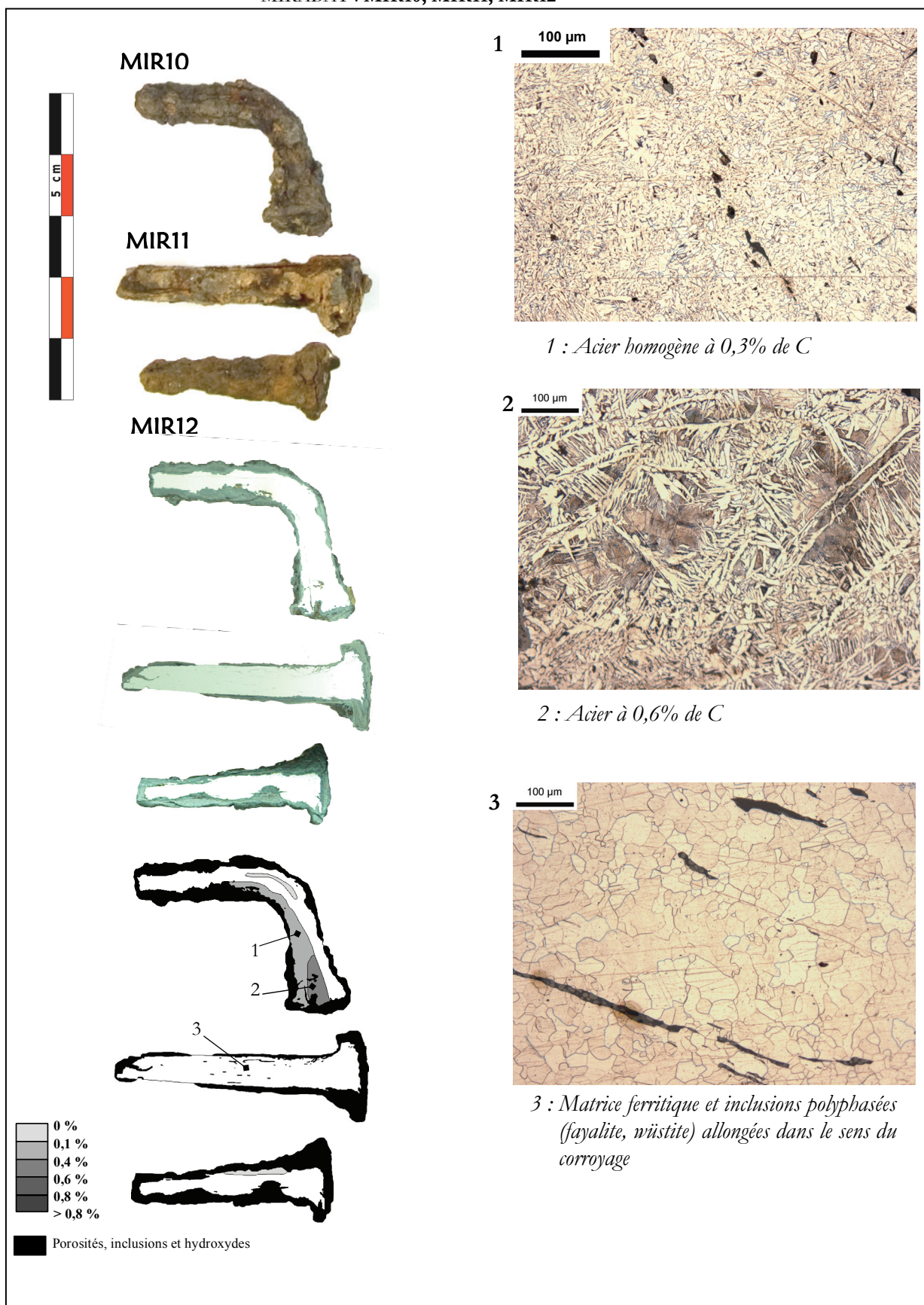
# Annexe P.25 - OBSERVATIONS METALLOGRAPHIQUES DES CLOUS DE MIRABAT : MIR5, MIR6, MIR7, MIR8, MIR9



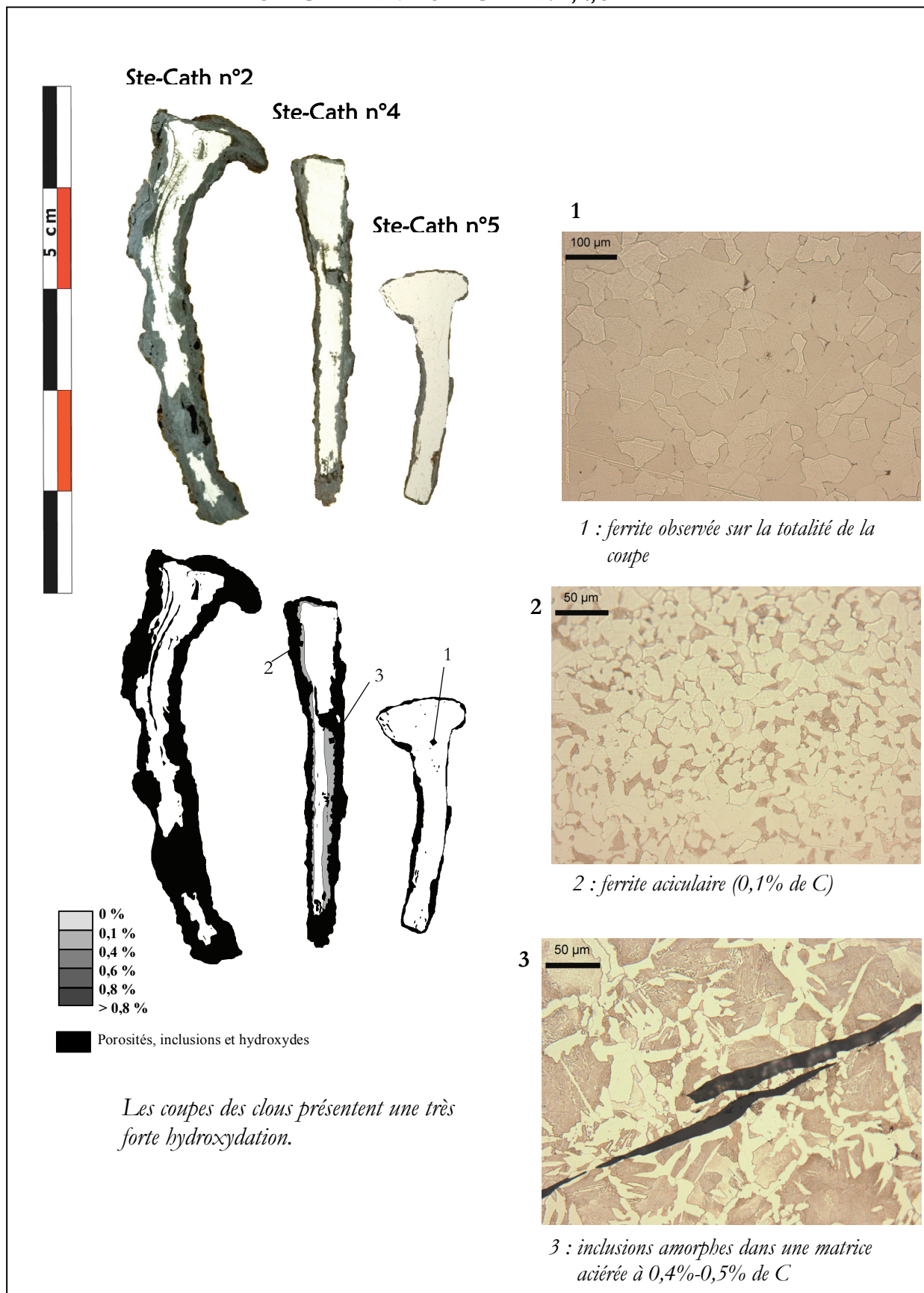
tel-00598796, version 1 - 7 Jun 2011



## Annexe P.26 - OBSERVATIONS METALLOGRAPHIQUES DES CLOUS DE MIRABAT : MIR10, MIR11, MIR12

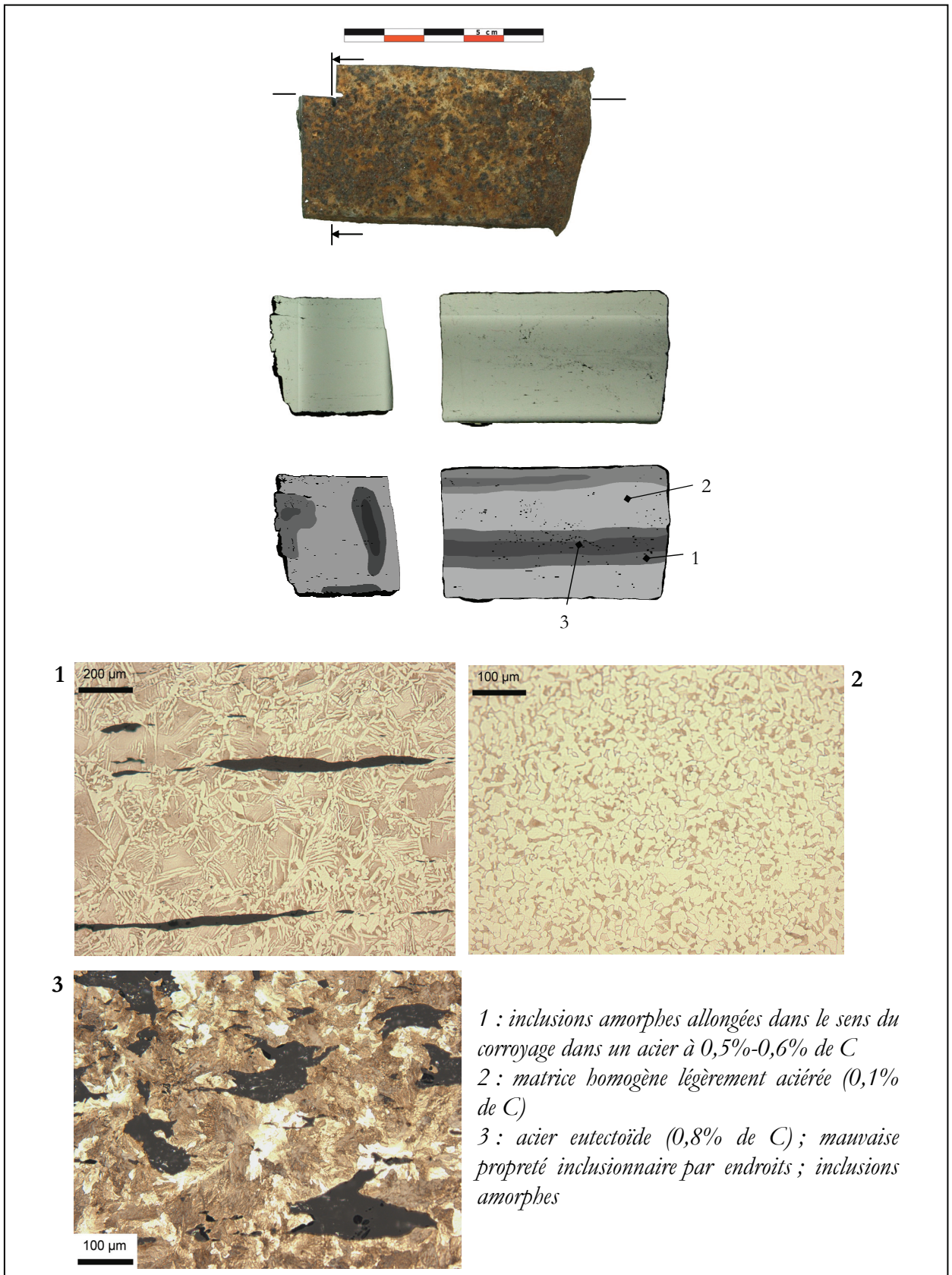


## Annexe P.27 - OBSERVATIONS METALLOGRAPHIQUES DES CLOUS DE STE-CATHERINE : STE-CATH N°2, 4, 5

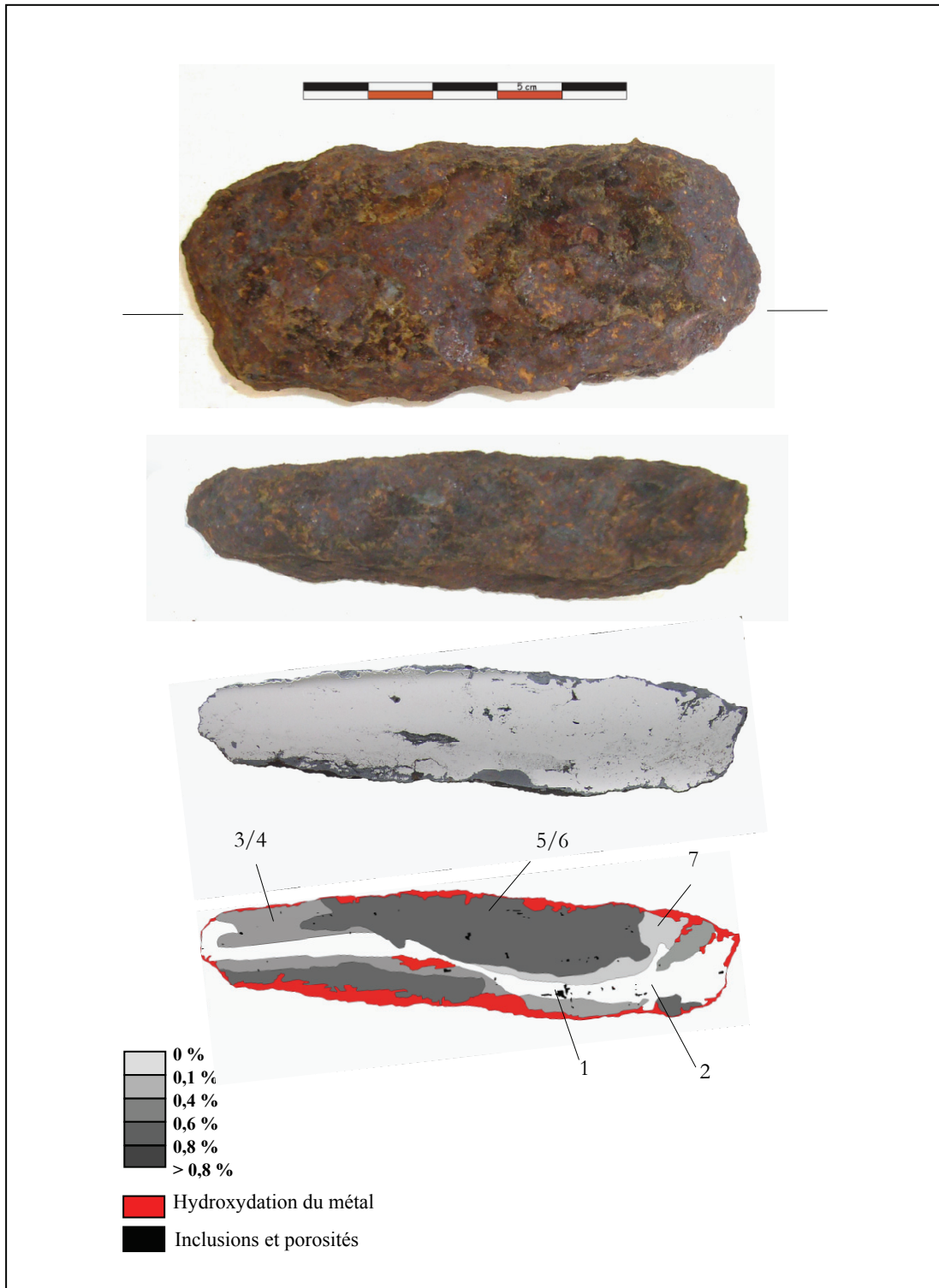




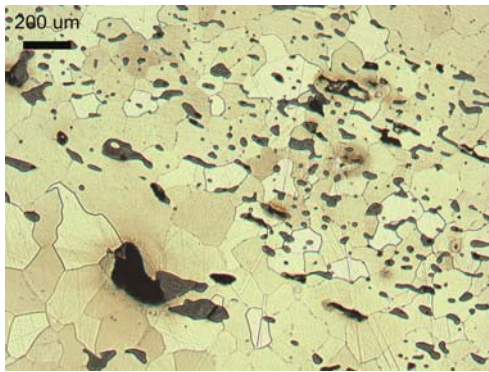
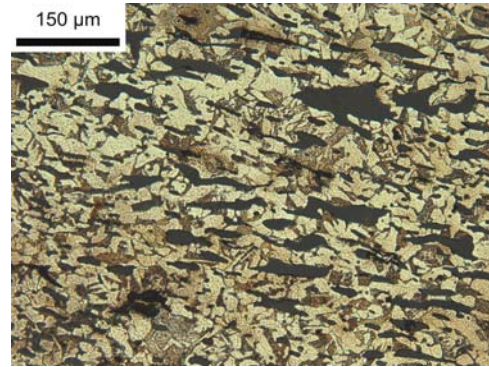
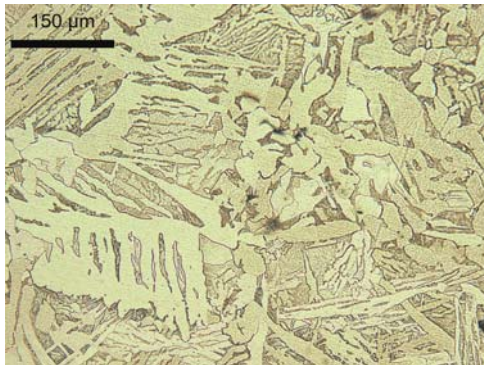
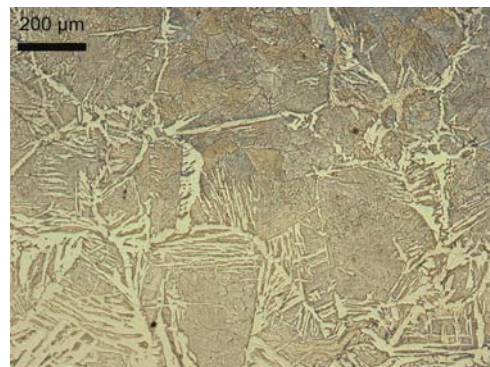
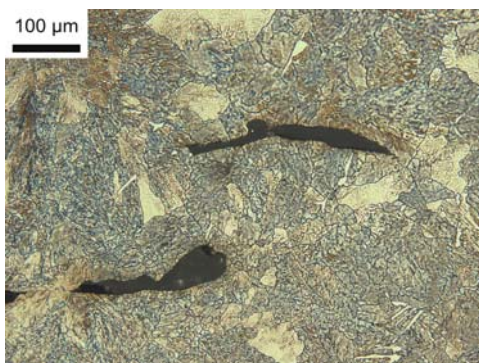
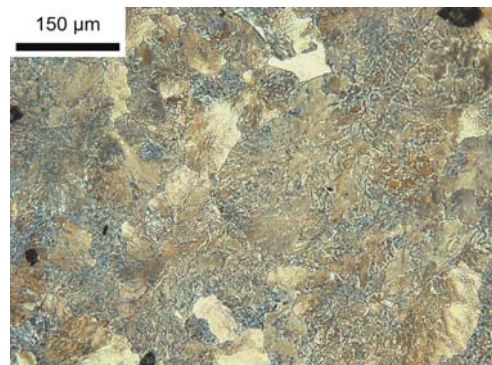
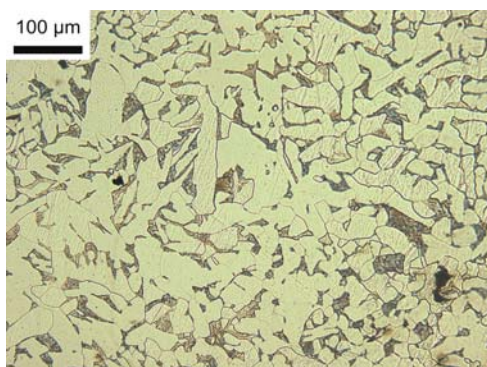
# Annexe P.28 - OBSERVATIONS METALLOGRAPHIQUES DU TIRANT GP3.4 (PALAIS-DES-PAPES)



# Annexe P.29 - OBSERVATIONS METALLOGRAPHIQUES DU LINGOT US1772 (LOMBARDIE)





**Micro 1****Micro 2****Micro 3****Micro 4****Micro 5****Micro 6****Micro 7**

## **MACROGRAPHIE**

Il s'agit d'un lingot de 8,5 cm de long et de section rectangulaire, dont la forme générale s'affine à l'une des extrémités. La coupe révèle un métal qui présente une très mauvaise propreté inclusionnaire par endroits. Les porosités et inclusions peuvent être de taille millimétrique. Les plus grosses inclusions comportent de nombreuses porosités circulaires ce qui indique une très forte viscosité, voire une liquéfaction lors de leur formation. Elles ne présentent pas de déformation longitudinale, parallèle aux bords ce qui semble indiquer une absence de corroyage.

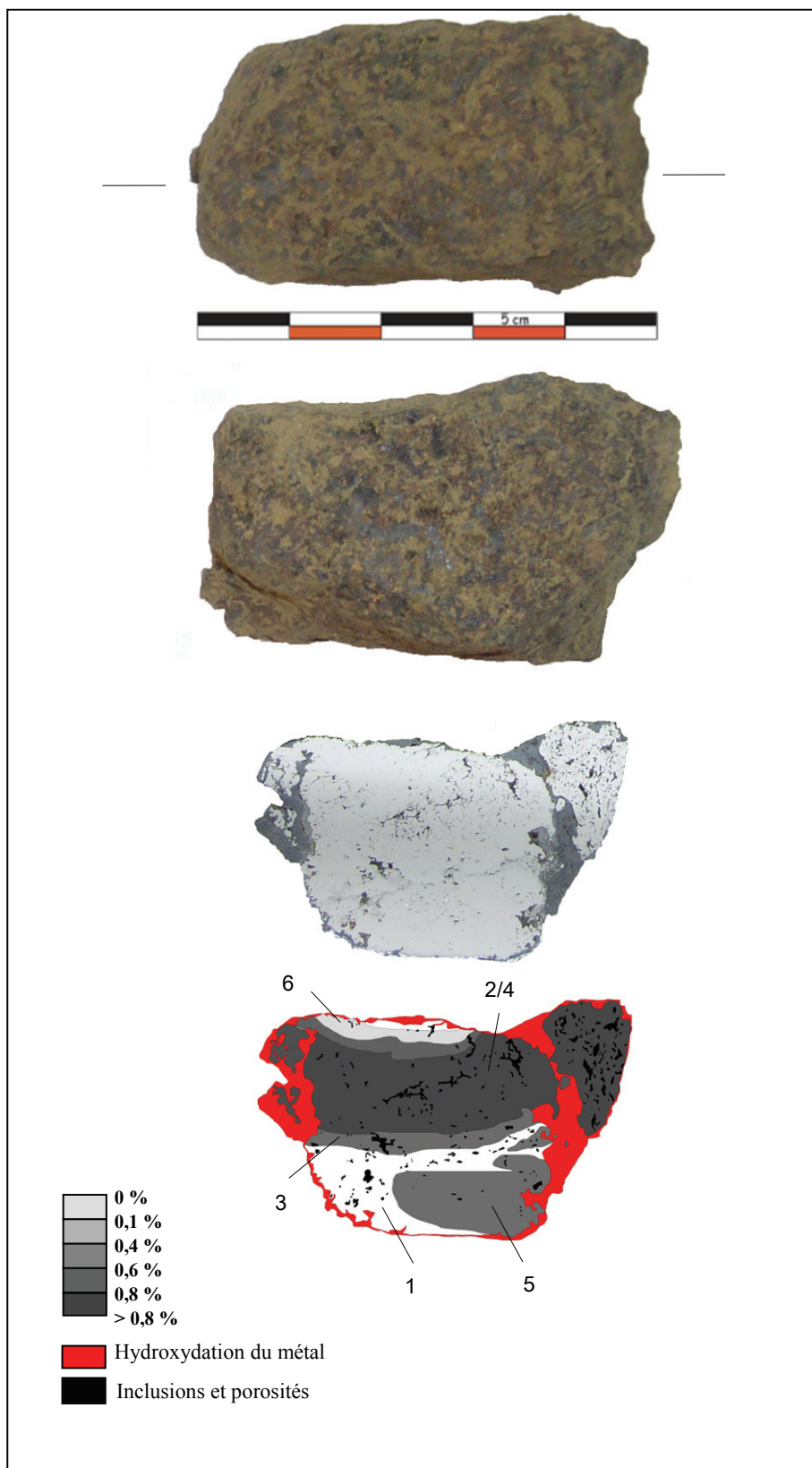
## **MICROGRAPHIE**

L'analyse métallographique révèle une propreté inclusionnaire de ce métal très mauvaise, visible notamment du côté de l'extrémité la plus large dans la partie (1/2).

Les inclusions observées, nombreuses et réparties de façon hétérogène, sont majoritairement amorphes (4), tandis que certaines sont composées de fayalite et globules de wüstite majoritairement présentes dans la ferrite. En plus des inclusions, la face polie présente un nombre non négligeable de porosités, remplies parfois d'oxydes et d'oxyhydroxydes de fer.

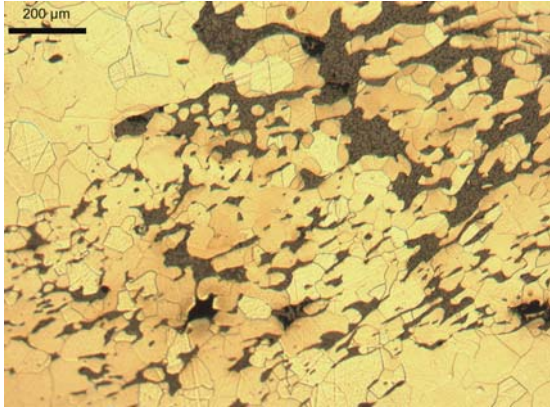
Après attaque au nital, on observe une composition hétérogène du métal composé de lignes plus ou moins aciérées. Le centre est plutôt ferritique (1) tandis que la périphérie est davantage aciérée allant de 0,2 (6) à 0,8% (5) de carbone. La majorité du métal est constitué d'acier très carburé, eutectoïde.

# Annexe P.30 - OBSERVATIONS METALLOGRAPHIQUES DU LINGOT US1660 (LOMBARDIE)

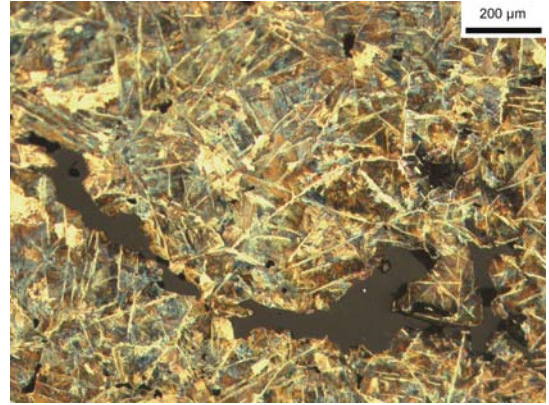




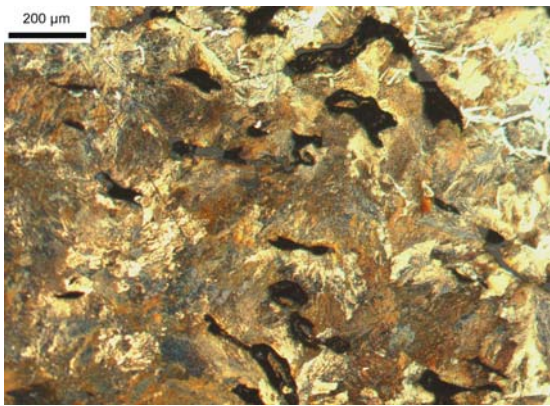
**Micro 1**



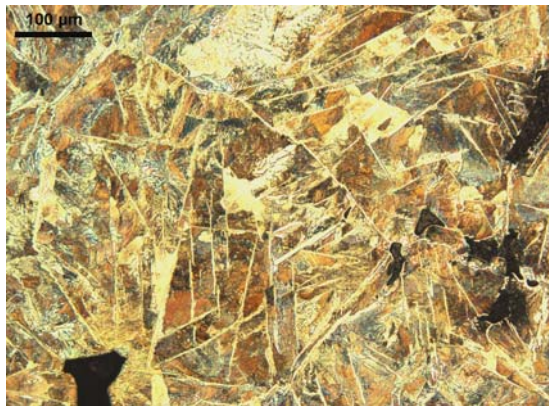
**Micro 2**



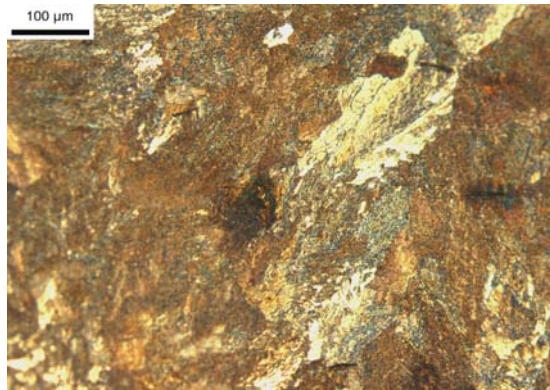
**Micro 3**



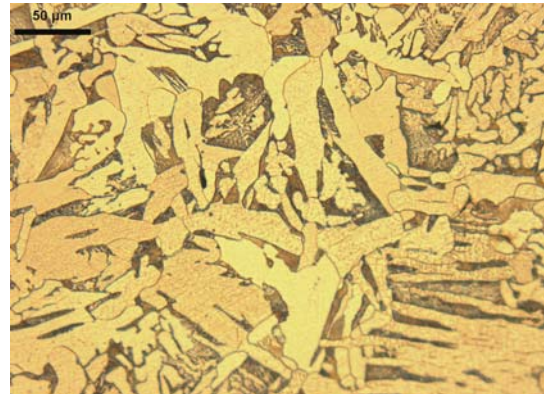
**Micro 4**



**Micro 5**



**Micro 6**



**MACROGRAPHIE :**

Il s'agit d'un lingot de 4,5 cm de long et de section beaucoup moins rectangulaire que le lingot US 1772. Le métal présente une très mauvaise propreté inclusionnaire sur toute la surface de l'échantillon. De nombreuses inclusions sont visibles.

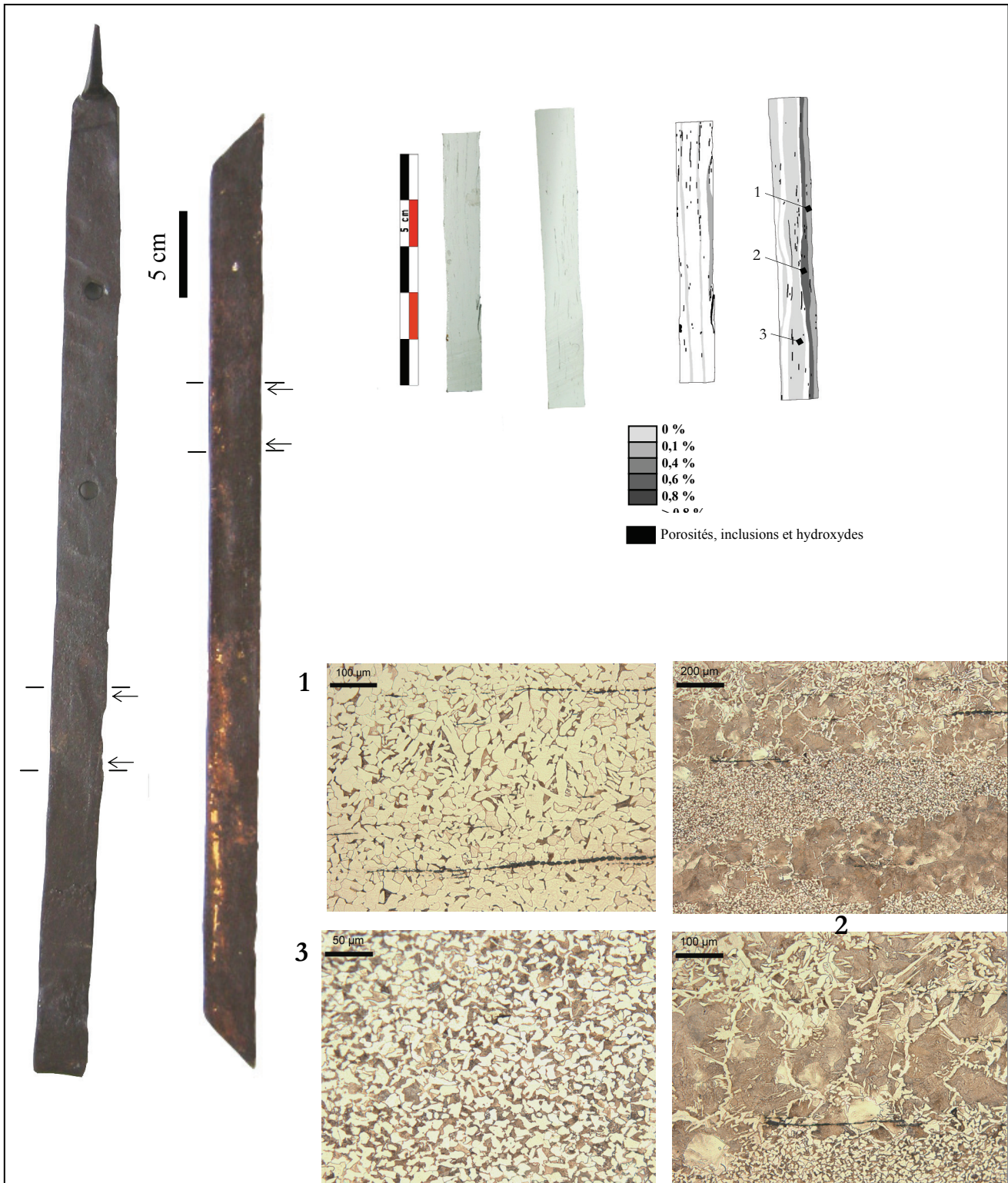
**MICROGRAPHIE :**

Comme pour l'autre lingot, un grand nombre d'inclusions d'aspect amorphe ont été observées au microscope optique mais, en revanche, aucune porosité n'est visible. De plus, les inclusions sont allongées dans le sens perpendiculaire au martelage (dans le sens de la longueur de l'objet) signe d'un martelage plus poussé que pour le lingot. Cet objet proviendrait d'une étape postérieure de la chaîne opératoire.

Le lingot a une matrice à dominante ferritique avec quelques zones faiblement carburées à moins de 0,35%<sub>mass</sub> de carbone. Les analyses métallographiques montrent que l'objet a une matrice à dominante eutectoïde (0,8%<sub>mass</sub> C) à hypereutectoïde (> 0,8%<sub>mass</sub> C). Sur la partie supérieure de l'objet, la teneur en carbone baisse (0,7%<sub>mass</sub> C).



# Annexe P.31 - OBSERVATIONS METALLOGRAPHIQUES DE L'ECHANTILLON Clé16 (PIEMOMT)



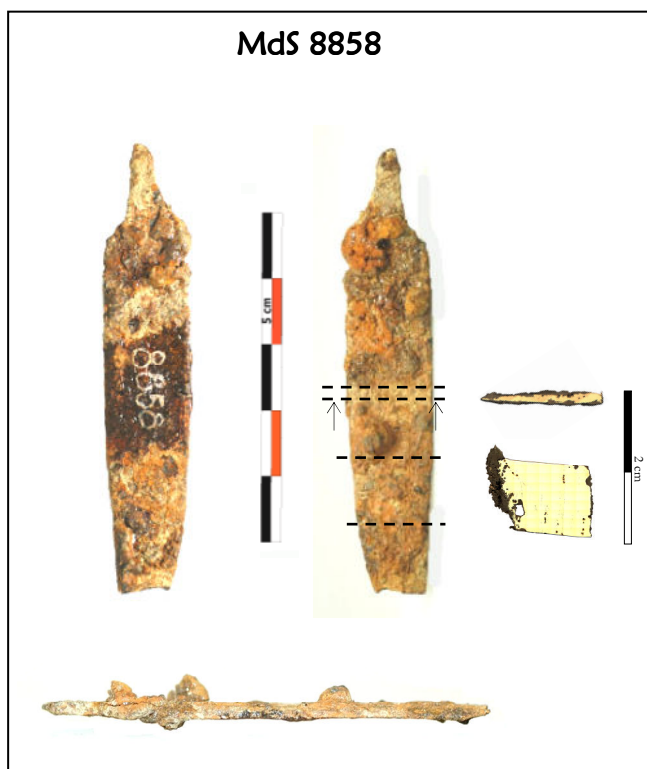
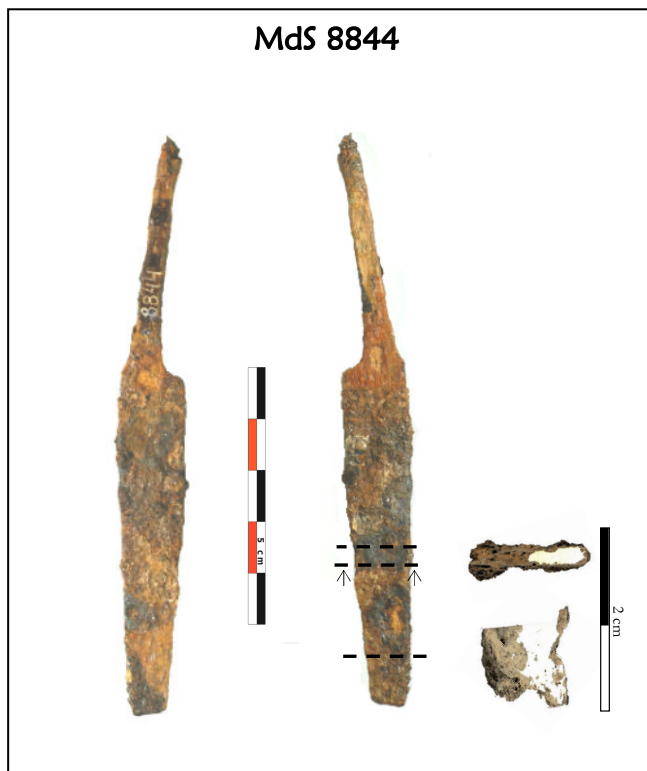
tel-00598796, version 1 - 7 Jun 2011



## **Annexe Q**

**CORPUS DES OBJETS DU SITE DE MONTRÉAL-DE-SOS  
ÉTUDIÉS DANS CE TRAVAIL**







Mds 29431



Mds 29522



Mds 29566



Mds 29591







## **Annexe R**

**LISTE DES ÉCHANTILLONS D'ORIGINE CONNUE  
COLLECTÉS ET ÉTUDIÉS DANS CE TRAVAIL  
(MINÉRAIS, SCORIES, OBJETS)**



**LISTE DES ECHANTILLONS DE MINERAIS (ARCHEOLOGIQUES ET  
GEOLOGIQUES) ET DE SCORIES**

ARIEGE		
Nom échantillon	Origine/Localisation	Remarques
CM06-2002/M1	Site de Castel-Minier US2002	Minerai archéologique grillé
CM06-2002/M2	Site de Castel-Minier US2002	Minerai archéologique grillé
CM06-2018/M1	Site de Castel-Minier US2018	Minerai archéologique grillé
CM06-2018/M2	Site de Castel-Minier US2018	Minerai archéologique grillé
CM06-2033/M1	Site de Castel-Minier US2033	Minerai archéologique grillé
CM06-2033/M2	Site de Castel-Minier US2033	Minerai archéologique grillé
CM06-2008/M1	Site de Castel-Minier US2008	Minerai archéologique grillé
CM06-2007/M1	Site de Castel-Minier US2007	Minerai archéologique rouge
CM06-2004/M1	Site de Castel-Minier US2004	Minerai archéologique grillé
R6	Site de Castel-Minier	Minerai archéologique grillé. Ramassage de surface
2190 Rancié	Mont-Rancié	Minerai géologique
GPS 45a	Mont-Rancié	Minerai géologique
GPS 52	Mont-Rancié	Minerai géologique

GPS 46a	Mont-Rancié	Minerai géologique
GPS 51a	Mont-Rancié	Minerai géologique
GPS 51b	Mont-Rancié	Minerai géologique
GPS 53	Mont-Rancié	Minerai géologique
2189 Rancié	Mont-Rancié	Minerai géologique
R1	Mont-Rancié	Minerai géologique
R2	Mont-Rancié	Minerai géologique
R3	Mont-Rancié	Minerai géologique
R5	Mont-Rancié	Minerai géologique
R7	Mont-Rancié	Minerai géologique
R8	Mont-Rancié	Minerai géologique
R9	Mont-Rancié	Minerai géologique
R10	Mont-Rancié	Minerai géologique
R11	Mont-Rancié	Minerai géologique
R12	Mont-Rancié	Minerai géologique
XP07-min	Mont-Rancié	Minerai utilisé pour XP07 grillé
Lerc-min/1	Site de Lercoul	Minerai archéologique grillé
Lerc-min/2	Site de Lercoul	Minerai géologique
XP07-sco1	XP07	Scorie coulée expérimentale
XP07-sco2	XP07	Scorie coulée expérimentale
CM06-2002/1	Site de Castel-Minier	Scorie coulée
CM06-1004/1	Site de Castel	Scorie coulée
CM06-2008/1	Site de Castel	Scorie coulée
CM06-1004/2	Site de Castel	Scorie coulée
CM06-2020/1	Site de Castel	Scorie coulée
SCCM1	Site de Castel	Fond de four
SCCM2	Site de Castel	Fond de four
CM06-2014/1	Site de Castel	Scorie dense coulée
CM06-2002/2	Site de Castel	Scorie coulée
CM06-2018/2	Site de Castel	Scorie coulée
CM06-2020/2	Site de Castel	Scorie coulée
CM06-1004/3	Site de Castel	Scorie coulée

CM06-2018/1	Site de Castel	Très fragmentée, peu dense, beaucoup de charbon
CM07-2099/1	Site de Castel	Scorie coulée
CM07-2088/1	Site de Castel	Pièce très cassée
CM07-2026/1	Site de Castel	Scorie plano convexe entière
CM06-2004/1	Site de Castel	Scorie coulée
SAV1	Site de Savignac	Scorie coulée
SAV2	Site de Savignac	Scorie coulée
SAV3	Site de Savignac	Scorie coulée
LERC1	Site de Lercoul	Scorie coulée
Lerc/1 (Lerc-sco 2072*)	Site de Lercoul	Scorie dense écoulée
Lerc/2 (Lerc-sco 2073*)	Site de Lercoul	Scorie dense
Lerc/3 (Lerc-sco 2074*)	Site de Lercoul	Scorie dense
Lerc/4 (Lerc-sco 2075*)	Site de Lercoul	Scorie dense
Lerc/5 (Lerc-sco 2076*)	Site de Lercoul	Scorie dense
Lerc/6 (Lerc-sco 2077*)	Site de Lercoul	Scorie dense
Lerc/7 (Lerc-sco 2078*)	Site de Lercoul	Scorie dense
Lerc/8 (Lerc-sco 2079*)	Site de Lercoul	Scorie de fond de four bulleuse
Lerc/9 (Lerc-sco 2080*)	Site de Lercoul	Scorie dense (quelques graviers)
Lerc/10 (Lerc-sco 2081*)	Site de Lercoul	Scorie dense (quelques graviers)
Lerc/11 (Lerc-sco 2082*)	Site de Lercoul	Scorie dense
Lerc/12 (Lerc-sco 2083*)	Site de Lercoul	Scorie dense
Lerc/15	Site de Lercoul	Scorie coulée
RIV 01	Riverenert	Scorie dense
RIV 02	Riverenert	Scorie dense
RIV 03	Riverenert	Scorie dense
RIV 04	Riverenert	Scorie dense
RIV 06	Riverenert	Scorie coulée
RIV 07	Riverenert	Scorie coulée

## LOMBARDIE

Nom échantillon	Origine/Localisation	Remarques
GAF1/M1	Mine de Gaffione	Minerai géologique
GAF1/M2	Mine de Gaffione	Minerai géologique
GAF1/M3	Mine de Gaffione	Minerai géologique
GAF2/M1	Mine de Gaffione	Minerai géologique
GAF/2	Mine de Gaffione	Minerai géologique
GAF/2bis	Mine de Gaffione	Minerai géologique
ST(M)/M1	Mine de Stendata	Minerai géologique
ST1/M1	Mine de Stendata	Minerai géologique
ST1/M2	Mine de Stendata	Minerai géologique
ST4/M1	Mine de Stendata	Minerai géologique
ST4/M2	Mine de Stendata	Minerai géologique
ST3/M1	Mine de Stendata	Minerai géologique
ST3/M2	Mine de Stendata	Minerai géologique
San.M/M1	Mine de San Marco	Minerai géologique
San M/M2	Mine de San Marco	Minerai géologique
San M/M3	Mine de San Marco	Minerai géologique
San M/M4	Mine de San Marco	Minerai géologique
San M/M5	Mine de San Marco	Minerai géologique
TRIO1/M1	Mine de Triomen	Minerai géologique
TRIO3/M1	Mine de Triomen	Minerai géologique
T1Z 021**	Ponte Val Gabbia	Minerai grillé
T1Z 031**	Piazza lunga	Hématite
T1Z 033**	Piazza lunga	Limonite
Lago D'inferno	Lago d'Inferno	Minerai géologique
CARISOLE	Mine de Carisole	Minerai géologique
VAL.BONDIONE	Mine de ValBondione	Minerai géologique
SCHz2s1/M1	Site de Schilpario	Minerai archéologique grillé
SCHI z1 S1/M1	Site de Schilpario	Minerai archéologique grillé
SCH min Hab/M1	Mines à proximité de Schilpario	Minerai géologique
SCH MINES /M2	Mines à proximité de Schilpario	Minerai géologique



SCH08/1	Site de Schilpario	Scorie coulée
SCH08/2	Site de Schilpario	Scorie coulée
SCH04/1	Site de Schilpario	Scorie coulée
SCH01/1	Site de Schilpario	Scorie de réduction très dense, peu poreuse
SCH06/1	Site de Schilpario	Scorie coulée
SCH06/2	Site de Schilpario	Scorie coulée
SCH07/1	Site de Schilpario	Scorie coulée
SCH03/1	Site de Schilpario	Scorie coulée
SCH02/1	Site de Schilpario	Scorie coulée
SCH02/2	Site de Schilpario	Scorie coulée
SCH03/2	Site de Schilpario	Scorie coulée
SCH05/1	Site de Schilpario	Scorie coulée
T1Z 002**	Ponte Val Gabbia	Scorie type p
T1Z 003**	Ponte Val Gabbia	Scorie type l
T1Z 004**	Ponte Val Gabbia	Scorie type k
T1Z 005**	Ponte Val Gabbia	Laitier l1
T1Z 006**	Ponte Val Gabbia	Scorie type h
T1Z 007**	Ponte Val Gabbia	Laitier b1

## ANDORRE

Nom échantillon	Origine/Localisation	Remarques
FR641/1	Forge Rossell couche de scories concassées	Scorie coulée très poreuse
FR641/2	Forge Rossell couche de scories concassées	Scorie coulée très poreuse
FR803/1	Forge Rossell	Fragment de scorie coulée dense
FA ss CTX	Forge Areny sol de la forge	Fragment informe de la sole du bas foyer
FA02UE9217/1	Forge Areny	Scorie coulée
FA2002UE9217/2	Forge Areny	Scorie coulée
FA9275/1	Forge Areny	Fragment de scorie denses scorie de la calotte du bas foyer ?

FA9275/2	Forge Areny	Fragment de scorie denses scorie de la calotte du bas foyer ?
FA9245/1	Forge Areny secteur de la soucherie du marteau	Fragment de scorie coulée concassée
FA9101/1	Forge Areny	Scorie coulée
FRUE600/1	Forge Rossell	Fragment de culot de foyer de réduction
FRUE645/1	Forge Rossell	Fragment de scorie dense, bulleuse, légèrement magnétique
FR1010/M1	Forge Rossell four de grillage	Fragment de minerai grillé
FR1010/M2	Forge Rossell four de grillage	Fragment de minerai grillé
FR1010/M3	Forge Rossell four de grillage	Fragment de minerai grillé
FA9245/M1	Forge Areny	Fragment de minerai grillé

## DAUPHINE

Nom échantillon	Origine/Localisation	Remarques
PEL 87 006*	Site de La Pelouse (Allevard)	Scorie dense
PEL 87 007*	Site de La Pelouse (Allevard)	Scorie dense
PEL 87 008*	Site de La Pelouse (Allevard)	Scorie dense
PEL 87 001*	Site de La Pelouse (Allevard)	Scorie coulée dense
PEL 87 002*	Site de La Pelouse (Allevard)	Scorie coulée dense
PEL 87 003*	Site de La Pelouse (Allevard)	Scorie coulée dense
PEL 87 005*	Site de La Pelouse (Allevard)	Scorie coulée dense
PEL 8810*	Site de La Pelouse (Allevard)	Minerai
PEL 8811*	Site de La Pelouse (Allevard)	Minerai

\* Notation de l'échantillon dans la base PalSid

\*\* Echantillons confiés pour analyses par V.Serneels

**LISTE DES OBJETS D'ORIGINE CONNUE, MIS AU JOUR**  
**SUR LES SITES ARCHEOLOGIQUES DE PRODUCTION**

ARIEGE		
Nom échantillon	Origine/Localisation	Remarques
CM06-2002-3	Site de Castel-Minier US2002 Niveau de scorie supérieur du ferrier 1	2 fragments de loupe reliés par de la scorie (masse : 368g)
CM06-F3	Site de Castel-Minier ferrier 3	Fragment de loupe (masse : 201g)
CM06-2003-2	Site de Castel-Minier US2003	Fragment de loupe (masse : 50g)
CM06-2008-1	Site de Castel-Minier US2008 niveau de scorie et de charbon du ferrier 1	Lingot -dimensions : 110x70x22 -masse : 595g
CM06-2002-2	Site de Castel-Minier US2002 Niveau de scorie supérieur du ferrier 1	Plaque élaborée -dimensions : 120x20x17 (1) 120x45x13 (2) -masse : 273g
CM06-2002-1	Site de Castel-Minier US2002 Niveau de scorie supérieur du ferrier 1	Tige -dimensions : 87x10x11 -masse : 49g
CM06-2003-1	Site de Castel-Minier US2001	Tige -dimensions : 100x17x17 -masse : 130g
CM06-2001-1	Site de Castel-Minier US2001 Niveau de terre végétale	Tige avec angle -dimensions : 2 sections 88x12x10 et 73x10x10 -masse : 69g

CM06-2004-1	Site de Castel-Minier US2004 amas de scories denses de la tranchée nord	Tôle courbée -dimensions : 112x50x(3-10) -masse : 179g
CM06-2004-2	Site de Castel-Minier US2004	-dimensions : 12x7x4,5 -masse : 982g
CM06-2004-3	Site de Castel-Minier US2004	Gromps -masse : 136g
CM07-2010-1	Site de Castel-Minier US2010	Gromps -masse : 539g
CM05-01-2--4	Site de Castel-Minier sondage 2004-2005	Gromps
CM05-01-2--17	Site de Castel-Minier sondage 2004-2005	Gromps
CM05-01-2--27	Site de Castel-Minier sondage 2004-2005	Tige

## LOMBARDIE

Nom échantillon	Origine/Localisation	Remarques
SCH-met1	Site de Schilpario (Surface)	Ebauche d'outil ? (masse : 97g)

## ANDORRE

Nom échantillon	Origine/Localisation	Remarques
FA-91/42	Forge Areny sol de travail du martinnet	Déchet de forgeage
FA02-9142	Forge Areny sol de travail du martinnet	Fragment de plaque
FR98-UE722	Forge Rossell couche du canal d'évacuation de la forge	Fragment de métal – échantillon de fer en cours de réduction
FR-UE629	Forge Rossell sol de la forge	Coin du bas-foyer qui servait à supporter le nez de la tuyère

FR 99	Forge Rossell martinet	Fragment de fer ayant la forme d'une tirette
FR98-UE600	Forge Rossell forn	Chute de plaque – fer commun

### AUTRES ORIGINES

Nom échantillon	Origine/Localisation	Remarques
MIMET	Site de Mimet (Bouches-du-Rhône)	Masse brute de réduction fournie pour l'analyse des éléments traces par M.Berranger (inclusions riches en manganèse)
LoupeLorraine	Loupe expérimentale	Produite à partir de la minette lorraine (minerai riche en phosphore) par P.Merluzzo. Analyses effectuées par A.Disser





## **Annexe S**

ARTICLE :  
PROTOCOLE DE MINÉRALISATION PAR  
ATTAQUE ACIDE  $\text{NH}_4\text{F}$  POUR LES ANALYSES ICP-MS

(Talanta (77) 445-450, 2008)



## Relevance of $\text{NH}_4\text{F}$ in acid digestion before ICPMS analysis

Clarisse Mariet<sup>\*</sup>, Oulfa Belhadj, Stéphanie Leroy, Francine Carrot, Nicole Métrich  
*Laboratoire Pierre Süe CEA – CNRS / UMR 9956 Centre de Saclay, Bât. 637 91191 Gif  
sur Yvette Cedex France*

*\* Corresponding author. Tel.: +33 1 69 08 49 60; fax: +33 1 69 08 69 23. E-mail address:  
clarisse.mariet@cea.fr*

**Keywords:** ICP-MS; trace elements; wet acid digestion; sample preparation

### ABSTRACT

In order to implement a simpler, less expensive and more safe sample dissolution procedure, we have substituted the  $\text{HF} - \text{HClO}_4$  mixture by  $\text{NH}_4\text{F}$ . By testing three certified reference materials, lichen 336, basalt BE-N, soil 7, it was found that the three-reagents digestion without  $\text{HF}$  and  $\text{HClO}_4$  ( $\text{HNO}_3 + \text{H}_2\text{O}_2 + \text{NH}_4\text{F}$  was used) was very effective for the pretreatment of ICP-MS measurement. The comparison was based on the measurement results and their uncertainties. All are reference material for amount contents of different trace elements. The accuracy and precision of the developed method were tested by replicate analyses of reference samples of established element contents. The accuracy of the data as well as detection limits (LOD's) vary among elements but are usually very good (accuracy better than 8%, LOD's usually below 1  $\mu\text{g/g}$  in solids). ICP-MS capabilities enable us to determine routinely 13 and 16 minor and trace elements in basalt and soil.

### ARTICLE

Atomic spectrometry is useful for analysis of solid samples of environmental and geological interest. To overcome the heterogeneous nature of the specimens, most of these samples are investigated for bulk analysis by atomic absorption spectrometry (AAS), inductively coupled plasma-atomic emission spectrometry (ICP-AES), or inductively coupled plasma-mass spectrometry (ICP-MS). Inductively Coupled Plasma Mass Spectrometry (ICP-MS) is the method with the highest potential with respect to its detection limits, sensitivity, precision and multi elemental determinations and speed.

Solution nebulisation is commonly used for the sample introduction system of these methods. Although improvements have been made in the existing solid sampling techniques (laser ablation, electrothermal vaporizer), the liquid introduction remains most widespread. Solid sample introduction offers some main advantages over liquid sample [1]. Sample preparation time and handling are reduced, thus diminishing the likelihood of cross-contamination from other samples or reagents. Because no solvent is present, molecular ion spectral interferences derived from solution are absent. However the lack of primary standards limits the quantitative viability of solid sample analysis [2, 3].

Finding the correct procedure for the complete dissolution of the samples by chemical digestion is the most critical aspect of ICP-MS analysis. The common dissolution techniques are the acid decomposition in open vessel, the microwave digestion and the alkali fusion. Alkali fusion requires a high flux to sample ratio (4:1) necessary to completely decompose the sample. This entails a strong matrix effect and the introduction of a great amount of polluting elements also leading to a possible contamination of the torch and other parts of the analytical apparatus (e.g. boron rich flux) [4-6]. By a consequence the solution must be strongly diluted ( $f_d$ , dilution factor,  $f_d = 5000$ ) dramatically lowering the detection limits. Moreover Si-rich samples generally result in solutions enriched in total dissolved solids (TDS) which can cause analytical drift by reducing the diameter of the cone orifice [5]. Furthermore high Si content may involve important isobaric interferences which prevent the determination of such element as  $^{45}\text{Sc}$  (interference:  $^{17}\text{OH}+^{28}\text{Si}$ ). Except alkaline fusion, multi elements analyses of geological samples, as basalts, are mainly carried out following acid digestion [7-11] and less with microwave digestion [12, 13]. The microwave digestion with open or closed oven frequently leaves undissolved residues [5, 14-16], making necessary the addition of flux, thus causing similar inconvenience of the alkali fusion. On the other hand, protocols requiring evaporations related to the change of medium are time consuming with even with microwave digestion.

Open vessel acid decomposition was chosen because it warrants low detection limits and the complete sample digestion while keeping a low pollution and limited matrix effect. It has the disadvantage of being the most time consuming and requiring a great quantity of acid [14]. A possible limitation of this procedure is represented by the incomplete sample decomposition due to the presence of refractory accessory minerals. A combination of  $\text{HNO}_3$  and HF is conventionally employed in the acid digestion of silicate matrix. However some recent studies have reported that good recoveries of many elements can be achieved without HF addition [6, 15, 17-19]. This information is essential because it has been recommended that the use of HF, very corrosive and toxic, should be avoided for safety reasons. Par consequent, new approaches to improve the digestion samples in elemental analysis are needed.

Our work aims at providing a simpler, less expensive and more safe dissolution procedure for lichen, soil and basalt leading to accurate ICP-MS determination of a few transition elements: Cr, Co, Ni, Zn, Pb, rare earth elements (La, Ce, Nd, Sm, Eu, Gd, Tb, Yb) and other trace elements like Sc, As, Rb, Sr, Mo, Ba, Cs, Hf, Ta, Th, U more seldom determined in such matrix. It is why we decided to remove the reagents more penalizing ( $\text{HClO}_4$  and HF) and to replace them by  $\text{NH}_4\text{F}$ . This last reagent has the same aptitudes that HF from the point of view of acid digestion without the disadvantages related to safety. To the knowledge of the authors, this is the first time  $\text{NH}_4\text{F}$  is used in a digestion procedure. Only tertiary ammonium or tetramethylammonium hydroxide (TMAH) are used in for biological samples [20, 21].  $\text{NH}_4\text{OH}$  appears in soils analysis in extraction procedures before ICP-MS but not in acid digestion [20].

## EXPERIMENTAL SECTION

**Materials and Equipment.** The quality control of the analytical technique was ascertained by applying digestion and analytical procedures for ICPMS to the following reference materials: the basalt geostandard BE-N from the SARM (Service of the Rocks and Minerals Analyses), the lichen 336 and soil 7 both provided by IAEA (International Atomic Energy Agency). We chose these samples because they illustrate most of the environmental and geological samples.

Trace analysis in solid materials with amount in the lower microgram per gram level requires clean working conditions and specialized sample handling equipment in order to keep the blank contribution and contamination risks small. Teflon flasks were rinsed with ultrapure water and then heated for at least 2 hours with HNO<sub>3</sub> (2%) followed by another rinsing and a drying step.

**Chemicals and Spike Materials.** For all dilutions and sample treatments, High purity de-ionized water (resistivity 18.2 MΩ.cm) obtained using a Milli-Q water purification system (Millipore, Bedford, MA, USA) was used throughout. All reagents used for digestion procedures are ® VWR Normatom purity grade. For the ICP-MS method, calibration solutions were prepared from certified stock multielemental 1000 mg. g<sup>-1</sup> solutions SPEX, Jobin Yvon. Analytical calibration standards were prepared daily over the range of 0–20 ng.g<sup>-1</sup> for all elements by suitable serial dilutions of multielement stock solution in 2 % (v/v) HNO<sub>3</sub>. Rhodium and Rhenium were used as internal standards at the concentration of 2 ng.g<sup>-1</sup>. The internal standards were diluted from 1000 mg. g<sup>-1</sup> stock standard.

All solutions were stored in high-density polyethylene bottles. Plastic bottles and glassware materials were cleaned by soaking in 10% (v/v) HNO<sub>3</sub> for 24 h, rinsing five times with Milli-Q water and dried in a class 100 laminar flow hood before use. All operations were performed in a clean bench.

**Digestion procedures.** The general conditions of the two digestion procedures are summarised in Table 1. About 50 mg (100 mg for lichen 336) of the sample were weighed into Teflon flasks.

In the case of A procedure, an HF-HNO<sub>3</sub>-HClO<sub>4</sub> mixture composed of 2 ml of HNO<sub>3</sub> (65 %), 1 ml HClO<sub>4</sub> (68 %) and 1 ml HF (47 %) was added to the sample. The flasks were closed and put on a sand bath at 240 °C during 10 hours. The Teflon flasks were cool down during ½ hours, then 1 ml of H<sub>2</sub>O<sub>2</sub> (30 %) was added. After 1/2 hours, the flasks were closed again and put on the sand bath at 190 °C overnight. The flasks were cool down. Then, after adding 1 ml HNO<sub>3</sub>, the flasks were opened and left on the sand bath at 240 °C for evaporation up to dryness. The operation has been repeated three times. 1 ml H<sub>2</sub>O purified with a Milli-Q system was added, the flasks were closed and put on a sand bath at 240 °C during 15 minutes. The resulting solution was transferred to a 50 ml flask and brought to volume with purified water.

As concerned B procedure, it is the same thing with a  $\text{HNO}_3\text{-NH}_4\text{F}$  mixture using 1 ml  $\text{NH}_4\text{F}$  (47 %) in the first step, then 1.5 mL  $\text{H}_2\text{O}_2$  in the second and 5 ml  $\text{H}_2\text{O}$  were added in the last. This is an attractive procedure because it doesn't require the more expensive acid  $\text{HClO}_4$  or the more hazardous acid HF.

A dilution factor  $f_d$  was applied to transform the concentration in solution ( $\mu\text{g.L}^{-1}$ ) into the concentration in solid ( $\mu\text{g.g}^{-1}$ ).  $f_d$  was calculated using the equation

$$f_d = \frac{\text{final solution volume (mL)}}{\text{sample weight (mg)}}$$

The resulting dilution factor is 1000; the reagent blank was prepared in the same manner.

**Instrumentation.** ICPMS measurements have been performed using a quadrupole ICP-MS spectrometer X7 series ICP-MS (*Thermo Fisher Corporation*) equipped with a concentric nebulizer. Instrumental parameters were fixed as indicated table 2. Although this instrument can be used in the CCT (collision cell technology) mode to remove polyatomic interferences, we operated it solely in standard mode, i.e., with the CCT valve vented, for the determination of metals.

table 2 : instrumental parameters

<b>ICP Parameters</b>	
plasma gas	argon
rf power	1350 W
nebulizer gas flow	0.74 L.min <sup>-1</sup>
Auxiliary gas flow	0.90 L.min <sup>-1</sup>
Coolant gas flow	13.8 L.min <sup>-1</sup>
Spray chamber water-cooled at 3°C	
<b>Mass spectrometer</b>	
Interface vacuum	1.9 x 10 hPa
Analyser vacuum	3.6 x 10 <sup>-7</sup> hPa
Ni made Xi sampler (1mm $\phi$ ) and skimmer (0.7mm $\phi$ )	
<b>Acquisition parameters</b>	
Full quantitative scan mode	
Dwell time	10 ms/element
Replicates	4
Ion collection mode	Pulse counting
Measuring time	90s



Signal optimization is obtained by using a 10 ng.g<sup>-1</sup> solution of Be, Mg, Co, Ni, In, Ce, Ba, Pb, Bi and U. The spectrometer is optimised to provide minimal values of the ratios CeO<sup>+</sup>/Ce<sup>+</sup> and Ba<sup>2+</sup>/Ba<sup>+</sup> and optimum intensity of the analytes. The optimum measurement conditions are summarised in Table 2 ; the isotopes used for analysis are listed in Table 3. Standards calibrations curves are built by measuring successively a mixed at different concentration levels 0, 0.1, 0.5, 2, 5, 10, 20 and 100 ng.g<sup>-1</sup> (calibration solutions were prepared from certified stock multielemental solutions). This method requires the use of internal standards to check for instrumental gain and to monitor short term analytical drifting. That is suitable by a 2 ng.g<sup>-1</sup> standard solution of Rh and Re added simultaneously to all samples just before the nebulise admission.

table 3 : Limits of detection

<b>Element</b>	<b>Analytical mass</b>	<b>Solution (ng.g<sup>-1</sup>) with 2% HNO<sub>3</sub></b>	<b>Sample blank (µg g<sup>-1</sup>)</b>
Sc	45	<0.01	0.52
Cr	52	<0.01	0.35
Co	59	0.10	0.20
Ni	60	0.19	0.52
Zn	66	0.69	3.6
As	75	0.73	0.70
Rb	85	0.16	0.20
Sr	88	0.18	0.43
Mo	95	0.78	0.89
Sb	121	0.38	0.50
Cs	133	0.05	0.10
Ba	137	0.06	0.09
La	139	0.10	0.39
Ce	140	0.11	0.35
Nd	146	0.88	0.90
Sm	147	0.89	0.89
Eu	153	0.43	0.43
Gd	157	1.04	1.05
Tb	159	0.20	0.20

<b>Yb</b>	<b>172</b>	<b>1.01</b>	<b>1.01</b>
<b>Hf</b>	<b>178</b>	<b>0.61</b>	<b>0.67</b>
<b>Ta</b>	<b>181</b>	<b>2.21</b>	<b>2.26</b>
<b>Pb</b>	<b>208</b>	<b>0.4</b>	<b>1.75</b>
<b>Th</b>	<b>232</b>	<b>0.19</b>	<b>0.23</b>
<b>U</b>	<b>238</b>	<b>0.29</b>	<b>0.29</b>

## RESULTS AND DISCUSSION

In order to avoid ICP-MS pollution,  $\text{H}_3\text{BO}_3$  is not used to eliminate fluorides. Moreover it has a negative matrix effect [22]. This is why, although it is longer, we chose evaporation to remove fluorides from geological and plant samples as volatile  $\text{SiF}_4$  [18, 23].

After the digestion, all samples formed yellowish solutions in the two procedures with no apparently visible residue.

**Detection limits.** The ICP-MS lower limits of detection (LOD's) were determined for each element (Table 3), with each procedure, in the following way: 15 individual chemical blanks prepared along with the other samples were measured as an unknown in 3 replicates. The detection limit in the solid sample was then assumed to three times the standard deviation of the blank solution counts, taking into account the dilution factor (1 mg of sample in 1 mL of solution). No difference was observed between the two procedures. Detection limits of ICP-MS mainly depend upon the cleanliness of digestion vessels, the purity of reagents adding during the mineralisation and on ICP-MS working conditions. In order to discriminate these different factors, about twenty solutions:  $\text{H}_2\text{O}$  with 2%  $\text{HNO}_3$  were analysed in the same manner than the samples blanks. We remark that there is a slight pollution for Zn, Mo and Pb most likely due to the cleanliness of digestion vessels or to the purity of reagents adding during the mineralisation. The interferences  $^{57}\text{Fe}^{16}\text{O}^1\text{H}^+$  plus  $^{58}\text{Ni}^{16}\text{O}^1\text{H}^+$  on  $^{75}\text{As}^+$  severely damage the detection limit. Meanwhile the LOD was generally below the lowest concentration observed in the samples.

**Reproducibility and accuracy.** As a test of procedure reproducibility, different aliquots (four aliquots for A procedure and the remainder for B one) of the same sample were dissolved and analysed. The average value  $X_i$  and the relative standard deviation (% RSD) were calculated (Tables 4, 5, 6). For the three references, the precision of analytical results characterized by the relative standard deviation was generally better than 8 %.

In the lichen 336 sample, the low reproducibility for Co (% RSD =12 %) and Tb (% RSD =9.1 %) is dependant on the low analyte concentration and sensibility in the sample. In the basalt BEN sample, the worse elements are Co (% RSD =24.7%), Sb (% RSD =15.9 %), Cs (% RSD =13.2%) and Sm (% RSD =20.6%) with A procedure.

As concerned soil 7, the elements for which the reproducibility is worse are Ni (% RSD =16.6%), Mo (% RSD =16.1%), Gd (% RSD =11.8%) and Tb (% RSD =10.1%) and with B procedure this time.

In order to compare the accuracy of the two procedures A and B, the measured concentrations were averaged and normalized against the certified values. There is a good agreement between the results and the reference values within 10% relative error, as illustrated in Figures 1, 2 and 3, respectively, for lichen 336, basalt BEN and soil 7.

First, one notes the procedure B is as good as procedure A for the majority of the elements.

The values obtained for Sb, Cs, Ba, Ta, Pb quite match the theoretical values by using A procedure. Whereas we thought the use of  $\text{NH}_4\text{F}$  brings to the digestion solution a new possible complexant because  $\text{NH}_3$  forms stable complexes with 3d elements [24], for others elements there is not only complexes but also precipitates. As an illustration, Ta, As, Sb easily form colloidal hydroxides in partially ammoniacal solution [25]. Besides, we can observe that these three elements are over-estimated in basalt BEN.

The measurement of  $^{121}\text{Sb}$  and  $^{137}\text{Ba}$  is always worst after the B procedure, most likely because of isobaric interferences respectively with the adducts  $^{103}\text{Rh}(^{15}\text{NH}_3)^+$  and  $^{103}\text{Rh}(^{14}\text{NH}_3)_2^+$  dependent on the addition of the internal standard. In the basalt BEN, the concentration of Sb is only of 0.26 ppm. Consequently, the contribution of the interference is all the more important as the concentration in the sample is weak. Selected interfering polyatomic ions can then be eliminated through ion molecule reaction cell with a small amount of gas [26]. A way of reducing these interferences consists in performing CCT mode with a mix collision gas  $\text{O}_2$  8% in He, oxygen being used to oxidize  $\text{NH}_3$  [2].

In contrast, the B procedure strongly improves the results for Gd even if its measured concentration remains over-estimated. One can imagine that the formation of  $^{140}\text{Ce}^{16}\text{OH}^+$  is put at a disadvantage.

In lichen 336, 6 traces elements ( $^{66}\text{Zn}$ ,  $^{85}\text{Rb}$ ,  $^{88}\text{Sr}$ ,  $^{139}\text{La}$ ,  $^{140}\text{Ce}$ ,  $^{208}\text{Pb}$ ) were founded in good agreement with the certified or recommended values, with RSD (%) near to 10 % or lower (table 4, figure 1). Since the concentrations of the other were lower than LOD's, no data were given for them.  $^{59}\text{Co}$  is slightly over-estimated in Lichen 336, but it should be noted that the required content is close to the LOD.

In basalt BEN (table 5), 13 elements ( $^{45}\text{Sc}$ ,  $^{52}\text{Cr}$ ,  $^{59}\text{Co}$ ,  $^{60}\text{Ni}$ ,  $^{85}\text{Rb}$ ,  $^{88}\text{Sr}$ ,  $^{95}\text{Mo}$ ,  $^{139}\text{La}$ ,  $^{140}\text{Ce}$ ,  $^{159}\text{Tb}$ ,  $^{178}\text{Hf}$ ,  $^{232}\text{Th}$ ) are accurately analyzed and their normalized concentrations lie between 1.1 and 1.15 for 5 others ( $^{121}\text{Sb}$ ,  $^{137}\text{Ba}$ ,  $^{146}\text{Nd}$ ,  $^{157}\text{Gd}$ ,  $^{172}\text{Yb}$ ). Nd is over-estimated in basalt BEN. This overestimation is possibly caused by the isobaric interference  $^{130}\text{Ba}^{16}\text{O}^+$ , when Ba is highly concentrated in the sample (as As it is the case of basalt BEN). This statement is

confirmed by the good agreement between the Nd measured concentrations and the certified value in the Ba poor, Soil 7 reference, whatever the procedure used.

In the case of Soil 7 (Table 6, Figure 3), the normalized values fall within the interval  $1 \pm 0.1$ , for 16 elements ( $^{45}\text{Sc}$ ,  $^{52}\text{Cr}$ ,  $^{59}\text{Co}$ ,  $^{60}\text{Ni}$ ,  $^{66}\text{Zn}$ ,  $^{75}\text{As}$ ,  $^{85}\text{Rb}$ ,  $^{88}\text{Sr}$ ,  $^{137}\text{Ba}$ ,  $^{139}\text{La}$ ,  $^{140}\text{Ce}$ ,  $^{147}\text{Sm}$ ,  $^{153}\text{Eu}$ ,  $^{208}\text{Pb}$ ,  $^{232}\text{Th}$ ,  $^{238}\text{U}$ ) with RSD (%) lower than 8 %

As previously demonstrated (Xu et al. [6]), the optimization of the digestion conditions without HF nor  $\text{HClO}_4$  led to the increase in the contribution of  $\text{H}_2\text{O}_2$ . This observation appears logical since the role of hydrogen peroxide is to increase the oxidizing capacity of the acids [27]. Thus, a part of the oxidizing effect of  $\text{HClO}_4$  is replaced by that of  $\text{H}_2\text{O}_2$ .

table 4 : Analytical results obtained by HF -  $\text{HClO}_4$  and  $\text{NH}_4\text{F}$  for lichen 336 (ppm)

Element	$X_A$ HF - $\text{HClO}_4$ (4)	RSD (%)	$X_B$ $\text{NH}_4\text{F}$ (10)	RSD (%)	Certified values	Standard deviation
$^{45}\text{Sc}$	<LD		<LD		0.17	0.01
$^{52}\text{Cr}$	<LD		1.07	14.6	1.06	0.085
$^{59}\text{Co}$	0.31	12.5	0.27	7.1	0.29	0.025
$^{60}\text{Ni}^*$	<LD		<LD			
$^{66}\text{Zn}$	32.8	3.1	29.7	3.4	30.4	1.7
$^{75}\text{As}$	<LD		0.62	8.5	0.63	0.04
$^{85}\text{Rb}$	1.8	3.1	1.9	7.1	1.76	0.11
$^{88}\text{Sr}$	9.1	2.5	10.0	6.9	9.3	0.55
$^{95}\text{Mo}^*$	<LD		<LD		0.15	
$^{121}\text{Sb}$	<LD		<LD		0.073	0.005
$^{133}\text{Cs}$	<LD		0.110	5.8	0.11	0.0065
$^{137}\text{Ba}$	6.8	2	6.38	3.2	6.4	0.55
$^{139}\text{La}$	0.64	7.9	0.61	10.2	0.66	0.05
$^{140}\text{Ce}$	1.3	6	1.24	7.0	1.28	0.085
$^{146}\text{Nd}$	<LD		0.63	8.2	0.6	0.09
$^{147}\text{Sm}$	<LD		0.11	8.6	0.106	0.007
$^{153}\text{Eu}$	<LD		<LD		0.023	0.002

<sup>157</sup> Gd*	<LD		<LD		0.5	
<sup>159</sup> Tb	0.017	39.1	0.017	17.3	0.014	0.001
<sup>172</sup> Yb	<LD		<LD		0.037	0.006
<sup>178</sup> Hf*	<LD		<LD		0.06	
<sup>181</sup> Ta*	<LD		<LD		0.01	
<sup>208</sup> Pb	4.4	4.6	4.8	8.9	4.9	0.3
<sup>232</sup> Th	<LD		0.12	13.0	0.14	0.01
<sup>238</sup> U*	<LD		0.05	11.6	0.037	

\* Recommended values ; (n) number of independent determinations (% RSD=100  $\sigma/m$ )

table 5 : Results obtained by HF - HClO<sub>4</sub> and NH<sub>4</sub>F for Basalt BEN (ppm)

Element	X <sub>A</sub>		X <sub>B</sub>		Certified values	Standard deviation
	HF - HClO <sub>4</sub> (4)	RSD (%)	NH <sub>4</sub> F (7)	RSD (%)		
<sup>45</sup> Sc	22	0.7	21	4.2	22	4.08
<sup>52</sup> Cr	378.	1.8	378	6.7	360	48.84
<sup>59</sup> Co	60.	24.7	63	1.0	60	7.78
<sup>60</sup> Ni*	279	1.4	274	1.6	267	26.48
<sup>66</sup> Zn	201	1.8	159	6.7	120	49.67
<sup>75</sup> As	1.5	2.1	2.2	6.7	1.8	0.56
<sup>85</sup> Rb	52	4.6	46	6.9	47	8.79
<sup>88</sup> Sr	1494	7.3	1318	7.1	1370	100
<sup>95</sup> Mo*	3.0	0.2	2.8	6.0	2.8	-
<sup>121</sup> Sb	0.3< LD	15.9	0.5	2.4	0.26	0.08
<sup>133</sup> Cs	0.8	13.2	1.0	3.6	0.8	0.33
<sup>137</sup> Ba	1058	3.2	1181	1.3	1025	125
<sup>139</sup> La	86	4.0	90	6.2	82	3
<sup>140</sup> Ce	160	3.7	168	2.6	152	24.08
<sup>146</sup> Nd	72	3.5	75	5.3	67	2.6
<sup>147</sup> Sm	13	20.6	13.	4.7	12.2	0.6

<sup>153</sup> Eu	4.0	4.8	3.13	3.9	3.6	0.52
<sup>157</sup> Gd*	12.3	2.0	10.9	1.4	9.7	1.4
<sup>159</sup> Tb	1.3	8.6	1.4	3.1	1.3	0.28
<sup>172</sup> Yb	2.0	8.0	2.0	3.4	1.8	0.68
<sup>178</sup> Hf*	5.8	8.2	5.2	2.7	5.6	0.37
<sup>181</sup> Ta*	6.1	5.1	6.8	4.8	5.7	0.88
<sup>208</sup> Pb	3.8	2.6	3.5	5.8	4	5.38
<sup>232</sup> Th	10.0	1.7	10.0	7.1	10.4	2.01
<sup>238</sup> U *	2.6	2.1	2.8	5.9	2.4	0.49

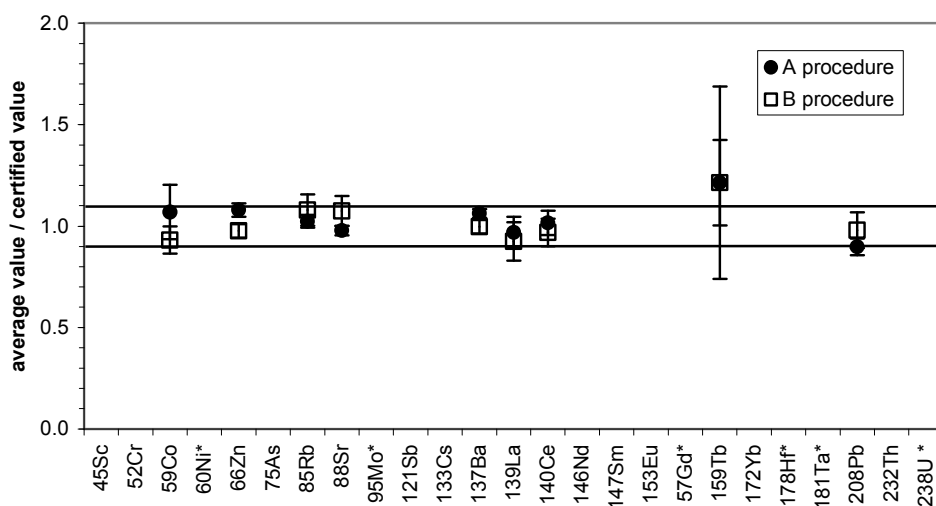
\* Recommended values ; (n) number of independent determinations

table 6: Analytical results obtained by HF - HClO<sub>4</sub> and NH<sub>4</sub>F for soil 7 (ppm)

Element	X <sub>A</sub>	RSD (%)	X <sub>B</sub>	RSD (%)	Certified values	Standard deviation
	HF - HClO <sub>4</sub> (4)		NH <sub>4</sub> F (6)			
<sup>45</sup> Sc	8.1	0.8	8.3	13.1	8.3	5.5
<sup>52</sup> Cr	60	1.2	63	3.1	60	4.5
<sup>59</sup> Co	9.0	0.7	8.2	6.7	8.9	0.4
<sup>60</sup> Ni*	28	1.0	24	16.6	26	2.5
<sup>66</sup> Zn	107	2.8	106	1.8	104	3
<sup>75</sup> As	14	18.7	14	9.2	13.4	1.3
<sup>85</sup> Rb	49	4.1	49	0.8	51	0.05
<sup>88</sup> Sr	113	3.1	109	0.5	108	0.5
<sup>95</sup> Mo*	1.4	0.5	2.8	16.1	2.5	18.5
<sup>121</sup> Sb	1.8	0.3	2	9.3	1.7	0.5
<sup>133</sup> Cs	5.3	0.2	5.8	8.4	5.4	1
<sup>137</sup> Ba	152	1.0	165	1.2	159	2
<sup>139</sup> La	27	0.4	30	0.8	28	0.2
<sup>140</sup> Ce	63	5.5	61	0.5	61	0.15
<sup>146</sup> Nd	28	2.5	33	8	30	

$^{147}\text{Sm}$	5	0.3	5	8.4	5.1	0.15
$^{153}\text{Eu}$	1.0	0.1	1.0	8.8	1	0.1
$^{157}\text{Gd}^*$	5.0	0.5	4.2	11.8	3.9	0.2
$^{159}\text{Tb}$	0.6	0.1	0.7	10.1	0.6	0.1
$^{172}\text{Yb}$	1.9	0.2	2.0	5.6	2.4	5.5
$^{178}\text{Hf}^*$	2.5	0.2	2.7	4.4	5.1	0.25
$^{181}\text{Ta}^*$	0.7<LD	0.0	0.9	6.2	0.8	0.35
$^{208}\text{Pb}$	62	5.3	57	0.1	60	5.5
$^{232}\text{Th}$	8.2	0.7	8.2	2.1	8.2	4.5
$^{238}\text{U}^*$	2.5	0.2	2.5	0.6	2.6	0.4

\* Recommended values ; (n) number of independent determinations (% RSD=100  $\sigma/m$ )



**Figure 1.** Ratio of the average values obtained with the certified values for each dissolution procedure for lichen 336. The solid lines indicate a variation of 10% compared to the certified value. \* when there is only recommended value.



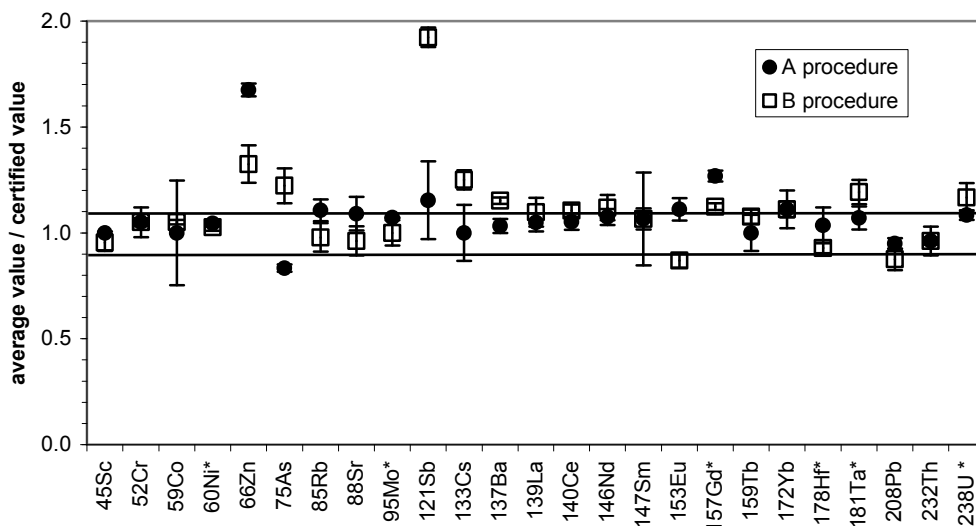


**Figure 2.** Ratio of the average values obtained with the certified values for each dissolution procedure for basalt BEN. The solid lines indicate a variation of 10% compared to the certified value. \* when there is only recommended value.

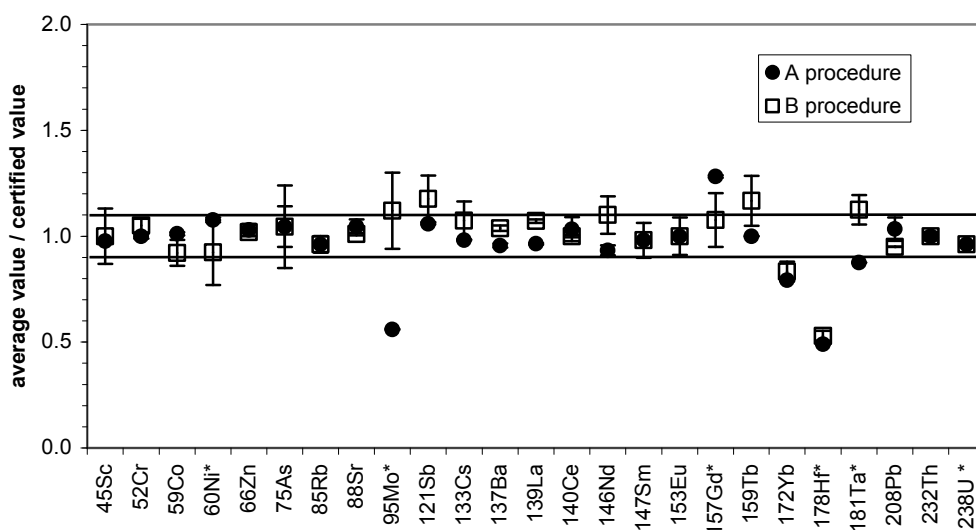


**Figure 3.** Ratio of the average values obtained with the certified values for each dissolution procedure for soil 7. The solid lines indicate a variation of 10% compared to the certified value. \* when there is only recommended value.

## CONCLUSION

As expected, for a multi-elemental analysis covering wide ranges of atomic masses and levels of occurrence, a single extraction method is not adequate. However, we developed a routine method for simultaneous determination of 13 and 16 elements (minor or trace) by ICP-MS, respectively, in basalt and soil. The final solutions are suitable for the ICP-MS instrument

because total dissolved solid is kept low and possible interferences mainly due to the use of HCl or HClO<sub>4</sub> are avoided.

A clear advantage of the digestion procedure with NH<sub>4</sub>F is the reduction of the number of acids used and the replacement of a prohibited acid of handling in laboratory for safety question by such an effective salt. The additional economic interest is obvious since ICPMS is the most popular method for trace element analysis.

Moreover, accurate determination of large spectra of trace elements has a broad interest for the knowledge of the geochemical cycles and element transfer through the different terrestrial reservoirs and in fine for Environmental and Earth Sciences. The NH<sub>4</sub>F-based digestion procedure apply to micro-samples (mass lower than 20 mg), too. The analytical precision is then strongly improved by the introduction of spiking aliquots.

## ACKNOWLEDGEMENTS

The authors are thankful to Anne - Marie Desaulty for her helpful discussions.

## REFERENCES

- [1] Gravel, J.-F., et al., *Analytical Chemistry*, 75(6) (2003)1442-1449.
- [2] Montaser, A., *Inductively coupled plasma mass spectrometry* ed. Wiley-VCH. (1998), Washington. 964.
- [3] Roper, P., *Applications of Reference Materials in Analytical Chemistry (2001)*: Royal Society of Chemistry.
- [4] Jarvis, I., I.M.M. Totland, and K.E. Jarvis, *Chemical Geology* (1997) 27-42.
- [5] Tsolakidou, A., J.B. Garrigós, and V. Kilikoglou, *Analytica Chimica Acta*, 474 (2002) 177–188.
- [6] Xu, Y., et al., *Talanta* 66 (2005) 58–64.
- [7] Beauchemin, D., et al., *Wilson and Wilson's Comprehensive Analytical Chemistry*, in: *Discrete sample introduction techniques for inductively coupled plasma mass spectrometry*. Elsevier, ed. D. Barcelo. Vol. 24. (2000), Amsterdam.
- [8] Yang, X.-J. and C. Pin, *The Analyst*, 125 (2000) 453–457.
- [9] Meisel, T., et al., *Simplified method for the determination of Ru, Pd, Re, Os, Ir and Pt in chromitites and other geological materials by isotope dilution ICP-MS and acid digestion*. *The Analyst*, 126 (2001) 322–328.

- [10] Makishima, A. and E. Nakamura, *Spectrochimica Acta Part B*, 15 (2000) 263-267.
- [11] Quitte, G. and F. Oberli, *Journal of Analytical Atomic Spectrometry*, 21 (2006) 1249–1255.
- [12] Valaram, V., S.L. Ramesh, and K.V. Anjaiah, *Fresenius J. Anal. Chem.*, 353 (1995) 153.
- [13] Totland, M.M., I. Jarvis, and K.E. Jarvis, *Chemical Geology*, 124 (1995) 21-28.
- [14] Ivanova, J., et al., *Talanta* 54 (2001) 567–574.
- [15] Iwashita, A., et al., *Fuel*, 85 (2006) 257–263.
- [16] Lachas, H., et al., *The analyst*, 124 (1999) 177–184.
- [17] Wang, J., et al., *Analytica Chimica Acta*, 514 (2004) 115–124.
- [18] Knapp, G., et al., *Microwave-Enhanced Chemistry*, ed. H.M. Kingston and S.J. Haswell. 1997, Washington: American Chemical Society.
- [19] Gupta, J.G.S. and N.B. Bertrand, *Talanta*, 42 (1995) 1947-1957.
- [20] Nobrega, J.A., et al., *Spectrochimica Acta Part B*, 61 (2006) 465-495.
- [21] Batista, B.L., et al., *Talanta*, (in Press) (2008).
- [22] Rodushkin, I., M.D. Axelsson, and E. Burman, *Talanta*, 51 (2000) 743-759.
- [23] Taylor, V.F., A. Toms, and H.P. Longrich, *Anal. Bioanal. Chem*, 372 (2002) 360-365.
- [24] Ringbom, A., *Complexation in analytical chemistry*. (1963), New York: J. Wiley and Sons.
- [25] Charlot, G., *L'analyse qualitative et les réactions en solution*. (1963), Paris: Masson. 433.
- [26] Erickson, B.E., *ICPMS Beyond quadrupole. Analytical Chemistry*, 71 (1999) 811A.
- [27] Mermet, J.M., *Microwave-enhanced chemistry. Fundamentals, sample preparation and applications*, ed. H.M. Kingston and S.J. Haswell. (1997), Washington: American chemical society. 772.

## **Annexe T**

### SHORT ENGLISH VERSION



## INTRODUCTION

Iron based materials, since their appearance, have played an essential role in the technical and economic history of ancient societies. Thus, research in paleo-iron metallurgy helps to understand some of their economical and technical aspects. The metallurgical operations on iron are linked to activities such as the exploitation and transformation of the ore, the production of iron objects, and the organisation of a production or transformation site. The remains of these metallurgical activities (metallic parts, waste, etc.) pile up with time and constitute a patrimony of material allowing us to address the questions linked to the understanding of these aspects as a whole.

Significant studies on ancient iron metallurgy appeared from the 19th century onwards<sup>13</sup>. These have, however, really increased over the past forty years<sup>14</sup>. It is in this context that a paleo-iron metallurgical methodology with a multidisciplinary vocation was expounded and structured around research groups. The archaeometric studies in association with data from historical sources - when they exist, archaeological sources on production sites, chemical and physical sources from metallurgy, and lastly, experimental sources contribute to reconstituting the evolution of the ancient techniques and the iron work organisation, that are so important in the societies' economies.

Subsequent activities to metallurgical ones are those linked to the distribution and the use of iron products. Whichever the periods taken into consideration, the issue raised by the circulation of iron materials found outside production sites is one that generates great interest among historians and archaeologists in iron metallurgy. As such, findings of paleo-iron metallurgy enable an understanding of some of its aspects. The understanding of the operating chain, associated with historical data, forms a preferred means of studying of the products' use

---

<sup>13</sup> Is found in *Annales des Mines*, a treatise from the chemist Dumas which describes the ancient processes of the elaboration of iron (Dumas, *Traité de Chimie Appliquée aux Arts*. Vol. 4. 1833: Béchét Jeune. 744 p) and articles from Daubrée (Daubrée, *Aperçu historique sur l'exploitation des métaux dans la Gaule*, Revue archéologique, 17, 1868 p.289-313.).

<sup>14</sup> With, in particular, works of R. Pleiner and J. Piaskowski (Pleiner, *Schmiedetechnik der Hallstattzeit im Lichte der Untersuchung des Hortfundes von Schlöben*. Archaeologické rozhledy **20**, 1968, p.33-42; Pleiner, *Iron Working in Ancient Greece*. National Technical Museum, 1969, Prague; Piaskowski, *Metallographische Untersuchungen der Eisenerzeugnisse in der Hallstattzeit im Gebiet zwischen Oder und Weichsel*. In: Beiträge zur Lausitzer Kultur, Dresden-Berlin, 1969, p.179-210; Piaskowski, *Le problème des débuts de la métallurgie de fer sur les territoires de la Pologne*. Przegląd Archaeologiczny 20/21, 1971, p.37-49).

that emerges from the circulation and markets studies. The study of the trade of siderurgic products from potential production zones and identified as such by archaeology, enable the reconstituting of technical, political and economical territories. Particularly, in the Middle Ages, the spread of iron objects, exchange tracers, as well as the supply of monuments construction is among the major questions concerning the geographical origin of iron-based objects. Nevertheless, research undertaken in this area has always remained restricted due to, on the one hand, the high number of ores that could have produced these materials and, on the other hand, the complexity of the operating chain.

A succession of chemical, physical and mechanical transformations is necessary to obtain a usable object from iron ore. Two processes followed one another in the history of iron metallurgy. The first one consists of the bloomery process that uses the low hearth. The operation occurs below the iron melting temperature. With this process, a large number of the iron ore compounds are not reduced, or not entirely, and become non-metallic slag inclusions trapped in the metal. The product of the smelting stage is a bloom composed of a metal and slag mix as well as slag inclusions. The treatments of post reduction are designed to transform this bloom in a semi-finished product (ingot, bar, plate) that can be offered for sale or be stored, transported and forged on site. The slag inclusions trapped in the metal of archeological objects made with the bloomery process carry the chemical signature of the iron ore initially used but also the conditions of production. However, the provenance studies on iron materials that attempted to correlate the chemical characteristics of the iron ores and smelting stage slags with the archaeological objects are extremely rare. Indeed, these are extremely difficult to conduct especially due to the complexity of the operations, in terms of the elements' thermochemistry and pollution phenomenon, which lead to its finality as a metal object.

Initially, the research on provenance was almost exclusively oriented towards the study of major elements due to the difficulty of the analysis of trace elements<sup>15</sup>. The research has gradually taken an interest in trace elements thanks to the development of new analytical methods. Therefore, it is only recently that the questions about provenance have been approached by both a study of major elements and of those present as traces<sup>16</sup>. A recent thesis (Desaulty, 2008) showed that these questions are possible for iron objects that come from the bloomery process, if one considers the appropriate elements to reach that goal. Our research is in line with these research works. They are set, in a general manner, in the line of a programme concerning the study of iron products developed in the laboratory "*Métallurgies et Cultures*"

---

<sup>15</sup> In this work, the trace elements are elements present as traces whose contents are inferior to 1000 ppm in the samples.

<sup>16</sup> Coustures *et al.* (2006), La provenance des barres de fer romaines des Saintes-Maries-de-la Mer (Bouches-du-Rhône). Etude archéologique et archéométrique. In Gallia, 63: p. 243-261 ; Desaulty (2008), *Apport des analyses chimiques multi technique à la compréhension du comportement des éléments traces dans les filières sidérurgiques anciennes. Application des études de provenance et à la distinction des procédés. Le cas du Pays de Bray normand*. Université Technologique de Belfort-Montbéliard.



(LMC; IRAMAT-CNRS-UMR 5060)<sup>17</sup>. This work was carried out at the branch of the LMC located at Saclay, at the “*Laboratoire Archéométrie et Prévision de l’Altération*” (LAPA; CEA-CNRS-UMR 9956). It has also been undertaken in collaboration with the interface of the SOLEIL synchrotron especially dedicated to cultural heritage and archaeology (Archaeology and Heritage Liaison Office HALO).

In the Middle Ages, the production areas that exploited deposits rich in manganese held a major place in the medieval economy of their region. These iron ores with high tracers – from a chemical composition point of view, and since they are characterized by manganese – were known for their qualities by the men working with iron in medieval times. These deposits linked to specific processes rendered possible – as it seems – the production of natural steel. Among the areas of iron metallurgical activities, one may find Ariège (France) and Lombardy (Italy). The two different geographical areas had in common spread domains for their production in the south of France.

The objective of this thesis is thus a study of provenance focused on the Middle Ages and concerning the geographic area from the Pyrenees to the Alps, in particular the Ariège and the Lombardy areas. The objects from these regions can be differentiated from other productions as their slag inclusions contain a high concentration of manganese. Furthermore, the particular content of the major element manganese is a first tool from which we can propose the study of the circulation and the diffusion of these products. In order to carry out this study of provenance, we will take a greater interest in tracking the objects that came from specific processes linked to the use of manganese-rich ore. Then, in order to distinguish more precisely the provenance of these objects, we will consider the trace element contribution.

Our reasoning is in line of a precise historical context. We will attempt to answer three historical and archaeological questions, each requiring a specific study approach:

- The characterisation of the siderurgical products’ circulation and the iron market’s organisation inside the production space in Ariège, in the Central Pyrenees, organised around a dominant mine that represents a structuring pole. Several reasons explain this choice. This work on provenance has, first of all, found in the Ariège region the historical and archaeological background necessary to conduct a study on provenance. Moreover, iron circulation in this production space is particularly hard to grasp due to the complexity and

<sup>17</sup> Thesis recently defended: Bauvais (2007), *Evolution de l’organisation des activités de forge dans le nord du Bassin parisien au second âge du fer. Etudes pluridisciplinaires de la chaîne opératoire en métallurgie du fer*. Thèse de doctorat, Université de technologie de Belfort-Montbéliard ; Desautly (2008), *Apport des analyses chimiques multi technique à la compréhension du comportement des éléments traces dans les filières sidérurgiques anciennes. Application des études de provenance et à la distinction des procédés. Le cas du Pays de Bray normand*. Université Technologique de Belfort-Montbéliard ; Pagès (2009), *La métallurgie du fer en France méditerranéenne de l’Antiquité au début du Moyen Âge : jalons d’une approche interdisciplinaire*, Doctorate thesis of the université Paul Valéry, Montpellier 3 ; Berranger (2009), *Le fer, entre matière première et moyen d’échange, en France du VII<sup>e</sup> au I<sup>er</sup> av. J.-C.. Approches interdisciplinaires*. Thèse de doctorat de l’Université Paris 1, Panthéon-Sorbonne.

the dynamism of its iron market sensed by historical sources. This work could clarify some of its aspects. Finally, the south of France witnessed the persistence of the bloomery process, an ideal condition to link the initial iron ore to the object, from a chemical point of view.

- The iron supplying in the monumental building of the Popes Palace in Avignon during the medieval period, localized at the confluence of the exporting areas of products from Lombardy and Ariège. Iron was massively used in the architecture of this building, one of the most important gothic constructions of the Middle Ages – and established in the south of France.
- We will also test the hypothesis of the Lombard origin accredited to pieces of armour by stylistic and technical analyses. This axis of research required a specific-methodological approach, based on the use of synchrotron radiation, due to the very tiny slags (<20µm) trapped in the samples from these armours, themselves extremely precious.

These questions must be conducted according to a resolutely interdisciplinary approach, in collaboration with the archaeologist, the historian, and the archaeometrist, in order to put in the best possible manner the hypothesis and the interpretations in their context. We have tried to maintain this multidisciplinary mindset throughout the execution of this works.

If the recent studies designed to determine the origin of iron objects have been based on the analysis of trace elements, they did not make good enough use, to date, of the great amount of elements selected to chemically characterize the iron-making areas. Consequently, before one addresses the historical and archaeological questions, it is necessary to set up an adapted methodology in order to treat the substantial amount of analytical data acquired in this work. The multivariate analysis represents a data treatment tool adapted to the description of a substantial set of data. For this reason, we propose to develop an ad-hoc methodology based on the multivariate approach to consider our question regarding provenance and to build on it for archaeological applications. This methodological approach will compose an important part of our research.

The presentation of this work will be organised in six chapters.

Chapter 1 will be dedicated to a bibliographical review the objective of which is to draw out the fundamental information and to orient our research. First, we will present, in a general and non-exhaustive manner, the elaboration processes of ancient iron metallurgy<sup>18</sup> and the examination of the waste of the smelting stage. A large place will be dedicated to the chemical elements' behaviour during the smelting stage of the iron ore up to the slag inclusions in the ancient irons, in order to track the provenance of archaeological objects. This presentation will be followed by the synthesis of the studies regarding the provenance of the iron objects that came from the bloomery process, and will present examples of studies from which significant

---

<sup>18</sup> By “ancient”, we mean iron metallurgy from its birth (~-2500 BC) to the second half of the 19th century, before the liquid state refining processes (Bessemer, Thomas, Martin).

results were obtained. The purpose of data characterisation by multivariate analysis of the present study will, then, be demonstrated. The historical background of our provenance study will finally allow to draw the unifying themes and to address the historical and archaeological questions.

Chapter 2 will refer to the description of the analytical methodology used to answer the fixed objectives. The necessity of applying a multi-technical approach (analysis of major elements and trace elements) and a multi-scale approach (macroscopic and microscopic analysis) will be put forward. It will be paired with the presentation of usual analysis techniques used and of the experimental methods created in this work context. Thus, the focus will be put on the microscopic characterisation techniques of slag inclusions in the object. We will describe, in particular, the use of synchrotron radiation to carry out X-ray microfluorescence experiments in confocal geometry on inclusions very small in size.

Chapter 3 will be dedicated to the presentation of a study corpus that was, in fact, considered for the chemical signature characterisation of the iron-making areas that were worth investigating. A brief description of the geological and archaeological sites studied will be outlined. The results of the composition and structural analysis of the samples will be paired with the corpus presentation.

The two following chapters will be dedicated to the results obtained by the different analytical methods on the iron ores, the slag samples and the slag inclusions in the objects. Chapter 4 essentially aims to present the new methodology created to determine the provenance of an object, and based on the multivariate analysis. The chemical signatures of the production areas will thus be characterised. The presentation of the general reasoning adopted and adapted to each historical application will close this chapter. Chapter 5 will describe the results of this methodology applied to objects of unidentified origin while differentiating the three aforementioned historical applications.

Finally, in chapter 6, will be discussed the overall results in order to draw characteristics of the circulation and supply of the iron materials studied. Then, we will draw conclusions concerning the contribution of this work to the provenance studies of the iron materials based on different methodological point of views.

## Chapter I: State of the art on provenance studies

The bibliographical study will not be translated as a whole. Only a synthesis of some selected aspects will be given here with reference to the major figures and tables.

### THE ELABORATION PROCESSES OF ANCIENT IRON METALLURGY

From the appearance of the first processes to obtain iron or steel until the 13th century, the ore was exclusively reduced according to the direct process -bloomery process- in the actual territory of France.

On this territory, in the last centuries of the Middle Ages, different ironmaking processes to obtain iron or steel were juxtaposed. In particular, mechanical installations caused the apparition of the indirect process (or blast furnace and finery process) that spreads in the North of Europe and in France. In spite of the diffusion of the indirect process, hydraulic forges that stick with the bloomery process, are still erected from the 14th to the 16th in Lorraine, Jura, the Alps and the Pyrenees for example. In this respect, they had a strong implantation in the Spanish and French Pyrenees until the development of indirect methods to the late 19th century (Bonhôte *et al.*, 1999). Thus, at the end of the 13<sup>th</sup> c., the *mouline*, which is “a direct reduction water-powered iron mill, in which the hydraulic force is used to move hammer and bellows and which produces iron and steel bars directly from iron ore and charcoal and not through the intermediary making pig-iron” (Verna, 2001) appears in the western part of the South of France, particularly in the County of Foix, and makes long term roots in the area from the Pyrenees to Périgord.

During ancient production sequences, the reduction of the ore for the direct process as well as the refining for the indirect one take place under the melting temperature of the metal. As a consequence, slag inclusions could remain entrapped in the metallic matrix.

### ORIGIN OF THE SLAG INCLUSIONS

#### **Element behaviour during the direct and indirect processes**

The general tendencies on the behaviour of the elements have been established thanks to the thermodynamical properties as well as the results from experimental smelting reconstructions (Ploquin, 1993 ; Serneels & Crew, 1997 ; Dillmann, 1998 ; Serneels, 2002 ; Dillmann & L’Héritier, 2007). More recently, the thesis work of Desaulty (2008) have added to the existing results, new data on the behaviour, during the direct and indirect processes, of the minor and major elements, and especially of numerous trace elements.

Figure I.2 schematically sums up the behaviour of the elements studied during the direct process (Desaulty, 2008). This table highlights elements which remain within the metal (Co,

Ni, As, Sb), those which partition between slag and metal (represented in orange), and those which pass into the slag (represented in light-blue). The compounds (major, minor, trace elements) which are not reduced during the process (i.e. passed into the slag), will be called in this summary “Non-Reduced Compounds” (NRC).

For the indirect process (Figure I.3), most of the elements are eliminated from the cast iron by mainly passing in the *laitier*. It thus appears that the slag inclusions in the artefacts from the indirect process are not formed from the NRC of the ores because of the thermodynamical and kinetic conditions during the process. An important consequence is that it seems to be difficult or even impossible to perform provenance studies using slag inclusion composition for indirect ferrous artefacts.

From a chemical point of view, the different materials that will be put in the furnace (i.e. the ore, the lining of the furnace, the charcoal or voluntary additives) will be present in the slag samples and in the slag inclusions. Several authors have concluded that raw materials were incorporated into bloomery smelting slag to some extent. Raw materials therefore contribute to the proportion of certain elements found in the slag (Eschenlohr & Serneels, 1991 ; Serneels & Crew, 1997 ; Serneels, 2002 ; Desaulty *et al.*, 2009). Table I.2 shows some examples of the contributions of these variables to the composition of the slag produced. Thus, the slag may be composed of up to 23% of the elements initially present in the raw materials.

Figure I.5 sums up the behaviour of the elements and the pollution contributions that could be introduced by the charcoal and the furnace lining during the bloomery smelting stage. These results are inferred from the literature as well as from the study of samples originally from three experimental smeltings (Desaulty, 2008).

### **Relating slag chemistry to ore chemistry for the bloomery process**

The elements which pass mainly into the slag during the smelting process preserve a constant ratio from the ore to the slag, then up to the slag inclusions. Nevertheless, there are several sources that may influence these ratios.

- The ratio of elements will not be preserved when one of these elements has its contents modified by the composition of the different materials put in the system (ore, charcoal, furnace lining, additives, etc.). To illustrate, Figure I.8 shows two examples of ratios of elements that are not constant from the ore to the slag inclusions because of pollution effects generated by the charcoal ashes. As a consequence, the ratios of these elements will not be characteristic of the ore’s chemical signature detected in the SI. Nevertheless, Dillmann & L’Héritier (2007) showed that the latter represent the chemical signature of a system, that is to say, a smelting operation with the same ore, charcoal, fluxes and furnace lining (Figure I.9).
- Another source of ratio variability could derive from the NRC within the artefact itself. Firstly, a high fragmentation of the inclusions and the presence of inclusions very small in

size lead to a local concentration effect (Figure I.10). This effect causes a relative variability of the ratio of the major elements. Secondly, the slag inclusions entrapped in the metal can arise from the use of sand or clay additives during the post smelting stage. In this case, the latter inclusions have a different composition than those coming from the smelting phase, so that their composition cannot be linearly fitted (Figure I.11). Considering these observations, it thus appears that these inclusions could not be used to track the chemical signature of the ore used.

The effect of the previous variables on slag composition must be thus considered when attempting to relate slag chemistry to ore chemistry. In this respect, Desaulty *et al.* (2009) and Coustures *et al.* (2003) have observed that the elements that pass completely in the slag without being contaminated by lining or charcoal during the smelting show a constant ratio from the ore to the slag inclusions remaining in the iron object (Figure I.7).

### **PROVENANCE STUDIES OF FERROUS MATERIALS**

Many researchers have tried to correlate iron objects, bloom, slag material and potential ores in order to establish the origin of iron artefacts made by the bloomery process. To do so, they have used several approaches such as the examination of isotopic ratios (Gale *et al.*, 1990; Schwab *et al.*, 2006; Degryse *et al.*, 2007), the analysis of trace elements in the metal of the iron artefacts (Devos *et al.*, 2000); the analysis of the major elements in slag inclusions (Hedges & Salter, 1979; Buchwald & Wivel, 1998) and more recently, those present as traces (Coustures *et al.*, 2003; 2006; Schwab *et al.*, 2006, Desaulty, 2008; Desaulty *et al.*; 2009). Since the isotopic ratios methods and measurements in the metallic matrix have hardly been employed to date and have not proved to be very effective for provenance studies, only brief comments will be made on the studies that have looked for slag inclusion analyses. Indeed, recent studies based on major and trace element analyses have underlined the potential for following chemical signatures from the iron ore to the slag inclusions in the artefacts to identify their provenance (Coustures *et al.*, 2006; Desaulty *et al.*; 2009).

#### **Studies of major elements in the slag inclusions**

Certain studies have underlined the possibility for major element ratios to chemically discriminate different ore sources and therefore distinguish typical ore compositions in favourable cases (minette de Lorraine, Danish ore) (Leroy, 1997; Buchwald & Wivel, 1998; Høst-Madsen & Buchwald, 1999). Nevertheless, this approach is limited since a majority of major elements may be affected by pollution and the number of these elements is clearly limited. In her works, Desaulty (2008; 2009) has shown that, for many iron-making areas, there is a lot of overlap between the major element ratios because of their dispersion (Figure I.13) Thus, considering these aspects, the major elements become in many cases low-selective.



Nevertheless, many researchers have exploited the major element compositional analyses made on the slag inclusions of ferrous artefacts in order to identify different ore sources (Hedges & Salter, 1979; Paynter, 2006; Dillmann & L'Héritier, 2007; L'Héritier, 2007; Pagès *et al.*, 2008; Berranger, 2009). Results from these studies show the potential for major elements to distinguish various origins in homogeneous corpus of artefacts. Even though it is possible to form homogeneous slag groups considering the NRC ratios, possibly indicating a common origin, it is nevertheless difficult with this approach to validate a link between a given iron-making area and the iron artefacts origin. Indeed, the chemical signatures of slag samples produced with the same ore sources but in two different reduction systems (i.e. ore, furnace lining, charcoal) will be more or less modified. The effect of the possible contaminants on slag composition must be considered when attempting to relate slag chemistry to ore chemistry. Considering these aspects, it is therefore crucial to consider, in addition to major elements, trace element analysis for provenance studies.

### **Studies of trace elements in the slag inclusions**

The most recent published work on the provenance (Desaulty *et al.*, 2009) confirms the effectiveness of combined analyses of major and trace elements on ores, slag samples and slag inclusions to evaluate the possibility that iron artefacts were produced using ore from a certain area. The authors have developed a methodology based on the complementarities of the major element ratios and trace elements analysis approaches in order to determine a chemical signature for the ore and slag of the Pays de Bray area (France, Normandy). In a first step, samples from several experimental smeltings with ores from this area were analysed in the perspective of characterizing the behaviour of numerous major and trace elements during the smelting process. From this analysis, elements that are not affected by any pollution and have the same partitioning coefficient between metal and slag were then selected to determine the chemical signature because their ratios should not change from the ore to the slag and the slag inclusions obtained from the smelting slag. From this selection, a second filter linked to geochemical considerations (i.e. exclusion of “quasi-isotopes” elements, selection of elements with similar valences and ionic radii) is applied to choose more specific couples. Considering all these parameters, couples finally selected to define the chemical signature of the Pays de Bray area are Sm/Th, Th/U, La/Yb, Y/Yb, Hf/Nb, Eu/Sm, Cs/Rb, Th/Sc (Figure I.19). The procedure combining major and trace elements was then followed to verify if the Pays de Bray could have been an important supplier for the ferrous reinforcements used in the Middle Ages for the building of churches and cathedrals in Rouen and Beauvais. The results show the effectiveness of the methodology in excluding the potential compatibility of samples with ore from a given area. It seems, on the other hand, to be more difficult to validate a provenance hypothesis. While previous studies (Høst-Madsen & Buchwald, 1999; Coustures *et al.*, 2003, Paynter, 2006) did not use such a rigorous approach, therefore showing some limits, this work reveals three momentous aspects to conduct a provenance study:

- It is necessary to select elements that pass completely into the slag (and therefore in the



slag inclusions) and are not significantly contaminated by lining and charcoal during the operation to preserve their ratio from ore to slag inclusions.

- ▶ It is necessary to analyse a large number of ore and slag samples in order to determine the chemical signature of a given area.
- ▶ It is necessary to select many ratios of elements in order to determine the chemical signature of a given area since several ratios of elements may be similar for many iron-making areas.

In this respect, Desaulty (2008) and Desaulty *et al.* (2008) select ratios of elements following, in part, geochemical information. If the procedure is interesting, it does not exclude the possibility of other element couples, not selected by the authors, which are not polluted to define the chemical signature of a given iron-making area. As a consequence, the number of trace element couples considered in Desaulty's works (8 ratios) is limited in comparison with the number of trace elements that pass into the slag completely and are not significantly contaminated by lining or charcoal (12 elements) to validate a provenance hypothesis. Since the elements capable to chemically define a given area may be numerous and therefore allow considering a large number of element ratios, it becomes difficult and tedious to compare the trace element ratios one by one (for example, 200 samples were analysed and 1926 analyses were so considered in Desaulty's works). Considering these observations, multivariate techniques can be thus invoked to treat the acquired data and to aid the extraction of significant information on the origin of an iron artefact with an unidentified origin.

### **MULTIVARIATE ANALYSIS FOR THE DATA DESCRIPTION**

Multivariate methods are relatively common in the areas of glass (Baxter & Freestone, 2006) and ceramic (Neff, 1995) research. On the other hand, they have been much less applied in the area of archaeometallurgy. In the literature, some studies in this field are nevertheless found (Hedges & Salter, 1979; Fells, 1983; Charlton, 2007; Giussani *et al.*, 2007) but mainly concern the slag samples chemistry. To our knowledge, no provenance study on ancient ferrous artefacts made by the bloomery process combining particular chemical element ratios and the multivariate analysis have been carried out to date. Research has always employed bivariate scatterplots as shown in the previous part.

A brief explanation of some multivariate methods used in this thesis will be given in this part. Some archaeological applications using standard methods routinely applied to investigate the chemical similarity between artefacts characterized by measurements on their chemical composition will be introduced in order to illustrate the multivariate methods. Mathematical details on the methods here described will be left out but can be found in reference literature: Shennan (1997) and Baxter (2003).

## Methods of unsupervised learning

### Hierarchical classification

Methods of hierarchical classification analysis represent statistical techniques widely used in archaeology (Baxter, 2003). They aim at describing the similarity (or dissimilarity) between samples and discovering homogeneous groups (or clusters) in a set of data. These methods can be used to identify groups of data without assuming *a priori* a structure of the data. Two types of classification are possible: the hierarchical ascendant analysis and the hierarchical descendant analysis.

The principle of the hierarchical ascendant analysis is to describe the proximity of the samples in the multivariate space. Thus, the most similar samples from a chemical point of view are grouped together until all individuals are joined in a single group. The representation of the results is a hierarchically arranged dendrogram. The construction of the dendrogram consists in connecting the samples with branches whose height describes the distance between the specimens in the multivariate space (Figure I.21). The number of groups in the data is decided from the appearance of the dendrogram. In contrast to hierarchical ascendant analysis, hierarchical descendant analysis initially views the set of data as a single cluster that is successively subdivided into smaller clusters. It has not been much used in archaeology.

A major aspect to point out is that there are many ways in which a classification might be carried out (many ways to measure the similarity between pairs, and numerous algorithms for grouping samples on the basis of their similarity). As a consequence, there is not a uniqueness of the obtained dendrograms.

Previous studies concerning iron artefacts (e.g. Fiset *et al.*, 2001) have shown the ability of the hierarchical classification analysis to identify groups of similar archaeological iron artefacts. Different constraints are nevertheless required to generate an explicit classification, particularly in the field of provenance studies. Indeed, the main objective in the present study is to relate iron artefacts with parent sources. Since the structure is not assumed *a priori*, each group of a particular origin should be the most homogeneous possible, and groups of different origins the most different possible to provide realistic groups in terms of provenance. But it will be seen later, with the PCA example, that the variation in the chemistry of samples defining a given iron-making area may be more significant than the variation between the iron-making area and the iron artefact, even if the latter was not produced in this area. Thus, the drawback is that this method may suggest clear structure in the set of data, even when data are random (Baxter, 1994). Moreover, the method may be poor at identifying even quite obvious outliers. If the hierarchical ascendant analysis is judged to be a powerful technique for explaining (dis)similarities between samples in a set of data (as the samples used to characterize a given area), it does not seem to be adapted to identify the provenance of an object with an unidentified origin.

**Principal component analysis**

The principal component analysis (PCA) is a common and powerful widely applied multivariate method for describing the variation in a set of data. As with the hierarchical cluster analysis, the PCA is an unsupervised method of descriptive analysis, so that each sample is treated as a separate cluster.

See Shennan (1997) and Baxter (2003) for more details on its principle. However, to give a brief summary, the idea is that the  $n$  original variables are linearly transformed to  $n$  new uncorrelated variables. As a consequence, the derived results are a new set of uncorrelated variables and each new axis (principal component noted PC) is a linear combination of the original variables. The structure of the original variables can be thus explored using simple graphical methods involving the first two or three PCs. The plot based on the first two PCs may be thought of as the plot that accounts for the greatest variation within the set of data. A single plot derived from the PCA can easily take the place of many bivariate scattergrams made up of the original variables. PCA is used to investigate the relationships between the samples. The positions of the original variables (scores) plotted into PC space exhibit patterns of variation in the initial structure of the set of data (example is shown in Figure I.24; Left). As a consequence, bivariate plots of PC scores can show groups in the data, corresponding to different chemical compositions and therefore suggesting distinction in the chemistry of samples.

In addition, a graphical representation that can be viewed as an approximation to the covariance matrix of the data permits to explain the relationship between the variables and the location of scores in PC space (Figure I.24; Right). On the latter plot, the variable is graphically loaded by displaying vectors emanating from the origin so as to show the magnitude of its influence on the principal component. From this, the variance of the variables is given by the extremes of the vectors and the correlation between variables can be inferred from the cosine of the angle subtended by pairs of variables. The two plots (plots of scores and loadings) can be superimposed with a common origin (involving the use of a biplot) in order to infer something about the chemical composition of the different groups evident in the plots of scores.

Concerning our research, the application of PCA may be interesting to treat the high dimensional data set acquired. In this way, the provenance of an iron artefact could be examined by comparing its data with the ones of the iron-making areas. Some previous studies have already used this statistical technique for identifying and describing chemical slag groups but not in the aim to identify the origin of an object (Fells, 1983; Charlton, 2007). On the contrary, Desaulty (2008) has tested the relevance of the PCA application for its provenance study. While Charlton, for example, used oxide concentrations, Desaulty used ratios of elements as variables as detailed previously (Sm/Th, Th/U, La/Yb, Y/Yb, Hf/Nb, Eu/Sm, Cs/Rb). To test the technique, the element couples defining the Pays de Bray area is compared, among others, to that of the region of Rennes. Note that the two previous chemical signatures using the selected ratios of elements are clearly distinguished with a bivariate scatterplot

(Figure I.27). The resulting plot of the scores based on the first two components from the PCA of the values of the element ratios are shown in Figure I.28. It appears that the two regions cannot be distinctly separated. In addition, it is important to observe that the dispersion within the scores describing the Pays de Bray is larger than the difference between the two regions.

Results of the PCA typically display the variation present in the set of variables. As a result, it is important to notice that while PCA may be intended to reveal the difference between the chemistry of the samples collected to characterize the chemical signature of a given area and the one of the iron artefact with an unidentified origin, it becomes also an effective means for investigating the variation of the composition within the set of data defining the iron-making area. This situation becomes particularly problematic when there is much more data that define the given area than the artefact itself as is the case in this study (200 samples on average for the iron-making area, 10 slag inclusions on average for the iron artefact with unknown origin). Indeed, the risk is to point out, as often as not, the dispersion of the data within a given area rather than the difference between its chemical signature and the one of the iron artefact. Considering all these parameters, the PCA does not seem to be an appropriate technique for identifying a provenance.

This problem may be partially resolved using the discriminant analysis.

### **The supervised discriminant analysis**

Discriminant analysis is another widely used multivariate method in archaeology. The principle of the method is discussed in other papers (see e.g. Baxter, 2003). The descriptive modeling of the discriminant analysis is Fisher's linear discriminant analysis (LDA). The prime aim of this approach is to identify the best discrimination between groups of data with the variables that have been measured. Thus, data can be previously classified in groups by site of origin and then groups so defined asked to be distinguished in terms of their chemical composition. LDA is closely related to the PCA since they both look for linear combinations of variables which best explain the data. Thus, each new axis from the LDA, or linear discriminant (LD), is a linear combination of the original variables. While PCA does not take into account any difference in class of data, LDA explicitly attempts to model the difference between the classes of data and to demonstrate group separation graphically. The first LD (LD1) can be represented as a line running through the set of data points that accounts for the greatest separation between the two or more groups of data defined *a priori*. If  $k$  groups of data are considered in the analysis, the LDA provides  $(k-1)$  discriminant functions and when  $k > 2$ , it is common to present results in the form of a bivariate plot based on the scores for the first few functions.

For our provenance study, the examined corpus and therefore the class related to each archaeological sample are known. Indeed, samples that characterize a given area can define a particular group and the slag inclusions of an artefact with an unidentified origin may define

another one. LDA can be used to assess how well separated these groups will be. The axis LD1 is particularly interesting for the present study since it could separate easily, from the descriptive variables assigned to the chemical elements, the chemical signatures of two groups of samples with a different origin. Due to its principle in the descriptive modeling, the LDA attributes to the data of the iron artefact, for which the origin is unknown, a single group. As a consequence, regarding the exclusion of an origin hypothesis, the principle of the distinction of the LDA could probably enable a more efficient treatment of the results acquired in the present provenance study than could be the case with the PCA. Nevertheless, this may make the validation of a provenance hypothesis difficult. However, it will be seen later that this analysis can also be used for this case of study thanks to a reasoning based on a postulate. To conclude, the investigative strategy that will be followed in this work rather uses the LDA.

### **Data transformation**

Baxter (2001; 2003; 2008) advises to transform the original variables since variables with larger variance dominate the results of methods of unsupervised learning, such as PCA and cluster analysis, than variables with relatively small variance. Several types of transformation are possible (centered data, standardized data, logged data, ratio transformed data, etc.) but the preferred choice consists in standardizing the variables<sup>19</sup>.

In archaeometric studies, the use of logarithmic transformation is also common (Pollard, 1986; Aitchison *et al.*, 2002; Baxter *et al.*, 2005; Baxter & Freestone, 2006). In our research, the study will be based on the use of log-ratio data but the aim of this transformation will not be to standardize the variables but rather to cancel out the dilution effect occurred in the slag during the smelting.

These commentaries particularly tend to show that the application of the multivariate analysis must begin with the application of transformation data to provide more meaningful results.

### **HISTORICAL QUESTIONS**

In the Middle Ages, many iron production areas where the practice of a bloomery smelting stage is attested, exploited manganese-rich ores. These areas occupied a major place in the medieval economy. We find in particular the Pyrenees, Catalonia, Lombardy, Burgundy, the Dauphine, Southern Germany, Styrie and Carinthie (Sclarfert, 1926; Verna & Benoît, 1991; Belhoste, 2001; Verna, 2001). These manganese-rich ores are recognized for their qualities by the men working iron at the Medieval age. These particular ores would allow to give natural steel in the bloomery smelting stage.

---

<sup>19</sup> Standardizing the element content variables  $E_{ij}$  consists in subtracting the element content mean ( $\bar{E}_j$ ) and dividing by the standard deviation ( $s_j$ ) :  $Y_{ij} = (E_{ij} - \bar{E}_j) / s_j$ .

### **The iron-making Ariège area**

A study of C. Verna, founded on documentary sources, permitted to shed light on the iron-making activities in the central Pyrenees, mainly in Ariège, during the period from the 13th to the 16th centuries (Verna, 2001). The iron-making basin of Ariège represents a true mining district centered around the Vicdessos valley within the haut Sabarthès (Figure I.30). The latter is composed of a number of iron concessions. In the Middle Ages, this basin was mainly supplied by the ore exploited by the Community of Vicdessos, in Sem (Mine of Rancié). Around the deposit of the haut Sabarthès, and in particular of the mine of Rancié, is organized an important iron-making activity, which makes the Ariège area a vast iron-making basin at the level of the Pyrenees and of Languedoc.

In the 13th century, the establishment of the *moulines* in Ariège will support the increase of production and will develop the trade. In the big metallurgical space composed of the County of Foix, then Ariège, ores and iron materials exchanges are organized (Figure I.31). The Vicdessos ore was exported in the Couserans following an exchange treaty concluded in 1347-1348 between the men from Vicdessos and those from Couserans, which remained in effect until the 19th century (Chevalier, 1956). Consequently, the Vicdessos supplies with ore some hydraulic forges in the Erce and Massat valleys, in Couserans, and receives in exchange the charcoal needed to supply the forges of Vicdessos valley. Concerning the iron-making products, the historical sources highlight a dynamic market in the County of Foix which thus makes its restitution complex. The iron of the *moulines* of the Ariège area also supplied a market further away from the production sites during the 13th century (Figure I.31). We thus can see, through all these possible exchanges, the difficulty in knowing the distribution conditions in the Ariège area. It is up to us to confront the historical and archaeological clues with the contribution of archaeometry. The complexity of the iron market sensed by the historical sources within the Ariège area at the Medieval age, its dynamism, the fact that it supplied a market which exceeds the local sphere, make the Ariège area an iron-making locus favouring a study of iron materials origin.

### **The iron-making Lombard area**

In the Italian Alps, the provinces of Brescia and Bergamo (Lombardy) constitute one of the most important iron-making areas, which occupied an essential place in the iron economy at the Medieval age. The iron metallurgy in Lombardy is thus directed mainly towards the manufacture of steel. Between the 13th and the middle of the 15th centuries, the Bergamask and Bresciane valleys produced the most abundant and the most famous steel in Europe. Lombard steel is delivered to the market and is widely circulated along the major commercial arteries. The spread of Lombard steels will run up against the diffusion of the products of other iron-making areas thus suggesting a common diffusion area in the South of France. Most of the iron-making industry, during the Middle Ages and at the modern age, was devoted to the



production of weapons and armours. Many samples of Italian armours, dating from the 14th to the 16th centuries, were studied by A. Williams. No study of source has been carried out to date on such samples. However, the armours are not always signed with a manufacture mark by the craftsmen. Thus, the attribution of a Milanese or Bresciane origin by the historians, and for many armours, is based on stylistic studies.

### **Popes' Palace of Avignon**

The Popes Palace of Avignon is a large building of the end of the Middle Ages located in the common diffusion area of several important iron-making production zones such as Ariège and Lombardy. A considerable quantity of iron used in its construction is still visible in various parts of the building site. Various ores seem to have been used for the realization of the pins and clamps. Thus, some of these irons would be from manganese-rich ore. These various clues suggest that the blacksmith qualified as “*maître des ferrures*” and exclusive supplier of the Palace, himself called upon several sources. However, the exact origin of these construction irons remains unknown to date. But the town of Avignon is located in an area where the markets of different important production zones compete.

### **SYNTHESIS**

The bibliographic synthesis enables to define this work's central issues in two major parts.

- ◆ Results obtained in previous provenance studies evidenced the need to use an approach combining major and trace elements which are not significantly contaminated by lining or charcoal during the operation. If we consider the trace elements and the analyses of numerous archaeological samples, a very large data set is thus provided. Due to the complexity of this high dimensional data treatment, a new multivariate methodology for the examination of an origin hypothesis has to be developed.
- ◆ This research work takes an interest in iron metallurgical areas for which ores contain a high concentration of manganese, in particular the Ariège and Lombardy areas. We propose to answer three specific historic and archaeological questions:
  - The iron market study of an iron production space: the Ariège: From the 13th c. to the 15th c., the production of *moulines*, a type of bloomery process forges in the Ariège area supplied the local iron market but also the more long-distance one. We aim at clarifying the iron market's organisation, also studied by historical approaches, inside the production space in Ariège. To this end, we took a close interest in studying the origin of objects uncovered on archaeological sites in Ariège, but also outside.
  - The supply of construction iron used in a medieval building: the Popes' Palace in Avignon: the most probable suppliers of this building are indicated by historical



studies. The palace is situated roughly at the borders of several iron-making areas including Ariège and Lombardy. Our research aims at revealing some supply sources of iron for different construction sites at the new palace by studying the reinforcements used in the monument.

- The verification of hypothetical origin assigned by historical stylistic studies: examples of some armours provided by the Wallace Collection: we propose to verify whether some armour samples are coming from the Italian Alps production centres as expected by the historians.

From these problematics, we can sum up the work's approach in three points:

- A reference corpus will be gathered for the determination of the chemical signatures defining the Ariège and the Lombardy areas. This will be done by analysing selected ore, slag samples and iron products from archaeological sites of these regions. Samples from an experimental smelting will also be studied. To study the iron market in Ariège, well dated objects of unknown origin from various archaeological sites in this area will be selected.
- Several analytical techniques will be coupled and used to characterize the samples on a macroscopic scale (ores and slag samples) and also on a microscopic scale (SI in the objects). In addition to ordinarily used methods, specific techniques will be employed to quantify the trace elements. We will develop a method especially focused on the analyses of the smaller SI.
- Due to the complexity of the high dimensional data set acquired, a multivariate statistical method has to be developed.

## Chapter II: Experimental methodologies. Analytical setups

The experimental methodologies adopted to examine the ancient samples either as powders for ore and slag samples or polished sections for iron objects are presented on Figure II.1.

### ORES AND SLAGS MACROSCOPIC ANALYSES

Archaeological ores and slags were analysed by macroscopic methods. Representative samples (i.e. about 80% of the initial slag or ore volume) were first crushed into powder in an agate shatter box before being sieved at 125  $\mu\text{m}$ . The study begins with the determination of the major element composition through Energy Dispersive Spectrometry coupled with a Scanning

Electron Microscope (EDS-SEM)<sup>20</sup>. Thus, compressed blocks were prepared from powders. All the surface of the pastilles were analysed and an average content was calculated.

This step is followed by the bulk trace element analyses. Two techniques enable this composition determination with specific low detection limits for each (Table II.1): Instrumental Neutron Activation Analyses (INAA) and Inductively Coupled Plasma Mass Spectrometry (ICP-MS) at the Pierre Süe laboratory and also at ALS Chemex Laboratory (Vancouver). Aliquots of 120mg of the samples for INAA and 50mg for ICP-MS analyses are prepared to perform these measurements.

ICP-MS measurements at Pierre Süe laboratory were performed using a Thermo Electron X7 quadrupole spectrometer equipped with a concentric nebuliser (Thermo Fisher Scientific). The analytical method is just like the one developed in Desaulty *et al.* (2008). For more details on ICP-MS analyses, see Desaulty (2008) and Desaulty *et al.* (2008). The relative error on results was estimated at 7%. Samples were prepared by acid decomposition in open vessels before ICP-MS analysis. Finding the correct procedure for the complete dissolution of the samples by chemical digestion is the most critical aspect of ICP-MS analysis. A combination of HNO<sub>3</sub> and HF is conventionally employed in the acid digestion of silicate matrix as done in Desaulty *et al.* (2008). Nevertheless, it has been recommended that the use of HF, which is very corrosive and toxic, should be avoided for safety reasons. As a consequence, our provenance study has required the development of a new acid digestion procedure. In order to implement a simpler, less expensive and more safe sample dissolution procedure, we have substituted the HF-HClO<sub>4</sub> mixture by NH<sub>4</sub>F (HNO<sub>3</sub> + H<sub>2</sub>O<sub>2</sub> + NH<sub>4</sub>F was used). By testing certified reference materials, it was found that the three-reagents digestion without HF and HClO<sub>4</sub> was very effective for the pretreatment of ICP-MS measurement. We have published the complete details of this procedure, which is recorded in the Appendix S (Mariat *et al.*, 2008).

The ICP-MS measurements performed by ALS Chemex laboratory<sup>21</sup> were regularly controlled by the comparison with results obtained by ICP-MS and INAA analyses at Pierre Süe laboratory (Figure II.2). The trace element composition by INAA was determined at Pierre Süe laboratory. All sample irradiations were carried out at the nuclear reactor Osiris of the Saclay CEA Centre (France) (Joron *et al.*, 1997). The determination of the element composition is followed by structural analysis for ore samples. XRD diagrams are registered on the powders to get global information on the nature of the present phases.

---

<sup>20</sup> An EDS system (IDEFIX setup, SAMx company) coupled with a SEM (Cambridge Stereoscan 120). Measurements were performed at 15 kV accelerating voltage. Accuracy and precision have been determined on synthesised iron containing slag samples analysed by other methods, such as Electron Probe Micro Analysis (EPMA). In iron containing slag, a relative error of 2% is estimated for measurements of major elements, and of 10% for minor elements with concentrations lower than 1%, down to 0.5 wt% (detection limit). Elements lighter than oxygen could not be measured, a factor which has precluded the analysis of some iron carbonates present in ore samples.

<sup>21</sup> ME-MS61 and ME-MS81 protocols were used.

## **IRON OBJECTS MICROSCOPIC ANALYSES**

The metallic samples were prepared in cross-section to enable the observation of the metallic matrix and the inclusions. They are embedded in epoxy resin, cut in transverse sections and successively polished using SiC abrasive paper (grades 80–4000). First, metallographic etchings were done on the artefacts using Nital 4% to determine the carbon content in the metal.

Then, samples were examined by optical microscopy with an OLYMPUS optical microscope under reflected light. This allows distinguishing different zones of interest on the artefact, the different kinds of inclusions and possible welding lines.

### **The analysis of the major elements**

Major element compositions of slag inclusions have been measured with SEM-EDS. Experimental conditions were unchanged in comparison to ore and slag samples' analyses. As mentioned in the bibliographic synthesis, inclusions coming from adding during forging are not representative of the ore smelting stage. Moreover, a local concentration effect due to the size of the inclusions can be observed. As a consequent, this kind of inclusions was eliminated and slag inclusions characteristic of the ore chemical signature were selected. To do so, the procedure proposed by Dillmann & L'Héritier (2007) was followed. It can be assumed that the defects are caused by local concentration effects or by adding during forging, and that the remaining ones, showing a linear relationship between NRC, are representative of the smelting stage (Figure II.4). Altogether, about 50 inclusions were analysed per artefact in order to evidence a linear relationship between the different NRC and to take into account the two previous points. At last, the diagram proposed by Dillmann & L'Héritier (2007) to distinguish direct from indirect process was used (Figure II.5).

### **The analysis of the trace elements**

#### **Application of LA-ICP-MS**

Between 10 and 15 inclusions representative of the smelting stage are selected for trace element analyses. Laser ablation inductively coupled plasma mass spectrometry (LA-ICP-MS) was applied for the investigation of the majority of SI because of the possibility to quantify a significant number of trace elements with low detection limits with this method. It has largely proved its capabilities for the analysis of solid samples such as the inclusions in iron objects (Devos *et al.*, 2000; Coustures *et al.*, 2003; Desaulty, 2008). These measurements were led in collaboration with the Centre Ernest Babelon (UMR5060 IRAMAT CNRS, Orléans) (Gratuze, 1999; Gratuze *et al.*, 2001). The analytical protocol developed is as follows: samples were ablated for 50 s, the repetition rate of the laser was 6Hz and the diameter of the ablation crater was about 80  $\mu\text{m}$ . These experimental conditions have been defined to obtain optimal signal in a SI. The calculation procedure involves matrix-matched standards, used as external

standardization, Nist 610 and Nist 612 whose composition is known and close to the one of the inclusions. As the amount of removed material is not the same for each ablation, the signal obtained for each trace element for the different ablations has been compared to the one for the internal standard: the isotope  $^{29}\text{Si}$ . Thus, each SI analysed by LA-ICP-MS should have previously been measured with SEM-EDS in order to know the concentration in silicon. The details of the calculation procedure can be found in several papers (Gratuze, 1999; Gratuze *et al.*, 2001; Speakman and Neff, 2005). Precision is usually of 12 relative per cent for trace elements, but could reach 20 relative per cent for trace elements below ppm level. In the present study, 39 elements are considered for LA-ICP-MS determination (Table II.2).

#### **Application of confocal $\mu\text{XRF}$ under Synchrotron Radiation for the smallest SI (example of armour samples)**

Due to the extremely well-preserved condition of the armours, only tiny specimens (surface from 1 to 3 mm<sup>2</sup>) were taken on each armour (Figure II.8). Inclusions entrapped in the metal are all smaller than 30  $\mu\text{m}$ . Nevertheless, LA-ICP-MS only allows to analyse areas larger than one tenth of micrometers. Moreover, the crucial specificity required for the analysis of precious armour samples is the preservation of their integrity. LA-ICP-MS can be regarded as destructive for the armour samples because the quantity of matter sampled by the laser is not negligible compared with the entire sample. If LA-ICP-MS is sufficient to analyse large inclusions, this method can not be used for smaller SI sizes or on valuable samples that cannot be destroyed even locally. As a consequence, we have tested the possibility of performing non-destructive elemental micro-analysis on the SI in armour samples by means of the microscopic X-Ray Fluorescence analysis under Synchrotron Radiation (SR- $\mu\text{XRF}$ ). To control the penetration depth of the analysis, a confocal setup was also used (Figure II.9). Main experiments have been performed on the FLUO beamline at ANKA (Figure II.10).

Figure II.11 shows a photograph of the setup at FLUO. The beam has been focalized with a planar polymer CRL to a spot size of a few micrometers (7.5x2.8  $\mu\text{m}^2$ ). For our study, where the size of the SI is less than 20  $\mu\text{m}$  diameter, we chose the spatial resolution by using a CRL instead of having a high photon flux by using a polycapillary. The confocal setup was constructed by mounting a polycapillary-half lens (X-ray Optics System) in front of the fluorescence detector. The sample was translated through the beam by means of a sample holder with two rotational and 3 translational stages. Excitation energy of 22 keV was chosen in order to detect trace elements of interest with a high atomic number: in particular, Rb, Sr, Y, Zr, whilst maintaining an acceptable photon flux (Figure II.13). Thus, a 20  $\mu\text{m}$  foil of Cr was placed between the polycapillary in detection and the detector window in order to suppress iron fluorescence when necessary.

In confocal setup, XRF signal of only a specific microvolume cube within the investigated sample can reach the detector. This microvolume of analysis is defined by the overlap of the foci of both X-ray optics (see Figure II.14). The acceptance (depth resolution) ( $d_{\text{FWHM}}$ ) of the polycapillary optic depends on the detected energy (Beckhoff *et al.*, 2006; Janssens *et al.*,

2004). As a consequence, the dimensions of the microvolume formed vary according to the experiment and the detected energy and has to be therefore characterised. In order to experimentally determine the dimensions of this microvolume, thin foils were used. Thus,  $d_{FWHM}$  was measured by scanning foils through the analysis volume. Foils were moved through the beam in 5  $\mu\text{m}$  steps in the horizontal plane (axe z shown in Figure II.11). The obtained full-width-at-half-maximum (FWHM) of the X-ray intensity profiles shown in Figure II.15 is relative to the foil thickness  $e$  and  $d_{FWHM}$  according to Equation II.2. In our work, the depth resolution is estimated to range from 26 $\mu\text{m}$  to 30 $\mu\text{m}$  at 5.9 keV (Mn-K $\alpha$ ) and from 12 $\mu\text{m}$  to 17 $\mu\text{m}$  in the energy range 13-16 keV according to the setup alignment (Figure II.16).

Second, our experimental protocol is performed in 4 steps:

- (i) As the inclusions are all rich in Mn (~2-10%), each SI was first roughly located on the surface by performing elemental map of Mn. Nevertheless, when the 20  $\mu\text{m}$  Cr filter was used, the Cr was excited by the Fe present in the metallic matrix but also in the SI. In this case, when the SI was not so rich in Mn (<2%), the Cr-K $\beta$  overlapped the Mn-K $\alpha$ . It was therefore decided to plot the map from the intensities ratio  $(K_{\beta}\text{Cr} + K_{\alpha}\text{Mn})/K_{\alpha}\text{Cr}$  map (Figure II.17).
- (ii) Then, each SI was scanned through the sampling volume in 5  $\mu\text{m}$  steps in depth (along the normal to the inclusion surface= $z$ -axis). The Mn intensity profiles plotted against depth permit to experimentally determine a position in depth for which the microvolume cube of analysis is situated within the SI. The penetration depth is so controlled. However, the obtained one-dimensional information may not be sufficient for the location of the position measurement.
- (iii) 3D information is required to study the inclusion composition for not arbitrarily position the microvolume cube within the inclusion being investigated. Elemental maps of Mn-K $\alpha$  (or  $K_{\beta}\text{Cr} + K_{\alpha}\text{Mn})/K_{\alpha}\text{Cr}$ ) were so performed at various depths below the surface (Figure II.20).
- (iv) Finally, spectrum was acquired to detect elements of interest without probing the metallic matrix around the inclusion. The acquisition time for each spectrum was generally of about 3600 seconds because of a poor transmission due to the confocal set-up and the Cr filter.

To convert the spectral lines intensities into elemental concentrations, we developed a procedure using the internal standard manganese. The determination of the trace elemental contents was performed by using the dedicated software PyMCA, which permits to calculate element amounts in a known matrix analysed by XRF (Solé *et al.*, 2007). Since PyMCA is not dedicated to confocal XRF experiments, some changes have been added for the setup modelling in the PyMCA software. Figure II.21 highlights several striking differences between the experimental setup taking into account by PyMCA and the confocal setup used in reality. These differences led us to calibrate the method by defining a transmission coefficient

( $\text{Coef}_{\text{trans}}$ ) depending on the polycapillary transmission and the radiation volume within the sample.  $\text{Coef}_{\text{trans}}$  was calculated at different depths in the inclusion by means of reference samples: homogeneous glasses synthesised in our laboratory with the same Fe content than SI but also SI whose composition is known by LA-ICP-MS analyses (Figure II.22; Figure II.23). For the SI of unknown trace elements composition (Rb, Sr, Y, Zr), the concentrations determined with PyMCA can be corrected by the transmission coefficients previously calculated (Figure II.24).

Reference materials and some inclusions of three armour samples were investigated by both LA-ICP-MS<sup>22</sup> and confocal SR-XRF to verify the relevance of the protocol developed. The standard deviation for the four trace elements is <10% in most of the cases and <20% in all cases, except for one data (Figure II.25). Figure II.26 shows that the contents determined using the analytical protocol developed for confocal  $\mu$ XRF measurements are in good agreement with the contents obtained by LA-ICP-MS. This evidences that the analytical process is both reproducible and accurate. Such a result can be obtained only because reference materials are made of a similar matrix to the SI ones.

## Chapter III: Description and characterisation of the corpus

A reference corpus has been gathered to define the chemical signatures of the Ariège and Lombardy areas. A sample list is available in Appendix R.

### THE ARIÈGE AREA

In the Middle Ages, the geological ore source localization together with historical documents and traces of extractions, suggest the wide exploitation of the ores from particularly the Mont Rancié in the Vicdessos and from Château-Verdun in the Ariège valley (Verna, 2001). Thus, ore samples were mainly collected from the Mont Rancié, on the north-west side (Figure III.1). In addition to these samples, geological ores were also collected on the east-south-east side (R<sub>10</sub>, 2190hém, 2189goeth, Lerc2070). Any geological ores from Château-Verdun could have been analysed in this work. Nevertheless, the ores deposits of Mont-Rancié and Château-Verdun are provided by the same geological formation (Figure III.2). It may be supposed that the ores from these two deposits have a similar geochemistry. Not many medieval iron mines are known in the Couserans region except Riverenert site (Verna, 2001) and no geological ores

---

<sup>22</sup> Measurements performed at the L.M.T.G (Laboratoire des Mécanismes et Transferts en Géologie) in Toulouse, in collaboration with D.Béziat (UMR 5563 UR 154 CNRS Université Paul-Sabatier IRD Observatoire Midi-Pyrénées) and M.P.Coustures (TRACES, Unité Toulousaine d'Archéologie et d'Histoire).



have been found in this area. All these geological ores analysed have a particular chemical characteristic: a high manganese content ( $\sim 4\text{wt}\%$  on average) and a low value for phosphorus ( $< 0.7\text{ wt}\%$ ) (Figure III.3). Ores from the Mont-Rancié are mainly made up of carbonates, iron and manganese oxides and hydroxides. X-ray diffraction allowed the identification of the different ore-forming iron phases. The essential type is defined as a mix of goethite ( $\alpha\text{-FeOOH}$ ) and hematite ( $\alpha\text{-Fe}_2\text{O}_3$ ) (Table III.1). A significant quantity of calcite ( $\text{CaCO}_3$ ) has been identified in ores containing a high content of Ca.

Four archaeological sites that provided evidence on the successive steps of the entire operating chain (ores, slags and products) were selected and sampled in Ariège. These sites are: Lercoul in the valley of Siguer, Riverenert within the Arize Massif, Savignac-les-Ormeaux in the south of Ariège and Castel-Minier in the Couserans.

### Castel-Minier archaeological site

Castel-Minier (Aulus-les-Bains) is situated in the Couserans (southeast western part of Ariège) in the immediate surroundings of the Vicdessos valley. A bed of argentiferous lead conducted to a significant silver-making activity in the Middle-Ages. Furthermore, research on the site revealed, in addition to the silver mining, an iron production area. The iron production was shown effective from the end of the 12th c. to the last quarter of the 16th c. as *terminus post quem*. Two slag heaps were located, one is associated to a castle, the other is not related to it (Figure III.5). Different types of samples (ores, slags but also iron materials) were selected in the areas of the iron-making disconnected from the castle. Figure III.6 (top) gives the major element composition of the ores sampled. Except for the CM2008/M1 sample, Fe is present to a significant level ( $>56\text{ wt}\%$ ). Moreover, manganese, which characterizes the ore's signature in Ariège is high ( $1.4 < \text{wt}\% < 10$ ). Figure III.6 (down) shows the trace element compositions of the ores plotted using a logarithmic scale. It underlines high contents of the following trace elements: Ti, Sr, Ba and Zn. Some of these ores are made up of goethite and hematite phases (CM06-2002/M1, CM06-2002/M2 and R<sub>6</sub>). For the others, a mix of magnetite ( $\text{Fe}_3\text{O}_4$ ), maghemite ( $\gamma\text{Fe}_2\text{O}_3$ ) and hematite is present (Table III.2).

The composition of respectively major and trace elements for slags integrated to the corpus are given in Figure III.8. Slag samples are rich in Fe ( $\sim 38\text{ wt}\%$ ), Si ( $\sim 11\text{ wt}\%$ ) and Mn ( $\sim 9\text{ wt}\%$ ) and their trace element compositions are relatively homogeneous.

In addition to ore and slag samples, the chemical signature of the site of Castel-Minier was also determined with metallic products, linked to the production of the iron-making site. These products correspond to *gromps*, pieces from the bloom but also several semi-finished metallic products. After etching, metallographic observations show that the metallic products are made of steel alloys (Figure III.11 and Appendix P).



### **Lercoul archaeological site**

The Lercoul site is situated on the east-south-east side of the Mont Rancié. The site comprises a slag heap, containing about 60 tons of slag, dated from the 3rd century AD. Tapped and bottom slags were collected and analysed by the C.R.P.G (Centre de Recherches Pétrographiques et Géochimiques). Samples were thus already under powders. Some of them were analysed in this work. Results obtained on the major element compositions (Figure III.12; top) show that slags are rich in Fe (up to 52 wt%) except Lerc8. Contents of Si ( $7.5 < \text{wt}\% < 25$ ), Al ( $\sim 3 \text{ wt}\%$ ) and Mn ( $\sim 4 \text{ wt}\%$ ) are also relatively high in most of the samples. It appears that the trace element compositions are relatively homogeneous (Figure III.12; down).

### **Riverenert archaeological site**

The Riverenert archaeological site is located within the Arize Massif in the Couserans (see the map in Figure III.2). Archaeological studies showed that iron ores were worked on this site from the 1st c. AD to the 16th-17th centuries. Measurements were performed on six slag samples (Figure III.13). Figure III.14 gives the sample compositions. Results underline that slags are siliceous; Ca and K contents are lower than 3 wt%. Manganese presents a particularly high content (up to 10 wt%). Zr ( $\sim 82 \text{ ppm}$ ), Ba ( $\sim 400 \text{ ppm}$ ), V ( $\sim 90 \text{ ppm}$ ) and As ( $\sim 166 \text{ ppm}$ ) contents can reach values above 100 ppm.

### **Savignac-les-Ormeaux archaeological site**

Savignac-les-Ormeaux<sup>23</sup> was an iron-making centre in the early modern period (16th-18th c.) near Ax-les-Thermes in eastern Ariège. Three tapped slags were collected in slag heaps to characterize the Ariège chemical signature. Previous research suggests that supply of ore for the Savignac forge was the ore from the Mont Rancié (Grimbert, 2006). The composition analyses evidence the use of ore characterised by a high manganese content ( $\sim 6 \text{ wt}\%$ ) (Figure III.15).

### **Experimental smelting**

In order to analyse samples of slag and metallic products obtained from well known ore and smelting conditions, an experimental reduction was conducted in a bloomery furnace. The experiment (XP07) processed a geological ore found on the Mont-Rancié (XP07.min). Tapped slags as well as lining and charcoal were recovered and analysed. Table III.3 shows the sample list for the samples collected from the XP07 experiment. Results on the sample compositions will be present in Chapter IV.

---

<sup>23</sup> Grimbert, L. (2006) dir., Savignac-les-Ormeaux, un atelier sidérurgique moderne (XVI<sup>e</sup>-XVIII<sup>e</sup> s.) DFS, INRAP, 2005.

## **THE LOMBARDY AREA**

In order to determine the chemical signature of the Italian Alps, geological ores extracted from the Alpine valleys of Lombardy were collected. The selection of the geological ore samples covers the iron rich deposits from East to West in the Lombardy area. Valleys sampled are Valtorta (Carisole mine), Valmora (mines of Parisola and San Marco), the di Lupi valley (Valbondione), Scalve valley (archaeological site of Schilpario, mines near Schilpario, mines of Stendata and Gaffione), Val Camonica (the iron-making site of Val Gabbia II and mines of Piazzalunga) (Figure III.18).

Results on the major element analyses are relatively scattered (Figure III.19). The majority of ores contains contents in Fe above 40 wt% except for one ore from Gaffione mines (Gaf.2bis), ores from Piazzalunga and Ponte Val Gabbia (named TIZ in purple). Characteristically the sedimentary, iron ores of the southern Alpine chain are manganese-rich ( $1 < \text{wt}\% < 6$ ). All samples exhibit very low P values ( $< 0.5 \text{ wt}\%$ ). Figure III.20 shows the trace element composition of the different ore samples represented for each geographic area. Concentration profiles underline a relative homogeneity in trace element compositions. The main trace elements are Ti and Sr accompanied by Ba which is major in variable amounts. The Ba contents are unusually high for some iron ores (68628ppm for Triomen mines and 23489ppm for Gaffione-Spiazzo mines).

Ore and slag samples were also collected on two archaeological sites from different periods: Schilpario (valley of Scalve) and Ponte di Val Gabbia II (Val Gabbia). Several slag heaps could have been surveyed at Schilpario, hence the datation has been determined to range from the 2<sup>nd</sup> to the 7<sup>th</sup> centuries. Slags typical of the bloomery process, two archaeological ores and one iron object were analysed (Figure III.21). The archaeological site of Ponte di Val Gabbia II, near Bienno, is of the Lombard period (C. Cucini Tizzoni, 1999). Measurements were performed on slags of the bloomery process but also on two typical slags of the indirect process reduction stage (laitiers) (TIZ005, TIZ007)<sup>24</sup>. All these specimens were supplied by Vincent Serneels<sup>25</sup>. Chemical analyses of the corpus corresponding to the above archaeological sites are given in Figure III.22. They show high Mn values ( $> 5 \text{ wt}\%$ ) coupled with very low P amounts ( $\sim 0.5 \text{ wt}\%$ ).

## **OTHER IRON-MAKING AREAS**

This part concerns other iron-making areas that will be considered in this work because their iron ores all have high amounts of manganese: Andorra, the Montagne Noire and the

---

<sup>24</sup> Desaulty (2008) has shown that lithophile elements present in the iron ores pass completely into the laitiers. The composition of these samples is therefore characteristic of the chemical heritage of the used ore.

<sup>25</sup> C.Cucini Tizzoni (1999) *La miniera perduta. Cinque anni di ricerche archeometallurgiche nel territorio di Bienno.*:Bienno. p.114.

Dauphine. We aimed at characterizing their chemical signature in order to compare them with the one defining the Ariège area. In this way, some provenance hypotheses could be tested.

Previous studies enable to date the iron production activity in Andorra between the 17th c. and the 19th c. (Codina *et al.*, 2001a) which is not the period studied in this work (13th-15th centuries). Nevertheless, Andorra's chemical signature has been characterized to test the multivariate method that will be developed in Chapter IV.

Archaeological studies revealed that iron was mass produced in the Montagne Noire area, located in the southwest of the Massif-Central. During the Middle Ages, iron production is attested in the south (in the Minervois) and in the north (in the Monts de Lacaune) (Verna, 2000). The characterization of its chemical signature in this work will be based upon results published by Coustures *et al.* (2003).

Finally, as mentioned in the bibliographic synthesis, the Dauphine area could have supplied the construction iron used in the Popes' Palace of Avignon. Samples from the PalSid database was chosen to define the chemical signature of this iron-making area. They were collected from the archaeological site of la Pelouse, dated from the 17th century, for which the use of the bloomery process is attested (Bruno-Dupraz & Peyre, 1988).

#### **COMPARISON OF THE COMPOSITION OF SAMPLES FROM THE DIFFERENT IRON-MAKING AREAS**

To conclude, the trace element compositions of ores and slag samples from the different medieval areas (Ariège, Lombardy, Montagne Noire and Dauphine) are compared in Figure III.27. Results reveal that concentrations are more or less of the same order of magnitude. As a consequence, it seems it is not possible to distinguish the samples of a different origin considering only absolute amounts of trace elements. Nevertheless, some peculiarities can be evidenced as, for example, a higher Ba value in ores from Lombardy.

### **Chapter IV: Provenance compatibility with the Ariège and Lombardy areas. Development of a methodology based on a multivariate approach**

This chapter is divided into four major parts. The first one will describe the element behaviour during the bloomery process and the element selection that will characterize the chemical signature of the iron-making areas. The second will explain the specific raw data transformation proposed to apply the multivariate analysis. The third will be dedicated to the description of the chemical signatures defining the Ariège and Lombardy areas. The last one

will deal with the multivariate statistical method developed to determine the provenance of the iron artefacts of unknown origin.

### **SELECTION OF THE DISCRIMINANT ELEMENTS**

An experimental smelting (XP07) using ore from Mont Rancié was conducted (see Chapter III) for the element behaviour study. In addition to ore and slag samples, charcoal and lining samples were analysed (Figure IV.1 and Figure IV.2). Charcoal composition is characterized by high values of Ca, K for major elements and Ba, Rb, Sr, Zn for trace elements. Ti, Ba, Zr are trace elements present in relatively high levels in lining (above 100 ppm). In order to understand the element behaviour, the composition of the samples analysed (ore, slags, charcoal and lining) was normalised to the ore composition, which means their compositions were divided by the one of the ore (Desaulty, 2008). Results of this normalisation are plotted in Figure IV.3 using a logarithmic scale. From this plot, the enrichment factor of slag compared to the ore for each element can be defined (named  $E_{sc}^m$  in Figure IV.3). The most frequent enrichment factor defined as a modal enrichment factor can be determined (Figure IV.3, down). A majority of the elements have an enrichment factor close to the modal factor. They represent the elements not affected by any pollution and having the same partitioning coefficient between metal and slag. It may thus be assumed that the ratio of their contents should not change from the ore to the slag inclusions obtained from the smelting slag. Three other behaviours may be observed. First, some elements have been contaminated by charcoal and/or lining during the experiment (they display a significantly higher enrichment factor than the modal one). Then, elements such as Mn have been partitioned between slag and metal (they are enriched in the slag but enrichment is lower than the modal factor). Last elements, such as Co, W, As are depleted in the slag (enrichment factor is lower than 1). These elements could be volatile or siderophile elements. Table IV.1 gathers results obtained with several experimental bloomery smeltings among which XP07 results. Elements are summed up according to the four behaviours observed. Some elements have a varying behaviour, being for example not polluted in some cases but polluted in other cases (such as Al, Zr, Sr.). These elements can not be selected to trace the chemical signature. On the contrary, most of the studied elements have the same behaviour in all the experiments (always polluted, never polluted,...). Considering these results, it may be assumed that elements which always pass mainly into the slag during the smelting process and are never contaminated by lining or charcoal can be used to characterize a chemical signature (Table IV.2). A constant ratio of these elements is preserved from the ore to the slag for samples from XP07 experiment as shown in Figure IV.4.

As the polluting effects cannot be generalised and depend on the ore composition, the element values present in the ores from the Ariège and Lombardy areas have to be considered in a second stage. The composition of the ores from these two iron-makings are compared, in Figure IV.5 and in Figure IV.6, with the ones of charcoal and lining proposed in the literature

(Crew 2000; Serneels, 2002; Chauvel, 2006; Desaulty, 2008; Senn *et al.*, 2009). It may be noted that Mn contents in ores from Ariège and Lombardy are mostly higher than in contaminant compositions. This could suggest that Mn pollution can be surely neglected for samples produced in these iron-making areas. If this element cannot be considered in a ratio regarding its behaviour during the different steps of the reduction process<sup>26</sup>, manganese oxide value can be nevertheless used as a helpful marker for discriminating samples coming from iron-making areas using manganese rich-ores to the other ones. Ba is also present in significant quantities in ores from Lombardy, so that a majority has higher Ba values than in lining or charcoal. Thus, the polluting effect for this element should not be visible for samples from Lombardy. Ba may be a marker of the chemical signature of Lombard ores and will be used in specific cases.

Characterization of the chemical signatures of the Ariège and Lombardy areas, based on the previous elements selected, will be investigated further in the third part of the chapter, after establishing terminology of the raw data transformation in the next section.

## **RAW DATA TRANSFORMATION**

### **Log-ratio data**

As mentioned above, it may be assumed that all ratios of the elements (E1, E2 ...) selected passing completely into the slag without being contaminated by lining or charcoal during the smelting remain constant from the ore to the slags and thus, to slag inclusions. Some of these ratios will be well-correlated, others more dispersed because of a variability of ore composition from an iron-making area according to their formation conditions. In a general manner, this property is simply expressed

$$E1 = aE2 \text{ where "a" is the elementary ratio non modified since the iron ores mining}$$

A first stage is to convert the data to logarithmic data. As a consequence, this transformation enables one to cancel out the dilution effect occurred in the slag during the smelting, so that analysis can only be based on the ratio value "a":

$$\begin{aligned} \text{Log}(E1) &= \text{Log}(E2) + \text{Log}(a) \\ X &= \text{Log} \left[ \frac{E1}{E2} \right] \quad (X = \text{Log}(a)) \end{aligned}$$

<sup>26</sup> It is not possible at this stage of the research to conclude about the Mn behaviour. Nevertheless, by analysing its content in SI and in metallic matrix, it is shown that this element does not have exactly the same behaviour as the other NRC. This point needs to be studied more in detail in the future in order to understand its behaviour better.

For a multivariate analysis, one element content  $E$  is compared with all the other contents. Each  $i$  sample is characterized by  $n$  elementary variables  $E_1, E_2, E_3, \dots, E_n$ . Considering the content of element  $j$  for sample  $i$  is denoted by  $E_{ij}$ . The extrapolation of the logged data transformation to the  $n$  elements is based on

$$X_{ij} = \log \left[ \frac{E_{ij}}{G(E_i)} \right]$$

where  $G(E_i) = (E_{i1} E_{i2} \dots E_{in})^{1/n}$  is the geometric mean of the elementary variables for the sample  $i$ .

This can be expressed as

$$X_{ij} = \log(E_{ij}) - \frac{1}{n} * \sum_{k=1}^n \log(E_{ik})$$

In the following, we will base multivariate analysis on the log-ratio data named  $X_{ij}$ .

Relative errors of  $E_{ij}$  induce, with logged data transformation, absolute errors on obtained  $X_{ij}$ . If the  $E_{ij}$  values are higher than detection limits, error occurred on  $X_{ij}$  will not be significant. On the other hand, if they are within detection limits, relative errors affected on  $E_{ij}$  become significant, so that an absolute error affects the  $X_{ij}$  values.

### Quality of data

In practice, analytical methods applied in this work (ICP-MS, INAA, LA-ICP-MS) do not measure all the trace elements with the same precision or efficiency. Regarding these parameters, elements measured for routine by the three previous methods and selected for multivariate analysis are the following:

Cs. U. Th. Hf. La. Ce. Sm. Eu. Yb. Y. Nb. Nd

In chemical composition studies data may be missing because values are below the level of detection. Nevertheless, because of the log-ratio transformation, any concentration information can be omitted from analysis. To deal with this problem in our work, a value in detection limit will be estimated to the mid-level of the detection.

Finally, the influence, on the  $X_{ij}$  scattering, of the presence of elements in detection limit involved in the mean ( $G(E_i)$ ) calculation has been tested. Figure IV.7 shows the frequency distribution of the  $X_{ij}$  defining the Ariège area for three different calculations of the mean  $G(E_i)$ . Results illustrate that data are less scattered when only elements often above the limit of detection are included in the mean expression:

$$\log G (E_i) = \frac{1}{5} [\log(Y) + \log(La) + \log(Ce) + \log(Sm) + \log(Eu)]$$

From this, the elements included in the multivariate analysis are summed up in Table IV.4.

### **DESCRIPTION OF THE CHEMICAL SIGNATURES DEFINING IRON-MAKING AREAS**

In this part, we deal with the definition and the characterization of the chemical signature of the Ariège and Lombardy areas. The aim of the two following paragraphs is to study the influence of two parameters on the chemical signature, more precisely on the  $X_{ij}$  scattering, defining these iron production spaces:

- Ores, slags and objects from various archaeological sites of an iron-making area contribute to its chemical signature definition. These samples represent different stages of the operating chain. The type of the sample (ore slag or object) would influence the dispersion of the chemical signature.
- Different archaeological sites were consistently considered for each iron production space. One can examine the contribution of samples from different geographical localizations, inside the area, on the chemical signature.

The effects of these two previous factors on the  $X_{ij}$  scattering must be considered before attempting to conduct a provenance study. To define and explain the formation of the chemical signature, the hierarchical cluster analysis, as explained in Chapter I, seems to be an appropriate technique for identifying groups in a structure of data (Baxter, 1994; Shennan, 1997; Gordon, 1999). One advantage of this method with respect to the data defining the chemical signature of Lombardy is that it does not require a minimal density of data.

#### **Influence of the sample type (place in the operating chain)**

The dendrogram produced by the hierarchical cluster analysis for data from Ariège is represented in Figure IV.11. A threshold from which groups can be identified is determined and illustrated on the figure. In this respect, six distinct chemical groups distinguish themselves (red n°1, orange n°3a, brown n°3b, purple and grey n°6b, blue n°6a and black n°5).

The main group (black n°5) is formed from ores, slags and objects, that is to say, samples from the different stages of the operating chain. The fact that the group is formed in the lower part of the dendrogram suggests that all included specimens are chemically similar. Thus, this group is homogeneous from a chemical point of view. As a consequence, it seems that the nature of the sample has no consequence on the variation of the chemical signature. Few elements are within the limit of detection for this group. Such observations can be made for the group n°3b (brown) made up of slags and ores.



The following groups, distinct from the two previous ones, cause variation in the data structure morphology. They are exclusively characterized by ore samples whose compositional analyses are reported in Table IV.5. For each group, several element contents are below the limit of detection in contrary to groups featuring a mixture of ores, slags and objects. Nearly all the measurements within the limit of detection are a feature of a specific element for the different groups. Therefore, this seems to be a characteristic of a particular type of ores. Nevertheless, when data is below limit of detection, their values are estimated. On log scale, the substitution of data below limit of detection can have a significant effect on the outcome of the analysis, so that the Euclidean distances in groups could be overestimated. As a consequence, variability observed within a group can be exaggerated with many data in limit of detection.

The dendrogram derived from data from Lombardy is shown in Figure IV.12. Results may be interpreted in the same way. If the main groups (brown n°7a, blue n°10b) are composed of samples representing different stages of the production, then nine distinct chemical groups of ores can be observable. The chemical variation of the signature is thus caused by these identifiable groups. The samples included inside each of them are characterized by element contents below the limit of detection (Table IV.6). Nevertheless, composition within a group displays strong similarities showing the same elements in limit of detection.

From the previous factors, the effect of the choice of samples type on the chemical signature evolution can be estimated:

- **1- Place of the sample in the operating chain:** specimens representing the different stages of production have been identified in homogeneous groups, from a chemical point of view, and for which few elements are below limit of detection. Thus, the place in the operating chain does not infer a variation of the chemical signature.
- **2- Influence of ores:** the dispersion of the chemical signature is mainly influenced by groups of ores. On the one hand, some of them do not contain elements below limit of detection. Because no slags from these ores are available, it can not make sense to remove these data from the analysis. On the other hand, other groups, constituting the majority, Euclidean distances in groups could be overestimated due to data substituted for elements present in limit of detection. Samples included in these groups are nevertheless aggregated according to specific chemical composition. Thus, it could be risky to exclude this data in statistical analysis since it may be informative and of interest for a chemical signature.
- **3-** In a general manner, it would make sense to remove these data from the analysis in order to get a better idea of the chemical signature scattering. However, involving the substituted data in the multivariate analysis is relevant in our work since they may represent the ore samples from which no slags are available. An additional reason is that few slags are available to define the chemical signature of Lombardy. This iron-making area is much characterized by ore samples. Data obtained on slag samples are not sufficient to characterize its chemical signature. In conclusion, as the substitution concerns a great

number of ore samples, we decide to conserve replacing data in the analysis to notably permit the characterization of the chemical signature of the Lombardy area.

### **Influence of the archaeological sites localization**

The aim now is to examine the influence of the geographical origin on the chemical signature of the samples. The previous dendrograms are now illustrated with colours indicating the archaeological origin of the samples.

The dendrogram from Ariège data is represented in Figure IV.13. The main homogeneous group, coloured in purple-pink, represents the samples from the Castel-Minier and Lercoul archaeological sites. As explained in Chapter III, the two aforementioned sites were supplied in ores by the Rancié mine located in the Vicdessos valley. The chemistry of this group is thus a direct reflection of the chemistry of the ores from the Mont Rancié. Moreover, slag samples collected from Savignac (yellow-orange) are not discriminated from the previous, therefore showing a similarity of the chemical signatures. This result suggests that the Savignac archaeological site was also supplied by the Rancié mine as expected by the archaeologists (Grimbert, 2006).

Slag samples collected from the Riverenert site, located in the Couserans valley, form a distinct group (green) most probably derived from a different chemical signature. This result will be an identification of slag especially formed with ores from Riverenert (in the Couserans valley). So, these slag samples contribute to the dispersion of the chemical signature of the Ariège area.

The dendrogram relative to the data from Lombardy is shown in Figure IV.14. In this area, only two archaeological sites were sampled (Schilpario and Val Gabbia II). Discrimination of two main groups is easily observed in the dendrogram (in purple and green). Samples included in the purple group are mainly slags and ores from Schilpario. The second is composed of slags from Val Gabbia II and also geological ores reduced on the site and coming from Piazzalunga. This distinction between both groups may be interpreted as a difference in their chemical signatures. As a consequence, within each of these groups can be identified a particular chemical heritage relative to samples from both valleys: Valle di Sclava and Val Gabbia.

In conclusion, considering samples from different archaeological sites supplied by various mines contributes to the scattering of the chemical signature of the Ariège and the Lombardy areas. It is thus possible to discern in detail chemistries reflective of varying ores within an iron production space.

## **METHODOLOGY BASED ON A MULTIVARIATE APPROACH**

The sample provenance can be examined from different points of view. In our work, the chemical signature of an object can be compared with the one of a single iron-production space, as it will be for the iron market's organisation study within the Ariège area. In addition, several iron production spaces can be considered simultaneously if various hypotheses of provenances are conceivable. This will be precisely the case for the study of the iron supplying in the monumental building of the Popes Palace in Avignon. As a consequence, this strategy suggests two approaches that will be described below.

As discussed in Chapter I, the Linear Discriminant Analysis (LDA) provides a means of efficiently discriminating groups of samples from various origins. This multivariate method will thus be applied for addressing the question of the provenance. Samples are classified according to their origin in such a way that samples from an iron-making area or SI of an object of unidentified origin are grouped into clusters. In this research, LDA is used primarily to demonstrate group separation graphically, so there is no need to invoke normality of data. Moreover, each  $X_{ij}$  involved in the expression of the geometric mean  $G(E_i)$  is a linear combination of the other  $X_{ij}$  of the mean. So, one element involved in this term must be excluded from the LDA analysis: the europium was arbitrarily chosen.

### **Compatibility with a provenance from Ariège**

Our approach consists in characterizing and quantifying the difference, on the discriminatory axis LD1, between the projections obtained with SI of objects from the iron-making area studied and from other areas.

In the following, the projection values on the LD1 axis for samples defining the Ariège area will be named  $\text{Proj}.X_{\text{ES.Ariège}}$  and those attributed to the object with an unknown origin  $\text{Proj}.X_{\text{OI}}$ . To investigate the compatibility between the chemical signatures, it is necessary to compare the  $\text{Proj}.X_{\text{ES.Ariège}}$  with the  $\text{Proj}.X_{\text{OI}}$ . Comparison is made between the frequency distribution of the  $\text{Proj}.X_{\text{ES.Ariège}}$  and the boxplot representation of  $\text{Proj}.X_{\text{OI}}$  on the LD1 axis. The boxplot is constructed from five values: the smallest value, the first quartile, the median, the third quartile, and the largest value. The two extreme values of the  $\text{Proj}.X_{\text{ES.Ariège}}$  on the LD1 axis represent the limit of the definition domain of the chemical signature of the Ariège area. Thus, because all the projections are generated consistently in a repeatable way on the LD1 axis, the calculation of both following distances may be especially useful when comparing the two classes of data on the discriminatory axis LD1 (Figure IV.16):

1/ distance between the median of the  $\text{Proj}.X_{\text{OI}}$  and the nearest extreme value of the  $\text{Proj}.X_{\text{ES.Ariège}}$ . This distance is named here "median distance":  $\mathcal{D}_{\text{méd.}}$

2/ distance between the quartile of the  $\text{Proj}.X_{\text{OI}}$  and the nearest extreme value of the  $\text{Proj}.X_{\text{ES.Ariège}}$ . This distance is named here "quartile distance":  $\mathcal{D}_{\text{quart.}}$

LDA analyses will be carried out separately, in a first stage, on iron artefact chemistries originally from the Ariège area and, in the second stage, from other areas.

(1) Figure IV.15 compares the Proj. $X_{OI}$  and the Proj. $X_{ES,Ariège}$  values on the LD1 axis for seven iron artefacts produced on the Castel-Minier production site and, thus, originally from the Ariège area. The values obtained for  $\mathcal{D}_{quart.}$  and  $\mathcal{D}_{méd.}$  are reported in Table IV.7. The first aim of two-group discriminant analysis is to identify the most significant separation between the two classes. As a consequence, even for an artefact produced with an ore from the Ariège area, the LDA can provide Proj. $X_{OI}$  extracted from the domain of the Proj. $X_{ES,Ariège}$  on the LD1 axis. Nevertheless, results also revealed that the distinction between the two classes of samples is not so important. In this respect, the Proj. $X_{OI}$  domain is always close to the one of the Proj. $X_{ES,Ariège}$ . The highest median and quartile distances estimated are respectively 0.27 and 0.01.

(2) Figure IV.17 and Table IV.9 summarize the results from LDA applied to artefacts not fabricated with ores from Ariège (Clé16, SCHmet1, Mimet, Loupelloiraine). In this case, the LDA analysis demonstrates clear separation between samples defining the area studied and the object from a different origin. Unlike the previous examples, the cluster of the iron object is now distinguished from the Proj. $X_{ES,Ariège}$  domain by higher values of the median and quartile distances than the maximal values obtained with artefacts from the Ariège production space. Thus, the resulting minimal values for median and quartile distances are respectively estimated 1.16 and 0.92 in the case that iron artefacts are not originally from the Ariège area.

In conclusion, the significant difference in the median and quartile distance values shows the LDA's utility in discerning groups of samples from the Ariège area to those from other provenances. If the values of  $\mathcal{D}_{méd.}$  and  $\mathcal{D}_{quart.}$  are lower than respectively 0.27 and 0.01, then the artefact with an unidentified origin could be originally from the Ariège area. If they are higher than 1.16 and 0.92, then it is possible to exclude an origin from Ariège. These values correspond to the threshold values, experimentally determined with our data, of the median and quartile distances from which the compatibility with a provenance from Ariège can be tested. It is important to bear in mind that future studies will be needed to confirm the above figures obtained in this study.

### **Compatibility with a provenance from Lombardy**

A similar pattern was highlighted for the Lombardy area. A single object originally from the Lombardy area (SCHmet1) could be used to experimentally determine the threshold values allowing the delimitation of the domain which defines the compatibility with a Lombard origin. Results are represented in Figure IV.18. The quartile and median distance values found are respectively 0.19 and 0.37.

As shown in Figure IV.19 and Table IV.9, objects from a different provenance are discriminated by higher median and quartile distances on the LD1 axis than an object fabricated in the Lombardy area. Thus, the LDA provides, once again, a very different set of inferences. In this case, the minimal values for median and quartile distances are respectively estimated 2.75 and 2.60.

From the previous observations, it is possible to establish subtle domains from which the compatibility with a provenance can be tested. Each of them depends on the iron-making area studied.

### **Establishment of a provenance compatibility graph**

The threshold values of the median and quartile distances can delimit three particular domains of compatibility with a provenance from the Ariège and the Lombardy areas: compatible, undetermined and incompatible. These threshold values are listed in Table IV.10. From these values, a graph, which expresses the quartile distance according to the median distance of the objects' projections and the iron-making area's, permits one to underline the different compatibility domains of signature with the production area. The provenance compatibility graph established for the Ariège and Lombardy areas are shown in Figure IV.20 and Figure IV.21.

These graphs, which allow us to test a hypothesis of provenance, will be subsequently applied on the data for objects with an unidentified origin in Chapter V.

In addition to the three aforementioned domains of compatibility, the graphs also highlight other domains (in grey). The latter correspond to SI analyses where data is probably too dispersed in reference to measurement errors. Thus, a compatibility of provenance cannot be obtained with these domains since they represent an uncertainty compared with the measures. If these domains seem not to be plausible, it may be conceivable that median and quartile distances belong to them but are nevertheless close to the threshold values of other domains. This is why a fourth domain may be determined as probably compatible. For the latter, the quartile distance value is included in the domain defined as "compatible" whereas the median distance value is included in the domain defined as "undetermined".

From this, we look for four domains of compatibility with a provenance from Ariège or Lombardy that might indicate the provenance of objects with an unidentified origin:

1/ **Compatible domain:** in this case, the object of unidentified origin has a similar chemistry to the iron-making area one, such that the object could be derived from ores of the iron production space.

2/ **Incompatible domain**: similarly, distance values included in the domain will prove that the hypothesis of provenance evaluated is not possible for the object examined.

3/ **Undetermined domain**: this domain suggests that both inclusion and exclusion of the tested origin are possible.

4/ **Probably compatible domain**: for this domain, the artefact is assumed to probably come from the tested origin.

A direct comparison of two classes of data thanks to these two previous graphs is a means of evaluating provenance hypotheses.

### **Comparison between several iron-making areas**

The aim is then to examine the provenance of an artefact when various hypotheses of provenances are considered. In this case, more than two classes are taken into account in the LDA, so that more than one plot based on the discriminant functions may be obtained.

To test the methodology, the LDA has been conducted with data from four iron-making areas: Ariège, the Montagne Noire, Lombardy and the Dauphine. First, we propose to perform the LDA on three classes of data: the Ariège and the Montagne Noire areas, and the SI of four artefacts from Ariège (Figure IV.22). Results show that scores assigned to the iron-making areas are successfully discriminated on the plot based on the (LD1, LD2) axes whereas the SI scores of each artefact show some overlap with the ones of the Ariège. Thus, the LDA confirms that the slag inclusions are structured much the same way as the samples from Ariège. When a data grouping is added to the previous (assigned to the Lombard samples), graphical representations of the samples in LD space are shown in Figure IV.23 and Figure IV.24. In this case, four clusters of data are considered; three discriminant functions (LD1, LD2, LD3) are thus generated. In the plot based on the two first discriminant axes (LD1, LD2), the projections of the slag inclusions of the object overlap significantly with those of the samples defining the Ariège area. The same pattern is observed between the clusters assigned to the Ariège and the Montagne Noire areas. The LDA analysis suggests that the clusters of the artefacts studied and that of the Montagne Noire area are less visually discriminated from the one assigned to the Ariège area. The other graphical representations in plots (LD1, LD3) and (LD2, LD3) are not particularly graphically informative, since they do not produce separate groups. It is generally possible to show most of the chemical information using the first LD axes. Thus, in practice, this is unlikely to require the use of any more than the first two or three LD axes. As a consequence, it will be common in this work to present results in the form of a bivariate plot based on the first two functions (LD1, LD2). Nevertheless, when a visible rapprochement between clusters in the plots of the first LDs axes will be highlighted, it could be advised, in the second stage, to confirm these results by the other plots, especially in the case where more than four clusters are considered.



Moreover, this example illustrates the fact that it may become difficult to visually identify various provenances when the number of clusters considered in the LDA is high. In conclusion, in the case where more than two classes are taken into account (various provenances are consequently considered), a visual approach will allow us, firstly, to possibly favour a specific hypothesis of provenance origin among those examined. The latter will be then individually compared to the variables of the object of an unidentified origin.

Finally, to ensure the possibility in excluding a provenance hypothesis for an artefact, the LDA has been performed on clusters assigned to four iron-making areas (Ariège, Montagne Noire, Lombardy, Dauphine) and one artefact of a different origin. For illustration, two examples of LDA applied on two iron artefacts (LoupeXP, Mimet) are illustrated on the plot based on the first two discriminant functions in Figure IV.25. Clusters of artefacts can be successfully separated from the other four, which show some overlap. A single plot is sufficient to exclude a provenance hypothesis. Thus, in the following, when the cluster assigned to the artefact with an unidentified origin will be separated from the ones of the iron production spaces in the plot (LD1, LD2), it will be possible to exclude the tested provenance hypotheses.

In conclusion, the LDA provides an ideal means of evaluating a hypothesis of provenance for archaeological objects with an unidentified origin and will be built on a general methodology.

### **GENERAL METHODOLOGY**

From the models introduced above, we proposed a general methodology, reported in Figure IV.27, intended to study and identify the resource-use of an iron object.

First, the absolute contents of the major elements manganese and phosphorus can be used as a first filter since the different ore types of the iron-making areas of interest (Ariège, Lombardy, Montagne Noire, Dauphine, Andorra) are all characterized by a significant presence of manganese and by the absence of phosphorus (see Chapter III). Thus, an artefact containing inclusions with low MnO\* content or/and very high P<sub>2</sub>O<sub>5</sub>\* content (more than about 4 wt%) could not come from the aforementioned iron production spaces.

In a second stage, the multidimensional strategy perfected for testing a provenance hypothesis as explained in the previous parts and summed up in Figure IV.27, will be applied on artefacts selected from the first filter. The proposed methodology begins by separating two approaches: when an object signature is compared to the one of a unique iron-making area, as for the study of the iron market organisation in Ariège, or when several hypotheses of provenance are estimated, as for the study of iron supplying in the monumental building of the Popes Palace situated at the borders of several iron-making areas. Both approaches will be respectively named **APPROACH n°1** and **APPROACH n°2** which are defined as follows:



**APPROACH n°1:** the chemical signature of an artefact is compared to the signature of a single iron-making area by performing LDA. The graph which underlines the different compatibility domains of signature with the same production area (compatible, probably compatible, undetermined and incompatible) subsequently allows to test the hypothesis of provenance. If the artefact could come from the considered area, the hierarchical cluster analysis can be thus invoked for eventually identifying the more probable valley sourcing within the iron production space. If the artefact origin is not compatible with the one of the area, it can be compared to samples assigned from other iron-making areas.

**APPROACH n°2:** in the case where more than two classes are taken into account (various provenances are consequently considered), a visual approach allows us, firstly, to favour a specific provenance in the graphs in LD space. The latter is then individually compared to the variables of the object with an unidentified origin.

This general model will be systematically used in the next chapter and applied to data of objects with unknown origin.

Nevertheless, this approach is incompatible with the study of armour samples supposed to be of Lombard origin because of the limited number of elements quantified in the SI. For the armour study, the manner in which these data will be processed and displayed will be thus separated from the previous methodology. Several filters will be applied. First, absolute trace element amounts quantified in slag inclusions will be compared to the ones in samples defining the Lombardy area in order to verify the compatibility of the SI composition with the Lombardy signature. Then, for SI analysed by confocal SR- $\mu$ XRF method, only the trace elements Sr and Y can be useful to distinguish areas due to the fact that they are probably not contaminated by lining or charcoal for ores from Lombardy (see Chapter IV). Thus, the ratio formed by the (Sr, Y) couple will be used to trace the chemical signature of the Lombardy area in the SI of these armour samples. For SI analysed by LA-ICP-MS, the quantified trace elements that are not contaminated will be selected to form couples and to determine their signatures. As such, the trace element Ba has proved to be of interest to characterize the chemical signature of the Lombardy area. This element could thus be used in a ratio of trace elements.

A result of such filters is that the hypothesis of a Lombard provenance for the armour samples could not be proved but only excluded in favourable cases.

## Chapter V: Provenance of iron materials. Historical and archaeological applications

The results obtained in the previous chapters (II, III, IV) make it possible to propose and develop a new multivariate analysis based methodology to determine or exclude a hypothesis of origin. It is now possible to apply it to iron artefacts with an unknown origin in order to answer the three historical and archaeological questions explained at the end of the bibliographic study, each requiring a specific study approach.

### STUDY OF THE IRON METALLURGICAL PRODUCTS' CIRCULATION OF A PRODUCTION SPACE: THE ARIÈGE AREA

#### Selected corpus of samples

During this study, we collected well-dated objects from four archaeological sites: the Montréal-de-Sos castle in the Vicdessos valley near the Mont-Rancié mine, the Castel-Minier production site in the Couserans area, and two other castles in the Couserans area : the Mirabat and the Sainte-Catherine castles. To underline the complexity and the dynamism of the iron marketing in the production area of Ariège, different types of objects were selected: nails, medieval projectiles, blades, etc..

The archaeological excavations carried out the Castel-Minier site allowed us to select 8 finished objects that are linked to the forge of the castle, the castle itself and also to the silver mine (a chisel). The origin of these objects can be thought of as unidentified because they are not directly related to the iron production area. Indeed, products of moulines are known from texts (massive products in the form of bar, plate or rough draught)<sup>27</sup> (Verna, 2001). The selected samples are not obviously compatible with this type of production. A description of these samples is given in Figure V.1.

On the Montréal-de-Sos site, numerous as well as various iron objects have been excavated. The selected corpus is diversified in order to study the provenance of different types of objects. It is therefore representative of the four functions identified on the site (Table V.1):

- Projectiles for armament or hunting,
- Frame nails,
- Horseshoe nails, equine iron linked to the horse equipment,
- Blades, an iron plate (Table V.1).

For the Mirabat and Sainte-Catherine castles situated in the Couserans area, a certain quantity of nails was excavated on both sites. In this respect, it was decided to collect only nails to

<sup>27</sup> *barra ferri rotunda, plata, merlaria, virgae ferrea, virgae platae, scapolones vomorum and ligonum.*

study their origin because one may suppose this type of objects often tended to be sold by the professionals of small metallurgical pieces (nailers, etc...) and bear witness to exchange contacts at forges or on markets. Moreover, in comparison with the objects from the Montréal-de-Sos castle, the study of a single type of objects enables in this case to observe a possible variety in the supply.

All of the evidence derived from excavation suggests that selected nails are dated from the end of the 13th c. to the 14th c (Tables V.2 and V.3).

### **Compatibility with a provenance from the Ariège area**

The chemical signature of the slag inclusions trapped in the objects previously described will be compared to that of the Ariège area by following the successive stages of the methodology based on the multivariate approach developed in Chapter IV..

As detailed in the previous chapter, a first filter using the absolute contents of the Mn and P major elements can be applied to test the hypothesis of provenance. Figure V.2 and Figure V.3 compare the MnO and P<sub>2</sub>O<sub>5</sub> values measured in samples from the Ariège area to the weighted average MnO\* P<sub>2</sub>O<sub>5</sub>\* contents in the slag inclusions of each artefact with an unidentified origin. It appears that a majority of objects have compatible amounts in these elements with that of the Ariège samples. Only the following artefacts: MdS n°29431 (Figure V.2) and MIR5 (Figure V.3) cannot come from this iron production area (too low MnO\* content for MdS n°29431 and too high P<sub>2</sub>O<sub>5</sub>\* content for MIR5). Samples whose major element composition is compatible with the Ariège signature will now be studied by the trace element analysis according to the approach n°1 of the detailed procedure suggested in Chapter IV which is established in two steps.

In a first stage, the compatibility of the objects with a provenance from Ariège can be investigated in this way. For the set of the results of the discriminant analysis, the plots showing the distribution of the projections (group separation) on the first discriminant function (LD1) will be reported in Appendix F (F.1, F.2, F.3, F.4). In the following, we will outline, for each archaeological site, the values obtained for median and quartile distances measured between the objects' projections (Proj.X<sub>OI</sub>) and the closest observation defining the iron-making area (Proj.X<sub>ES.Ariège</sub>).

#### Castel-Minier site :

Concerning objects found on the Castel-Minier site, the values for these distances are given in Table V.4 and illustrated in the abacus which underlines the different compatibility domains of the chemical signature with the Ariège production area (Figure V.4).

For specimens CM07-2044, CM05-2-36, CM05-2-59, CM05-2-54 and i10013, distances clearly belong to the domain of provenance compatibility defined as compatible with a provenance from Ariège. Given the definition of this specific domain, these objects may come from of local production. Regarding iron artefact CM05-2-34, the median and quartile

distances are slightly apart from the latter domain. They are included in the domain defined in chapter IV as probably compatible. It thus appears to be possible to suppose ores from Ariège as ore sources for this artefact. On the other hand, two of them, a nail (CM06-2002-1) and possibly a piece of equine iron (CM05-2-31), display quartile and median distances distant from the two previous domains. The fact that these distances are included in the domain defined as “incompatible” suggests that these objects appear to be of a different origin, imported in the Ariège area.

#### Montréal-de-Sos site :

The results obtained from the samples found on the Montréal-de-Sos castle are illustrated in Table V.5 and Figure V.6.

Three groups of samples are different from each other in the abacus. First, some of the specimens (MdS8844, MdS8858, MdS29336, MdS29522, and MdS29566), belonging to the “compatible” domain, can be related to ores from Ariège, while others (MdS29409, MdS29421 and MdS8889) exhibit distances that are included in the “undetermined” domain for which clear conclusion on their origin cannot be drawn. In this respect, for the latter, an origin from the Ariège area can neither be excluded, nor validated. Finally, for the three latest objects (MdS29591, MdS9297 and MdS29342), such provenance can be clearly ruled out.

#### Mirabat site :

Results of the Xij projections on the discriminant function LD1 for nails from the Mirabat castle are reported in Figure V.8 and in Table V.6.

From these results, it appears that four groups of samples are different from each other. First, some objects (MIR1, MIR3, MIR6, MIR8, MIR10 and MIR12) are distinguished by high distance values included in the domain defined as non compatible, so that they can not have been fabricated without any doubt in the Ariège iron-making area. The latter are split into two distinct fields discerned by different distance values that could testify of various origins. Then, a single nail (MIR7) could be originally from the Ariège area. Finally, since the distances assigned to the nails constituting the last group (MIR2, MIR9, and MIR11) are included in the undetermined domain, we assume that they could be either a product of Ariège ore, or of other iron-making areas. In fine, of the ten nails, four to the maximum were potentially produced using ore from the Ariège area.

#### Sainte-Catherine site :

Discriminant analysis results concerning the nail samples from the Sainte-Catherine castle are displayed in Table V.7. The median and quartile distance values separating the objects' projections on the discriminant axis LD1 to the closest projection defining the iron-making area (Figure V.9) argue that one of the three nails (Ste Cath n°4) would have been fabricated with ore from the Ariège area. For the other two, the high values of these distances permit to

definitively exclude such origin. Note, in addition, that these values between these nails are different, suggesting they may be related to distinct ores.

### **Comparison of the chemical signature with the ones of the Ariège valleys**

As shown in chapter IV, the hierarchical analysis permits to identify samples especially formed either with ores from Riverenert (the Couserans valley) or with ores from Mont Rancié. Thus, this analysis is here applied to objects identified as originally from Ariège with the intention of identifying a particular relation with one of these areas (Figure V.10). The chemical signatures assigned to the ore deposits of each of them are bordered in the resulting dendrogram.

The dendrogram shows that the chemical signatures measured on the slag inclusions of the objects from the Castel-Minier and Montréal-de-Sos archaeological sites are compatible with that of ore used in the Vicdessos valley rather than the Riverenert mine (Couserans). These observations confirm, in a predictable manner, the large hegemony of the Rancié mine for Ariège ore supplying of many iron metallurgical installations. On the other hand, the chemical heritage detected in the slag inclusions of nail MIR7 is more similar to the chemical signature of ore from the Riverenert mine. This result illustrates in this way that a basic supply for some ironwork sites in the Couserans area was probably guaranteed by the local ore deposits at Riverenert.

### **Provenance of the objects that do not come from the Ariège area**

Concerning samples with a chemical signature not compatible or of undetermined compatibility with a provenance from the Ariège area, other possible provenance hypotheses due to the high amount of manganese in their ore deposits can be investigated in this study. In the immediate surroundings and at some distance of the Ariège, ores from the Andorra and the Montagne Noire areas can be included as possible sources for these objects. Note that there is nevertheless no archaeological and historical evidence for an iron-smelting industry in Andorra before the 16th century. On the other hand, the historical sources indicate that iron produced in the South of the Montagne Noire, in the Minervois area, were provided in the haut Sabarthès area in Ariège during the Middle Ages (Verna, 2000). As a consequence, according to the approach n°1 of the procedure developed, a discriminant analysis will be performed on data defining the Ariège, the Andorra, the Montagne Noire areas and the objects with an unidentified origin (four classes of data are thus considered in the analysis).

The blades found on the Montréal-de-Sos site constitute a particular case of study. Specifically for this type of objects, a fifth provenance hypothesis can be tested since ores from Lombardy can be included as a possible source. Indeed, there is indication by textual sources for trade of knives from Parma in the haut Sabarthès during the Middle Ages, most probably through Lombard peddlers (Verna, 2001). In this case, five classes of data will be taken into account in

the discriminant analysis (Ariège, Montagne Noire, Andorra, Lombardy, and objects with an unidentified origin).

We propose to analyse the origin of these objects in three steps:

- **1.** First, iron artefacts for which no information on their origin (“undetermined” domain) has been retained will be examined.
- **2.** Then, artefacts for which the ores from Ariège as possible raw material could be rejected will be regarded.
- **3.** Finally, results obtained on the two blades will be presented.

**1-** For the first group, the resulting plots based on the first two discriminant functions (LD1, LD2) are shown in Figure V.11. On the one hand, the separation between the objects’ projections and the ones attributed to the Andorra (blue) and the Montagne Noire (green) areas seems to be large enough for chemical signatures of objects with an unidentified origin to be differentiated. Therefore, it can be concluded that a positive assignment to one of these both specific ore deposits is impossible.

On the other hand, results do not allow us to clearly distinguish scores of objects MIR11, MIR9 and MdS29421 from scores defining the Ariège area. In the same manner, projection representations in the plots based on the other discriminant axes (Appendix H) corroborate the conclusions drawn from the previous results. Nevertheless, projections linked to the artefacts of unidentified origin are not totally included in the domain defining the Ariège chemical signature. This means that, keeping to the methodology, clear conclusions cannot be drawn about their origin in this study. On the contrary, score groups assigned to the equine iron MdS29409 and the nail MIR2 display reasonable separation with the Ariège one, so that none of these artefacts was made with iron or steel coming from this area. It is therefore not possible in this work to identify where these ferrous materials were produced.

**2-** For the second group, results are reported in Figure V.12. The graphical representation in the plot (LD1, LD2) allows us to distinguish the chemical heritage detected in the slag inclusions of the iron artefacts from the genetic environments of the iron-making areas tested. A separation between two groups displayed on a single plot being sufficient to exclude an origin hypothesis, Figure V.12 suggests the incompatibility of chemistry between the artefacts of unidentified origin and the tested iron production areas. From these results, it appears that these artefacts were probably not produced in these regions, so we must look for iron production areas elsewhere, as will be discussed in Chapter VI.

**3-** Finally, concerning the blades (MdS9297 and MdS88), for the present results (Figure V.13) it is sufficient to note that the chemical signature of both samples are not exactly the same as the ones of the iron-making areas tested in this study. As a consequence, these samples would be originated from other iron production areas.

## Construction iron in the St-Etienne collegiate church of Capestang

Our aim is now to examine the origin of ferrous materials found outside the production area of Ariège, more than about a hundred kilometres. In the vicinity of Narbonne, at Capestang, the St-Etienne collegiate church was built in the beginning of the 14th century by the same architect as that of the Narbonne cathedral. The study of the iron materials used in the Church construction is thus a fair means of examining the possible presence of iron from the Ariège area around Narbonne. In this respect, it would be verified if iron produced in the County of Foix and transported to Narbonne could be used in the construction of the building.

The analysed samples, presented in Table V.8, were taken from the pinnacle pins of the church. Previous studies showed that pinnacles are subjected of several restorations during the centuries. It is thus possible that the pins buttressing them were not put in place during the initial construction but are rather the result of more recent restorations. So, it was verified, by applying the abacus proposed by Dillmann & L'Héritier (2007), if the iron studied comes from the direct process or from the finery (Figure V.14). Results show that the CAP2 sample was manufactured by the indirect process whereas the others were made by the bloomery process. Due to the fact that it has been shown that the ore chemical signature is removed from the final slag inclusions during the indirect process, the following study will only focus on the two artefacts CAP1 and CAP3. The weighted average composition in  $P_2O_5^*$  and  $MnO^*$  in the slag inclusions of both pins CAP1 and CAP3 are compared to the contents measured in samples from the Ariège area in Figure V.15. The results show that CAP1 inclusions have slightly higher  $P_2O_5^*$  amounts than the Ariège samples but not in sufficient amounts to exclude a provenance from this area<sup>28</sup>. The chemical signatures of both samples are thus compatible with the Ariège signature, and as a result the methodology based on the multivariate analysis can be applied.

Table V.9 gathers the median and quartile values obtained for the variable projections of the objects. They belong to the domain compatible with an origin from Ariège as Figure V.16 suggests it. It can thus be concluded that these construction irons can be derived from ores of the Ariège production space.

### **STUDY OF THE ORIGIN OF THE CONSTRUCTION IRONS USED IN THE MEDIEVAL BUILDING: THE POPES' PALACE IN AVIGNON**

#### **Selected corpus of samples**

At different places of the Popes' Palace of Avignon, ferrous reinforcements were evidenced by archaeological studies and prospecting. Some clamps used in the construction of the palace,

<sup>28</sup> Indeed, phosphorus can be added by the charcoal and moreover, a small part of this element passes in the metal during the smelting.



built in 1335, have been the subject of yearly studies conducted by Dillmann & Bernardi (2003). The authors observed that numerous samples have slag inclusions with a high manganese content, related to the use of a Mn-rich ore.

In order to characterize the iron supply sources in a quantitative way, it was decided to analyse samples representative of different construction sites of the new palace. The corpus of samples from the Popes Palace, dated from the 14th century, is thus composed of (Figure V.17 and Table V.10):

- ▶ Three pins from the Grand Promenoir, finished in 1351, and three others from the Conclave' Gallery, constructed in 1360.
- ▶ One clamp from the Trouillas tower, finished in 1347.
- ▶ Six clamps from different brackets (C, G, E) of the Latrines tower, interestingly built in a single year (1338).

### **Comparisons of the chemical signatures and provenance**

As described in Chapter I, various supply sources are obviously conceivable for construction iron of the palace, since there are many iron production spaces that have systematically provided the town of Avignon with iron. Some of these possible sources, like the Ariège, the Dauphine, the Lombardy and the Montagne Noire areas, will be tested in this research. Their chemical signatures will thus be compared with those of the selected samples.

The research conducted by Dillmann & L'Héritier (2007) observes that this medieval building was essentially reinforced with construction iron of the bloomery iron. It is thus conceivable to perform a provenance study and apply the developed procedure.

The major element concentrations measured within the slag inclusions of a majority of samples, except for both specimens from the clamp Eg7, reveal high manganese concentrations (Figure V.18) indicative of Mn-rich ores. The provenance hypotheses tested can thus be ruled out for samples from clamp Eg7. For the others, the phosphorus and manganese contents in the slag inclusions are relevant with concentrations defining the iron-making areas, so that these possible sources cannot be excluded. Thus, according now to the two-stage approach n°2, it is first suggested to apply the discriminant analysis to the different iron ore occurrences proposed as sources and the construction irons.

Nevertheless, a discriminant analysis will be carried out beforehand only on the construction irons in order to highlight possible various origins. Results represented in the plot based on the first two discriminant functions (LD1, LD2) (Figure V.19) show interestingly that iron from the Trouillas tower and the Conclave' Gallery seem to have very close ratios of trace elements in this graphical representation. The scores assigned to these construction irons are thus proposed to form a group n°1. Samples from the Grand Promenoir can be ruled out from this group n°1, therefore suggesting a different origin. Moreover, samples from this construction

site seem not to have similar chemical signatures between them, therefore forming two distinct groups (group n°2 and 4). Two different origins at least may coexist within this site of the palace as previously indicated by the  $MnO^*$  and  $P_2O_5^*$  contents. One of the samples collected in the Grand Promenoir, GP3.4, constitutes, with the majority of the clamps from the Latrine tower (with the exception of sample Se1), a group that exhibits related chemical signatures (group n°4). It nevertheless appears that the chemical signatures show a certain variation within this group. Regarding clamp Se1 (group n°3), a clear differentiation of ore source compared with the previous one is obvious. It is argued that this four group arrangement is the result of four different origins at the minimum detected in the slag inclusions of the construction irons: one group composed by the samples collected on the Trouillas tower and the Conclave' Gallery (group n°1), one of two samples from the Grand Promenoir (group n°2), one of the clamp from the Latrines tower Se1 (group n°3), and the last one composed of a single sample from the Grand Promenoir (GP3-4) and other clamps from the Latrines tower (group n°4). At this level of study, a diversity of origins is thus observed.

The previous conclusions drawn from the observation in the plot based on the first two discriminant functions (LD1, LD2) must then be corroborated by the graphical representations obtained in the plots based on the remaining functions. In this particular case, the graphical demonstration must be based on a lot of plots since the LDA provides numerous discriminant functions (11). Nevertheless, demonstration such as this can be assessed informally only by reference to the plots based on the first few discriminant functions because it can be expected to be possible to represent most of the separation present in the sample's variables with only the first functions.. On the contrary, as shown in Chapter IV, the plots based on the last discriminant functions tend to show a lot of overlap between groups.

From the results illustrated in Figure V.20, it can be concluded that the information provided from the other projection plots is consistent with previous results for many of the samples with the exception of Eg1 sample. For the latter, included in group n°4, the scores seem to be more separated from the others in the graphical representation (LD1, LD4). In conclusion, it may thus be assumed that artefacts within each group, with the exception of the Eg1 sample, have the same origin.

### **Group n°1**

About the four samples constituting group n°1, the graphical representations of the discriminant analysis in the plot based on the two first functions (LD1, LD2) is shown in Figure V.21. From these results, it appears that the scores assigned to the slag inclusions of construction irons can not be related to those of ores used in the Ariège, Lombardy and the Montagne Noire areas, so that there is no doubt that these specific ores as ore sources for the iron supply of the Trouillas tower and the Conclave' Gallery can be excluded.

On the other hand, the plot (LD1, LD2) shows that the artefact and the Dauphine scores are rather closely related. The plots based on the other discriminant axes (Appendix I) also display

a strong correlation between the two groups of scores, therefore corroborating this observation. Thus, according to the two-stage approach n°2 of the suggested procedure, our analyses only allow firstly to favour this hypothesis of origin among those examined.

In a second step, it is thus necessary to test this specific hypothesis of provenance by individually comparing the variables of the Dauphine samples with those of the slag inclusions of the construction irons. This analysis can not, however, be performed as part of this work, since the chemical signature of the Dauphine area is defined with few samples. As a consequence, based on the established protocol and in need of sufficient data, it is not possible to conclude on the origin of these construction irons.

### **Group n°2**

The results dealing with samples of group n°2 (Figure V.22) indicate that chemical signatures of both construction irons are completely incompatible with that of the iron-making areas tested in this research. This means that none of these artefacts were made with iron from these regions.

### **Group n°3**

The provenance compatibility abacus for Se1 is plotted in Figure V.23. Similar observations as the ones made for group n°2 can be suggested for this sample.

### **Group n°4**

On the other hand, the results obtained for the samples of group n°4 (Figure V.24 and Figure V.25), reveal that the signatures of the construction irons of group 4 are not comparable to those of the Montagne Noire, Lombardy and the Dauphine. It appears that these artefacts were not produced in these regions. On the contrary, the iron artefact scores are close to the domain defining the signature of Ariège. In the same way, no other projection plot allows to differentiate irons from this group of the samples defining the Ariège area (Appendix I). Therefore, this first stage of established methodology doesn't allow to exclude a production from Ariège for these samples. According to the approach n°2 of the protocol, we must compare, in a second step, their chemical signature in a more precise way by projection on the discriminant axis LD1. The values of the median and quartile distances resulting from this analysis are consigned in Table V.11 and are deferred in the graph of Figure V.26. For the three samples Ec2, Ec3 and Eg3, these values belong to the domain defined as compatible with a provenance from Ariège, which is inclined to show their chemical signatures correspond well with the Ariège one. We therefore suggest that these construction irons could be produced in the Ariège area. On the other hand, it is not possible to clearly account for the source of iron Eg1 insofar as its projections are in the domain of undetermined compatibility with an Ariège origin. Finally, the GP3-4 sample is located at the limit of the "incompatible" domain with an origin from Ariège. It thus seems possible to exclude such a provenance for this construction iron.

Thus, according to our methodology, three samples of the Latrines tower would come from Ariège basin. Such an origin for Eg1 is not excluded but we will not be able to confirm or invalidate such a hypothesis in this work. On the contrary, the GP3-4 sample does not seem to come from the Ariège area.

An assessment of these results will be proposed in Chapter VI.

### **VERIFICATION OF HYPOTHETICAL ORIGIN: ARMOURS SUPPOSED TO BE LOMBARD**

As developed in Chapter I, Lombardy was an important manufacture center for armour. This military material was then provided to all Western Europe.

The armours are not always signed with a manufacture mark by the craftsmen. Thus, for many artefacts, the attribution of a Milanese or Bresciane origin by the historians is only based on stylistic and technical studies. We will here confront some of the interpretations with the archaeometric approach and the analysis by the trace elements.

#### **The corpus of samples**

We have takings of armours entrusted for study by the Wallace Collection<sup>29</sup>. Most of these armours were the subject of stylistic studies consigned in the catalog of the museum (Mann, 1961). The whole of the information relating to these samples is summarized in Table V.12. These armours were all identified as Italian, except for the armet W.C A.153 for which a Spanish origin was rather proposed. However, for the latter, it is not excluded, according to some historians, that this armet was manufactured in Milan for the Spanish market. It thus appeared interesting to us to add this sample to the corpus of study.

#### **Selection of the slag inclusions from the reduction**

Armours are highly manufactured artefacts for which high quantities of additives were certainly used during forging. Indeed, the more the artefact is manufactured, the more a massive use of additives or a local concentration effect is probable. For this reason, it is essential to verify that at least a minority of inclusions in the armour samples are coming from the smelting stage.

According to the methodology proposed by Dillmann & L'Héritier (2007), SI composition of two NRC is plotted and fitted by a linear model passing through zero. The results (Figure V.27) show that a constant NRC ratio can be identified in the inclusion composition of the armour samples studied in this work. Considering these results, it appears that SI coming from the smelting stage is present in the armour samples. The trace elements present in these inclusions can thus be analysed for a provenance study.

---

<sup>29</sup> Samples entrusted by A. Williams (The Wallace Collection, Londres, Grande Bretagne).

## Results

Insofar as these armours are dated from the 15th to the 17th centuries, it is necessary to identify beforehand those which are obtained by the direct process. To this aim, we use the abacus proposed by Dillmann & L'Héritier (2007) allowing to distinguish the objects from the two ancient processes (Figure V.28, left). The results reveal that most armours belong to the bloomery process domain. It is thus possible to examine their chemical signature to discuss their origin. However, the W.C A.148 morion is situated in the unspecified domain. This part of armour could as much come from the direct process as the indirect one. We nevertheless decide to study its chemical signature. We must note, however, that the conclusions which could be drawn from the results will have to be considered with prudence.

In Figure V.28 (Right), the manganese and phosphorus oxide concentrations contained in the slag inclusions of armour samples are compared with those defining the Lombard area. We see that those are compatible, except for three armours W.C A.215 (too low MnO content), W.C A.153 and W.C A.148 (too high P<sub>2</sub>O<sub>5</sub> content). It seems possible to exclude a fabrication of these armours from the ores of the Lombard valleys studied in this work. These results would fit with the idea of the Spanish origin suggested by the historians for the armet W.C A.153. On the other hand, it calls into question the Lombard origin of morion W.C A.148 on the hypothesis that this one results from the bloomery process.

Now, let's confront these first observations with the results of the analysis in trace elements. On the seven armours compatible with the Lombard samples, two (W.C A.215 and W.C A.152) of them could not be the subject of such an analysis because of the insufficient size of their slag inclusions (< 6 µm). For the other armours, an assessment of the elements which could be quantified in slag inclusions, by LA-ICP-MS or by SR-µXRF in confocal geometry, is consigned in Table V.13.

Due to a lack of a sufficient number of trace elements detected, we know that the comparison between the armours signature and the one from Lombardy is carried out in two stages:

1. Confrontation of the absolute contents (Figure V.29):

For the majority of the elements, these contents are approximately compatible with those of the Lombard samples. Nevertheless, armour samples W.C A.144 and W.C A.143 seem to be characterized by rather high Yb, Hf and Th amounts. Nevertheless, a variation in concentrations can be related to variation of the reduction outputs during the smelting. Moreover, this result only concerns the analysis of very few slag inclusions. Consequently, for the Lombard source hypothesis, no armour can be excluded thanks only to the absolute contents filter of trace elements.

2. In a second stage, the signature comparison will be carried out in a specific way, adapted to the number of trace elements quantified by armour (see Chapter IV):

- When contents of the elements Rb, Sr, Y and Zr, only, could be determined, only the Sr/Y ratio will be observed
- When several trace elements have been quantified, we will compare several of their ratios. The possible ratios to form in this study are: Y/Yb, Nb/Hf, Nd/Y, Nb/Cs, Ba/Sr, Y/Sr, La/Yb, Y/La.

We will successively consider the results obtained for each armour by applying the comparison filters of the ratios.

○ **W.C A.180**

For this sample, only the values of the Sr/Y ratio can be compared with those of the Lombard samples (Figure V.30). W.C A.180 presents values of this ratio which are not significantly different from those from the Lombard area. This work will thus not permit to invalidate its Lombard origin.

○ **W.C A.73**

The yttrium contents for armour W.C A.73 could not be quantified because of a value within detection limit, which is about 10 ppm, with the use of SR- $\mu$ XRF for this element. The contents in the slag inclusion are thus lower than this value and the minimal value of Sr/Y ratio are thus higher than Sr/10. If we represent the possible minimal value of this ratio in Figure V.31 (light green line), we note that for the Y contents close to the detection limit although lower than this one, the Sr/Y ratio can be of the same order of magnitude as those observed in the Lombard samples (green zone) (Figure V.31). We thus can not exclude a Lombard origin for armour W.C A.73.

○ **W.C A.235**

For this sample, four trace elements ratios (Ba/Sr, Y/Sr, Nb/Cs, Y/La) can be considered. It appears, in Figure V.32, that the slag inclusion signatures of sample W.C A.235 belong to the domain defining the Lombard signature. Consequently, the manufacture of this armour made from a Lombard ore can not be denied.

○ **W.C A.144**

For armour W.C A.144, we note that for the Y/Yb ratio the signature of the armour is clearly different from the Lombard one (Figure V.33). Nevertheless, this differentiation is obtained with the data of a single slag inclusion, the only one for which the contents were not within the limit of detection, which means we have to be careful about the interpretation of the results. Complementary analyses, carried out on a bigger number of slag inclusions, would be necessary to confirm this tendency.

○ **W.C A.143**

For the slag inclusions of armour W.C A.143, among the ratios formed of non-polluted elements, Y/Yb and Nb/Hf do not belong to the domain representing the Lombard signature and are clearly different (Figure V.34). It would thus seem that we could exclude a Lombard origin for this armour. However, we note that only few values are available for each ratio (one to two analysed slag inclusions).

These results are corroborated for a large number of slag inclusions by those obtained with Ba/Sr ratio. This difference could however be due to strontium pollution during the elaboration of the armour's metal. It appears, however, that the armour's signature could not be compatible with the Lombard signature studied in this work. These observations bring into question the origin of this morion. The possibility we may have to exclude this armour from the Lombard area is new information and would deserve to be thoroughly examined by complementary analyses. The scarcity of armour's takings nevertheless constitutes an important obstacle with such a prospect.

## **Chapter VI: Circulation and supply of iron materials. Report and prospects**

In the previous chapter, we presented in detail the results obtained thanks to the methodology based on both the multivariate approach implemented in this work and those relating to the specific case of armours. We are now going to gather all these results and discuss them.

### **THE CIRCULATION AND THE IRON MARKET'S ORGANISATION OF IRON PRODUCTS IN THE ARIÈGE AREA**

#### **Diversity in the provenances**

Firstly we are going to focus on the information provided by the multivariate approach on the origin of the objects collected on the archeological sites of the haut Sabarthès and the Couserans. In Table VI.1 is erected a balance sheet of the provenance indexes of these objects gathered in previous Chapter.

By considering the Ariège area in its "global nature" and in a diachronic manner, at least 13 objects studied and taken from the sites in Ariège (out of 34) were made from metal coming from the *moulines* of this iron-making area. Among these irons, the majority (12 out of 13) comes from the iron ores of the Mont Rancié (valley of the Vicdessos). These observations seem to confirm the hegemony of the mine of Rancié during the medieval period for the ore supplies to the iron and steel installations, at least to a part of the haut Sabarthès and the



Couserans. Nevertheless, we can also see that an important amount of the objects does not come from the iron production zone. These results therefore show that, within a region of production of iron products, we can also find objects made from a non-local iron.

We can apply a more subtle reading of these results by examining the localization of the archeological sites in relation to the ore sources and their nature (castle, production site, etc.), but also on the one hand the type of objects and on the other hand the chronology.

### **The influence of the objects' typology, the location and the kind of archaeological sites**

#### **Consumption sites**

##### *Typology of the objects*

For the site of Montréal-de-Sos, even if half of the objects studied, dating from the 13th and 14th centuries, were produced from iron ores of the valley of Vicdessos, probably from that of the Mont Rancié, the amount of iron coming from other regions must not be neglected. It amounts for precisely half of the objects under study. Thus, for five objects (projectile, nail, blades), it is certain that an elaboration from the ores of the basin of Vicdessos can be rejected. Other objects are of a possible but not confirmed origin from Ariège: a nail of a framework and a mule iron. Eventually, by taking into account at first only the factor of the typology of the objects, it seems that, for this site, whatever the type of object (nail, projectile, equine iron, knife), some of them are of origin from Ariège (5 out of 12) and others are not (5 out of 12). Thanks to the archaeometry, a combination of the supply sources on a site located in the Vicdessos thus emerges.

For the castles of Mirabat and Sainte-Catherine, only one type of object has been studied (nails dating from the 13th-14th centuries). Concerning the site of Mirabat, the results show that the majority of the nails analysed (8 out of 12) does not seem to come from neither from the Vicdessos nor from the Couserans. For the latter, provenance from the Montagne Noire or Andorra can also be rejected. Thus, only one nail presumably comes from the Ariège area (MIR7) and would have moreover been made from ores probably extracted from around the mine of Riverenert (Couserans). For the site of Sainte-Catherine, two nails out of three were not fabricated in Ariège. It is unfortunately impossible to determine where they come from in this research work. A single nail thus seems to be from Ariège in this part of the iron production space. We would have to analyse a much more significant number of nails to be able to bring to light the amount of objects coming from the production zone of Ariège on the site.

We have studied the homogeneity, from the point of view of their chemical signature, of nails that do not come from the Ariège and unearthed on these castles. Thanks to the discriminant analysis (Figure VI.1), it appears at first that the supply sources for the two castles were not

identical, their nails possessing distinctive chemical signatures on the plot (LD1, LD2). Several groups of signatures also differ for the nails of the castle of Mirabat. Moreover, we can assume that some of them could have the same origin. It is indeed possible to form two specific groups of objects, in the plot (LD1, LD2) for which the chemical signatures would be close to one another in each of them within the multivariate space (the pointed outline of the figure). This result is further confirmed by that of the projection in the first few discriminant plots (Figure VI.2). As a consequence, the possibility of a common provenance for the nails of these two groups must not be excluded.

The supply sources in iron for the framework nails from Mirabat are thus multiple, as demonstrated by the different chemical heritages detected in their slag inclusions. The nails come with the carpenter or are bought aside. Their origin can depend on that of the carpenter himself. The carpenters in charge of the construction or of the maintenance of the framework could have also provided for themselves from other sources. Moreover, we have shown that these differ from that of the castle of Sainte-Catherine.

Thanks to these results, a diversity of provenance is also put forward for one single type of object. Once more, a combination of the supply sources on these two consumption sites of the Ariège area is observed.

#### *Site location*

The site of Montréal-de-Sos is located approximately five kilometers from the mine of Rancié. The results obtained in this work therefore confirm that the geographical situation of the castle of Montréal-de-Sos favors the buying of iron coming from the mine of Rancié. Nevertheless, the iron produced locally was not the only consumption. The site is also located in the vicinity of important steel areas, which also leaves us to suppose that they could supply in iron produced in these regions. The results seem to show that the proximity of the mine of Rancié and economical power go with one another. Moreover, the site benefits from a relatively easy to get to location, in the vicinity of the trade routes. Thus, the transport of iron products of diverse origins on these commercial routes can facilitate the presence of supplies exterior to the County of Foix on the site of Montréal-de-Sos.

The haut Sabarthès supplied by the mine of Rancié is thus not only a production space. It is as much a site of open-market where products from multiple origins circulate. The results obtained on the provenance of the artefacts under study in this work thus seem to illustrate the complexity of the iron market in the haut Sabarthès on an economical point of view.

As for the artefacts that were not fabricated in Ariège, we have been able to eliminate the production zones of the Montagne Noire and Andorra. We will have to focus mainly on the irons from the Minervois, which also combine places of extraction and of transformation of the iron. The Catalan iron, mainly produced on the sides of the Mont Canigou in haut Vallespir

and Conflent<sup>30</sup>, as well as the iron of the Mont-de-Lacaune are also two other hypotheses concerning their provenance.

The Mirabat castle is located in the east of the Couserans, in the haut Salat. It is further away of the production sites and not located in the Vicdessos. Contrary to the fortification of Montréal-de-Sos located in the Vicdessos, it is more difficult to attest of the presence of iron made from ores of Rancié for a site established in this zone of the Couserans. We have seen that the unique origin from Ariège put forward for the nails of Mirabat would therefore be the iron ores exploited at Riverenert (MIR7). There are only about fifteen kilometers in between the two sites. Several hypotheses can be made to further explain the previous observations:

**1-**In a first approach, these results can coherently illustrate the distance of the castle from the production sites supplied in ores from the Mont Rancié.

**2-**From a chronological point of view, it might therefore be possible that some nails under study here be dated from the period before of the agreement of the treaty., that is to say before the *moulines* of the valleys of Ercé and of Massat were supplied by the ores of Vicdessos. In this case, the small number of nails coming from Ariège can also restore the almost exclusive usage of iron ores from the mine of Rancié by the *moulines* of Vicdessos.

**3-**Finally, this result could also testify of an opening of the market in the region of the Couserans. Nevertheless, only one type of object (nail) has been here examined. We therefore have to extremely cautious regarding our conclusions.

Even if the Couserans is a sector isolated by passes, exchanges with the close-by sectors exist (Verna, 2001). The castle of Mirabat is located next to the high passes of the south side that communicated with the Pallars (Spain). The iron ore deposits of this region also having a high percentage of manganese, we therefore must not exclude the fact that certain nails could have been made from the iron of the Pallars.

The castle of Sainte-Catherine, also in the Couserans, is located in the Castillonais (west zone of the Couserans). Whereas only one nail seems to have been melted from an iron ore of on the mine of Rancié (Ste Cath n4), none of them are fabricated from ore of the mine of Riverenert. The castle of Sainte-Catherine is located on the borders of Ariège, near the Comminges in the west. The pass linking the valley to the haut Comminges has been a privileged communication route. In this region, the extraction and reduction activities are vouched for, especially in the Aspet, and the existence of *moulines* is mentioned (Verna, 2001). The site of Sainte-Catherine was also politically dependent on the County of the Comminges in the 13th-14th centuries (Lasnier, 2007). This political integration<sup>31</sup> could therefore also be an opening for exchanges both with the Comminges and the Gascogne. The fact that the nails could have come from this region is therefore a hypothesis that we have to verify.

<sup>30</sup> See Chapter I.

<sup>31</sup> Even if the latter is blurred because of the treaty organizing the exchange between iron ore from the valley of the Vicdessos and coal from the woods of the Couserans.

In fact, it seems that the majority of nails have an origin exterior to the Ariège area (Videssos, Couserans).

#### **Production site**

The iron ore from the valley of Videssos, in the 14th century, supplied the *mouline* of Castel-Minier located in the Couserans (see Chapter IV). Out of the eight objects collected on the site (dating from the 14th and 15th centuries), a majority comes from ores of the valley of the Videssos.

In this precise case, the results give rise to an entirely different landscape compared to the other sites. We have seen that the geographical zone where the site is located is submitted to the tricky problem of the supply in iron ore, the Couserans not being able to provide for the needs in ore of its *moulines*. Since the treaty was signed in 1347-1348, the *mouline* of Castel-Minier has been supplied with ore from the Rancié. This ore does not come out freely from the valley of the Videssos but is the result of a controlled distribution and therefore of a withholding policy. The production of the *mouline* of Castel-Minier is entirely dependent on this supply. The results obtained here are thus the reflection of the political control of the supply in iron ore and not that of a market.

This study seems therefore to show that the men of the castle, notably, forged and used metal produced in the vicinity. The presence of the neighbouring *mouline* directly influences the supplies in iron, which was not the case for any of the consumption sites previously examined. To this, we have to add the fact that the site is located at the bottom of the valley, a fact which makes the presence of exterior supplies much more rare at Castel-Minier than their could have been at Montréal-de-Sos, castle that by the way is itself located in the vicinity of the *moulines* of the valley of the Videssos. The two objects that were not made out of iron ore from the Mont Rancié are but an exception here. On the location of Castel-Minier, whatever the type of artefact, nail, ring, but also a chisel found in the silver mines of the site, the object is manufactured from iron of the *mouline*.

*In fine*, two aspects can be emphasized:

- The controlled exchanges between the coal of the Couserans and the iron ore of the Videssos valley in the light of the treaty for this part of the Couserans.
- The geographical isolation of the site of Castel-Minier: the men of the castle only forged the iron from the *mouline*.

#### **A provenance from Ariège for some construction irons present in the St-Etienne collegiate church of Capestang**

We have considered the presence of iron from Foix in the vicinity of Narbonne at Capestang. In Table VI.2, we have listed the provenance results obtained in the previous Chapter on the

construction irons obtained thanks to the bloomery process of the Saint-Etienne collegiate church of Capestang.

The construction irons CAP1 and CAP3 being made from the bloomery process, it is possible to study their origin. These irons seem to have been produced from an iron ore from Ariège, probably that of the Vicdessos. It is therefore possible to demonstrate the presence of iron from Foix in the construction of the collegiate church. At first, this result would come and confirm that the town of Narbonne was able to receive iron produced in the Vicdessos from the County of Foix. The fact that we also find some at Capestang is an even more interesting result as its presence is not registered in the textual sources. In the next paragraph, the quality of this product (iron or steel) will be discussed.

### **Synthesis of the trade routes**

All previous data enable us to restore some circulation routes, in the Couserans and the Vicdessos, used by the iron ore from the mine of Rancié and the iron products. We have seen that the results obtained on the provenance of the objects under study differ in function of the site. The Figure VI.3 summarizes the provenance of the objects under study, and more largely, the major roads of circulation put forward in this work. We confront them to the contribution of the textual sources.

Note that we have made the two periods coexist, 13th-14th and 14th-15th centuries, on the map. The dates are therefore specified for each circulation routes. Circular diagrams are here to help visualize the provenance of the objects for each archeological site. For the latter, the figures represent the number of artefacts associated to each category of provenance.

To finish, based on the observations made in this part as well as those made in Chapter IV, the Figure VI.4 presents other hypotheses of provenance suggested for the objects discovered on the archeological sites of the Vicdessos and the Couserans and that are not of an origin from Ariège.

### **Nature of the iron matrix**

Up to now, we have not yet considered the nature of the material. Yet, we know that some authors have emphasized the production of particularly carburized alloys in Ariège probably linked to the use of an iron ore rich in manganese. It therefore appears interesting to put in relation both the composition of iron alloys under study in this work and their origin. We offer to examine the information brought by the metallographic analysis for the objects collected on the sites in Ariège<sup>32</sup> and the construction irons of the St-Etienne collegiate church. It appeared to us as being of interest to consider the objects whose function does not require a particular

---

<sup>32</sup> The artefacts of the site of Montréal-de-Sos have not undergone a metallographic study. They have therefore not dealt with in this part of the work.

carburization *a priori*. We have thus been careful to avoid all objects (or part of the object) whose function requires to be carburized.

The selected objects are often heterogeneous from the point of view of the carbon distribution. In order to express a degree of carburization, we have used the metallographic typology coined by Pagès (2009) that takes into account the proportion of the different types of alloy to the total surface<sup>33</sup>. This typology takes two parameters into account, the proportion of the carburized surface and the contents in weighted average carbon. The results are represented in Figure VI.6. The reader will find, in Appendix P, the detailed metallographic study of each of these objects. The areas of the four classes suggested by Pagès figure on the graph: ferritic, heterogeneous, composite steel and steel. We can observe that, for more than a third of the objects, the metal ranks in the “ferritic” category. A major point to note is that only one object of an origin from Ariège can be ranked in this category. Then, the nature of the metal of three other objects, coming or not from Ariège is ranked in the category of the “heterogeneous” alloys. Finally, the last two types of iron alloys, composite steel and steel, are formed by half of the analyzed samples. In these two last classes of iron alloys, we mainly find objects made of iron from Ariège. In order to illustrate these observations, we have listed in a histogram (stacked) the objects in function of their origin (“Ariège”, “Others”) and of the different classes of alloys. The objects, which have a ferritic tendency (“ferritic” and “heterogeneous” classes), have been put together as well as those who have a steel tendency (“composite steel” and “steel” classes) (Figure VI.7).

It is possible to note that the objects that have a ferritic tendency in majority (9 samples out of 12 in total) have not been made from iron produced in Ariège. On the contrary, the most important amount of the objects that has a steel tendency comes from the Ariège area (7 out of 10 in total). The analytic corpus is of course not sufficient to draw general conclusions, but at this level of observation, we can see that a significant tendency stands aside. The artefacts fabricated in Ariège are made from rather steel metal in comparison to those which do not come from Ariège. We can link these observations to those of historical sources that indicate that the iron produced in the *moulines* located in Ariège is designed as a heterogeneous metal (*merlaria*) comprising irons and steels resulting from different degrees of carburization inside the furnace (Verna, 2001). We would therefore find in these results, the specificity of the iron produced in Ariège<sup>34</sup>.

### **THE IRON SUPPLYING IN THE CONSTRUCTION SITES OF THE POPES PALACE OF AVIGNON**

In this part, the problematic of provenance deals with the supply in iron of the Popes' Palace of Avignon. This monument lends itself to this study as it is located in the area of common spread of the iron-making areas of interest. The data collected in the Chapter IV enable us to give a

<sup>33</sup> Note that this typology is initially used for a classification of semi-finished products from the bloomery metallurgy. See Pagès (2009), p.208-209.

<sup>34</sup> On that matter, note that for the production of the *mouline* of Castel-Minier, we are in the presence of a steel process (See Chapter III).



few answers as concern their origin. The results obtained on the steels of four building sites of the new palace (Conclave Gallery, Trouillas tower, Grand Promenoir and Latrines tower) are listed in the Table VI.4.

The bars used in the Conclave Gallery and in the Trouillas tower seem to have the same supply sources (Provenance 1). This report is interesting because the dates of construction of both the Trouillas tower (finished in 1347) and the Conclave Gallery (built in 1360) are not contemporaries. We have therefore confirmed the fact that the supply regions can vary in function of the different construction campaigns of a building<sup>35</sup>. The irons from the Grand Promenoir form two other groups deriving from the use of distinct iron ores (Provenance 2 and 3). The iron from Foix is said to have been used for the Latrines tower to carve some of clamps reinforcing the corbel C (Ec2 and Ec3) and one of the clamp coming from the corbel G (Eg3). For the latter (corbel G), a third clamp could also come from the County of Foix, nevertheless this origin remains uncertain, whereas that of the clamp Eg7 differs from the previous ones as its inclusions do not contain manganese. Finally, the only clamp of the corpus coming from the south of the Latrines tower (Se1) was created from an iron different to that of the other iron materials of the same building site. Note here that the Latrines tower was built in a single year (1338) and that, even in such a short amount of time, our work further demonstrates that iron of various origins supplied the building site.

In conclusion, we can say that, at the minimum, six provenances can be distinguished for four building sites of the new palace. Moreover, on a same building site (either Latrines tower, or Grand Promenoir), various iron origins are testified. These results would tend to confirm that the apostolic Chamber got from the “*maître des ferrures*”, the exclusive supplier of the palace, productions of various origins and therefore that the latter bought iron from different provenances to urban sellers or directly from the producer. We now have to try and explain the reasons of his choices (economical or political?).

None of these iron artefacts are said to be of Lombard origin or from the Montagne Noire. On the contrary, this work underlines the presence of iron coming from other iron production areas using manganese-rich ores, presumably the haut Sabarthès and hypothetically the Dauphine:

**1-** For the construction iron of Trouillas tower and the Conclave Gallery, the origin that is privileged among those that were tested in the course of this work, is that of the Dauphine. The latter however still needs to be confirmed and it is not excluded that another area of production containing manganese-rich ore not studied here is at the origin of the metal of these materials. It will therefore be essential to undertake further analytic works on other samples of the steel zone of the Dauphine in order to characterize as precisely as possible its chemical signature.

---

<sup>35</sup> On that matter, look back at the works of M. L'Héritier on the use of iron in the monumental construction (L'Héritier *et al*, 2007).



We will therefore have the ability to validate, or not, this area of production as being one of the possible supply sources in iron of the Popes Palace in Avignon in the 14th century.

2- The origin of the pins of the Grand Promenoir (Provenances 2 and 3) remains more mysterious as it has not been possible to establish a link between them and a specific origin. The inquiry to determine their provenance remains therefore open. The samples of this part of the palace differ from the other irons in terms of their quality, being mainly made of steel with few residual slag inclusions for the samples GP3 and GP3.2. Note that the sample GP3.4 is also made of steel but the amount of the residual slag inclusions is higher. The quality of these materials is therefore not comparable to that observed for the irons of provenance 1<sup>36</sup>, statement which conforms itself to the fact that they have a distinctive origin. The pins of the Grand Promenoir might have required specific quality material as it was submitted to specific constraints, especially during the construction on the Grand Chapel adjacent. By doing so, their origin being distinct from that of the irons used in the other parts of the palace could be the consequence of a will to use a material with higher mechanical qualities.

3- Finally, the results of this research work put into light the fact that the supplies for the archeological elements of the Latrines tower, built in 1338, are various and that one of them seems to be the iron from Foix. This result is further important as we do not find any written mention of the presence of iron from Foix in Avignon. However, we do have the proof, thanks to texts, that some iron from Foix was used in the Tour du Lion in Arles, located next to Avignon<sup>37</sup> (Verna, 2001).

In Avignon, the steel markets coming from other regions are in competition with one another. The master builders therefore had a large choice of iron products supplies and always managed to get the iron in the constructions. In order to grasp the importance of the iron from Foix supply for this part of the palace, some clamps reinforcing other brackets of the tower have to be examined.

We intend to summarize all the results concerning the supply in iron of the building sites of the Popes' Palace in Figure VI.8.

### **THE ARMOUR COMPATIBILITY WITH A LOMBARD ORIGIN**

In a third move and parallel to the study of the commerce of iron metallurgical products from the Ariège area, we have tried to verify the hypothesis of a Lombard origin for the pieces of armours exhibited in the Wallace Collection. For these samples, it was possible to partly verify the compatibility of the chemical signatures detected in the slag inclusions of the armours with that of the Lombardy thanks to the help of a selection of ratios of elements. In Table VI.5, are listed the different compatibility or incompatibility clues of a Lombard origin for the samples studied.

<sup>36</sup> See the metallographic study done by Dillmann & Bernadi (2003) for these samples.

<sup>37</sup> The iron from Foix was used in the refectory works of the Tour du Lion in 1486.

Regarding these results, certain provenances from Lombardy can be questioned. However, as only a small amount of inclusions (and elements) have been studied for each sample, we have to be extremely cautious as regards our interpretations on the provenances of these pieces of armours. Indeed:

- We have seen that the sample W.C A.148 could come from both the bloomery and indirect process.
- For the armour W.C A.125, analysed only by major elements, the contents in manganese oxides in the slag inclusions are detectable ( $\sim 0.5\%_{\text{wt}} \text{MnO}^*$ ) but inferior to those of the ores and slag samples from Lombardy. A study in trace elements would however be necessary to definitely reject the possibility of a Lombard origin.
- For the “Spanish” morion W.C A.144, the analysis of the trace elements could enable us to reject a Lombard provenance. However, this result only concerns results obtained from a single slag inclusion, which is more than insufficient to conclude definitively.
- For the “Spanish” morion W.C A.143, the analysis in trace elements also enables us to question its Lombard origin.

Nevertheless, the fact that these armours might not be fabricated from Lombard ores can be explained easily enough. Indeed, the armours under study could have been sold under the etiquette of a false Italian provenance, as the latter was a pledge of quality. The “Spanish” morions could have thus been counterfeits put on the market by the rival centers.

## **BILAN AND PROSPECTS: CONTRIBUTION TO THE PROVENANCE STUDIES**

### **Methodology based in the multivariate analysis**

One of the objectives of this thesis work was to establish a methodology capable of dealing with a great number of data thus contributing to the methodological development in provenance studies. The development of this new approach is in itself one of the important results of this work. It imposes:

- That a significant number of elements (major, minor and trace) be considered. This requires that it is possible to establish an adapted analytic approach, enabling the quantification of an important number of trace elements.
- That only the lithophiles and non-polluted elements (major, minor and trace) be used.
- That, during the comparison of several iron-making areas, a common base of elements be selected, which brings us not to take into account the chemical specificities of each of these regions.
- That the threshold contents or *a minima* the values of the ratios of elements be comparable from one analytical technique to another.

- To consider the problems linked to the limits of detection.

Moreover, this method requires two preliminary studies:

- processing of the elementary data<sup>38</sup> in order to look for the most efficient expression of the  $X_{ij}$  to characterize the signature of the iron production spaces (Chapter IV),
- definition of the conditions of the provenance compatibility with the iron production spaces (Chapter IV).

We have established a practical methodology that has the advantage of being able to describe a great number of data. Once the conditions of the provenance compatibility with the iron-making areas characterized, this multivariate analysis approach turns out to be operational, efficient and quick to deal with the data and observe the reactions.

For the future studies on the provenance of iron artefacts, it would be interesting to continue this multivariate approach by trying:

- to optimize the discrimination between signatures from the different areas. This result can be obtained thanks to the help of a procedure of selection of the elementary variables.
- to characterize the errors associated to the  $X_{ij}$  that present several elements within the limit of detection. The expanse of the chemical signatures' domain in the multivariate space would therefore be better characterized.

An abacus, which expresses the quartile distance in function of the median distance, was established to enable us to test a provenance hypothesis. We thus have to underline the fact that the abacus relies on threshold values based on the totality of the measures used in this work. In future studies, it will therefore be essential to provide the abacus with values of quartile and median distances obtained thanks to provenance tests done on objects whose provenance is known by the archeology.

### **Analytical methodology**

The analytical approach used relies on the synergy of the methods enabling us to obtain the maximum of information on the elementary composition of the macroscopic samples (iron ores, slags) and of the microscopic slag inclusions trapped in the metal of the objects. The determination of the contents of the trace elements is the trickiest analysis to undertake. The ICP-MS by laser ablation is an accessible means, very much adapted to the analysis of a majority of the slag inclusions. However, this method is not sufficient enough for the analysis of the smaller ones of those. It is the reason why we have used the X-ray microfluorescence

---

<sup>38</sup> Notably a research of the elements that have no contents in limit of detection, for the common denominator in the expression  $X_{ij}$ .

experiments in confocal geometry under synchrotron radiation and implemented a work methodology adapted to the study of pieces of armours. Nevertheless, the number of non-polluted lithophile trace elements detected is however not sufficient to enable us to confirm an origin, and even less, to apply our methodology based on the multivariate approach. It would therefore be convenient to test other analytical methods, enabling the quantification of a more significant number of trace elements in a manganese-rich matrix, with a beam of a size inferior to 30 micrometers:

- The Laser Induced Breakdown Spectroscopy (LIBS), enabling it to reach a beam of around 5 micrometers, can be used for this purpose.
- The analysis by wavelength dispersive XRF system (XRF-WDS) under synchrotron radiation is also an approach which would be worth analyzing.

## CONCLUSION

The thesis had two main objectives. Firstly, the research work was aimed at conducting a provenance study of iron-based objects focused on the Middle Ages and concerning a geographical area including the South of France and the Lombardy. We took a close interest in the circulation and the diffusion of objects coming from specific processes linked to the use of manganese-rich ores. We drew three historical and archaeological questions for which a specific study approach was adapted:

- The study of iron-made products in the production area of Ariège, but also nearby, in order to contribute to the understanding of the iron market organisation in Ariège;
- The study of iron supplying in the building of the Popes Palace situated at the borders of several iron-making areas, which include Lombardy and Ariège;
- The verification of the Lombard origin accredited to pieces of armour supposed to be Lombard by stylistic studies.

To treat these historical questions, it was necessary to develop a new methodology combining the trace element analysis to a multivariate analysis approach and capable to treat a substantial amount of acquired analytical data.



In order to reach our objectives, we first had to set up a corpus representative of the chemical signatures of the Ariège and Lombard iron-making areas. It was composed of both archaeological and geological samples, and slags, and of semi-finished products from different archaeological sites of these production areas. The obtained samples from an experimental reconstitution were attached to the corpus of Ariège.

Subsequently, our work consisted in setting up a multi-technical analytical approach (analyses of major elements and elements present as traces) and multi-scale analyses (macroscopic and microscopic analysis), which allowed us to determine the composition of all the samples. For this reason, in addition to the usual method of analysis used such as the EDS coupled to the

SEM for the quantifying of major elements, we were led to use experimental methods that were more specific for the element traces analysis: the ICP-MS and INAA for the ores and the slag samples, as well as the microscopic characterisation techniques for the slag inclusions in the objects: the ICP-MS by laser ablation and X-ray microfluorescence in confocal geometry under synchrotron radiation. The use of ICP-MS for the entire element traces analysis in the slags and in the ores required the creation of a digestion procedure well adapted to the composition of iron rich slag samples. Finally, regarding the slag inclusions, the non-destructive ultimate analysis of very small slag inclusions ( $<30\mu\text{m}$ ) had never been the object of thorough studies. Therefore, we have emphasised on the relevance of using the X-ray microfluorescence in confocal geometry under synchrotron radiation. This method, necessary for the analysis of slag inclusion in the armours, required not only the creation an adapted work methodology, but also the forming of a quantification strategy for the detected element traces. All this enabled us to obtain satisfactory results, which were validated by LA-ICP-MS. We demonstrated the potentialities and limits of this analytical technique in our study context and pointed out the possibilities of testing other methods.



One of the two objectives consisted in establishing a methodology based on the multivariate approach in order to characterise the chemical signature of iron-making areas in Ariège and Lombardy, and to track it in the slag inclusions of archaeological objects. This must only take into account the elements that completely pass in the slags and that are not polluted during the different stages of the direct operating chain. Thus, the methodology that we set up consists in:

- 1. In a first approach, the selection of the discriminatory elements. For this work, twelve elements were taken into account in the multivariate analysis.
- 2. The standardization of the elementary data using a logarithmic transformation of a ratio of chemical elements that we have named “ $X_{ij}$ ”.
- 3. The application of the discriminant analysis to these logarithms of ratios associated with the variables that define the iron-making areas and the objects from an unidentified origin. This supervised method of multivariate statistics allows us to compare the chemical signatures of the production areas with those of the objects. This work is executed in two different manners: when an object signature is compared to the one of a unique iron-making area or when several provenance hypotheses are estimated.

In the case that only two classes are considered in the discriminant analysis (the object class and the iron-making area class), the determination of the object’s origin is based on a provenance compatibility abacus established from the absolute values of the variables’ projections on the discriminatory axis (LD1). This graph, which expresses the quartile distance

according to the median distance of the objects' projections to the closest observation defining the iron-making area, underlines the different compatibility domains of the chemical signature with the production area (compatible, probably compatible, undetermined and not compatible) and subsequently allows us to test the provenance hypothesis. The limit values of these domains were established for Ariège and Lombardy, the two principal production areas considered in our study. The different domains of compatibility delimitations are based on the threshold values of the median and quartile distances, which were experimentally determined. The latter can be improved as a result of the analysis of other objects that come from the considered area and those from a different origin.

In the case where more than two classes are taken into account (various provenances are consequently considered), a visual analysis allows us, firstly, to favour a specific provenance on the projection LDA plots. The latter is then individually compared to the variables of the object with an unidentified origin.

This work has allowed us to elaborate an efficient tool that was applied to our data. This tool enabled the development of a general work methodology set up to compare the chemical signatures of the iron-making areas studied with the ones of objects with an unidentified origin that could come from these areas:

- *The first filter of absolute contents*

Considering a preliminary stage, the observation of absolute contents in manganese serves as the first filter to the exclusion of the archaeological object made out of an ore that does not have these strong signatures.

- *The use of the multivariate analysis: application of the linear discriminant analysis*

The multivariate approach is applied in two specific ways depending on whether one attempts to compare the chemical signature of the object with the signature of only one or several iron-making areas (see previous paragraph).

- *Special case: the application of specific filters for very small slag inclusions (from 10 to 30 $\mu$ m)*

If the X-ray microfluorescence in confocal geometry under synchrotron radiation is used for the inclusion analysis, the number of permitted elements to characterise a chemical signature is low and, the multivariate analysis cannot be applied. Therefore, the absolute contents in element traces located in the slag inclusions in the objects are first compared to those contained in the samples of the iron-making area, then the ratios of non-polluted lithophile element traces are compared.



As it was mentioned, the other objective of this research, with a historical background, is in three parts. It refers to the application of our methodology to the provenance question focused around three historical case studies.



- We have reconstructed certain characteristics concerning the circulation of iron products in Ariège based on the study of the objects' origin uncovered in different archaeological sites of Vicdessos and of Couserans, and based on Ariège's abacus of provenance compatibility. First, the results confirmed the large hegemony of the Rancié mine for Ariège ore supplying of the moulins in the Vicdessos and some siderurgical installations in the Couserans. Secondly, it was demonstrated that a large part of the analysed objects, and collected in Ariège, was probably not fabricated from the local iron and that the sources of supply were diverse. We were able to illustrate the fact that Ariège, in addition to being an effective production area, was also a market area where products of different origins were exchanged. The critical examination, along with the historical data, allows us to point out three aspects of this market:

- In the area of Vicdessos, the complexity of the market, from an economical point of view, thanks to the analysis of objects uncovered in a site located near Mont Rancié (Montréal-de-Sos). This complexity is related to the site's location which is closed to the trade routes.
- In the Couserans area, the remoteness of the castles in comparison to the production sites supplied with ores from Rancié or, in a political way, the vision of an area not supplied by this ore in the 13th -14th centuries before its exporting was controlled toward the Couserans in the mid-14th century.
- Opposed to this, the vision of the political control over the supply of ore from Mont Rancié in the valleys of Couserans neighbouring Vicdessos (the valleys of Ercé and Massat) in the 14th-15th centuries, rather than that of a free market.

Finally, a significant result of this work underlines that iron from Ariège is present in the Church St-Etienne of Capestang, which proves that the diffusion of iron went from Foix to Capestang.

- In the South of France, choosing the Popes Palace in Avignon to study the iron supply sources of a medieval building site was obvious. This choice was all the more evidenced in this research so as it is localized at the confluence of the marketing areas of products from Lombardy and Ariège. We have demonstrated that at least six provenance groups can be identified in four construction sites of the new palace. These results seem to confirm that the Apostolic Chamber, which was the unique supplier of the palace, bought iron from different origins from the "maître des ferrures". The supply for the architectural elements of the Latrine tower which was built in a single year, are also diverse. One of them is compatible from an iron production from the Ariège area. The favoured origin for the iron of the Trouillas tower and the Conclave' Gallery is from the Dauphine, although this remains to be confirmed through the carrying out of a corpus more representative of the siderurgical space. However, interestingly it was not possible to link the iron used in the Grand Promenoir to any provenance in particular.

- The study of the armours said to be from Lombardy could not be made with a multivariate approach. Based on the comparison of the absolute contents and the ratios of non-polluted elements traces quantified in the slag inclusions, we demonstrated that some Lombard provenances accredited three to four armours from the Wallace Collection can be questioned.



In conclusion, this work had a double dimension.

From a methodology point of view, we have established an approach based on a multivariate analysis adapted to large number of data and that meets the requirements of studies on geographical origin. We have showed, that by focusing our questions on a theme, whose historical and archaeological background is well documented, the obtained results turned out to be highly convincing. On this account, the archaeometric results obtained for the study of the iron market in Ariège revealed a consistency with the available historical data. By these means, we were able to demonstrate the validity of the approach.

As for the experimental techniques, we have contributed to the development of the X-ray microfluorescence in confocal geometry, bringing into play synchrotron radiation, to allow us to analyse in a non destructive way the small slag inclusions (from 10 to 30µm). This method however needs to be consolidated by the quantifying of a larger amount of elements.

From a historical point of view, we have contributed to a better understanding of the iron market in Ariège and revealed the Popes Palace supply sources during its construction, which until now were unknown. Finally, the study of the armour samples offered us the opportunity to question the Lombard origin of certain pieces of armour.

The entire results show the extent of the means offered by archaeometry to supply solutions to the historical studies on ancient metals.



This work offers several perspectives for future research.

The compatibility abacus with a provenance from Ariège and Lombardy must be refined, particularly for Lombardy, in order to reduce the extent of the undetermined domain. For that purpose, new analytical data must be gathered on objects that come from the area studied but also from different origins. Moreover, to improve the discrimination between the signatures of different iron-making areas, a specific study on a selection of elemental variables should be considered.

The examination of new objects from Ariège will also allow one to deal thoroughly with the question related to the circulation of iron products in Ariège by considering a two-level sampling in the archaeological sites: on one hand, by selecting only one type of object delivered to the dig in order to grasp the diversity of the supplies, and on the other hand, by selecting variants of iron products to identify the eventual specificities in the supplies. In the same time, one must take interest in other production areas identified by history and archaeology as potential iron suppliers in Ariège (Catalogne, Minervois, Comminges, Roussillon) to identify the extent of the relations between Ariège and these production areas. From another angle, to understand the diffusion of the iron from Ariège and to study the trade close by, further away and even the long distance trade, the examination of iron from constructions built outside of the production area of Ariège and in different regions, is crucial.

The studies conducted here did not enable us to characterise the provenance of a great part of the samples collected to date in the Popes Palace of Avignon. It would be interesting, on one hand to confirm certain supply hypothesis, and on the other hand, to quantify the diversity of the supply sources, to broaden the samples to a larger number of iron in the palace. An analysis of a larger corpus of samples taken from Dauphine will be required, with the objective of confirming this provenance hypothesis.

The non destructive analysis of the composition of small slag inclusions in the manufactured and precious samples take on an essential meaning in the study of their provenance. Additional studies should be executed with confocal X-ray microfluorescence, particularly at low energy, to detect a more significant number of non-polluted lithophile element traces. Thus, the quantifying of the element barium could reveal itself particularly profitable in the signature characterisation of samples from Lombardy. Furthermore, other analytical methods such as LIBS, could eventually help in reaching this goal.

Finally, we wish to make available the results of the chemical signature characterisation of Ariège and Lombardy. By giving access to the use of provenance compatibility abacus suggested here as well as very large databases acquired, this would enable the archaeological and archaeometrical communities, interested by the questions concerning provenance of iron products, to benefit from these results and to test the provenance hypothesis. The abacus would constitute a concrete foundation enabling the continuation of the research; it could benefit from a more systematic use by the scientific community.